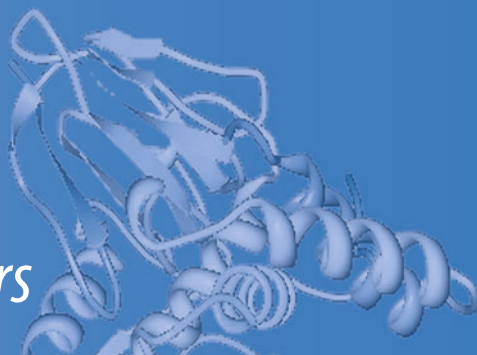Baoxue Yang
Jeff M. Sands *Editors*

Urea Transporters

Springer

Subcellular Biochemistry

Volume 73

Series editor

Robin Harris, Northumberland, UK

More information about this series at http://www.springer.com/series/6515

Baoxue Yang · Jeff M. Sands
Editors

Urea Transporters

Springer

Editors
Baoxue Yang
Department of Pharmacology
School of Basic Medical Sciences
Peking University
Beijing
China

Jeff M. Sands
Renal Division, Department of Medicine
  and Department of Physiology
Emory University School of Medicine
Atlanta, GA
USA

Foreword

Urea Transporters edited by B. Yang and J.M. Sands is a compendium of chapters about urea transport across membranes and the transporters/channels that mediate it. This is the first book on urea transport since a classic book *Urea and the Kidney* edited by Bodil-Schmidt Nielsen in 1970. The editors have recruited the top workers in the field worldwide to provide us with a far-reaching accounting of the world's knowledge about urea transport. The book deals with most aspects of urea transport from urea transporter molecules, illustrating that the SLC14 family of proteins most likely function as urea channels and not carriers. The chapter on the use of transgenic knockout mice to study renal urea transporters by Fenton and Yang is particularly informative, providing the latest information on the relationship between urea transport and the urinary concentrating mechanism. An exciting chapter on small molecule inhibitors of urea channels by Verkman and colleagues provides insight into urea channels as pharmacological targets. Since SLC14 isoforms UT-A1 and UT-A3 are expressed in the inner medullary collecting duct, downstream from sites of sodium chloride transport, inhibition of these transporters can be expected to increase water excretion without affecting sodium chloride balance. Thus, this family of drugs may provide us with new therapeutic agents for the treatment of water balance disorders.

I expect that this book will be highly useful as a comprehensive reference work to provide a foundation for future studies of urea transport. We are living in an era of information glut, and works such as the one provided by Yang and Sands are invaluable as a means to rapidly assimilate information on a given topic going back to the earliest studies. The scholarship is exceptional and book is as up-to-date as it can be in this era of rapidly expanding knowledge. I wish that more books with this level of focus and scholarship were available.

Mark A. Knepper

Contents

Contributors

Marc O. Anderson Department of Chemistry and Biochemistry, San Francisco State University, San Francisco, CA, USA

Lise Bankir INSERM UMRS 1138, Centre de Recherche Des Cordeliers, Paris, France; Université Pierre et Marie Curie, Paris, France

Mitsi A. Blount Renal Division, Department of Medicine and Department of Physiology, Emory University School of Medicine, Atlanta, GA, USA

Guangping Chen Department of Physiology, and Renal Division Department of Medicine, Emory University School of Medicine, Atlanta, GA, USA

Onur Cil Departments of Medicine and Physiology, University of California, San Francisco, CA, USA

Zixun Dong Department of Pharmacology, School of Basic Medical Sciences, Peking University, Beijing, China

Cristina Esteva-Font Departments of Medicine and Physiology, University of California, San Francisco, CA, USA

Robert A. Fenton Department of Biomedicine, Interpret Center, Aarhus University, Aarhus, Aarhus, Denmark

Lirong Guo Department of Pathophysiology, Norman Bethune College of Medicine of Jilin University, Changchun, China

Tinghai Hu Department of Nephrology, The Second Affiliated Hospital, Chongqing Medical University, Chongqing, China

Tao Jiang Department of Pharmacology, School of Basic Medical Sciences, Peking University, Beijing, China

Janet D. Klein Renal Division, Department of Medicine and Department of Physiology, Emory University School of Medicine, Atlanta, GA, USA

Anita T. Layton Department of Mathematics, Duke University, Durham, NC, USA

Tianluo Lei Department of Pharmacology, School of Basic Medical Sciences, Peking University, Beijing, China

Elena J. Levin Verna and Marrs McLean Department of Biochemistry and Molecular Biology, Baylor College of Medicine, Houston, USA

Xin Li Department of Pharmacology, School of Basic Medical Sciences, Peking University, Beijing, China

Fei Li Department of Pharmacology, School of Basic Medical Sciences, Peking University, Beijing, China

Min Li Department of Pharmacology, School of Basic Medical Sciences, Peking University, Beijing, China

Chunling Li Institute of Hypertension and Kidney Research, Zhongshan School of Medicine, Sun Yat-sen University, Guangzhou, China

Yan Meng Department of Pathophysiology, Norman Bethune College of Medicine of Jilin University, Changchun, China

Jianhua Ran Department of Anatomy and Neuroscience Center, Basic Medical College, Chongqing Medical University, Chongqing, China

Huiwen Ren Department of Pharmacology, School of Basic Medical Sciences, Peking University, Beijing, China

Jeff M. Sands Renal Division, Department of Medicine and Department of Physiology, Emory University School of Medicine, NE, Atlanta, GA, USA

Alan S. Verkman Departments of Medicine and Physiology, University of California, San Francisco, CA, USA

Hongkai Wang Department of Anatomy and Neuroscience Center, Basic Medical College, Chongqing Medical University, Chongqing, China

Weidong Wang Institute of Hypertension and Kidney Research, Zhongshan School of Medicine, Sun Yat-sen University, Guangzhou, China

Baoxue Yang State Key Laboratory of Natural and Biomimetic Drugs, Key Laboratory of Molecular Cardiovascular Sciences, Ministry of Education, Department of Pharmacology, School of Basic Medical Sciences, Peking University, Beijing, China

Xuejian Zhao Department of Pathophysiology, Norman Bethune College of Medicine of Jilin University, Changchun, China

Ming Zhou Verna and Marrs McLean Department of Biochemistry and Molecular Biology, Baylor College of Medicine, Houston, USA

Chapter 1
Overview and Historical Perspective

Baoxue Yang and Jeff M. Sands

Keywords Urea · Urea transporter · Membrane transporter · Solute

Urea (O = C(-NH$_2$)$_2$; radius 2 Å; mol. wt. 60 Da) is a small planar, trigonal, and water soluble molecule that was recognized as a main constituent of urine in the seventeenth century. It was also the first organic molecule synthesized from inorganic salts. It was initially isolated from urine in 1773 by Hillaire-Marin Ronelle. Subsequently, Friedrich Wöhler discovered in 1828 that evaporation of an aqueous solution of inorganic ammonium cyanate salt resulted in the production of urea. This finding was the first evidence to refute the doctrine that an essential vital force inherent in living cells was necessary to make organic compounds. In the nineteenth century, the role of the kidneys in ensuring the clearance of this waste product from the body was revealed by the observation of urea accumulation in the blood after experimental bilateral nephrectomy.

Urea has a low solubility in lipids and a correspondingly low permeability through artificial lipid bilayers (4×10^{-6} cm/s [1]) that lack any transport proteins to facilitate its transfer. Urea permeability through human erythrocytes is high (1.2×10^{-3} cm/s [5]) as a result of a specific urea transporter, UT-B. Urea transporters in erythrocytes and in the kidney play a pivotal role in the urine concentrating mechanism and the conservation of body water. In 1934, Gamble and colleagues wrote that it is "…an interesting instance of biological substances that the largest 'waste product' in urine incidentally performs an important service

B. Yang (✉)
State Key Laboratory of Natural and Biomimetic Drugs, Key Laboratory of Molecular Cardiovascular Sciences, Ministry of Education, Department of Pharmacology, School of Basic Medical Sciences, Peking University, 100191 Beijing, China
e-mail: baoxue@bjmu.edu.cn

J.M. Sands
Renal Division, Department of Medicine and Department of Physiology, Emory University School of Medicine, WMB Room 338, 1639 Pierce Drive, NE, Atlanta, GA 30322, USA
e-mail: jeff.sands@emory.edu

to the organism" [2]. Two seminal papers from 1972, Kokko and Rector [3] and Stephenson [8], proposed passive equilibration models for urine concentration in the inner medulla that depend upon the delivery of large quantities of urea to the deep inner medulla. The accumulation of urea in the inner medullary interstitium is accomplished through the axial heterogeneity of urea permeabilities along the collecting duct, which delays urea reabsorption to the deepest portion of the inner medullary collecting duct (IMCD) [6, 7], and the asymmetry of urea transport across the erythrocyte, which minimizes the loss of urea from the inner medulla by increasing the efficiency of countercurrent exchange of urea in the vasa recta [4]. Thus, the ability to produce concentrated urine and conserve body water depends upon urea transporters in both the kidney medulla and erythrocytes.

The reader of this book may wonder why the kidney or the erythrocyte needs urea transporters when most textbooks state that urea is freely permeable across cell membranes. Even though the permeability of urea in artificial lipid bilayer membranes is quite low, urea will diffuse across cell membranes and achieve equilibrium given enough time. In the kidney, the transit time, both for tubule fluid through the collecting duct and for erythrocytes through the vasa recta, is too fast to allow urea concentrations to reach equilibrium by passive diffusion. In addition, the need to concentrate urea within the inner medullary interstitium in order to maintain the urea gradient that is required for the generation of concentrated urine [3, 8] indicates the need for urea transport process(es) that can be regulated. This book is the first on urea transporter proteins. In the remainder of this chapter, we provide brief highlights of the content of each chapter.

Urea is generated by the urea cycle enzymes, which are mainly in the liver but are also ubiquitously expressed at low levels in other tissues. Urea is then eliminated through fluids, especially urine. Blood urea nitrogen has been utilized to evaluate renal function. The metabolic processing of urea is altered in several conditions, including changes in diet, hormones, and several diseases. Available clinical information and experimental data suggest the importance of urea in renal function, extra renal physiology and as a diagnostic tool in several clinical conditions (Chap. 2).

From a relatively low concentration in the plasma and glomerular ultrafiltrate (4–10 mM), urea is progressively concentrated along the nephron up to 40–400 mM in human urine and 100–l,000 mM in rat urine. The kidney transforms large quantities of urea-poor plasma into a small volume of urea-rich urine. The structural organization is believed to result in preferential interactions among tubules and vasa recta, interactions that may contribute to more efficient countercurrent exchange or multiplication, to urea cycling and urea accumulation in the inner medulla, and to sequestration of urea or NaCl in particular tubular or vascular segments (Chap. 3).

As mentioned above, urea is a small, highly polar molecule with low lipid solubility, and it has a low permeability through artificial lipid bilayers (4×10^{-6} cm/s). Traditional wisdom (and most textbooks) states that urea is freely permeable across cell membranes. A specific facilitated urea transport process was first proposed in 1987 in rabbit and rat terminal IMCDs. The existence of

urea transport proteins was confirmed when the first urea transporter was cloned in 1993. The urea transporters have two major subgroups, designated UT-B and UT-A. There are 6 distinct protein isoforms of UT-A: UT-A1 to UT-A6 (Chap. 4).

To date, crystal structures of two evolutionarily distant urea transporters have been solved. These structures reveal a common urea transporter fold involving two structurally homologous domains that encircle a continuous membrane-spanning pore and indicate that urea transporters transport urea via a channel-like mechanism. Examination of the conserved architecture of the pore, combined with crystal structures of ligand-bound proteins, molecular dynamics simulations, and functional data on permeation and inhibition by a broad range of urea analogs and other small molecules, provides insight into the structural basis of urea permeation and selectivity (Chap. 5).

Urea transporters are subject to regulation both acutely and by long-term measures. Rapid regulation of UT-A1 results from the combination of phosphorylation and membrane accumulation. Other acute influences on urea transporter activity are ubiquitination and glycosylation. Long-term regulation of urea transport closely associates with the environment that the kidney experiences. Low protein diets and low osmotic diuresis prompt an increase in urea transporter protein abundance in the kidney. Urea transporter abundances are reduced in aging animals and animals with angiotensin converting enzyme deficiencies (Chap. 6).

UT-A1 can be polyubiquitinated and degraded through the proteasome pathway and can also be monoubiquitinated and degraded in the lysosomal system. Ubiquitination could be a key regulator of UT-A1 sorting, trafficking, and protein turnover. The caveolin-mediated pathway is responsible for constitutive UT-A1 internalization, whereas the clathrin-coated pit pathway may regulate UT-A1 endocytosis stimulated by vasopressin in vivo (forskolin in vitro), and the latter pathway is accelerated by monoubiquitination. The monoubiquitinated UT-A1 is trafficked to the lysosome for degradation. In contrast, cytosolic UT-A1, misfolded UT-A1 from the endoplasmic reticulum, and constitutively internalized cell surface UT-A1 (mostly from the caveolae-mediated endocytic pathway) are polyubiquitinated and targeted to the proteasome for degradation (Chap. 7).

UT-B represents the major urea transporter in erythrocytes. UT-B is highly permeable to urea and chemical analogues formamide, acetamide, methylurea, methylformamide, ammonium carbamate, and acrylamide. Urea analogues dimethylurea, acrylamide, methylurea, thiourea, and methylformamide inhibit UT-B-mediated urea transport by >60 % by a pore-blocking mechanism. UT-B is also a water channel in erythrocytes with similar single-channel water permeability as aquaporin-1. Whether UT-B is an NH_3 channel still needs further study. The urea permeability of erythrocytes varies depending upon the mammalian species from which the erythrocytes are harvested (Chap. 8).

In kidney, UT-B is located primarily in the descending vasa recta. UT-A1 and UT-A3 are found in the inner medullary collecting duct, while UT-A2 is located in the thin descending limb. These transporters are crucial to the kidney's ability to concentrate urine. Physiological roles of urea transporters in kidney have been studied using genetically engineered mouse models. Mice lacking UT-A1/UT-A3,

UT-A2, UT-B, or UT-A2 and UT-B have decreased maximal urine concentrating ability. The reported phenotypes demonstrate that urea transporters mediate intrarenal urea recycling, which plays an important role in the urine concentration mechanism (Chap. 9).

The urea transporter UT-B is expressed in erythrocytes, kidney, brain, heart, liver, colon, bone marrow, spleen, lung, skeletal muscle, bladder, prostate, testis, etc., in mammals. Extrarenal phenotype analysis of UT-B null mice has found that UT-B deletion results in urea accumulation in the hippocampus, which induced depression-like behavior probably by interfering with the NOS/NO system. UT-B deletion causes a cardiac conduction defect, and TNNT2 and ANP expression changes in the aged UT-B null heart. UT-B also plays a very important role in protecting bladder urothelium from DNA damage and apoptosis by regulating the urea concentration in urothelial cells. UT-B functional deficiency results in urea accumulation in the testis and early maturation of the male reproductive system (Chap. 10).

Since knockout mice lacking the urea transporters are polyuric, urea transporter inhibitors are potential targets for the development of a novel class of diuretics. Recently, several classes of urea transporter inhibitors were reported. Further development of these intriguing compounds would be quite exciting. An Inhibitor of the inner medullary collecting duct urea transporters, UT-A1 and UT-A3, is particularly attractive as a drug target since they are located in the last portion of the nephron and hence should have minimal downstream effects on electrolyte excretion, in contrast to conventional diuretics that act in more proximal portions of the nephron (Chap. 11).

UT-B in the plasma membrane of erythrocytes was identified as the Jk antigen, which determines the Kidd blood type in humans, and is involved in transfusion medicine and organ transplantation. The Jk (a-b-) blood type is a consequence of a silent *Slc14A1* gene caused by various mutations related to lineage. In addition, the specific mutations in the *Slc14A1* gene related to hypertension and metabolic syndrome cannot be ignored. Genome-wide association studies established *Slc14A1* as a related gene for bladder cancer and some genotypes are associated with higher morbidity (Chap. 12).

Clearance of urea from the body is usually considered to result only from glomerular filtration with some reabsorption of urea along the nephron. Active urea secretion is not thought to take place in the mammalian nephron. However, several pieces of evidence, obtained in humans and experimental animals, not only suggest but also prove that a large fraction of urea found in the urine must have been added by secretion. Active urea uptake or secretion is present in early forms of life (bacteria and yeast) and lower vertebrates (elasmobranchs, some amphibians). It is thus not unlikely that such function has been conserved through evolution up to mammals (Chap. 13).

Aquaporins (AQPs) are a family of membrane water channels that basically function as regulators of intracellular and intercellular water flow. Some of AQPs, the glyceroaquaporins, also transport urea, glycerol, ammonia, hydrogen peroxide, and gas molecules. AQP-mediated osmotic water transport across epithelial

plasma membranes facilitates transcellular fluid transport and thus water reabsorption. AQP-mediated urea and glycerol transport are involved in energy metabolism and epidermal hydration. AQP-mediated CO_2 and NH_3 transport across membranes maintain intracellular acid–base homeostasis. AQPs are also involved in the pathophysiology of a wide range of human diseases (Chap. 14).

References

1. Galluci E, Micelli S, Lippe C (1971) Non-electrolyte permeability across thin lipid membranes. Arch Int Physiol Biochim 79:881–887
2. Gamble JL, McKhann F, Butler AM, Tuthill E (1934) An economy of water in renal function referable to urea. Am J Physiol 109:139–154
3. Kokko JP, Rector FC (1972) Countercurrent multiplication system without active transport in inner medulla. Kidney Int 2:214–223
4. Macey RI, Yousef LW (1988) Osmotic stability of red cells in renal circulation requires rapid urea transport. Am J Physiol 254:C669–C674
5. Mayrand RR, Levitt DG (1983) Urea and ethylene glycol-facilitated transport systems in the human red cell membrane: saturation, competition, and asymmetry. J Gen Physiol 81:221–237
6. Sands JM, Knepper MA (1987) Urea permeability of mammalian inner medullary collecting duct system and papillary surface epithelium. J Clin Invest 79:138–147
7. Sands JM, Nonoguchi H, Knepper MA (1987) Vasopressin effects on urea and H_2O transport in inner medullary collecting duct subsegments. Am J Physiol 253:F823–F832
8. Stephenson JL (1972) Concentration of urine in a central core model of the renal counter flow system. Kidney Int 2:85–94

Chapter 2
Urea

Hongkai Wang, Jianhua Ran and Tao Jiang

Abstract Urea is generated by the urea cycle enzymes, which are mainly in the liver but are also ubiquitously expressed at low levels in other tissues. The metabolic process is altered in several conditions such as by diets, hormones, and diseases. Urea is then eliminated through fluids, especially urine. Blood urea nitrogen (BUN) has been utilized to evaluate renal function for decades. New roles for urea in the urinary system, circulation system, respiratory system, digestive system, nervous system, etc., were reported lately, which suggests clinical significance of urea.

Keywords Urea · Urea cycle · BUN

Generation of Urea

Urea is a polar, highly water soluble, and charge-neutral molecule, with an oxygen and two nitrogen atoms serving as hydrogen bond acceptors, and two amino functions providing a total of four hydrogen bonds for donation (Fig. 2.1). A solution

———————————

H. Wang · J. Ran (✉)
Department of Anatomy and Neuroscience Center, Basic Medical College,
Chongqing Medical University, Yixueyuan Road 1, Chongqing 400016, China
e-mail: ranjianhua@cqmu.edu.cn

H. Wang
e-mail: wanghongkai1993@gmail.com

T. Jiang
Department of Pharmacology, School of Basic Medical Sciences,
Peking University, Beijing 100191, China
e-mail: 151355076@qq.com

Fig. 2.1 The molecular
structure of urea. The
molecular formula is
$CO(NH_2)_2$; the molecular
mass is 60.06 g/mol
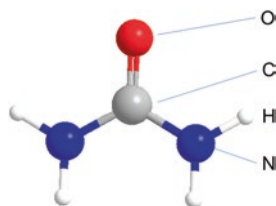
Fig. 2.2 The urea cycle. The
process happens around the
membrane of mitochondria
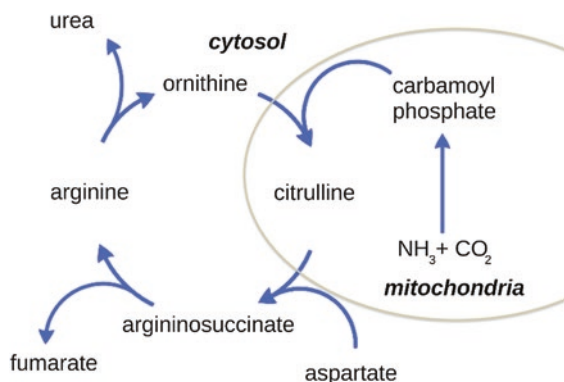
of urea is colorless, odorless, and neither acidic nor alkaline. In 1932, Hans Krebs
and Kurt Henseleit discovered the biosynthesis pathway of urea in mammalian
liver in vitro, and this pathway was subsequently named as the urea cycle (also
known as the ornithine cycle) [95]. The urea cycle is as necessary to life as is the
Krebs cycle (also known as the TCA cycle). The generation of urea serves a key
role in protein catabolism in mammals.

The urea cycle consists of five enzymatically controlled reactions: The first two
steps happen in the mitochondria and the rest happen in the cytosol (Fig. 2.2). This
ammonia disposal mechanism, i.e., the urea cycle, was expounded by a series of
studies [71, 75, 108, 136, 143, 144, 145, 146, 147, 148, 153, 154, 163, 166].

Step 1: Location: mitochondria; catalyzed by carbamoyl phosphate synthetase I
(CPS-1); rate-limiting step

$$NH_3 + CO_2 + H_2O + 2ATP \rightarrow \text{carbamoyl phosphate} + 2ADP + Pi$$
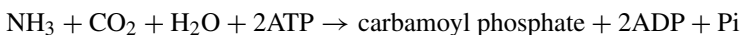
Step 2: Location: mitochondria; catalyzed by ornithine transcarbamoylase (OTC)

$$\text{carbamoyl phosphate} + \text{ornithine} \rightarrow \text{citrulline} + Pi$$

Step 3: Location: cytosol; catalyzed by argininosuccinate synthetase (ASS); rate-
limiting step

$$\text{citrulline} + \text{aspartate} + ATP \rightarrow \text{argininosuccinate} + AMP + PPi$$
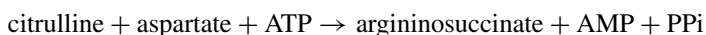
Step 4: Location: cytosol; catalyzed by argininosuccinate lyase (ASL)

$$\text{argininosuccinate} \rightarrow \text{arginine} + \text{fumarate}$$
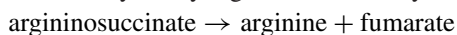
Step *5*: Location: cytosol; catalyzed by arginase I (ARG-1)

$$arginine + H_2O \rightarrow ornithine + urea$$

Therefore, the overall equation of the urea cycle is:

$$NH_3 + CO_2 + aspartate + 3ATP + 2H_2O \rightarrow urea + fumarate + 2ADP + 2Pi + AMP + PPi$$

Or it sums up as:

$$2NH_3 + CO_2 + 3ATP + H_2O \rightarrow urea + 2ADP + AMP + 4Pi$$
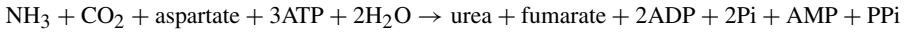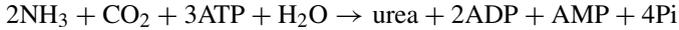
Apart from the above five enzymes, several other proteins participate in efficient functioning of the pathway in vivo, including glutaminase, glutamate dehydrogenase, N-acetylglutamate synthetase, mitochondrial aspartate/glutamate transporter, and mitochondrial ornithine/citrulline transporter [17, 28, 43, 83, 93, 126, 130, 202]. The complete urea cycle also exists in enterocytes in mammals [45], whereas the three cytoplasmic enzymes are found in a variety of other tissues such as stratum corneum [118], brain [36], mammary gland [149], kidney [149], submaxillary salivary gland [149], epididymis [149], eye [142], and endothelium [211]. (Fig. 2.3). The physiology of the incomplete urea cycle in these organs is to synthesize products, such as polyamines and NO, which catalyzed the conversion of arginine to ornithine.

In ureotelic animals such as mammals, the physiological significance of the urea cycle in liver is to convert the cytotoxic ammonia to much less toxic urea, even though the synthesis has a net energy cost [48, 117, 156]. Urea is not able to be further metabolized by mammalian tissues but urea markedly inhibits ureagenesis itself as negative feedback regulation [50]. Though it converts a basic substance to a neutral one, the urea cycle is not involved in the regulation of acid–base homeostasis because it cannot be regulated by acid or base load [21, 25, 26]. In conditions where the urea cycle in liver fails, such as in cirrhosis [125, 195], the accumulation of ammonia that causes hepatic encephalopathy is fatal [40, 191]. Body nitrogen balance is controlled via regulation of the generation of urea [217].

Protein in the diet can raise urea synthesis through upregulation of urea cycle enzymes to 300 % above what is present at the onset of a fast [160]. Under conditions of varying dietary protein quality, the liver level of free amino acids may limit the rate of the urea synthesis, primarily without a change of enzyme activities [72]. Infusion of glucose-alone elicits a significant reduction in ureagenesis [67, 69]. Xylitol inhibits urea synthesis and alanine metabolism [68]. In rats fed with a high-fat diet, ARG-1 is downregulated, which may lead to a lower rate of urea generation [122]. Defects in the urea cycle enzyme systems may be present in rats fed with a zinc-deficient diet, which is linked to deficiency of OTC [141].

Urea biosynthesis is susceptible to regulation by hormones. Insulin decreases the capacity for urea synthesis [69]. In insulin-dependent diabetes mellitus, the generation of urea in rat liver is elevated through upregulation of CPS-1 and OTC, causing negative nitrogen balance [88]. When cultured hepatocytes are supplemented with amino acids, high insulin preconditioning downregulates urea synthesis by means of downregulating CPS-1, OTC, ASS, and ARG-1 [98]. Additional dexamethasone induces the expression of CPS-1, ASS, ASL, and
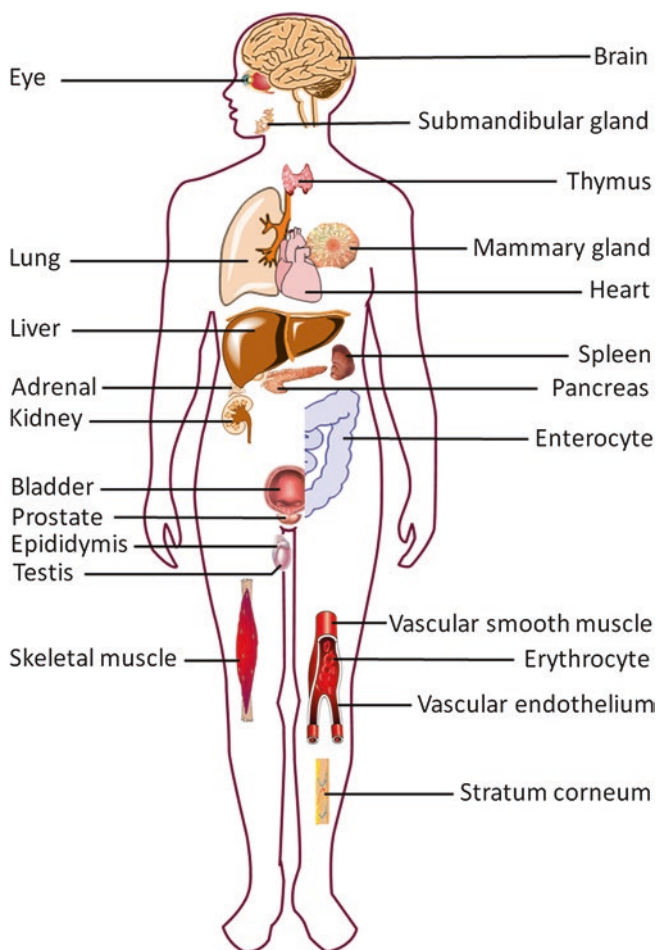
Fig. 2.3 The organs generating urea. The organs generating urea include liver, brain, eye, submandibular gland, thymus, lung, mammary gland, heart, spleen, adrenal, pancreas, kidney, intestine, bladder, prostate, testis, epididymis, skeletal muscle, vessel, erythrocyte, and skin

ARG-1 in cultured fetal hepatocytes, which can be inhibited by insulin treatment [80]. Contrarily, glucagon infusion independently accelerates the rate of urea generation in both humans and rodents [4, 67, 196]. The urea synthesis rate is markedly reduced in patients with chronic pancreatitis whose glucagon secretion is impaired [66]. The effect of glucagon administration on the urea cycle relies on upregulating CPS-1, ASL, and ARG-1 in cultured fetal hepatocytes [79, 81]. Hyperinsulinemic-induced hypoglycemia patients, whose glucagon concentration is doubled, have a markedly high rate of urea biosynthesis [64]. Adrenergic agonists (phenylephrine and norepinephrine) stimulate the generation of urea, as compared to untreated hepatocytes in vitro [91]. Both exogenous and endogenous glucocorticoids can upregulate hepatic urea synthesis [62, 79, 80, 161, 206, 207],

which can be reversed by a glucocorticoid receptor blocker [73]. Growth hormone and insulin-like growth factor I can either singly or in combination decrease urea biosynthesis by downregulating all five enzymes [62, 63, 206]. Patients infused with somatostatin display higher rate of the urea synthesis [74].

The generation of urea is also affected in other conditions. Iron overload in liver can be found in patients with hemochromatosis, alcoholic liver disease, and chronic viral hepatitis, or secondary to repeated blood transfusions. Based on a proteomic analysis, elevated CPS-1, OTC, and ARG-1 levels were found in iron-overloaded patients, which may lead to higher rate of the urea synthesis [137]. Liver cirrhosis decreases the level of urea cycle enzymes [191], resulting in low efficacy of urea synthesis [195]. Release of endotoxin lipopolysaccharide (LPS) during infection in cirrhosis can separately impair the urea synthesis process by decreasing urea cycle enzymes as well [125]. Thus, the reduced capacity to detoxify ammonia may be the reason why infection exacerbates hepatic encephalopathy in patients with cirrhosis [40]. The levels of all five urea cycle enzymes are significantly lower in hepatoma, which is considered as the next step of cirrhosis [27].

Moreover, the rate of urea synthesis is also elevated in other cachectic tumor-bearing rats, which implies negative nitrogen balance in cancer cachexia [41]. Inflammatory cachexia, such as in rheumatoid arthritis, shows elevated generation of urea in liver [216]. Severe stress, like pain, upregulates liver function including urea synthesis [61]. The rate of urea synthesis rises during the TNF-α induced acute-phase response [185]. Further study suggested that IL-6 contributes to downregulation of urea cycle genes but displays no effects on the upregulated rate of urea synthesis [184]. What is more, the LPS-induced acute-phase response upregulates urea synthesis in vivo [124].

The urea cycle enzymes are significantly increased in chronic vitamin A deficiency, which causes a much higher rate of urea generation [51]. In acute and chronic uremia, the urea production rate in liver is increased by means of elevated levels of urea cycle enzymes after it went through a temporary early-stage downregulation [3, 76, 123]. This phenomenon is probably induced by varied glucagon levels in uremia [3]. In rats with obesity, as a result of which the rate of urea biosynthesis is low, all urea enzymes are decreased especially CPS-1 and ASS [16]. The deficit of ureagenesis is also found in fatty liver with low levels of urea cycle enzymes [116, 186]. The generation of urea is increased in patients with active inflammatory bowel disease due to an unknown mechanism [106].

Some compounds have the capacity to influence the generation of urea in liver. Diuretics such as xipamide, mefruside, chlortalidone, and chlorothiazide but not furosemide inhibit urea synthesis from the first step in liver due to an inhibition of mitochondrial carbonic anhydrase that supplies CO_2 to the urea cycle [82]. In contrast, acute moderate dehydration caused by furosemide downregulates urea synthesis; this effect is mediated by reduced glucagon levels [84]. The increased rate of urea synthesis in non-insulin-dependent diabetes mellitus can slow down after prostaglandin E1 infusion [113]. In large-dose caffeine-treated rats, increased urea synthesis has been found as a consequence of upregulated CPS-1 and ASS [89]. Acute exposure to low ethanol concentrations transiently leads to suppression

Table 2.1 Urea concentration in mammalian

	Mice	Rats	Dogs	Humans	Cows
Plasma urea concentration, mmol/l	9	5	4	5	5
Urine urea concentration, mmol/l	1,800	700	620	285	260
U/P urea	200	140	155	60	52
References	Yang and Bankir [215]	Yang and Bankir [215]	Spector et al. [174]	Yang and Bankir [215]	Spek et al. [175]

of the capacity for urea synthesis, presumably due to the decrease in the NAD/NADH ratio during catabolism of ethanol [86]. Protein amounts of CPS-1, ASS, and OTC are all decreased in perfluoroalkyl acids (synthetic toxicant with worldwide environmental distribution)-treated rats [199]. L-carnitine protects mice from an acute ammonia load by means of accelerating the rate of urea generation [42].

Excretion of Urea

Urea, as a terminal product, is subsequently excreted out of the organism after generation. It is well known for centuries that approximately 90 % of urea is eliminated in urine by the kidney, which is the origin of its name [44]. In humans, the daily excretion of urea in urine is around 30 g. Urea is excreted not only by glomerular filtration, but also by tubular secretion [96, 162]. Studies have also found excretion of urea in sweat [164], tears [183], saliva [2, 31], and digestive fluid (feces) [23, 29, 170] in humans.

Table 2.1 illustrates in numbers the special features of urea handling in different mammals. It shows the wide differences among humans, cows, dogs, rats, and mice in urinary urea concentration. The plasma urea level is relatively low (5–10 mmol/l) in these mammals, and the urea concentration in the urine may be 60 times higher than in the plasma in humans and up to 200 times in mice. Thus, a very large fraction of the concentrating effort of the kidney is devoted to the concentration of urea. Though the kidney is the main organ to dispose of urea, the process herein is not just as simple as filtration and concentration. Urea is "sequestrated" in the inner medulla [193] via urea transporters that mediate intrarenal urea recycling process [15] (see Chaps. 9 and 13).

Clinical Significance of Urea

Urinary System

Clinicians usually use blood urea nitrogen (BUN) to measure the amount of nitrogen coming from urea in the blood as an index of renal function [187]. An increase in BUN is associated with many factors including the following: (1) Prerenal

causes. The most common manifestation is hypovolemia. Due to a shortage of renal blood supply, the glomerular filtration rate is reduced, causing an increase of BUN. This can occur as a result of massive hemorrhage or diarrhea. (2) Intrarenal causes, such as glomerulonephritis, chronic pyelonephritis, and toxic nephritis. A deficiency of renal function causes reduced excretion and leads to urea accumulation. (3) Postrenal causes. Whatever etiology leads to the blockage of the urinary tract can produce a high BUN level, such as prostatic hypertrophy, urolithiasis, and bladder cancer. These pathological changes press on the urethra and block urine flow, which interferes the major urea excretion pathway.

Above all, urea acts as an indispensable contributor in laboratory diagnosis and has a strong relevance with kidney. Unfortunately, BUN is inferior to other markers to evaluate renal function, even without mentioning that dysfunction of one kidney is often masked by the healthy one. BUN is not a reliable marker because it is easily influenced by causes unconnected to glomerular filtration rate, including tissue breakdown, high protein intake, and major gastrointestinal hemorrhage [187, 197]. It can be elevated in patients suffering from non-alcohol fatty liver disease [104]. Besides, BUN even increases with age while the fractional excretion of urea decreases with age [121]. The importance of evaluating renal function only by urea fades away due to the factors mentioned above.

Nonetheless, recent studies also unveiled clinical significance of urea in other fields. Fractional excretion of urea below 40 % was found to be a sensitive and specific index to differentiate transient from persistent acute kidney injury in patients [47], while another study showed fractional excretion of urea less than 35 % can distinguish acute kidney injury from its two main causes: prerenal state and acute tubular necrosis [33]. But other studies discovered that fractional excretion of urea changes are age related, suggesting that the above statistics may call for a reanalysis [121]. A study even declared that the fractional excretion of urea is a poor predictor of acute kidney injury, especially in distinguishing transient and persistent acute kidney injury [205]. The relationship between fractional excretion of urea and acute kidney injury is still waiting for clarification. Patients with diabetes mellitus and hypertension are predisposed to kidney diseases, and those with significantly low urinary urea concentration as a biomarker have a worse prognosis [20]. For geriatric patients, BUN is an independent predictor of morbidity to get urinary tract infections [60]. BUN is also one of the factors that predict the need for nephrectomy in patients with renal trauma [169].

Acute renal failure is a common complication of rhabdomyolysis [179]. BUN may be one of the important predictive factors to indicate the patients with rhabdomyolysis that may develop acute renal failure [38]. A similar trial in New York suggests that only BUN and blood creatinine can predict which patients with rhabdomyolysis will develop the complications of acute renal failure and require hemodialysis [56]. On the contrary, a case report exhibited the opposite result that BUN is not reliable [198]. The argument whether BUN is an appropriate predictor in this situation may need a further multicenter clinical trial or meta-analysis.

Kidney dialysis adequacy is determined presently through the use of a dimensionless parameter called the urea reduction ratio that compares the predialysis

with the postdialysis levels of BUN as determined through laboratory analyses of blood samples taken at the beginning and at the end of a dialysis treatment [12]. Patients with low or high urea levels exhibited higher mortality than those with medium levels, while both low and high levels of urea are independent predictors of all-cause mortality [177]. Dialysis disequilibrium syndrome is prevented by the use of dialysate-containing urea at a concentration similar to that of the patient's blood [87].

Circulation System

The BUN level has a strong predictive significance for cardiovascular outcomes and all-cause mortality. A number of studies strongly recommend monitoring BUN as a predictor of prognosis in both acute heart failure and chronic heart failure, resulting from the high correlation between increasing BUN and bad outcomes [7, 9, 34, 35, 37, 55, 57, 59, 78, 92, 97, 133, 151, 157, 168, 172, 214]. Quantitatively, a significant cardiovascular risk is associated with the diagnosis of chronic renal failure through the hematocrit, urea in plasma, and gender (HUGE) formula [152]. Moreover, during treatments for heart failure, BUN can identify patients destined-to-experience adverse outcomes associated with the use of high-dose loop diuretics—the patients can get maximum benefit from this double-edged sword by properly monitoring the BUN [128, 182]. A further study also considered BUN as a predictor to reflect the response of diuretics in acute heart failure [192].

The BUN level is a better factor than the creatinine level when it is associated with the hardness of decision to perform a cardiac catheterization on patients who present symptoms of unstable angina without known prior history of coronary artery disease [129, 158]. Still as a predictor, increasing BUN level correlates with a high long-term mortality in patients diagnosed as myocardial infarction [8, 107]. Even after coronary artery bypass grafting, a high BUN is still an independent risk factor for mortality, which strongly suggests cardiologists should monitor a patient's BUN level throughout their hospital course [70].

Respiratory System

Community-acquired pneumonia is common and is associated with a considerable risk of death [6]. After international multicenter derivation/validation studies, CURB-65 score (an abbreviation of confusion, BUN >7 mmol/L, respiratory rate ≥30/min, BP ≤60 mmHg, and age ≥65 years) gets commonly used and widely practiced as an assessment tool of the severity and short-term mortality of community-acquired pneumonia in daily clinical work. Each element of the CURB-65 score counts 1 point and a bad outcome is revealed when the CURB-65 score is >3 points [99, 120, 213]. Considering its effective prediction of both bacterial

pneumonia [213] and viral pneumonia [120], the CURB-65 score may be an assessment tool regardless of pathogen. The CURSI score, in place of BP and age by shock index (SI), was also established for elderly patients [127]. A recent study of bacteremic pneumococcal pneumonia in elder patients also found a relation between BUN and mortality [155]. Another score called the PORT rule (respiratory rate, temperature, pH, BUN, and sodium concentration) was created to help pulmonologists make decisions about whether to hospitalize patients with mild community-acquired pneumonia [58]. Stevens–Johnson syndrome and toxic epidermal necrolysis are severe life-threatening conditions. Once bronchial epithelial is implicated in these conditions, they can cause acute respiratory failure. Elevated BUN is a variable in a multivariate analysis to predict at-risk patients who need early management of mechanical ventilation [139]. To assist physicians with difficult decisions about hospital admission for patients with an acute exacerbation of chronic obstructive pulmonary disease (COPD) presenting in the emergency department, 5 risk factors including prior intubation, initial heart rate $\geq$110/min, being too ill to do a walk test, hemoglobin <100 g/L, and urea $\geq$12 mmol/L were set up [176]. Patients who are assessed at score of 2 or higher are strongly recommended for hospitalization.

Digestive System

A large proportion of the digestive tract and glands are associated with urea in clinical practice. *Helicobacter pylori* infection is associated with a wide range of gastrointestinal diseases such as functional dyspepsia, gastroesophageal reflux disease, chronic active gastritis, peptic ulcers, and even gastric malignancies [39, 46, 132]. The marvelous discovery of *Helicobacter pylori* almost kicked peptic ulcer out of the surgical department, except for severe complications such as perforation and massive hemorrhage [201]. Nowadays, diagnosing *H. pylori* infection and then starting an eradication therapy is routine and fundamental knowledge for gastroenterologists in clinical practice around the world [111]. ^{13}C and ^{14}C urea breath tests are broadly used to probe the presence of *H. pylori* in stomach as the best type of noninvasive method in this field [10]. Patients firstly swallow a capsule containing urea labeled with ^{13}C or ^{14}C. If *H. pylori* is present in stomach, the bacterium metabolizes the urea into nitrogen and carbon (as CO_2). The CO_2 would be absorbed across the lining of the stomach into blood. It is eventually excreted through the lungs by breath. The result of a urea breath test is quantitative so as to estimate the integral load of the bacteria and severity of gastritis [134]. Physicians always call for another round of urea breath test to evaluate the eradication treatment, which is helpful for determining the next prescription [171]. As a mature technique and an easily acceptable one, as contrasted with endoscopic biopsy, the efficiency and safety when it is performed on children have been well proved and all-age stages of children have been benefited from this test [32, 194]. However, clinicians and technicians are supposed to realize the influences of baseline caused

by age and gender [115, 219]. Furthermore, in a proof-of-concept study, ^{13}C urea may be a suitable marker to assess the in vivo fate of colon-targeted dosage forms given by mouth (a special type of capsule) [159]. The ^{13}C urea breath test was found as a novel biomarker of diagnosis and treatment for tuberculosis in rabbits, so further research on humans can be valuable [85].

In acute hepatitis A, BUN level >36 mg/L is a predictor of mortality [110]. High BUN level independently contributes to prediction of mortality in pyogenic liver abscess patients [5]. In patients who have a paracetamol overdose, BUN per se can predict hepatotoxicity [200]. A new score consisted of BUN, hemoglobin, systolic blood pressure, and comorbid conditions apply to identify the risk stratification of acute upper-gastrointestinal hemorrhage. It marks the severity of the bleeding and judges whether the patient needs clinic intervention and hospital admission [22].

Acute pancreatitis is a devastating disease with extensive morbidity and mortality so that it is imperative that clinicians recognize patients who may end up in severe outcomes at an early stage. BUN, as a single marker, is a useful, routine, easy-to-perform sensitive index to predict the severity and the mortality of the acute pancreatitis in the early assessment [53, 190, 209, 210]. Pancreaticoduodenectomy, which is performed on patients with pancreatic carcinoma, etc., has a high morbidity rate of complications. A BUN level of 20 mg/dL or greater can help surgeons identify patients who are at increased risk of morbidity and mortality after pancreaticoduodenectomy [204]. Further study exhibited that high BUN on the first postoperative day is associated with an increased occurrence and severity of complications, including the occurrence of pancreatic fistula [150].

A BUN level of more than 40 mg/dL is also an independent preoperative predictor of higher 30-day mortality after esophagectomy [14]. Preoperative BUN/creatinine ratio in primary gastrointestinal cancer patients requiring surgery would be useful to predict the mortality caused by postoperative enteric fistulas [101], and a high BUN level independently predicts worse overall survival in patients with malignant bowel obstruction in the setting of Stage IV non-curative cancer [208]. After colectomy for colon cancer, preoperative BUN is one of the predictive risk factors for 30-day mortality and complications such as pneumonia and systemic sepsis [105].

Nervous System

Urea also plays multiple clinical roles in neuropsychiatry. It has been firmly proved that acute ischemic stroke patients have a bad outcome with renal dysfunction [30, 52, 100, 109, 140, 180, 188, 212]. Just based on the above, studies displayed that the BUN/creatinine ratio may be a novel predictor of early deterioration of stroke [102] and elevated BUN is an independent predictor associated with poor clinical outcome and mortality in acute ischemic stroke patients after

treatment with i.v. tPA [220]. Even though elevated BUN has been precluded as a predictor of pre-eclampsia during pregnancy [112], the decreased fractional excretion of urea ($\leq$35 %) in pre-eclampsia is relevant. Soon after delivery, the fractional excretion of urea would return toward the normal range (50–65 %) [218]. What is more, BUN is considered as one of the biochemical indicators of delirium happening in the emergency department and intermediate care units [114, 24].

Others

Low BUN in routine pretherapeutic laboratory testing is significantly correlated with a higher T stage in patients with head and neck cancer and also correlates with the appearance of neck metastasis [135]. BUN, one of the elements in day +7 score, identifies risk of transplant-related mortality after hematopoietic stem cell transplantation in the first seven days [13, 173]. By measuring the concentration of urea in diluted lavage synovial fluid, we can estimate intra-articular synovial fluid volume in normal joints and joints with chronic arthritides [94].

In the past, dietary history was depended heavily on an individual's memory and level of motivation, nevertheless based on a randomized double-blind crossover feeding trial, urinary urea holds promise as a quantifiable bioindex of dietary protein intake with a formula: protein intake (g/day) = 63.844 + 1.11 × (urinary urea, g/creatinine, g) [19]. Higher BUN in premature newborns may be associated with the chance of metabolic diseases in later stages of life, such as diabetes, hypertension, and metabolic syndrome [119]. Vaginal fluid urea is a helpful marker in diagnosing premature rupture of membranes because fetal urine is the most important source of amniotic fluid, which helps us avoid unwanted obstetric complications such as chorioamnionitis and preterm birth [90].

Using a logistic model, a retrospective study displayed that the only variable that was independently associated with mortality in *Clostridium difficile* infection was renal failure by observing fourfold higher BUN levels in the non-survivor group [131]. A 13-year-old boy who was eventually diagnosed with blastomycosis after orthopedic surgery had an elevated BUN as his first sign [103]. BUN $\geq$10 mmol/L is a risk factor for bacterial coinfection in dengue patients [165]. BUN is significantly associated with a low concentration of efavirenz, which is widely prescribed for people infected with HIV, in blood [178]. It can hence improve the prediction of efavirenz plasma concentration and optimize its dosing in antiretroviral therapy. In patients with Fournier's gangrene, BUN is significantly different between survivors and non-survivors and it is the only parameter that deceases to normal at the end of the treatment in the survivor group [189].

Urea-containing cream is prescribed for dermatitis, xerosis, ichthyosis, psoriasis, onychomycosis, eczema, tinea pedis, etc., as a topical antifungal emollient and moisturizer [1, 49, 138, 167, 181]. Urea clearance can be used as a relatively simple method to estimate drug-induced blood flow changes in human skin during microdialysis of vasoactive substances [54].

Patients who underwent emergency laparotomy have high 12-month mortality if preoperative BUN >7.5 mmol/L, suggesting that this is an independent predictor [11]. Elevated BUN is a valuable predictor for increased long-term mortality in various critically ill patients regardless of their precise disease [18, 77]. The significance of urea/albumin ratio in predicting the stay and mortality of critical patients was found, based on a retrospective study of patients admitted to ICU with non-chronic kidney disease [65]. These results are accordant with finding that BUN is linked to mortality in a number of diseases. A simple 5-point scoring system, NaURSE (Na$^+$, Urea, Respiratory Rate and Shock Index in the Elderly), was created to predict in-hospital mortality in acutely ill older patients. The crude mortality rates were 9.5, 19.9, 34.4, 66.7, and 100 % for scores 0, 1, 2, 3, and 4, respectively [203].

References

1. Ademola J, Frazier C, Kim SJ, Theaux C, Saudez X (2002) Clinical evaluation of 40 % urea and 12 % ammonium lactate in the treatment of xerosis. Am J Clin Dermatol 3:217–222
2. Albrectsen SR, Thaysen JH (1955) The excretion of urea by the human parotid gland. Scand J Clin Lab Invest 7:231–238
3. Almdal TP, Egfjord M, Hansen BA, Vilstrup H (1991) Increased hepatic capacity of urea synthesis in acute and chronic uraemia in rats. Clin Nutr 10:206–212
4. Almdal TP, Vilstrup H (1988) Loss of nitrogen from organs in rats induced by exogenous glucagon. Endocrinology 123:2182–2186
5. Alvarez Pérez JA, González JJ, Baldonedo RF, Sanz L, Carreño G, Junco A, Rodríguez JI, Martínez MaD, Jorge JI (2001) Clinical course, treatment, and multivariate analysis of risk factors for pyogenic liver abscess. Am J Surg 181:177–186
6. Angus DC, Linde-Zwirble WT, Lidicker J, Clermont G, Carcillo J, Pinsky MR (2001) Epidemiology of severe sepsis in the United States: analysis of incidence, outcome, and associated costs of care. Crit Care Med 29:1303–1310
7. Aokage T, Sato N, Kajimoto K, Asai K, Yumino D, Sakata Y, Keida T, Mizuno K, Tanaka K, Takano T (2011) Baseline blood urea nitrogen as a marker for predicting cardiac events in patients hospitalized for acute heart failure syndrome-beyond other renal variables. Eur Heart J 32:126–127
8. Aronson D, Hammerman H, Beyar R, Yalonetsky S, Kapeliovich M, Markiewicz W, Goldberg A (2008) Serum blood urea nitrogen and long-term mortality in acute ST-elevation myocardial infarction. Int J Cardiol 127:380–385
9. Aronson D, Mittleman MA, Burger AJ (2004) Elevated blood urea nitrogen level as a predictor of mortality in patients admitted for decompensated heart failure. Am J Med 116:466–473
10. Atherton J, Spiller R (1994) The urea breath test for *Helicobacter pylori*. Gut 35:723
11. Awad S, Herrod PJ, Palmer R, Carty HM, Abercrombie JF, Brooks A, de Beer T, Mole J, Lobo DN (2012) One- and two-year outcomes and predictors of mortality following emergency laparotomy: a consecutive series from a United Kingdom teaching hospital. World J Surg 36:2060–2067

12. Azar AT, Wahba K, Mohamed AS, Massoud WA (2007) Association between dialysis dose improvement and nutritional status among hemodialysis patients. Am J Nephrol 27:113–119

13. Bacigalupo A, Oneto R, Bruno B, Soracco M, Lamparelli T, Gualandi F, Occhini D, Raiola A, Mordini N, Berisso G (1999) Early predictors of transplant-related mortality (TRM) after allogeneic bone marrow transplants (BMT): blood urea nitrogen (BUN) and bilirubin. Bone Marrow Transplant 24:653–659

14. Bailey SH, Bull DA, Harpole DH, Rentz JJ, Neumayer LA, Pappas TN, Daley J, Henderson WG, Krasnicka B, Khuri SF (2003) Outcomes after esophagectomy: a ten-year prospective cohort. Ann Thorac Surg 75:217–222

15. Bankir L, Yang B (2012) New insights into urea and glucose handling by the kidney, and the urine concentrating mechanism. Kidney Int 81:1179–1198

16. Barber T, Viña J, Viña J, Cabo J (1985) Decreased urea synthesis in cafeteria-diet-induced obesity in the rat. Biochem J 230:675–681

17. Begum L, Jalil MA, Kobayashi K, Iijima M, Li MX, Yasuda T, Horiuchi M, del Arco A, Satrústegui J, Saheki T (2002) Expression of three mitochondrial solute carriers, citrin, aralar1 and ornithine transporter, in relation to urea cycle in mice. Biochim Biophys Acta 1574:283–292

18. Beier K, Eppanapally S, Bazick HS, Chang D, Mahadevappa K, Gibbons FK, Christopher KB (2011) Elevation of blood urea nitrogen is predictive of long-term mortality in critically ill patients independent of "normal" creatinine. Crit Care Med 39:305–313

19. Bihuniak JD, Simpson CA, Sullivan RR, Caseria DM, Kerstetter JE, Insogna KL (2013) Dietary protein-induced increases in urinary calcium are accompanied by similar increases in urinary nitrogen and urinary urea: a controlled clinical trial. J Acad Nutr Diet 113:447–451

20. Bispo JAM, de Sousa Vieira EE, Silveira L, Fernandes AB (2013) Correlating the amount of urea, creatinine, and glucose in urine from patients with diabetes mellitus and hypertension with the risk of developing renal lesions by means of Raman spectroscopy and principal component analysis. J Biomed Opt 18:87004

21. Bjerrum K, Vilstrup H, Almdal T, Ostergaard L (1990) No effect of bicarbonate-induced alkalosis on urea synthesis in normal man. Scand J Clin Lab Invest 50:137–141

22. Blatchford O, Murray WR, Blatchford M (2000) A risk score to predict need for treatment for uppergastrointestinal haemorrhage. Lancet 356:1318–1321

23. Bliss DZ, Stein TP, Schleifer CR, Settle RG (1996) Supplementation with gum arabic fiber increases fecal nitrogen excretion and lowers serum urea nitrogen concentration in chronic renal failure patients consuming a low-protein diet. Am J Clin Nutr 63:392–398

24. van den Boogaard M, Schoonhoven L, Maseda E, Plowright C, Jones C, Luetz A, Sackey PV, Jorens PG, Aitken LM, van Haren FM, Donders R, van der Hoeven JG, Pickkers P (2014) Recalibration of the delirium prediction model for ICU patients (PRE-DELIRIC): a multinational observational study. Intensive Care Med 40:361–369

25. Boon L, Blommaart PJ, Meijer AJ, Lamers WH, Schoolwerth A (1994) Acute acidosis inhibits liver amino acid transport: no primary role for the urea cycle in acid–base balance. Am J Physiol Renal Physiol 267:F1015–F1020

26. Boon L, Blommaart PJ, Meijer AJ, Lamers WH, Schoolwerth AC (1996) Response of hepatic amino acid consumption to chronic metabolic acidosis. Am J Physiol 271:F198–F202

27. Brebnor LD, Grimm J, Balinsky JB (1981) Regulation of urea cycle enzymes in trans-plantable hepatomas and in the livers of tumor-bearing rats and humans. Cancer Res 41:2692–2699

28. Brosnan JT, Brosnan ME (2002) Hepatic glutaminase—a special role in urea synthesis? Nutrition 18:455–457

29. Brown RL, Gibson JA, Fenton JC, Snedden W, Clark ML, Sladen GE (1975) Ammonia and urea transport by the excluded human colon. Clin Sci Mol Med 48:279–287

30. Brzosko S, Szkolka T, Mysliwiec M (2009) Kidney disease is a negative predictor of 30-day survival after acute ischaemic stroke. Nephron Clin Pract 112:c79–c85

31. Carco P, Canciullo D (1958) Urea excretion through the human salivary glands. Ann Otol Rhinol Laryngol 67:1050–1065
32. Cardinali LdCC, Rocha GA, Rocha AMC, de Moura SB, de Figueiredo Soares T, Esteves AMB, Nogueira AMMF, Cabral MMDÁ, de Carvalho AST, Bitencourt P (2003) Evaluation of ^{13}C urea breath test and *Helicobacter pylori* stool antigen test for diagnosis of *H. pylori* infection in children from a developing country. J Clin Microbiol 41:3334–3335
33. Carvounis CP, Nisar S, Guro-Razuman S (2002) Significance of the fractional excretion of urea in the differential diagnosis of acute renal failure. Kidney Int 62:2223–2229
34. Cauthen CA, Lipinski MJ, Abbate A, Appleton D, Nusca A, Varma A, Goudreau E, Cowley MJ, Vetrovec GW (2008) Relation of blood urea nitrogen to long-term mortality in patients with heart failure. Am J Cardiol 101:1643–1647
35. Cauthen CA, Tong M, Wu Y, Jain A, Tang W (2011) Prognostic importance of serial evaluation of blood urea nitrogen in ambulatory patients with chronic systolic heart failure and preserved renal function. J Card Fail 17:S86
36. Cederbaum SD, Shaw KN, Spector EB, Verity MA, Snodgrass PJ, Sugarman GI (1979) Hyperargininemia with arginase deficiency. Pediatr Res 13:827–833
37. Chen CY, Yoshida A, Asakura M, Hasegawa T, Takahama H, Amaki M, Funada A, Asanuma H, Yokoyama H, Kim J, Kanzaki H, Kitakaze M (2012) Serum blood urea nitrogen and plasma brain natriuretic Peptide and low diastolic blood pressure predict cardiovascular morbidity and mortality following discharge in acute decompensated heart failure patients. Circ J 76:2372–2379
38. Chen C-Y, Lin Y-R, Zhao L-L, Yang W-C, Chang Y-J, Wu H-P (2013) Clinical factors in predicting acute renal failure caused by rhabdomyolysis in the ED. Am J Emerg Med 31:1062
39. Chey WD, Wong BC (2007) American College of Gastroenterology guideline on the management of *Helicobacter pylori* infection. Am J Gastroenterol 102:1808–1825
40. Coltart I, Tranah TH, Shawcross DL (2013) Inflammation and hepatic encephalopathy. Arch Biochem Biophys 536:189–196
41. Corbello Pereira SR, Darronqui E, Constantin J, da Silva MHdRA, Yamamoto NS, Bracht A (2004) The urea cycle and related pathways in the liver of Walker-256 tumor-bearing rats. Biochim Biophys Acta 1688:187–196
42. Costell M, O'Connor J-E, Míguez M-P, Grisolía S (1984) Effects of L-carnitine on urea synthesis following acute ammonia intoxication in mice. Biochem Biophys Res Commun 120:726–733
43. Curthoys NP, Watford M (1995) Regulation of glutaminase activity and glutamine metabolism. Annu Rev Nutr 15:133–159
44. Cushny AR (1917) The excretion of urea and sugar by the kidney. J Physiol 51:36–44
45. Davis PK, Wu G (1998) Compartmentation and kinetics of urea cycle enzymes in porcine enterocytes. Comp Biochem Physiol B: Biochem Mol Biol 119:527–537
46. Debongnie J, Pauwels S, Raat A, De Meeus Y, Haot J, Mainguet P (1991) Quantification of *Helicobacter pylori* infection in gastritis and ulcer disease using a simple and rapid carbon-14-urea breath test. J Nucl Med 32:1192–1198
47. Dewitte A, Biais M, Petit L, Cochard J-F, Hilbert G, Combe C, Sztark F (2012) Fractional excretion of urea as a diagnostic index in acute kidney injury in intensive care patients. J Crit Care 27:505–510
48. Dimski DS (1994) Ammonia metabolism and the urea cycle: function and clinical implications. J Vet Intern Med 8:73–78
49. Elewski BE, Haley HR, Robbins CM (2004) The use of 40 % urea cream in the treatment of moccasin tinea pedis. Cutis 73:355–357
50. Emmanuel B (1981) Autoregulation of urea cycle by urea in mammalian species. Comp Biochem Physiol 70A:79–81
51. Esteban-Pretel G, Marín MP, Cabezuelo F, Moreno V, Renau-Piqueras J, Timoneda J, Barber T (2010) Vitamin A deficiency increases protein catabolism and induces urea cycle enzymes in rats. J Nutr 140:792–798

52. Fabjan TH, Hojs R, Tetičkovič E, Balon BP (2007) Ischaemic stroke–impact of renal dysfunction on in-hospital mortality. Eur J Neurol 14:1351–1356

53. Faisst M, Wellner UF, Utzolino S, Hopt UT, Keck T (2010) Elevated blood urea nitrogen is an independent risk factor of prolonged intensive care unit stay due to acute necrotizing pancreatitis. J Crit Care 25:105–111

54. Farnebo S, Zettersten EK, Samuelsson A, Tesselaar E, Sjöberg F (2011) Assessment of blood flow changes in human skin by microdialysis urea clearance. Microcirculation 18:198–204

55. Felker GM, Leimberger JD, Califf RM, Cuffe MS, Massie BM, Adams KF Jr, Gheorghiade M, O'Connor CM (2004) Risk stratification after hospitalization for decompensated heart failure. J Card Fail 10:460–466

56. Fernandez WG, Hung O, Bruno GR, Galea S, Chiang WK (2005) Factors predictive of acute renal failure and need for hemodialysis among ED patients with rhabdomyolysis. Am J Emerg Med 23:1–7

57. Filippatos G, Rossi J, Lloyd-Jones DM, Stough WG, Ouyang J, Shin DD, O'Connor C, Adams KF, Orlandi C, Gheorghiade M (2007) Prognostic value of blood urea nitrogen in patients hospitalized with worsening heart failure: insights from the acute and chronic therapeutic impact of a vasopressin antagonist in chronic heart failure (ACTIV in CHF) study. J Card Fail 13:360–364

58. Fine MJ, Auble TE, Yealy DM, Hanusa BH, Weissfeld LA, Singer DE, Coley CM, Marrie TJ, Kapoor WN (1997) A prediction rule to identify low-risk patients with community-acquired pneumonia. N Engl J Med 336:243–250

59. Fonarow GC, Adams KF Jr, Abraham WT, Yancy CW, Boscardin WJ (2005) Risk stratification for in-hospital mortality in acutely decompensated heart failure. JAMA 293:572–580

60. Ginde AA, Rhee SH, Katz ED (2004) Predictors of outcome in geriatric patients with urinary tract infections. J Emerg Med 27:101–108

61. Greisen J, Grofte T, Hansen PO, Jensen TS, Vilstrup H (1999) Acute non-traumatic pain increases the hepatic amino- to urea-N conversion in normal man. J Hepatol 31:647–655

62. Grofte T, Jensen DS, Gronbaek H, Wolthers T, Jensen SA, Tygstrup N, Vilstrup H (1998) Effects of growth hormone on steroid-induced increase in ability of urea synthesis and urea enzyme mRNA levels. Am J Physiol 275:E79–E86

63. Grofte T, Wolthers T, Jensen SA, Moller N, Jorgensen J, Tygstrup N, Orskov H, Vilstrup H (1997) Effects of growth hormone and insulin-like growth factor-I singly and in combination on in vivo capacity of urea synthesis, gene expression of urea cycle enzymes, and organ nitrogen contents in rats. Hepatology 25:964–969

64. Grofte T, Wolthers T, Jorgensen JO, Poulsen PL, Vilstrup H, Moller N (1999) Hepatic amino- to urea-N clearance and forearm amino-N exchange during hypoglycemic and euglycemic hyperinsulinemia in normal man. J Hepatol 30:819–825

65. Gundpatil DB, Somani BL, Saha TK, Banerjee M (2014) Serum urea: albumin ratio as a prognostic marker in critical patients with non-chronic kidney disease. Indian J Clin Biochem 29:97–100

66. Hamberg O, Andersen V, Sonne J, Larsen S, Vilstrup H (2001) Urea synthesis in patients with chronic pancreatitis: relation to glucagon secretion and dietary protein intake. Clin Nutr 20:493–501

67. Hamberg O, Vilstrup H (1994) Regulation of urea synthesis by glucose and glucagon in normal man. Clin Nutr 13:183–191

68. Hansen BA, Almdal TP, Vilstrup H (1989) Effects of xylitol versus glucose on urea synthesis and alanine metabolism in rats. Clin Nutr 8:109–112

69. Hansen BA, Krog B, Vilstrup H (1986) Insulin and glucose decreases the capacity of urea-N synthesis in the rat. Scand J Clin Lab Invest 46:599–603

70. Hartz AJ, Kuhn EM, Kayser KL, Johnson WD (1995) BUN as a risk factor for mortality after coronary artery bypass grafting. Ann Thorac Surg 60:398–404

71. Havir EA, Tamir H, Ratner S, Warner RC (1965) Biosynthesis of urea XI. Preparation and properties of crystalline argininosuccinase. J Biol Chem 240:3079–3088

72. Hayase K, Yokogoshi H, Yoshida A (1980) Effect of dietary proteins and amino acid deficiencies on urinary excretion of nitrogen and the urea synthesizing system in rats. J Nutr 110:1327–1337

73. Heindorff H, Almdal TP, Vilstrup H (1991) Blockade of glucocorticoid receptors prevents the increase in urea synthesis after hysterectomy in rats. Eur J Clin Invest 21:625–630

74. Heindorff H, Billesbolle P, Pedersen SL, Hansen R, Vilstrup H (1995) Somatostatin prevents the postoperative increases in plasma amino acid clearance and urea synthesis after elective cholecystectomy. Gut 36:766–770

75. Hoberman HD, Havir EA, Rochovansky O, Ratner S (1964) Biosynthesis of urea X. Stereospecificity of the argininosuccinase reaction. J Biol Chem 239:3818–3820

76. Hoppe-Seyler G, Maier K, Schollmeyer P, Frohlich J, Talke H, Gerok W (1975) Studies on urea cycle enzymes in rat liver during acute uraemia. Eur J Clin Invest 5:15–20

77. Huang Y, Xi Q, Xia S, Wang X, Liu Y, Huang C, Zheng W, Yu S (2014) Development and validation of a prognostic scale for hospitalized patients with terminally ill cancer in China. Support Care Cancer 22:145–152

78. Hummel SL, Ghalib HH, Ratz D, Koelling TM (2013) Risk stratification for death and all-cause hospitalization in heart failure clinic outpatients. Am Heart J 166(895–903):e891

79. Husson A, Bouazza M, Buquet C, Vaillant R (1983) Hormonal regulation of two urea-cycle enzymes in cultured foetal hepatocytes. Biochem J 216:281–285

80. Husson A, Bouazza M, Buquet C, Vaillant R (1985) Role of dexamethasone and insulin on the development of the five urea-cycle enzymes in cultured rat foetal hepatocytes. Biochem J 225:271

81. Husson A, Buquet C, Vaillant R (1987) Induction of the five urea-cycle enzymes by glucagon in cultured foetal rat hepatocytes. Differentiation 35:212–218

82. Häussinger D, Kaiser S, Stehle T, Gerok W (1986) Liver carbonic anhydrase and urea synthesis the effect of diuretics. Biochem Pharmacol 35:3317–3322

83. Indiveri C, Tonazzi A, Stipani I, Palmieri F (1997) The purified and reconstituted ornithine/citrulline carrier from rat liver mitochondria: electrical nature and coupling of the exchange reaction with H^+ translocation. Biochem J 327(Pt 2):349–355

84. Ivarsen P, Greisen J, Vilstrup H (2001) Acute effects of moderate dehydration on the hepatic conversion of amino nitrogen into urea nitrogen in healthy men. Clin Sci (Lond) 101:339–344

85. Jassal MS, Nedeltchev GG, Lee J-H, Choi SW, Atudorei V, Sharp ZD, Deretic V, Timmins GS, Bishai WR (2010) ^{13}C-urea breath test as a novel point-of-care biomarker for tuberculosis treatment and diagnosis. PLoS ONE 5:e12451

86. Jensen SA, Almdal TP, Vilstrup H (1991) Acute in vivo effects of low ethanol concentration on the capacity of urea synthesis in rats. Alcohol Clin Exp Res 15:90–93

87. Johnson W, Hagge W, Wagoner R, Dinapoli R, Rosevear J (1972) Effects of urea loading in patients with far-advanced renal failure. Mayo Clin Proc 47:21–29

88. Jorda A, Gomez M, Cabo J, Grisolia S (1982) Effect of streptozotocin diabetes on some urea cycle enzymes. Biochem Biophys Res Commun 106:37–43

89. Jorda A, Portoles M, Guasch R, Bernal D, Saez GT (1989) Effect of caffeine on urea biosynthesis and some related processes, ketone bodies, ATP and liver amino acids. Biochem Pharmacol 38:2727–2732

90. Kafali H, Öksüzler C (2007) Vaginal fluid urea and creatinine in diagnosis of premature rupture of membranes. Arch Gynecol Obstet 275:157–160

91. Kashiwagura T, Erecińska M, Wilson D (1985) pH dependence of hormonal regulation of gluconeogenesis and urea synthesis from glutamine in suspensions of hepatocytes. J Biol Chem 260:407–414

92. Klein L, Massie BM, Leimberger JD, O'Connor CM, Pina IL, Adams KF Jr, Califf RM, Gheorghiade M (2008) Admission or changes in renal function during hospitalization for worsening heart failure predict postdischarge survival: results from the outcomes of a prospective trial of intravenous milrinone for exacerbations of chronic heart failure (OPTIME-CHF). Circ Heart fail 1:25–33

93. Kobayashi K, Sinasac DS, Iijima M, Boright AP, Begum L, Lee JR, Yasuda T, Ikeda S, Hirano R, Terazono H, Crackower MA, Kondo I, Tsui LC, Scherer SW, Saheki T (1999) The gene mutated in adult-onset type II citrullinaemia encodes a putative mitochondrial carrier protein. Nat Genet 22:159–163

94. Kraus VB, Stabler TV, Kong S, Varju G, McDaniel G (2007) Measurement of synovial fluid volume using urea. Osteoarthritis Cartilage 15:1217–1220

95. Krebs HA, Henseleit K (1932) Untersuchungen uber die Harnstoffbildung im Tierkörper. Hoppe-Seyler's Zeitschrift für physiologische Chemie 210:33–66

96. Layton AT, Bankir L (2013) Impacts of active urea secretion into pars recta on urine concentration and urea excretion rate. Physiol Rep 1

97. Lee DS, Austin PC, Rouleau JL, Liu PP, Naimark D, Tu JV (2003) Predicting mortality among patients hospitalized for heart failure. JAMA 290:2581–2587

98. Li Z, Yarmush ML, Chan C (2004) Insulin concentration during preconditioning mediates the regulation of urea synthesis during exposure to amino acid-supplemented plasma. Tissue Eng 10:1737–1746

99. Lim W, Van der Eerden M, Laing R, Boersma W, Karalus N, Town G, Lewis S, Macfarlane J (2003) Defining community acquired pneumonia severity on presentation to hospital: an international derivation and validation study. Thorax 58:377–382

100. Lima HN, Cabral NL, Franklin J, Moro CHC, Pecoits-filho R, Goncalves AR (2012) Age dependent impact of estimated glomerular filtration rate on long-term survival after ischaemic stroke. Nephrology 17:725–732

101. Lin HL, Chen CW, Lu CY, Sun LC, Shih YL, Chuang JF, Huang YH, Sheen MC, Wang JY (2012) High preoperative ratio of blood urea nitrogen to creatinine increased mortality in gastrointestinal cancer patients who developed postoperative enteric fistulas. Kaohsiung J Med Sci 28:418–422

102. Lin LC, Yang JT, Weng HH, Hsiao CT, Lai SL, Fann WC (2011) Predictors of early clinical deterioration after acute ischemic stroke. Am J Emerg Med 29:577–581

103. Listernick R (2013) A 13-year-old boy with elevated BUN and creatinine. Pediatr Ann 42:96–98

104. Liu X, Zhang H, Liang J (2012) Blood urea nitrogen is elevated in patients with non-alcoholic fatty liver disease. Hepatogastroenterology 60:343–345

105. Longo WE, Virgo KS, Johnson FE, Oprian CA, Vernava AM, Wade TP, Phelan MA, Henderson WG, Daley J, Khuri SF (2000) Risk factors for morbidity and mortality after colectomy for colon cancer. Dis Colon Rectum 43:83–91

106. Lundsgaard C, Hamberg O, Thomsen OO, Nielsen OH, Vilstrup H (1996) Increased hepatic urea synthesis in patients with active inflammatory bowel disease. J Hepatol 24:587–593

107. Luria MH, Knoke JD, Margolis RM, Hendricks FH, Kuplic JB (1976) Acute myocardial infarction: prognosis after recovery. Ann Intern Med 85:561–565

108. Lusty C, Ratner S (1972) Biosynthesis of urea XIV. The quaternary structure of argininosuccinase. J Biol Chem 247:7010–7022

109. MacWalter RS, Wong SY, Wong KY, Stewart G, Fraser CG, Fraser HW, Ersoy Y, Ogston SA, Chen R (2002) Does renal dysfunction predict mortality after acute stroke? A 7-year follow-up study. Stroke 33:1630–1635

110. Mackinney-Novelo I, Barahona-Garrido J, Castillo-Albarran F, Santiago-Hernandez JJ, Mendez-Sanchez N, Uribe M, Chavez-Tapia N (2012) Clinical course and management of acute hepatitis A infection in adults. Ann Hepatol 11:652–657

111. Malfertheiner P, Megraud F, O'Morain C, Bazzoli F, El-Omar E, Graham D, Hunt R, Rokkas T, Vakil N, Kuipers EJ (2007) Current concepts in the management of *Helicobacter pylori* infection: the Maastricht III Consensus Report. Gut 56:772–781

112. Manjareeka M, Nanda S (2013) Elevated levels of serum uric acid, creatinine or urea in preeclamptic women. Int J Med Sci Public Health 2:43–47

113. Marchesini G, Zaccheroni V, Brizi M, Natale S, Forlani G, Bianchi G, Baraldi L, Melchionda N (2001) Systemic prostaglandin E1 infusion and hepatic aminonitrogen to urea nitrogen conversion in patients with type 2 diabetes in poor metabolic control. Metabolism 50:253–258

114. Mariz J, Santos NC, Afonso H, Rodrigues P, Faria A, Sousa N, Teixeira J (2013) Risk and clinical-outcome indicators of delirium in an emergency department intermediate care unit (EDIMCU): an observational prospective study. BMC Emerg Med 13:2

115. Marusic M, Majstorovic Barac K, Bilic A, Jurcic D, Gulic S, Grubic Rotkvic P, Bago J (2013) Do gender and age influence the frequency of *Helicobacter pylori* infection? Wien Klin Wochenschr 125:714–716

116. Maswoswe SM, Tremblay GC (1989) Biosynthesis of hippurate, urea and pyrimidines in the fatty liver: studies with rats fed orotic acid or a diet deficient in choline and inositol, and with genetically obese (Zucker) rats. J Nutr 119:273–279

117. Meijer AJ, Lamers WH, Chamuleau R (1990) Nitrogen metabolism and ornithine cycle function. Physiol Rev 70:701–748

118. Michels VV, Beaudet AL (1978) Arginase deficiency in multiple tissues in argininemia. Clin Genet 13:61–67

119. Monroy-Torres R, Naves-Sánchez J, Ortega-García JA (2011) Breastfeeding and metabolic indicators in Mexican premature newborns. Rev Invest Clin 64:521–528

120. Mulrennan S, Tempone SS, Ling ITW, Williams SH, Gan G-C, Murray RJ, Speers DJ (2010) Pandemic influenza (H1N1) 2009 pneumonia: CURB-65 score for predicting severity and nasopharyngeal sampling for diagnosis are unreliable. PLoS ONE 5:e12849

121. Musch W, Verfaillie L, Decaux G (2006) Age-related increase in plasma urea level and decrease in fractional urea excretion: clinical application in the syndrome of inappropriate secretion of antidiuretic hormone. Clin J Am Soc Nephrol 1:909–914

122. Nakano K, Kurimoto S, Ashida K (1971) Effect of previous high fat diet on body protein metabolism in rats. J Nutr 101:895–900

123. Nielsen SS, Grofte T, Gronbaek H, Tygstrup N, Vilstrup H (2007) Opposite effects on regulation of urea synthesis by early and late uraemia in rats. Clin Nutr 26:245–251

124. Nielsen SS, Grofte T, Tygstrup N, Vilstrup H (2005) Effect of lipopolysaccharide on in vivo and genetic regulation of rat urea synthesis. Liver Int 25:177–183

125. Nielsen SS, Grofte T, Tygstrup N, Vilstrup H (2007) Cirrhosis and endotoxin decrease urea synthesis in rats. Hepatol Res 37:540–547

126. Nissim I, Horyn O, Luhovyy B, Lazarow A, Daikhin Y, Yudkoff M (2003) Role of the glutamate dehydrogenase reaction in furnishing aspartate nitrogen for urea synthesis: studies in perfused rat liver with 15 N. Biochem J 376:179–188

127. Nullmann H, Pflug MA, Wesemann T, Heppner HJ, Pientka L, Thiem U (2014) External validation of the CURSI criteria (confusion, urea, respiratory rate and shock index) in adults hospitalised for community-acquired pneumonia. BMC Infect Dis 14:39

128. Núñez J, Núñez E, Miñana G, Bodí V, Fonarow GC, Bertomeu-González V, Palau P, Merlos P, Ventura S, Chorro FJ (2012) Differential mortality association of loop diuretic dosage according to blood urea nitrogen and carbohydrate antigen 125 following a hospitalization for acute heart failure. Eur J Heart Fail 14:974–984

129. Ostfeld R, Spinelli M, Mookherjee D, Holtzman D, Shoyeb A, Schaefer M, Kawano T, Doddamani S, Spevack D, Duc Y (2010) The association of blood urea nitrogen levels and coronary artery disease. Einstein J Biol Med 25:3–7

130. Palmieri L, Pardo B, Lasorsa FM, del Arco A, Kobayashi K, Iijima M, Runswick MJ, Walker JE, Saheki T, Satrustegui J, Palmieri F (2001) Citrin and aralar1 are Ca^{2+}-stimulated aspartate/glutamate transporters in mitochondria. EMBO J 20:5060–5069

131. Pant C, Madonia P, Minocha A, Manas K, Jordan P, Bass P (2010) Laboratory markers as predictors of mortality in patients with *Clostridium difficile* infection. J Investig Med 58:43–45

132. Parsonnet J, Friedman GD, Vandersteen DP, Chang Y, Vogelman JH, Orentreich N, Sibley RK (1991) *Helicobacter pylori* infection and the risk of gastric carcinoma. N Engl J Med 325:1127–1131

133. Pellicori P, Carubelli V, Zhang J, Castiello T, Sherwi N, Clark AL, Cleland JG (2013) IVC diameter in patients with chronic heart failure: relationships and prognostic significance. JACC Cardiovasc Imaging 6:16–28

134. Perri F, Clemente R, Pastore M, Quitadamo M, Festa V, Bisceglia M, Bergoli ML, Lauriola G, Leandro G, Ghoos Y (1998) The ^{13}C-urea breath test as a predictor of intragastric bacterial load and severity of *Helicobacter pylori* gastritis. Scand J Clin Lab Invest 58:19–28

135. Peter F, Wittekindt C, Finkensieper M, Kiehntopf M, Guntinas-Lichius O (2013) Prognostic impact of pretherapeutic laboratory values in head and neck cancer patients. J Cancer Res Clin Oncol 139:171–178

136. Petrack B, Ratner S (1958) Biosynthesis of urea VII. Reversible formation of argininosuccinic acid. J Biol Chem 233:1494–1500

137. Petrak J, Myslivcova D, Man P, Cmejla R, Cmejlova J, Vyoral D, Elleder M, Vulpe CD (2007) Proteomic analysis of hepatic iron overload in mice suggests dysregulation of urea cycle, impairment of fatty acid oxidation, and changes in the methylation cycle. Am J Physiol Gastrointest Liver Physiol 292:G1490–G1498

138. Pigatto P, Bigardi A, Cannistraci C, Picardo M (1996) 10 % urea cream (Laceran) for atopic dermatitis: a clinical and laboratory evaluation. J Dermatolog Treat 7:171–175

139. de Prost N, Mekontso-Dessap A, Valeyrie-Allanore L, Van Nhieu JT, Duong TA, Chosidow O, Wolkenstein P, Brun-Buisson C, Maitre B (2014) Acute respiratory failure in patients with toxic epidermal necrolysis: clinical features and factors associated with mechanical ventilation. Crit Care Med 42:118–128

140. Putaala J, Haapaniemi E, Gordin D, Liebkind R, Groop P-H, Kaste M, Tatlisumak T (2011) Factors associated with impaired kidney function and its impact on long-term outcome in young ischemic stroke. Stroke 42:2459–2464

141. Rabbani P, Prasad AS (1978) Plasma ammonia and liver ornithine transcarbamoylase activity in zinc-deficient rats. Am J Physiol 235:E203–E206

142. Rao GN, Cotlier E (1984) Urea cycle enzymes in retina, ciliary body-iris, lens and senile cataracts. Exp Eye Res 39:483–495

143. Ratner S, Anslow WP, Petrack B (1953) Biosynthesis of urea VI. Enzymatic cleavage of argininosuccinic acid to arginine and fumaric acid. J Biol Chem 204:115–125

144. Ratner S, Pappas A (1949) Biosynthesis of urea I. Enzymatic mechanism of arginine synthesis from citrulline. J Biol Chem 179:1183–1198

145. Ratner S, Pappas A (1949) Biosynthesis of urea II. Arginine synthesis from citrulline in liver homogenates. J Biol Chem 179:1199–1212

146. Ratner S, Petrack B (1951) Biosynthesis of urea III. Further studies on arginine synthesis from citrulline. J Biol Chem 191:693–705

147. Ratner S, Petrack B (1953) Biosynthesis of urea IV. Further studies on condensation in arginine synthesis from citrulline. J Biol Chem 200:161–174

148. Ratner S, Petrack B, Rochovansky O (1953) Biosynthesis of urea V. Isolation and properties of argininosuccinic acid. J Biol Chem 204:95–113

149. Reddi PK, Knox WE, Herzfeld A (1975) Types of arginase in rat tissues. Enzyme 20:305–314

150. Relles DM, Richards NG, Bloom JP, Kennedy EP, Sauter PK, Leiby BE, Rosato EL, Yeo CJ, Berger AC (2013) Serum blood urea nitrogen and serum albumin on the first postoperative day predict pancreatic fistula and major complications after pancreaticoduodenectomy. J Gastrointest Surg 17:326–331

151. Riegel B, Knafl GJ (2013) Electronically monitored medication adherence predicts hospitalization in heart failure patients. Patient Prefer Adherence 8:1–13

152. Robles NR, Felix FJ, Fernandez-Berges D, Perez-Castan J, Zaro MJ, Lozano L, Alvarez-Palacios P, Garcia-Trigo A, Tejero V, Morcillo Y, Hidalgo AB (2013) The HUGE formula (hematocrit, urea and gender): association with cardiovascular risk. Eur Rev Med Pharmacol Sci 17:1889–1893

153. Rochovansky O, Ratner S (1961) Biosynthesis of urea IX. Further studies on mechanism of argininosuccinate synthetase reaction. J Biol Chem 236:2254–2260

154. Rochovansky O, Ratner S (1967) Biosynthesis of urea XII. Further studies on argininosuccinate synthetase: substrate affinity and mechanism of action. J Biol Chem 242:3839–3849

155. Ruiz LA, Zalacain R, Capelastegui A, Bilbao A, Gomez A, Uranga A, Espana PP (2014) Bacteremic pneumococcal pneumonia in elderly and very elderly patients: host- and pathogen-related factors, process of care, and outcome. J Gerontol A Biol Sci Med Sci 69:1018–1024

156. Saheki T, Atsuko U, Hosoya M, Katsunuma T, Ohnishi N, Ozawa A (1980) Comparison of the urea cycle in conventional and germ-free mice. J Biochem 88:1563–1566

157. Salah K, Kok WE, Eurlings LW, Bettencourt P, Pimenta JM, Metra M, Bayes-Genis A, Verdiani V, Bettari L, Lazzarini V, Damman P, Tijssen JG, Pinto YM (2014) A novel discharge risk model for patients hospitalised for acute decompensated heart failure incorporating N-terminal pro-B-type natriuretic peptide levels: a European collaboration on acute decompensated heart failure: ELAN-HF score. Heart 100:115–125

158. Saygitov RT, Glezer MG, Semakina SV (2010) Blood urea nitrogen and creatinine levels at admission for mortality risk assessment in patients with acute coronary syndromes. Emerg Med J 27:105–109

159. Schellekens R, Olsder G, Langenberg S, Boer T, Woerdenbag H, Frijlink H, Kosterink J, Stellaard F (2009) Proof-of-concept study on the suitability of ^{13}C-urea as a marker substance for assessment of in vivo behaviour of oral colon-targeted dosage forms. Br J Pharmacol 158:532–540

160. Schimke RT (1962) Differential effects of fasting and protein-free diets on levels of urea cycle enzymes in rat liver. J Biol Chem 237:1921–1924

161. Schimke RT (1963) Studies on factors affecting the levels of urea cycle enzymes in rat liver. J Biol Chem 238:1012–1018

162. Schmidt-Nielsen B, Sands JA (2001) Urea excretion in white rats and kangaroo rats as influenced by excitement and by diet. J Am Soc Nephrol 12:856–864

163. Schulze IT, Lusty C, Ratner S (1970) Biosynthesis of urea XIII. Dissociation-association kinetics and equilibria of argininosuccinase. J Biol Chem 245:4534–4543

164. Schwartz IL, Thaysen JH, Dole VP (1953) Urea excretion in human sweat as a tracer for movement of water within the secreting gland. J Exp Med 97:429–437

165. See KC, Phua J, Yip HS, Yeo LL, Lim TK (2013) Identification of concurrent bacterial infection in adult patients with dengue. Am J Trop Med Hyg 89:804–810

166. Shambaugh G (1977) Urea biosynthesis I. The urea cycle and relationships to the citric acid cycle. Am J Clin Nutr 30:2083–2087

167. Shemer A, Nathansohn N, Kaplan B, Weiss G, Newman N, Trau H (2000) Treatment of scalp seborrheic dermatitis and psoriasis with an ointment of 40 % urea and 1 % bifonazole. Int J Dermatol 39:532–534

168. Shenkman HJ, Zareba W, Bisognano JD (2007) Comparison of prognostic significance of amino-terminal pro-brain natriuretic peptide versus blood urea nitrogen for predicting events in patients hospitalized for heart failure. Am J Cardiol 99:1143–1145

169. Shoobridge JJ, Bultitude MF, Koukounaras J, Royce PL, Corcoran NM (2013) Predicting surgical exploration in renal trauma: assessment and modification of an established nomogram. J Trauma Acute Care Surg 75:819–823

170. Skala I, Mareckova O, Ruzickova J, Blaha J, Strakova M, Reneltova I, Jirka J, Kocandrle V, Zvolankova K (1978) Urea and ammonia excretion into gastric juice in regularly dialyzed patients and patients after renal transplantation. I Dialyzed patients. Czech Med 1:180–190

171. Slomianski A, Schubert T, Cutler A (1995) ^{13}C Urea breath test to confirm eradication of *Helicobacter pylori*. Am J Gastroenterol 90:224–226

172. Smith GL, Shlipak MG, Havranek EP, Foody JM, Masoudi FA, Rathore SS, Krumholz HM (2006) Serum urea nitrogen, creatinine, and estimators of renal function: mortality in older patients with cardiovascular disease. Arch Intern Med 166:1134

173. Sormani M, Oneto R, Bruno B, Fiorone M, Lamparelli T, Gualandi F, Raiola A, Dominietto A, Van Lint M, Frassoni F (2003) A revised day +7 predictive score for transplant-related mortality: serum cholinesterase, total protein, blood urea nitrogen, gamma glutamyl transferase, donor type and cell dose. Bone Marrow Transplant 32:205–211

174. Spector DA, Yang Q, Wade JB (2007) High urea and creatinine concentrations and urea transporter B in mammalian urinary tract tissues. Am J Physiol Renal Physiol 292:F467–F474

175. Spek JW, Bannink A, Gort G, Hendriks WH, Dijkstra J (2012) Effect of sodium chloride intake on urine volume, urinary urea excretion, and milk urea concentration in lactating dairy cattle. J Dairy Sci 95:7288–7298

176. Stiell IG, Clement CM, Aaron SD, Rowe BH, Perry JJ, Brison RJ, Calder LA, Lang E, Borgundvaag B, Forster AJ, Wells GA (2014) Clinical characteristics associated with adverse events in patients with exacerbation of chronic obstructive pulmonary disease: a prospective cohort study. CMAJ 186:E193–E204

177. Stosovic M, Stanojevic M, Simic-Ogrizovic S, Jovanovic D, Djukanovic L (2009) Relation between serum urea and mortality of hemodialysis patients. Ren Fail 31:335–340

178. Sukasem C, Chamnanphon M, Koomdee N, Santon S, Jantararoungtong T, Prommas S, Puangpetch A, Manosuthi W (2014) Pharmacogenetics and clinical biomarkers for sub-therapeutic plasma efavirenz concentration in HIV-1 infected Thai adults. Drug Metab Pharmacokinet [Epub ahead of print], PMID: 24477223

179. Sułowicz W, Walatek B, Sydor A, Ochmański W, Miłkowski A, Szymczakiewicz-Multanowska A, Szumilak D, Kraśniak A, Lonak H, Wojcikiewicz T (2002) Acute renal failure in patients with rhabdomyolysis. Med Sci Monit 8:CR24

180. Sweileh WM (2008) Predictors of in-hospital mortality after acute stroke: impact of renal dysfunction. Int J Clin Pharmacol Ther 46:637–643

181. Syed TA, Ahmadpour OA, Ahmad SA, Shamsi S (1998) Management of toenail onychomycosis with 2 % butenafine and 20 % urea cream: a placebo-controlled, double-blind study. J Dermatol 25:648–652

182. Testani JM, Cappola TP, Brensinger CM, Shannon RP, Kimmel SE (2011) Interaction between loop diuretic-associated mortality and blood urea nitrogen concentration in chronic heart failure. J Am Coll Cardiol 58:375–382

183. Thaysen JH, Thorn NA (1954) Excretion of urea, sodium, potassium and chloride in human tears. Am J Physiol 178:160–164

184. Thomsen KL, Aagaard NK, Gronbæk H, Holst JJ, Jessen N, Frystyk J, Vilstrup H (2011) IL-6 has no acute effect on the regulation of urea synthesis in vivo in rats. Scand J Clin Lab Invest 71:150–156

185. Thomsen KL, Jessen N, Moller AB, Aagaard NK, Gronbaek H, Holst JJ, Vilstrup H (2013) Regulation of urea synthesis during the acute-phase response in rats. Am J Physiol Gastrointest Liver Physiol 304:G680–G686

186. Tomomura M, Tomomura A, Musa DAA, Horiuchi M, Takiguchi M, Mori M, Saheki T (1997) Suppressed expression of the urea cycle enzyme genes in the liver of carnitine-deficient juvenile visceral steatosis (JVS) mice in infancy and during starvation in adulthood. J Biochem 121:172–177

187. Traynor J, Mactier R, Geddes CC, Fox JG (2006) How to measure renal function in clinical practice. BMJ 333:733

188. Tsagalis G, Akrivos T, Alevizaki M, Manios E, Stamatellopoulos K, Laggouranis A, Vemmos KN (2009) Renal dysfunction in acute stroke: an independent predictor of long-term all combined vascular events and overall mortality. Nephrol Dial Transplant 24:194–200

189. Tuncel A, Keten T, Aslan Y, Kayali M, Erkan A, Koseoglu E, Atan A (2014) Comparison of different scoring systems for outcome prediction in patients with Fournier's gangrene: Experience with 50 patients. Scand J Urol 48:393–399

190. Ueda T, Takeyama Y, Yasuda T, Matsumura N, Sawa H, Nakajima T, Ajiki T, Fujino Y, Suzuki Y, Kuroda Y (2007) Simple scoring system for the prediction of the prognosis of severe acute pancreatitis. Surgery 141:51–58

191. Ugarte G, Pino ME, Valenzuela J, Lorca F (1963) Urea cycle enzymatic abnormalities in patients in endogenous hepatic coma. Gastroenterology 45:182–188

192. Valente MA, Voors AA, Damman K, Van Veldhuisen DJ, Massie BM, O'Connor CM, Metra M, Ponikowski P, Teerlink JR, Cotter G, Davison B, Cleland JG, Givertz MM, Bloomfield DM, Fiuzat M, Dittrich HC, Hillege HL (2014) Diuretic response in acute heart failure: clinical characteristics and prognostic significance. Eur Heart J 35:1284–1293

193. Valtin H (1966) Sequestration of urea and nonurea solutes in renal tissues of rats with hereditary hypothalamic diabetes insipidus: effect of vasopressin and dehydration on the countercurrent mechanism. J Clin Invest 45:337–345

194. Vandenplas Y, Blecker U, Devreker T, Keppens E, Nijs J, Cadranel S, Pipeleers-Marichal M, Goossens A, Lauwers S (1992) Contribution of the ^{13}C-urea breath test to the detection of *Helicobacter pylori* gastritis in children. Pediatrics 90:608–611

195. Vilstrup H (1980) Synthesis of urea after stimulation with amino acids: relation to liver function. Gut 21:990–995

196. Vilstrup H, Hansen BA, Almdal TP (1990) Glucagon increases hepatic efficacy for urea synthesis. J Hepatol 10:46–50

197. Waikar SS, Bonventre JV (2006) Can we rely on blood urea nitrogen as a biomarker to determine when to initiate dialysis? Clin J Am Soc Nephrol 1:903–904

198. Walid M (2008) Blood urea nitrogen/creatinine ratio in rhabdomyolysis. Indian J Nephrol 18:173

199. Walters M, Wallace K (2010) Urea cycle gene expression is suppressed by PFOA treatment in rats. Toxicol Lett 197:46–50

200. Waring W, Stephen A, Robinson O, Dow M, Pettie J (2008) Serum urea concentration and the risk of hepatotoxicity after paracetamol overdose. QJM 101:359–363

201. Warren JR (2006) Helicobacter: the ease and difficulty of a new discovery (nobel lecture). ChemMedChem 1:672–685

202. Watford M (1993) Hepatic glutaminase expression: relationship to kidney-type glutaminase and to the urea cycle. FASEB J 7:1468–1474

203. Wilson AH, Kidd AC, Skinner J, Musonda P, Pai Y, Lunt CJ, Butchart C, Soiza RL, Potter JF, Myint PK (2014) A simple 5-point scoring system, NaURSE (Na$^+$, Urea, Respiratory Rate and Shock Index in the Elderly), predicts in-hospital mortality in oldest old. Age Ageing 43:352–357

204. Winter JM, Cameron JL, Yeo CJ, Alao B, Lillemoe KD, Campbell KA, Schulick RD (2007) Biochemical markers predict morbidity and mortality after pancreaticoduodenectomy. J Am Coll Surg 204:1029–1036

205. Wlodzimirow KA, Abu-Hanna A, Royakkers AA, Spronk PE, Hofstra LS, Kuiper MA, Schultz MJ, Bouman CS (2014) Transient versus persistent acute kidney injury and the diagnostic performance of fractional excretion of urea in critically Ill patients. Nephron Clin Pract 126:8–13

206. Wolthers T, Grofte T, Jorgensen JO, Vilstrup H (1997) Growth hormone prevents prednisolone-induced increase in functional hepatic nitrogen clearance in normal man. J Hepatol 27:789–795

207. Wolthers T, Hamberg O, Grofte T, Vilstrup H (2000) Effects of budesonide and prednisolone on hepatic kinetics for urea synthesis. J Hepatol 33:549–554

208. Wright FC, Chakraborty A, Helyer L, Moravan V, Selby D (2010) Predictors of survival in patients with non-curative stage IV cancer and malignant bowel obstruction. J Surg Oncol 101:425–429

209. Wu BU, Bakker OJ, Papachristou GI, Besselink MG, Repas K, van Santvoort HC, Muddana V, Singh VK, Whitcomb DC, Gooszen HG, Banks PA (2011) Blood urea nitrogen in the early assessment of acute pancreatitis: an international validation study. Arch Intern Med 171:669–676

210. Wu BU, Johannes RS, Sun X, Conwell DL, Banks PA (2009) Early changes in blood urea nitrogen predict mortality in acute pancreatitis. Gastroenterology 137:129–135

211. Wu G, Meininger CJ (1993) Regulation of L-arginine synthesis from L-citrulline by L-glutamine in endothelial cells. Am J Physiol 265:H1965–H1971

212. Yahalom G, Schwartz R, Schwammenthal Y, Merzeliak O, Toashi M, Orion D, Sela B-A, Tanne D (2009) Chronic kidney disease and clinical outcome in patients with acute stroke. Stroke 40:1296–1303
213. Yamada M, Kubo H, Ishizawa K, Kobayashi S, Shinkawa M, Sasaki H (2005) Increased circulating endothelial progenitor cells in patients with bacterial pneumonia: evidence that bone marrow derived cells contribute to lung repair. Thorax 60:410–413
214. Yancy CW, Lopatin M, Stevenson LW, De Marco T, Fonarow GC (2006) Clinical presentation, management, and in-hospital outcomes of patients admitted with acute decompensated heart failure with preserved systolic functionA report from the acute decompensated heart failure national registry (ADHERE) database. J Am Coll Cardiol 47:76–84
215. Yang B, Bankir L (2005) Urea and urine concentrating ability: new insights from studies in mice. Am J Physiol Renal Physiol 288:F881–F896
216. Yassuda Filho P, Bracht A, Ishii-Iwamoto EL, Lousano SH, Bracht L, Kelmer-Bracht AM (2003) The urea cycle in the liver of arthritic rats. Mol Cell Biochem 243:97–106
217. Young VR, El-Khoury AE, Raguso CA, Forslund AH, Hambraeus L (2000) Rates of urea production and hydrolysis and leucine oxidation change linearly over widely varying protein intakes in healthy adults. J Nutr 130:761–766
218. Zar T, Kohn OF, Kaplan AA (2011) Fractional excretion of urea in pre-eclampsia. Iran J Kidney Dis 5:398–403
219. Zevit N, Niv Y, Shirin H, Shamir R (2011) Age and gender differences in urea breath test results. Eur J Clin Invest 41:767–772
220. Zhang Y, Churilov L, Meretoja A, Teo S, Davis SM, Yan B (2013) Elevated urea level is associated with poor clinical outcome and increased mortality post intravenous tissue plasminogen activator in stroke patients. J Neurol Sci 332:110–115

Chapter 3
Mathematical Modeling of Urea Transport in the Kidney

Anita T. Layton

Abstract Mathematical modeling techniques have been useful in providing insights into biological systems, including the kidney. This article considers some of the mathematical models that concern urea transport in the kidney. Modeling simulations have been conducted to investigate, in the context of urea cycling and urine concentration, the effects of hypothetical active urea secretion into pars recta. Simulation results suggest that active urea secretion induces a "urea-selective" improvement in urine concentrating ability. Mathematical models have also been built to study the implications of the highly structured organization of tubules and vessels in the renal medulla on urea sequestration and cycling. The goal of this article is to show how physiological problems can be formulated and studied mathematically, and how such models may provide insights into renal functions.

Keywords Mathematical modeling · Urea · Urea transportation · Urine concentrating mechanism

Introduction

There has been a long history of interaction between mathematics and physiology. In renal physiology, mathematical modeling techniques have been used to attain a better understanding of renal hemodynamics [1–25], renal oxygenation [26–33], epithelial transport [34–49], and urine concentrating mechanism [50–67]. Given the essential role that urea plays in the urine concentration process, mathematical models of the urine concentrating mechanism requires the representation of urea transport in the renal medulla, a subject that is the focus of this chapter.

A.T. Layton (✉)
Department of Mathematics, Duke University, Durham, NC, USA
e-mail: alayton@math.duke.edu

Fig. 3.1 Schematic drawing for model renal tubule, illustrating water flow (F_V), water flux (J_V), and solute flux (J_S)
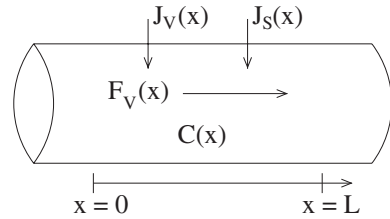
Modeling Water and Urea Conservation

The first step in constructing a model for urea transport is to represent water and urea flows along a renal tubule. To that end, we will derive equations that model tubular flow and transmural fluxes along a renal tubule.

   We will derive model equations that describe the conservation of water and urea along a renal tubule, which extends from $x = 0$ to $x = L$, as shown in Fig. 3.1. First, we will consider water transport along the tubule. For simplicity, we assume that the tubule is rigid. Technically speaking, tubular walls are comprised of cells that are, to some extent, flexible. However, the structures surrounding the tubules in vivo likely reduce that degree of compliance, which makes the rigid-wall assumption reasonable. (One instance in which this rigid-tubule assumption is violated is the papillary collecting duct undergoing peristaltic contractions, where the collecting duct is collapsed for up to 95 % of the time [68].) In most cases, it is also reasonable to describe the flow in the tubules as plug flow (i.e., flow with no radial component and constant velocity across any cross section). With this assumption, the problem can be formulated using only one spatial dimension (x).

Water Conservation

To derive a differential equation that describes water conservation along the tubule, consider the tubular segment in Fig. 3.1. Assume a tubule radius of r. Because water is effectively incompressible, the change in water flow rate must equal the sum of the water flux out of (or into) the tubule through its walls between $x = 0$ and $x = L$. Following this reasoning, we can relate the outflow to the inflow and total water flux by

$$F_V(L) = F_V(0) + 2\pi r \int_0^L J_V(x)dx, \tag{3.1}$$

where $F_V(x)$ denotes the volume flow rate along the tubule, typically with units of nl/min for renal tubules, and $J_V(x)$ denotes water flux through the tubular walls, taken positive into the tubule. We use the notation that J_V is computed at a point

along the circumference of the tubule, which necessitates the multiplication by the factor $2\pi r$. Equation (3.1) can be rewritten as a differential equation

$$\frac{\partial}{\partial x}F_V(x) = 2\pi r J_V(x).$$

(3.2)

Water can be driven through a cell membrane by hydrostatic pressure, oncotic pressure, or osmotic pressure. To derive the equation that describes water flux across a renal tubule, we make another simplifying assumption, which is that water transport across tubular walls can be represented as single-barrier transport. We make the same assumption in our description of solute fluxes below as well. Given this assumption, water flux into a renal tubule in Fig. 3.1 can be described by

$$J_V(x) = L_p RT \sum_k \sigma_k \big(C_k(x) - C_k^e(x)\big),$$

(3.3)

where L_p is the water permeability of the tubule, σ_k is the osmotic coefficient of solute, k, C_k is the luminal concentration of that solute, and $C_k^e(x)$ is the interstitial (i.e., external) solute concentration of that solute. Oncotic and hydrostatic pressures are assumed negligible.

Urea Conservation

Next, we will derive a differential equation to describe the conservation of urea along the tubule. The flow rate of urea at position x is given by the product of its concentration $C(x)$ and the flow rate of water $F_V(x)$, i.e., $F_V(x)C(x)$. Let the amount of urea transported inward through the tubule walls at x (given per unit area per unit time) be denoted by $J_S(x)$. Then, following an approach similar to what we used to derive the water conservation Eq. (3.2), we describe urea conservation along the renal tubule by

$$\frac{\partial}{\partial x}(F_V(x)C(x)) = 2\pi r J_S(x).$$

(3.4)

It is noteworthy that the urea conservation Eq. (3.4) is general and can be applied to all types of renal tubules and indeed applies to other solutes such as NaCl or protein. The water conservation Eq. (3.2) also applies to many biological tubules, renal, or otherwise. Of course, tubules in the kidney differ widely in their transport properties, and those differences are reflected in the flux terms J_V and J_S.

Modeling Urea Fluxes

Transepithelial urea transport can proceed via transcellular and/or paracellular pathways. Solutes moving across the paracellular route must traverse through tight junctions. Transcellular transport can be passive or active. Passive transport by definition does not require energy, as opposed to active transport.

Modeling Passive Fluxes

We will first describe how to represent passive urea fluxes, which include paracellular fluxes and passive transcellular fluxes. In passive transport, the flux goes in the direction that reduces the Gibbs free energy of the system. In open systems at constant temperature and pressure, the change in the Gibbs free energy is proportional to the change in the electrochemical potentials of the system components. Because urea is uncharged, its flux is described by the Kedem–Katchalsky equation [69]

$$J_S = J_V(1 - \sigma)\bar{C} + P\Delta C, \tag{3.5}$$

where the first term represents the contribution from advection, s denotes the reflective coefficient of urea, and $\bar{C}$ is an average membrane concentration, which in dilute solution is given by

$$\bar{C} = \frac{\Delta C}{\Delta \ln C}. \tag{3.6}$$

The second term in Eq. (3.5) arises from diffusion, characterized by P, which denotes the permeability of the membrane to urea.

Modeling Active Fluxes

Some nephron segments contain transporters that can reabsorb or secret solutes against a transmembrane electrochemical gradient. The best-known example is perhaps the Na^+/K^+-ATPase, which is an antiporter enzyme that can pump sodium out of and potassium into the cells. Na^+/K^+-ATPase is responsible for the active reabsorption of NaCl along the thick ascending limb segments.

The active reabsorption of a solute can be modeled by the Michaelis–Menten kinetics, which is a simple biochemical model of enzyme kinetics. Given the luminal concentration C, the active solute flux is

$$J_S = -\frac{V_{\max}C}{K_m + C}. \tag{3.7}$$

Here, $V_{\max}$ represents the maximum rate achieved by the system, at maximum (saturating) substrate concentrations. The Michaelis constant K_m is the substrate concentration at which the reaction rate is half of $V_{\max}$.

While several nephron segments are known to actively reabsorb salt, no significant active urea reabsorption has been reported. Nonetheless, Bankir and colleagues [70] recently reviewed a number of observations, in different species including humans, that suggest the existence of active urea *secretion* that probably takes place in the S3 segment of the straight proximal tubule in the deep cortex and the outer stripe of the outer medulla. Those authors have suggested that, by extracting urea from the medullary vasculature, active secretion delivers urea in the nephron lumen in addition to the previously filtered urea that is delivered to the inner medulla through the terminal collecting duct and recycled by countercurrent exchange. This active secretion
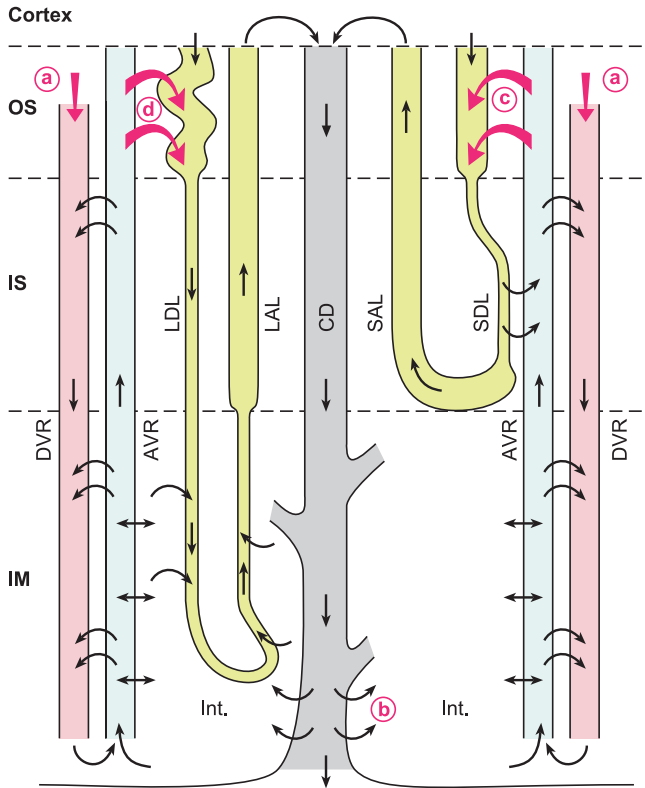
Fig. 3.2 Schematic representation of the fate of urea secreted in the pars recta. A short-looped and a long-looped nephron are represented, as well as two descending and ascending vasa recta (*DVR* and *AVR*, respectively). Not shown here: the DVRs in the outer stripe (*OS*) are main branches of the efferent arterioles of the deep glomeruli and have only limited surface area for contact with the AVR. In contrast, in the inner stripe (*IS*), DVRs and AVRs are closely packed in vascular bundles, a configuration that increases contact area and favors countercurrent exchanges. DVRs bring into the medulla plasma that has not been filtered and that contains urea (**a**). Note that DVRs express UT-B and AVRs are fenestrated. This allows very rapid and efficient exchanges between both structures. In rodents, the short descending limbs (*SDL*) in the IS are close to the vascular bundles (rat) or are even incorporated among the AVRs and DVRs, forming so-called complex vascular bundles. IM segments of long loops are assumed to have high urea permeabilities, consistent with preliminary data in rat (Pannabecker and Dantzler, personal communication). The present model assumes that urea is actively secreted in the pars recta of both short-looped (**c**) and long-looped (**d**) nephrons. Some of this urea can be added to the urea that cycles in the renal medulla, brought to the interstitium via the terminal IMCD (**b**). This improves the ability to accumulate urea in the deep IM and to selectively concentrate urea in the urine. Abbreviations: LDL/LAL, long descending/ascending limb; SAL, short ascending limb; CD, collecting duct; IM, inner medulla; and Int. interstitium. Reprinted from Ref. [55]

may account for the difference between the urea flow remaining in the late superficial proximal convoluted tubule and the urea flow observed in the early distal tubule, as well as for fractional excretion of urea exceeding 50 % [70]. A schematic representation of the urea cycle with active urea secretion into the pars recta is shown in Fig. 3.2.

Table 3.1 A comparison of model predictions with and without active urea secretion

Urine		Without urea secretion	With urea secretion	Difference (%)
Urine composition				
Osmolality	(mosm/(kg · H$_2$O))	1,077	1,195	+11.0
U$_{urea}$	(mM)	388	591	+52.3
U$_{Na}$	(mM)	298	251	−15.8
U$_{NR}$	(mM)	82.3	87.2	−6.0
Excretion rates				
Flow rate	(nl/(min · nephron))	0.0854	0.0863	+1.1
Osmole	(pmol/(min · nephron))	92	103	+12.0
Urea	(pmol/(min · nephron))	33	51	+54.5
Na$^+$	(pmol/(min · nephron))	25	22	−11.9
NR	(pmol/(min · nephron))	7.03	7.53	+7.11

Differences in model predictions are given as percentage of values computed without active urea secretion

To represent urea secretion, transmural urea flux is computed based on interstitial concentration C_e rather than luminal concentration C:

$$J_S = \frac{V\text{max}\,C_e}{K_m + C_e}.$$ (8)

Layton and Bankir [55] used a mathematical model of the renal medulla of the rat kidney to investigate the impact of active urea secretion in the intrarenal handling of urea and in the urine concentrating ability. They compared urea flow rates and other related model variables without and with the hypothetical active urea secretion in the pars recta. Key simulation results are summarized in Table 3.1. The two models (with and without active urea secretion) predicted similarly concentrated urines (1,077 vs. 1,195 mosm/(kg·H$_2$O)). The major difference is found in urea excretion, where the model with active urea secretion did so at a rate that is 52.3 % higher. That result is particularly noteworthy in that the higher urea excretion rate was achieved with only minimal increase in urine flow (1.1 % increase). These simulations suggest that active urea secretion induces a "urea-selective" improvement in urine concentrating ability by enhancing the efficiency of urea excretion without requiring a higher urine flow rate and with only modest changes in the excretion of other solutes.

Modeling Urea Sequestration

Anatomic studies have revealed a highly structured organization of tubules and vasa recta in the outer medulla of some mammalian kidneys [71, 72], with tubules and vessels organized concentrically around vascular bundles, tightly packed clusters of parallel vessels and tubules containing mostly vasa recta. Recent studies of three-dimensional architecture of rat inner medulla and expression of membrane proteins

associated with fluid and solute transport in nephrons and vasculature have revealed transport and structural properties that likely impact the inner medullary urine concentrating mechanism in the rat kidney. These studies have shown that the inner medulla portion of the descending limbs has at least two or three functionally distinct subsegments and that clusters of collecting ducts form the organizing motif through the first 3–3.5 mm of the inner medulla [73–75]. The structural organization is believed to result in preferential interactions among tubules and vasa recta, interactions that may contribute to more efficient countercurrent exchange or multiplication, to urea cycling and urea accumulation in the inner medulla, and to sequestration of urea or NaCl in particular tubular or vascular segments [63, 65, 71, 72, 76–79]. (We will say that a solute is "sequestered" when its fractional contribution to local fluid osmolality substantially exceeds its fractional contribution to blood plasma osmolality.)

Several investigators have sought to represent aspects of three-dimensional medullary structure in mathematical models of the urine concentrating mechanism (e.g., Ref. [80, 81]). Notably, Wexler, Kalaba, and Marsh [63, 82] developed a model (the "WKM" model) that represented a very substantial degree of structural organization by means of weighted connections between tubules and vessels. Although the WKM model was formulated primarily to investigate the concentrating mechanism of the inner medulla, outer medullary function played a large role in both the original [63] and subsequent WKM studies [65, 83].

More recently, Layton and co-workers developed highly detailed mathematical models for the rat kidney's concentrating mechanism. Their models represent radial organization with respect to a vascular bundle in the outer medulla, or a collecting duct cluster in the inner medulla, by means of "interconnected regions" (see Fig. 3.3), with radial structure incorporated by assigning appropriate tubules and vasa recta to each region. The portion of each interconnected region that is exterior to both tubules and vasa recta represents merged capillaries, interstitial cells, and interstitial space. At a given medullary level, each interconnected region is assumed to be a well-mixed compartment with which tubules and vasa recta interact. To specify the relative positions or distributions of the tubules and vasa recta and to simulate the potential preferential interactions among them, each tubule or vas rectum is assigned to a particular concentric region, or, in some cases, fractions of a tubule or vas rectum are distributed to two interconnected regions. Tubules and vasa recta that are in contact with different interconnected regions are influenced by differing interstitial environments. However, tubules or vasa recta that do not contact the same region may still interact via interstitial diffusion of solutes around tubules and vasa recta; these diffusive fluxes are simulated by assigning nonzero solute permeabilities to the boundaries that separate adjacent regions.

To specify the relative positions of the tubules and vessels, each tubule or vessel i is assigned a series of parameter $\kappa_{i,R}$, for $R = R1, R2, \ldots, R7$, where $\kappa_{i,R}$ is the fraction of the tubule in contact with region R. Thus, these parameters must satisfy the condition $\sum_R \kappa_{i,R} = 1$. For example, according to the configuration shown in Fig. 3.3, in the inner stripe, the position of the collecting duct is specified by $\kappa_{CD,R4} = 1$ and $\kappa_{CD,R} = 0$ for $R \neq R4$; the position of the short ascending limb, which straddles the two interbundle regions R3 and R4, is specified by $\kappa_{SAL,R3} = 0.25$ and $\kappa_{SAL,R4} = 0.75$, and $\kappa_{SAL,R} = 0$ for $R \neq R3$ or R4.
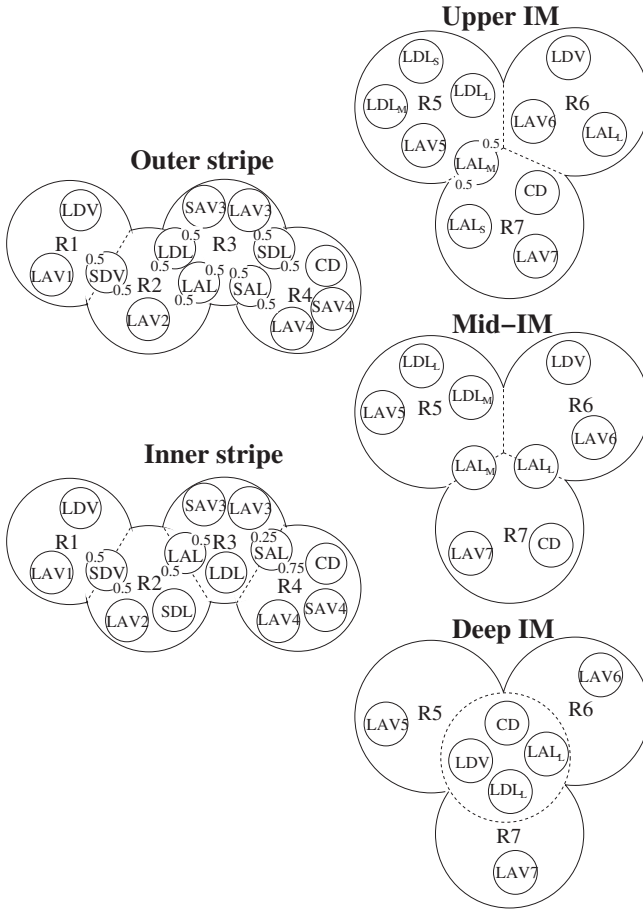
Fig. 3.3 Schematic diagram of a cross section through the outer stripe, inner stripe, upper inner medulla (*IM*), mid-IM, and deep IM, showing regions and relative positions of tubules and vessels. Decimal numbers in panel A indicate relative interaction weightings with regions. R1, R2, R3, and R4, regions in the outer medulla; R5, R6, and R7, regions in the IM. SDL, descending limbs of short loops of Henle. SAL, ascending limbs of long loops of Henle. LDL, descending limb of long loop of Henle. LAL, ascending limb of long loop of Henle. Subscripts "S," "M," and "L" associated with a LDL or LAL denote limbs that turn with the first mm of the IM (S), within the mid-IM (M), or reach into the deep IM (L). CD, collecting duct. SDV, short descending vasa recta. SAV3 and SAV4, two populations of short ascending vasa recta. LDV, long descending vas rectum. LAV1, LAV2, ..., LAV7, populations of long ascending vasa recta. Reprinted from Ref. [59]

To compute urea fluxes, the model takes into account the position of the tubule or vessel. Passive urea flux is given by a weighed average of the fluxes with each region:

$$J_S = \sum_R \kappa_R (J_{V,R}(1 - \sigma)\bar{C}_R + P(C_R - C)), \tag{3.9}$$

Fig. 3.4 Interstitial fluid
urea concentration profiles
in the different regions,
predicted by the region-based
model in Ref. [60]
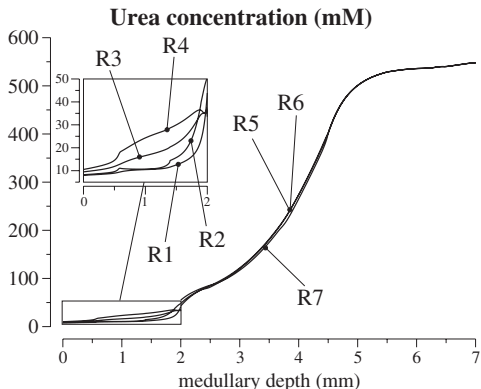
where $J_{V,R}$ denotes the water fluxes between the tubule or vessel and region R, and C_R denotes interstitial fluid urea concentration in region R. The average membrane concentration $\bar{C}_R$ is taken between the luminal concentration and the interstitial concentration of region R, i.e.,

$$\bar{C}_R = \frac{C_R - C}{\ln C_R - \ln C}. \tag{3.10}$$

This "region-based" approach was used to first develop a model of the rat outer medulla [56, 57, 84] and then used in a series of models of the rat renal medulla [58–60]. These models predicted moderately concentrated urine at flow rates consistent with experimental measurements, but were unable to predict highly concentrated urine. Urea cycling is predicted within the vascular bundles in the inner stripe between the descending and ascending vasa recta that reach into the inner medulla, but inter-region urea concentration exhibits only a small radial gradient in the inner medulla; see Fig. 3.4.

Conclusions

Mathematical modeling is a useful tool for understanding the underlying mechanisms of an observed physiological phenomenon, or for investigating "what-if" scenarios. In particular, modeling studies have suggested that the three-dimensional architecture of the renal medulla leads to preferential interactions among tubules and vessels, which in turn give rise to sequestration of urea. By incorporating a hypothetical active urea secretion process into a mathematical model of the urine concentrating mechanism, we obtained simulation results that suggest that active urea secretion in the pars recta of the proximal tubule may allow more efficient excretion of urea with negligible impact on the amount of water required for that excretion. While further progress may be contingent upon new experimental data, especially on the transport properties of the tubules, some of which remain poorly characterized, we nonetheless hope these "in silico" results will stimulate further experimental research.

References

1. Chang R, Robertson C, Deen W, Brenner B (1975) Permselectivity of the glomerular capillary wall to macromolecules. I. Theoretical considerations. Biophys J 15:861–886
2. Deen W, Robertson C, Brenner B (1972) A model of glomerular ultrafiltration in the rat. Am J Physiol 223(5):1178–1183
3. Deen W, Bridges C, Brenner B, Myers B (1985) Heteroporous model of glomerular size selectivity: application to normal and nephrotic humans. Am J Physiol Renal Physiol 249:F374–F389
4. Deen W, Lazzara M, Myers B (2001) Structural determinants of glomerular permeability. Am J Physiol Renal Physiol 281:F579–F596
5. Drumond M, Deen W (1994) Structural determinants of glomerular hydraulic permeability. Am J Physiol Renal Physiol 266:F1–F12
6. Edwards A, Layton A (2013) Calcium dynamics underlying the afferent arteriole myogenic response. Am J Physiol Renal Physiol (in press)
7. Edwards A, Daniels B, Deen W (1997) Hindered transport of macromolecules in isolated glomeruli. II. Convection and pressure effects in basement membrane. Biophys J 72:214–222
8. Edwards A, Daniels B, Deen W (1999) Ultrastructural model for size selectivity in glomerular filtration. Am J Physiol Renal Physiol 276:F892–F902
9. Guasch A, Deen W, Brenner B (1993) Charge selectivity of the glomerular filtration barrier in healthy and nephrotic humans. J Clin Invest 92:2274–2282
10. Holstein-Rathlou N, Marsh D (1990) A dynamic model of the tubuloglomerular feedback mechanism. Am J Physiol (Renal Fluid Electrolyte Physiol 27) 258:F1448–F1459
11. Layton A (2010) Feedback-mediated dynamics in a model of a compliant thick ascending limb. Math Biosci 228:185–194
12. Layton A, Moore L, Layton H (2006) Multistability in tubuloglomerular feedback and spectral complexity in spontaneously hypertensive rats. Am J Physiol Renal Physiol 291:F79–F97
13. Layton A, Moore L, Layton H (2009) Multistable dynamics mediated by tubuloglomerular feedback in a model of coupled nephrons. Bull Math Biol 71:515–555
14. Layton A, Moore L, Layton H (2009) Tubuloglomerular feedback signal transduction in a compliant thick ascending limb. Am J Physiol Renal Physiol, submitted
15. Layton A, Pham P, Ryu H (2012) Signal transduction in a compliant short loop of Henle. Int J Numer Methods Biomed Eng 28(3):369–380
16. Layton H, Pitman E, Moore L (1991) Bifurcation analysis of TGF-mediated oscillations in SNGFR. Am J Physiol (Renal Fluid Electrolyte Physiol 30) 261:F904–F919
17. Layton H, Pitman E, Moore L (1995) Instantaneous and steady-state gains in the tubuloglomerular feedback system. Am J Physiol Renal Physiol 268:F163–F174
18. Layton H, Pitman E, Moore L (1997a) Nonlinear filter properties of the thick ascending limb. Am J Physiol (Renal Fluid Electrolyte Physiol 42) 273:F625–F634
19. Layton H, Pitman E, Moore L (1997b) Spectral properties of the tubuloglomerular feedback system. Am J Physiol (Renal Fluid Electrolyte Physiol 42) 273:F635–F649
20. Marsh D, Sosnovtseva O, Chon K, Holstein-Rathlou N (2005) Nonlinear interactions in renal blood flow regulation. Am J Physiol Regul Integr Comp Physiol 288:R1143–R1159
21. Marsh D, Sosnovtseva O, Mosekilde E, Rathlou NH (2007) Vascular coupling induces synchronization, quasiperiodicity, and chaos in a nephron tree. Chaos 17:015,114–1—015,114–10
22. Ryu H, Layton A (2012) Effect of tubular inhomogeneities on feedback-mediated dynamics of a model of a thick ascending limb. Med Math Biol (in press)

23. Ryu H, Layton A (2012) Tubular fluid flow and distal nacl delivery mediated by tubuloglomerular feedback in the rat kidney. J Math Biol (in press)
24. Sgouralis I, Layton A (2012) Autoregulation and conduction of vasomotor responses in a mathematical model of the rat afferent arteriole. Am J Physiol Renal Physiol 33:F229–F239
25. Sgouralis I, Layton A (2013) Control and modulation of fluid flow in the rat kidney. Bull Math Biol, (in press)
26. Chen J, Layton A, Edwards A (2009) A mathematical model of oxygen transport in the rat outer medulla: I. model formulation and baseline results. Am J Physiol Renal Physiol 297:F517–F536
27. Chen J, Edwards A, Layton A (2009) A mathematical model of oxygen transport in the rat outer medulla: II. impacts of outer medullary architecture. Am J Physiol Renal Physiol 297:F537–F548
28. Chen J, Edwards A, Layton A (2009 a) Effects of pH and medullary blood flow on oxygen transport and sodium reabsorption in the rat outer medulla. Am J Physiol Renal Physiol, submitted
29. Edwards A, Layton A (2009) Nitric oxide and superoxide transport in a cross-section of the rat outer medulla. II. Reciprocal interactions and tubulo-vascular cross-talk. Am J Physiol Renal Physiol 299:F634–F647
30. Edwards A, Layton A (2010) Nitric oxide and superoxide transport in a cross-section of the rat outer medulla. I. Effects of low medullary oxygen tension. Am J Physiol Renal Physiol 299:F616–F633
31. Edwards A, Layton A (2012) Impacts of nitric oxide-mediated vasodilation on outer medullary NaCl transport and oxygenation. Am J Physiol Renal Physiol (in press)
32. Gardiner B, Smith D, O'Connor P, R RE (2011) A mathematical model of diffusional shunting of oxygen from arteries to veins in the kidney. Am J Physiol Renal Physiol 300:F1339–F1352
33. Gardiner B, Thompson S, Ngo J, Smith D, Abdelkader A, Broughton B, Bertram J, Evans R (2012) Diffusive oxygen shunting between vessels in the preglomerular renal vasculature: anatomic observations and computational modeling. Am J Physiol Renal Physiol 303:F605–F618
34. Weinstein A (1986) A mathematical model of the rat proximal tubule. Am J Physiol (Renal Physiol 250:F860–F873
35. Weinstein A (1992) Chloride transport in a mathematical model of the rat proximal tubule. Am J Physiol Renal Physiol 263:F784–F798
36. Weinstein A (1995) A kinetically defined Na^+/H^+ antiporter within a mathematical model of the rat proximal tubule. J Gen Physiol 105:617–641
37. Weinstein A (1997) Dynamics of cellular homeostasis: recovery time for a perturbation from equilibrium. Bull Math Biol 59(3):451–481
38. Weinstein A (1998) A mathematical model of the inner medullary collecting duct of the rat: pathways for Na and K transport. Am J Physiol (Renal Physiol 43) 274:F841–F855
39. Weinstein A (1999) Modeling epithelial cell homeostasis: steady-state analysis. Bull Math Biol 61:1065–1091
40. Weinstein A (2000) A mathematical model of the outer medullary collecting duct of the rat. Am J Physiol Renal Physiol 279:F24–F45
41. Weinstein A (2001) A mathematical model of rat cortical collecting duct: determinants of the transtubular potassium gradient. Am J Physiol Renal Physiol 280:F1072–F1092
42. Weinstein A (2002) A mathematical model of rat collecting duct I. Flow effects on transport and urinary acidification. Am J Physiol Renal Physiol 283:F1237–F1251
43. Weinstein A (2008) A mathematical model of distal nephron acidification: diuretic effects. Am J Physiol Renal Physiol 295:F1353–F1364
44. Weinstein A (2009) A mathematical model of rat ascending henle limb. I. Cotransporter function. Am J Physiol Renal Physiol 298:F512–F524
45. Nieves-Gonzalez A, Clausen C, Marcano M, Layton A, Layton H, Moore L (2012) Fluid dilution and efficiency of Na^+ transport in a mathematical model of a thick ascending limb cell. Am J Physiol Renal Physiol 304:F634–F652
46. Nieves-Gonzalez A, Clausen C, Layton A, Layton H, Moore L (2013) Transport efficiency and workload distribution in a mathematical model of the thick ascending limb. Am J Physiol Renal Physiol 304:F653–F664

47. Chang H, Fujita T (1999) A numerical model of the renal distal tubule. Am J Physiol Renal Physiol 276:F931–F951
48. Thomas S, Dagher G (1994) A kinetic model of rat proximal tubule transport—load-dependent bicarbonate reabsorption along the tubule. Bull Math Biol 56(3):431–458
49. Tournus M, Seguin N, Perthame B, Thomas S, Edwards A (2013) A model of calcium transport along the rat nephron. Am J Physiol Renal Physiol 305:F979–F994
50. Layton H (1986) Distribution of Henle's loops may enhance urine concentrating capability. Biophys J 49:1033–1040
51. Layton H (1990) Urea transport in a distributed model of the urine-concentrating mechanism. Am J Physiol (Renal Fluid Electrolyte Physiol 27) 258:F1110–F1124
52. Layton H, Davies J (1993) Distributed solute and water reabsorption in a central core model of the renal medulla. Math Biosci 116:169–196
53. Layton H, Davies J, Casotti G, Braun E (2000) Mathematical model of an avian urine concentrating mechanism. Am J Physiol Renal Physiol 279:F1139–F1160
54. Layton H, Knepper M, Chou C (1996) Permeability criteria for effective function of passive countercurrent multiplier. Am J Physiol (Renal Fluid Electrolyte Physiol 39) 270:F9–F20
55. Layton A, Bankir L (2013) Impacts of active urea secretion into pars recta on urine concentration and urea excretion rate. Physiol Rep 1(e00):034
56. Layton A, Layton H (2011) Countercurrent multiplication may not explain the axial osmolality gradient in the outer medulla of the rat kidney. Am J Physiol Renal Physiol 301:F1047–F1056
57. Layton A, Layton H (2005) A region-based mathematical model of the urine concentrating mechanism in the rat outer medulla: I. Formulation and base-case results. Am J Physiol Renal Physiol 289:F1346–F1366
58. Layton A (2011) A mathematical model of the urine concentrating mechanism in the rat renal medulla: I. Formulation and base-case results. Am J Physiol Renal Physiol 300:F356–F371
59. Layton A (2011) A mathematical model of the urine concentrating mechanism in the rat renal medulla: II. Functional implications of three-dimensional architecture. Am J Physiol Renal Physiol 300:F372–F394
60. Layton A, Dantzler W, Pannabecker T (2012) Urine concentrating mechanism: impact of vascular and tubular architecture and a proposed descending limb urea-Na$^+$ cotransporter. Am J Physiol Renal Physiol 302:F591–F605
61. Layton A, Pannabecker T, Dantzler W, Layton H (2010) Functional implications of the three-dimensional architecture of the rat renal inner medulla. Am J Physiol Renal Physiol 298:F973–F987
62. Layton A, Gilbert R, Pannabecker T (2012) Isolated interstitial nodal spaces may facilitate preferential solute and fluid mixing in the rat renal inner medulla. Am J Physiol Renal Physiol 302(7):F830–F839
63. Wexler A, Kalaba R, Marsh D (1991a) Three-dimensional anatomy and renal concentrating mechanism. I. Modeling results. Am J Physiol (Renal Fluid Electrolyte Physiol 29) 260:F368–F383
64. Hervy S, Thomas S (2003) Inner medullary lactate production and urine-concentrating mechanism: a flat medullary model. Am J Physiol Renal Physiol 284:F65–F81
65. Thomas S (1998) Cycles and separations in a model of the renal medulla. Am J Physiol (Renal Fluid Electrolyte Physiol 44) 275:F671–F690
66. Thomas S, Wexler A (1995) Inner medullary external osmotic driving force in a 3-D model of the renal concentrating mechanism. Am J Physiol (Renal Fluid Electrolyte Physiol 38) 269:F159–F171
67. Thomas S (2000) Inner medullary lactate production and accumulation: a vasa recta model. Am J Physiol Renal Physiol 279:F468–F481
68. Reinking L, Schmidt-Nielsen B (1981) Peristaltic flow of urine in the renal papillary collecting ducts of hamsters. Kidney Int 20:55–60
69. Kedem O, Katchalsky A (1958) Thermodynamic analysis of the permeability of biological membranes to non-electrolytes. Biochim Biophy Acta 27:229–246
70. Bankir L, Trinh-Trang-Tan MM (2000) Urea and the kidney. In: BM B, FC R (eds) Brenner and Rector's The Kidney, 6th edn, Saunders, Philadelphia, pp 637–679

71. Bankir L, de Rouffignac C (1985) Urinary concentrating ability: insights from comparative anatomy. Am J Physiol (Regulatory Integrative Comp Physiol *18*) 249:R643–R666
72. Kriz W, Kaissling B (2000) Structural organization of the mammalian kidney. The Kidney: Physiology and Pathophysiology, 3rd edn. Lippincott Williams & Wilkins, Philadelphia, pp 587–654
73. Pannabecker T, Abbott D, Dantzler W (2004) Three-dimensional functional reconstruction of inner medullary thin limbs of Henle's loop. Am J Physiol Renal Physiol 286:F38–F45
74. Pannabecker T, Dantzler W (2004) Three-dimensional lateral and vertical relationship of inner medullary loops of Henle and collecting duct. Am J Physiol Renal Physiol 287:F767–F774
75. Pannabecker T, Dantzler W (2006) Three-dimensional architecture of inner medullary vasa recta. Am J Physiol Renal Physiol 290:F1355–F1366
76. Bankir L, Bouby N, Trinh-Trang-Tan MM (1987) Heterogeneity of nephron anatomy. Kidney Int (supplement 20) 31:S–25–S–39
77. Knepper M, Roch-Ramel F (1987) Pathways of urea transport in the mammalian kidney. Kidney Int 31:629–633
78. Kriz W, Lever A (1969) Renal countercurrent mechanisms: structure and function. Am Heart J 78(1):101–118
79. Lemley K, Kriz W (1987) Cycles and separations: the histotopography of the urinary concentrating process. Kidney Int 31:538–548
80. Chandhoke P, Saidel G (1981) Mathematical model of mass transport throughout the kidney: effects of nephron heterogeneity and tubular-vascular organization. Ann Biomed Eng 9:263–301
81. Knepper M, Saidel G, Palatt P (1976) Mathematical model of renal regulation of urea excretion. Med Biol Eng 14:408–425
82. Wexler A, Kalaba R, Marsh D (1991b) Three-dimensional anatomy and renal concentrating mechanism. II. Sensitivity results. Am J Physiol (Renal Fluid Electrolyte Physiol 29) 260:F384–F394
83. Wang X, Thomas S, Wexler A (1998) Outer medullary anatomy and the urine concentrating mechanism. Am J Physiol (Renal Physiol 43) 274(3):F413–F424
84. Layton A, Layton H (2005) A region-based mathematical model of the urine concentrating mechanism in the rat outer medulla: II. Parameter sensitivity and tubular inhomogeneity. Am J Physiol Renal Physiol 289:F1367–F1381

Chapter 4
Genes and Proteins of Urea Transporters

Jeff M. Sands and Mitsi A. Blount

Abstract A urea transporter protein in the kidney was first proposed in 1987. The first urea transporter cDNA was cloned in 1993. The *SLC14a* urea transporter family contains two major subgroups: *SLC14a1*, the UT-B urea transporter originally isolated from erythrocytes; and *SLC14a2*, the UT-A group originally isolated from kidney inner medulla. *Slc14a1*, the human UT-B gene, arises from a single locus located on chromosome 18q12.1-q21.1, which is located close to *Slc14a2*. *Slc14a1* includes 11 exons, with the coding region extending from exon 4 to exon 11, and is approximately 30 kb in length. The *Slc14a2* gene is a very large gene with 24 exons, is approximately 300 kb in length, and encodes 6 different isoforms. *Slc14a2* contains two promoter elements: promoter I is located in the typical position, upstream of exon 1, and drives the transcription of UT-A1, UT-A1b, UT-A3, UT-A3b, and UT-A4; while promoter II is located within intron 12 and drives the transcription of UT-A2 and UT-A2b. UT-A1 and UT-A3 are located in the inner medullary collecting duct, UT-A2 in the thin descending limb and liver, UT-A5 in testis, UT-A6 in colon, UT-B1 primarily in descending vasa recta and erythrocytes, and UT-B2 in rumen.

Keywords Urea · Urea transporter · Vasopressin · Kidney · Erythrocytes

J.M. Sands (✉) · M.A. Blount
Renal Division, Department of Medicine and Department of Physiology, Emory University
School of Medicine, WMB Room 338, 1639 Pierce Drive, NE, Atlanta, GA 30322, USA
e-mail: jeff.sands@emory.edu

M.A. Blount
e-mail: mabloun@emory.edu

Cloning and Gene Structures of Urea Transporters

The Slc14a1 (UT-B) Gene

The *Slc14a1* (UT-B) gene was initially cloned from a human erythropoietic cell line [87] and subsequently cloned from rat and mouse [19, 104, 127, 142]. *Slc14a1*, the human UT-B gene, arises from a single locus located on chromosome 18q12.1-q21.1 (Fig. 4.1), which is located close to *Slc14a2*, the human UT-A gene [63, 84, 85, 117]. The analogous mouse genes, UT-B (*Slc14a1*) and UT-A (*Slc14a2*), also occur in tandem on mouse chromosome 18 [25]. Interestingly, the Kidd (Jk) blood group antigen, one of the minor blood group antigens, is located in the same region of human chromosome 18 as are the two urea transporter genes [63]. In humans, the Kidd antigen is the UT-B protein [7, 16, 63, 67, 81, 84, 85]. Several mutations in the human UT-B/Kidd antigen (*Slc14a1*) gene have been reported [42, 43, 63, 64, 86, 109, 134]. Red blood cells from humans lacking the Kidd antigen (Jk(a-b-) or Jk null) do not exhibit phloretin-sensitive facilitated urea transport, in contrast to red blood cells from humans expressing a Kidd antigen [32].

The human UT-B gene, *Slc14a1*, includes 11 exons, with the coding region extending from exon 4 to exon 11, and is approximately 30 kb in length [63]. There are two mRNA transcripts, 4.4 and 2.0 kb, which result from alternative polyadenylation signals; both are expressed in reticulocytes and encode a single 45-kDa protein [63]. Two rat cDNA sequences were originally reported for UT-B1 that differed by only a few nucleotides at their 3' end [19, 127]. It is unknown whether these small differences may represent polymorphisms or sequencing artifacts.

The Slc14a2 (UT-A) Gene

The *Slc14a2* (UT-A) gene was initially cloned from rat [78] and subsequently cloned from human and mouse [5, 24]. UT-A is encoded by a different gene than UT-B (reviewed in [4]). However, UT-A and UT-B contain tandem repeat sequences that may represent a urea transporter signature sequence [100].

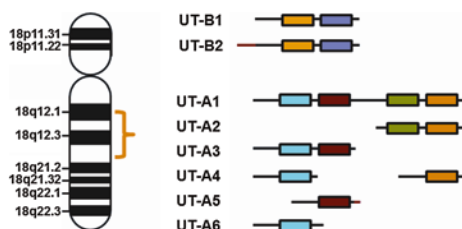**Fig. 4.1** Schematic representation of Slc14a1 and Slc14a2, the human UT-B and UT-A gene, respectively, and resulting the different isoforms of UT-A and UT-B urea transporters. The different boxes represent regions of hydrophobic amino acids. The *black lines* show coding sequences which are common, while the *red lines* show coding sequences that are unique to that particular isoform (i.e., derived from novel exons)

The rat UT-A gene is a very large gene (Fig. 4.2) with 24 exons and is approximately 300 kb in length [78, 112]. UT-A1 is encoded by exons 1–12 spliced to exons 14–23 (exon 13 is not used for UT-A1). UT-A3 is encoded by exons 1–12. UT-A4 is encoded by exons 1–7 spliced to exons 18–23. There is a common transcription start site in exon 1 and translation start site in exon 4 for UT-A1, UT-A2, and UT-A4. In contrast, UT-A2 is encoded by exons 13–23 with a unique translation start site in exon 16. UT-A1b and UT-A2b utilize exon 24, which is located in the 3' untranslated region of the UT-A gene. UT-A1b and UT-A2b have the same coding regions as UT-A1 and UT-A2, respectively, but their cDNA transcripts differ due to use of exon 24 in the 3' untranslated region [6]. UT-A3b also results from expression of an alternative 3'-untranslated region and results in a transcript that is ~1.5 kb longer than UT-A3 cDNA [6]. UT-A1b, UT-A2b, and UT-A3b mRNAs are expressed in rat inner medulla [6].

The rat *Slc14a2* (UT-A) gene contains two promoter elements: promoter I is located in the typical position, upstream of exon 1, and drives the transcription of UT-A1, UT-A1b, UT-A3, UT-A3b, and UT-A4; while promoter II is located within intron 12 and drives the transcription of UT-A2 and UT-A2b. UT-A1 and UT-A3 are located in the inner medullary collecting duct, UT-A2 in the thin descending limb and liver, UT-A5 in testis, UT-A6 in colon, UT-B1 primarily in descending vasa recta and erythrocytes, and UT-B2 in rumen [6, 78]. When the 1.3 kb of UT-A promoter I that is located immediately 5' to exon 1 is cloned into a luciferase reporter gene construct and transfected into mIMCD3, MDCK, or LLC-PK1 cells, it shows evidence of promoter activity [79, 92]. This 1.3-kb promoter sequence does not contain a TATA motif but does contain three CCAAT elements [79]. UT-A promoter I activity is significantly increased by hyperosmolality, and it contains a tonicity enhancer (TonE) element [79]. Dexamethasone, at a dose equivalent to a level found during stress, reduces the activity of UT-A promoter I by 70 % and decreases the mRNA abundances of UT-A1, UT-A3, and UT-A3b in the rat inner medulla [92]. The repressive effect of dexamethasone on UT-A
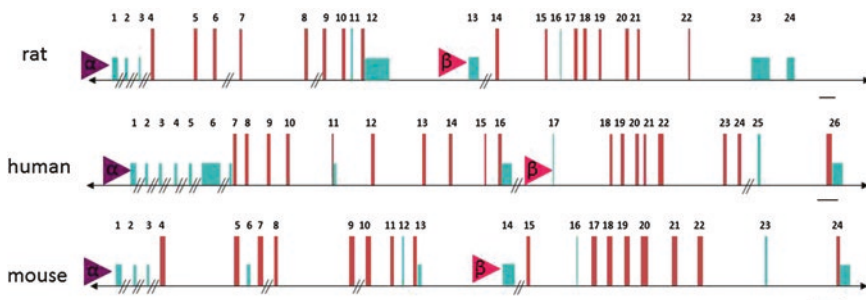
Fig. 4.2 Comparison of the genomic organization of the urea transporter UT-A gene (Slc14a2) for human, rat, and mouse. Above are schematic representations of the gene structure for each species. Exon width is representative of actual size, and intronic distance is scaled. Introns >5 kb are represented by //and are not scaled. Triangles denote the α (*green*) and β (*red*) promoters. Coding exons (*dark blue*) and untranslated exons (*light blue*) are drawn to scale. Figure is reproduced with permission of the American Physiological Society from Klein et al. [51]

promoter I activity does not occur via the consensus glucocorticoid response element (GRE) that is present in UT-A promoter I [92].

UT-A2 is under the control of a unique internal promoter, UT-A promoter II, which is located within intron 12 [6, 78]. The transcription start site for UT-A2 is located in exon 13, which is almost 200 kb downstream from exon 1 [6, 78]. Within intron 12, there is a TATA box 40 bp upstream of the UT-A2 transcription start site and a cAMP response element (CRE) 300 bp upstream of the UT-A2 transcription start site [6, 78]. This internal promoter region of intron 12 shows evidence of promoter activity when it is transfected into mIMCD3 cells, along with a luciferase reporter gene, and the cells are stimulated with cAMP; no promoter activity is detected under basal conditions [6, 78].

The human UT-A gene is located on chromosome 18 and is approximately 67.5 kb in length (Fig. 4.2). The human gene is significantly shorter than the rat gene because: (1) it does not contain an exon in the 3'-untranslated region that is analogous to rat exon 24; and (2) the 5'-untranslated region is almost entirely located in exon 1 in humans, while in rat, it spans the first 3 widely spaced exons [5, 78]. However, human UT-A does contain an extra exon, exon 5a, which has not been reported in rat [114]. Exon 5a was subsequently renumbered as exon 6, with a renumbering of all the downstream exons [112]. The human UT-A gene gives rise to UT-A1, UT-A2, and UT-A3, similar to rat, and to a shorter isoform, UT-A6 [112]. UT-A6 is encoded by human exons 1–11 (original nomenclature is exons 1–10 but including exon 5a) and is expressed in colon [114]. Single nucleotide polymorphisms in human SLC14A2 are predictive of the antihypertensive efficacy of nifedipine, an L-type voltage-gated calcium channel blocker [35]. These polymorphisms are detected in human UT-A2 and are associated with variation in blood pressure in men but not in women [97].

The structure of the mouse UT-A gene is very similar to the rat UT-A gene (Fig. 4.2), with the exception that a mouse UT-A4 isoform has not been detected [24]. The mouse UT-A gene contains 24 exons, is >300 kb in length, and has two promoter elements, which are named α and β [24, 112]. UT-A promoter α, which corresponds to promoter I in rat, contains a TonE element, and its promoter activity is increased by hypertonicity [24]. In contrast to rat, the activity of mouse UT-A promoter I (α) is increased by cAMP, even though no consensus CRE element is present in promoter I (α) from either species [24, 78]. The mouse gene also gives rise to a testis-specific isoform, UT-A5, which is encoded by exons 6–13 [24, 26, 112]. While all mouse UT-A isoforms originate from a single mouse gene, the transcription start site of UT-A5 has not been determined and may be located downstream from mouse UT-A1 and UT-A3 [24]. Thus, whether UT-A5 is driven by promoter α or by a novel promoter element is not known, nor is it known whether UT-A5 is expressed in humans or rat (Table 4.1).

UT-A promoter α has been further characterized using a transgenic mouse in which 4.2 kb of the 5'-flanking region of the UT-A gene is linked to a β-galactosidase reporter gene [27]. This transgene drives IMCD-specific expression of β-galactosidase in the terminal IMCD [27]. The regulation of β-galactosidase transgene by water restriction and glucocorticoids is similar to the regulation of the endogenous UT-A promoter I (α) [24, 27, 79, 92].

Table 4.1 Mammalian facilitated urea transporter gene families

Gene	Isoform	RNA (kb)	Protein (kDa)	AVP	Location	References
Slc14a1	UT-B1	3.8	43		DVR, RBC[a]	Olives et al. [87], Couriaud et al. [19], Promeneur et al. [96], Tsukaguchi et al. [127], Berger et al. [9], Timmer et al. [124]
	UT-B2	3.7	43–54	No	Bovine rumen	Stewart et al. [119], Tickle et al. [123]
Slc14a2	UT-A1	4.0	97, 117	Yes	IMCD	Shayakul et al. [107], Bradford et al. [13], Bagnasco et al. [5]
	UT-A1b	3.5			medulla[b]	Bagnasco et al. [6], Nakayama et al. [78]
	UT-A2	2.9	55	No[c]	tDL, liver	You et al. [144], Smith et al. [113], Olivès et al. [84], Promeneur et al. [96], Nielsen et al. [82], Doran et al. [21], Potter et al. [94]
	UT-A2b	2.5			medulla[b], heart	Karakashian et al. [46], Bagnasco et al. [6], Duchesne et al. [22]
	UT-A3	2.1	44, 67	Yes	IMCD	Karakashian et al. [46], Fenton et al. [26], Shayakul et al. [108], Terris et al. [122]
	UT-A3b	3.7			medulla[b]	Bagnasco et al. [6]
	UT-A4[d]	2.5	43	Yes	medulla[b]	Karakashian et al. [46]
	UT-A5[e]	1.4			testis	Fenton et al. [26]
	UT-A6[f]	1.8			colon	Smith et al. [114]

Isoform names are based upon the urea transporter nomenclature proposed in [104]; *AVP*, urea flux is stimulated by vasopressin; *DVR* descending vasa recta; *RBC* red blood cells

[a]also expressed in several other tissues and endothelial cells; *IMCD* inner medullary collecting duct; *tDL* thin descending limb

[b](exact tubular location unknown)

[c]no in rat but yes in mouse

[d]cloned from rat only

[e]cloned from mouse only

[f]cloned from human only

Non-Mammalian Urea Transporters

In addition to the two mammalian urea transporters discussed above, there are several non-mammalian urea transporters that have been cloned (Table 4.2). Based upon a bioinformatic analysis, it appears that vertebrates acquired urea transporter genetic information from bacteria [74]. This analysis suggests that all current vertebrate orthologues and paralogues arose from this one primordial system, followed by two gene duplication events during development of the vertebrate lineage [74]. The cloned non-mammalian urea transporters are most homologous to UT-A2.

The non-mammalian urea transporters permit urea to be transported specifically, which is important to the ability of marine life to cope with their shifting environment [2, 70,129, 135, 139]. For example, urea transporters help elasmobranch fish retain urea in their gills and kidneys against a large external environmental gradient. Urea transporters contribute to urea removal or excretion rather than retention in teleost fish. A unique urea transporter, UT-C, has been cloned from the Japanese eel, Anguilla japonica [75]. Zebrafish also express a urea transporter, and this transporter is responsible for 90 % of urea excretion [14, 15].

Table 4.2 Non-mammalian urea transporters

Species	Common name	References
Alcolapia grahami	Lake Magadi tilapia	Walsh et al. [132]
Anguilla japonica	Japanese eel	Mistry et al. [75]
Balaenoptera acutorostrata	Whale	Birikawa et al. [10]
Bufo marinus	Toad	Konno et al. [55], Konno et al. [56]
Callorhinchus milii	Holocephalan elephant fish	Kakumura et al. [45]
Danio rerio	Zebrafish	Braun et al. [14]
Dasyatis sabina	Atlantic stingray	Walsh et al. [133], McDonald et al. [70]
Oncorhynchus mykiss	Rainbow trout	Pilley and Wright [93], Hung et al. [37]
Opsanus beta	Gulf toadfish	Rodela et al. [99], [71], McDonald et al. [73], Wood et al. [138], Laurent et al. [58], Wood et al. [137]
Physeter macrocephalus	Whale	Birikawa et al. [10]
Porichthys notatus	Plainfin midshipman	McDonald et al. [72]
Protopterus annectens	African lungfish	Hung et al. [38]
Protopterus dolloi	Slender lungfish	Wood et al. [136]
Raja erinacea	Skate	Morgan et al. [76, 77]
Squalus acanthias	Dogfish shark	[29]
Trachemys scripta elegans	Red-eared slider turtle	Uchiyama et al. [128]
Triakis scyllia	Dogfish	Hyodo et al. [39]
Triakis scyllium	Houndshark	Yamaguchi et al. [141]

Isoforms of Urea Transporters

UT-B1

UT-B1 mRNA is widely expressed and has been detected in many tissues (Fig. 4.3), including kidney, brain, liver, colon, small intestine, pancreas, testis, prostate, bone marrow, spleen, thymus, heart, skeletal muscle, lung, bladder, and cochlea [9, 18–20, 33, 36, 40, 41, 57, 62, 64, 84, 87, 95, 96, 124, 125, 127, 142]. Several polyclonal antibodies have been made to either the N- or C-terminus of human UT-B1 [36, 124, 140]. These antibodies also detect UT-B1 in rodents [36, 124, 140]. On Western blot, UT-B1 protein is detected as a broad band between 45 and 65 kDa in human red blood cells and 37–51 kDa in rat or mouse red blood cells [124, 142]. UT-B1 protein is detected in kidney medulla as a broad band between 41 and 54 kDa [124]. In both red blood cells and kidney medulla, deglycosylation converts the broad band detected on Western blot to a sharp band of 32 kDa [124]. In addition, a 98-kDa band is detected in kidney, but this band is non-specific since it is still present in kidney lysates from UT-B knock-out mice [53, 124].

Human, mouse, and rat kidney show UT-B1 immunostaining (Fig. 4.4) in the non-fenestrated endothelial cells that are characteristic of descending vasa recta [36, 88, 124, 126, 140, 142], most notably in the descending vasa recta that are external to collecting duct clusters [90]. UT-B1 protein is also present in rat liver, colon, testis, brain, heart, lung, aorta, cochlea, spinotrapezius muscle, and mesenteric artery [18, 20, 23, 36, 40, 57, 62, 124, 125, 131]. UT-B1 has been identified in rat urothelia, which was previously thought to be impermeable to urea and water [115]. Immunohistochemistry of ureter and bladder shows UT-B1 localized

Fig. 4.3 UT-B1 mRNA is widely expressed and has been detected in many tissues, including kidney, brain, liver, colon, small intestine, pancreas, testis, prostate, bone marrow, spleen, thymus, heart, skeletal muscle, lung, bladder, and cochlea
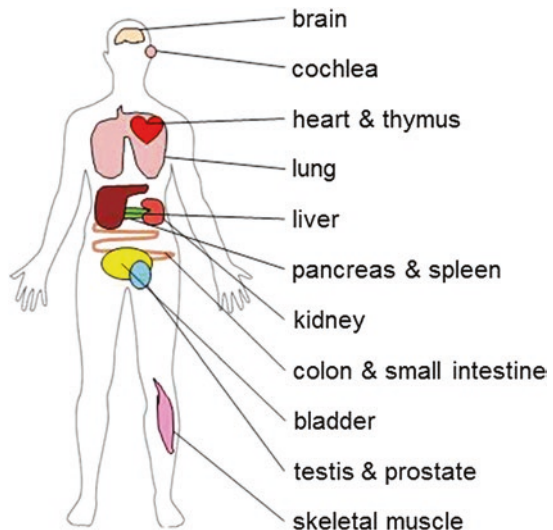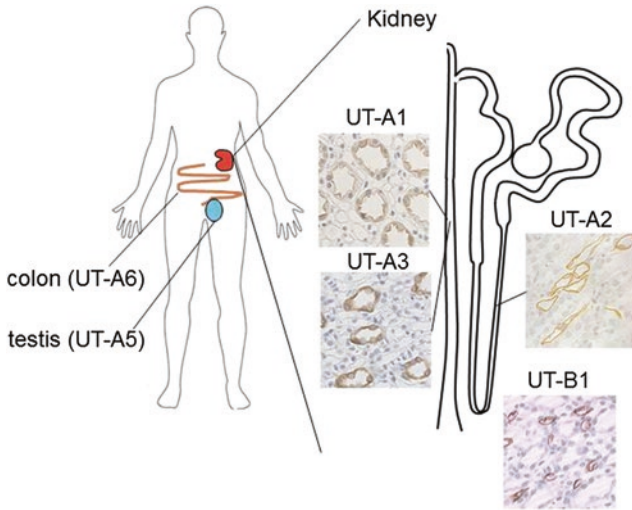
Fig. 4.4 UT-A1 and UT-A3 proteins are expressed in the inner medullary collecting duct, UT-A2 in the thin descending limb, UT-A5 in testis, UT-A6 in colon, and UT-B1 in descending vasa recta (and erythrocytes, not shown)

to the epithelial cell membrane [116]. UT-B1 protein is also expressed in several cultured endothelial cell lines, where it promotes urea entry, which in turn, inhibits L-arginine transport [124, 131].

UT-B1 transports urea when it is expressed in Xenopus oocytes, and urea transport is inhibited by phloretin, thiourea, and pCMBS [69]. UT-B1 also transports several chemical analogs of urea, including methylurea, formamide, acetamide, acrylamide, methylformamide, and ammonium carbamate [147]. Two studies show that rat and mouse UT-B1 can function as a water channel, in addition to its role as a urea transporter, when expressed in Xenopus oocytes [142, 143]. However, questions have been raised regarding the physiological significance of water transport through UT-B1 since a third study showed that rat UT-B1 specifically transports urea when a physiological expression level is achieved in oocytes, but only higher levels of UT-B1 expression result in increases in urea and water permeability [110]. Several small molecule inhibitors of UT-B1 have been identified that have a good UT-B1 versus UT-A selectivity and that do not inhibit water transport through AQP1 [59]. UT-B1 acts as an active water transporter in C6 glial cells [83].

Mice lacking UT-B1 have a urine concentrating defect that is similar in magnitude to humans lacking Kidd antigen [8, 103]. This is consistent with the decreased concentrating ability observed in animal models where UT-B1 protein abundance is decreased, such as water loading [61], potassium deprivation [44], ureteral obstruction [60], and severe inflammation [105]. The reader is referred to Chap. 10 for a detailed discussion of the extrarenal phenotype of UT-B knockout mice.

UT-B2

UT-B2 mRNA is expressed in the rumen of sheep and cow [1, 49, 65, 98, 111, 119, 123] but has not been detected in other tissues. Vasopressin does not alter UT-B2 abundance [123]. UT-B2 levels in their gastric system are responsive to shifting pH environments and ruminal ammonia concentrations, and are highly dependent on the type of food consumed [1, 49, 65, 68, 111, 119]. The response of UT-B2 abundance in ruminants to the level of nitrogen in their food is consistent with the response of UT-B1 abundance in rodents to variation in the urea load or the urea content of the urine [41, 47].

UT-A1

UT-A1 protein expression (Fig. 4.4) is detected in the apical plasma membrane and in the cytoplasm of the IMCD in rat [12, 20, 48, 52, 61, 82] and human medulla [5]. It is also expressed in the apical plasma membrane and in the cyto-plasm of cells that are stably transfected with UT-A1: UT-A1-MDCK cells [17, 30, 31] and UT-A1-mIMCD3 cells [52]. When expressed in Xenopus oocytes, rat, mouse, and human UT-A1 are stimulated by cyclic AMP [5, 28, 96, 106, 107].

Polyclonal antibodies have been raised against three portions of UT-A1: the N-terminus [130], the intracellular loop region [121], and the C-terminus [80, 82]. These antibodies often detect more than one UT-A protein since the vari-ous UT-A proteins result from alternative splicing of the UT-A gene. However, they can be distinguished by the different size bands that are detected on Western blot. The N-terminus antibody detects UT-A1 (97 and 117 kDa), UT-A3 (44 and 67 kDa), and UT-A4 (43 kDa); the loop region antibody detects only UT-A1; and the C-terminus antibody detects UT-A1, UT-A2 (55 kDa), and UT-A4 [46, 101, 121, 122]. In the inner medullary tip region, all anti-UT-A1 antibodies detect pro-tein bands at 97 and 117 kDa by Western blot [80, 82, 121]. The 97- and 117-kDa proteins are glycosylated versions of a non-glycosylated 88-kDa UT-A1 protein [13]. In one study, UT-A1 was also detected as a 206-kDa protein complex in native inner medullary membranes [13]. UT-A1 protein is most abundant in the inner medullary tip, present in the inner medullary base, and not detected in outer medulla or cortex [50, 82, 102].

UT-A2

UT-A2 and UT-A1 have the same C-terminal amino acid (and 3' cDNA) sequence but differ at the N-terminal (5' cDNA) end [5, 24, 107]. Hence, UT-A2 is essen-tially the C-terminal half of UT-A1. UT-A2 is detected as a 55-kDa protein band on Western blot of inner medullary proteins [130]. UT-A2 is also detected in

heart and liver as 39- and 55-kDa protein bands [20, 22, 54]. UT-A2 is expressed (Fig. 4.4) in the thin descending limb of the loop of Henle [48, 66, 82, 88, 89, 91, 130, 145]. UT-A2 is only detected in the last 28–44 % of the thin descending limb of short-looped nephrons [146]. UT-A2 is highly specific for urea and does not transport water, ammonia, methylurea, dimethylurea, formamide, or acetamide when expressed in Xenopus oocytes [66]. Both phloretin and thiourea inhibit urea transport through UT-A2, but pCMBS does not, in Xenopus oocytes [69]. For UT-A2, the single transporter flux rate is 46,000 urea molecules/second/channel [66].

Cyclic AMP analogs do not stimulate UT-A2 when it is expressed in either Xenopus oocytes or human embryonic kidney (HEK) 293 cells [3, 46, 96, 106, 107, 113, 144]. However, vasopressin does increase urea flux in MDCK cells that are stably transfected with mouse UT-A2, mUT-A2-MDCK cells [94]. Urea flux is also increased by forskolin and increased intracellular calcium in mUT-A2-MDCK cells [94]. However, inhibiting PKA with H-89 has no effect on forskolin-stimulated urea flux in mUT-A2-MDCK cells [94].

UT-A3

UT-A3 and UT-A1 have the same N-terminal amino acid (and 5' cDNA) sequence but differ at the C-terminal (3'-cDNA) end [26, 46, 108]. Hence, UT-A3 is essentially the N-terminal half of UT-A1. A polyclonal antibody to the unique C-terminus of UT-A3 shows that UT-A3 is expressed (Fig. 4.4) in the IMCD [122]. This antibody, as well as the N-terminal antibody to UT-A1, detects protein bands at 44 and 67 kDa by Western blot of inner medullary tip proteins; both bands represent glycosylated versions of a non-glycosylated 40-kDa UT-A3 protein [11, 122]. UT-A3 protein is most abundant in the inner medullary tip, weakly detected in the inner medullary base and outer medulla, and absent in cortex [122].

UT-A3 exhibits a 7.5-fold increase in urea transport but no increase in water transport in Xenopus oocytes, indicating that UT-A3 is selective for urea versus water [34]. UT-A3 is highly specific for urea and does not transport water, ammonia, methylurea, dimethylurea, formamide, or acetamide, [66]. For UT-A3, the single transporter flux rate is 59,000 urea molecules/second/channel, a value that is similar to UT-A2 [66]. Cyclic AMP analogs stimulate urea transport by UT-A3 when it is expressed in Xenopus oocytes (in 3 studies) or HEK 293 cells [28, 46, 114], but not in a fourth study of oocytes [108]. Vasopressin stimulates urea transport via a PKA-dependent pathway in cells that are stably transfected with mouse UT-A3, mUT-A3-MDCK cells [120].

The immunolocalization of UT-A3 within the IMCD has varied in different studies. The initial rat studies detected UT-A3 immunostaining in the apical plasma membrane and intracellular cytoplasmic vesicles of terminal IMCDs, but no immunostaining was seen in the basolateral plasma membrane [82, 122]. Subsequent studies detected UT-A3 staining only in the basolateral plasma membrane in mouse IMCD and in mUT-A3-MDCK cells [118, 120]. More recently,

UT-A3 immunostaining was detected only in the basolateral plasma membrane in control rat IMCDs, but in both the basolateral and apical plasma membranes following vasopressin administration [11]. UT-A3 expression in the basolateral plasma membrane provides a mechanism for transepithelial urea transport across the IMCD, with UT-A1 in the apical plasma membrane and UT-A3 in the basolateral plasma membrane.

UT-A4

UT-A4 and UT-A1 have the same N- and C-terminal amino acid (and 5' and 3' cDNA) sequences, but UT-A4 is smaller and essentially consists of the N-terminal quarter of UT-A1 spliced into the C-terminal quarter of UT-A1 [46]. UT-A4 mRNA is detected in rat kidney medulla (although its exact tubular location is unknown) and is stimulated by cyclic AMP analogs when expressed in HEK-293 cells [46]. In contrast to rat, UT-A4 has not been detected in mouse kidney.

UT-A5

UT-A5 is expressed in mouse testis but not in kidney [26]. UT-A5's deduced amino acid sequence begins at methionine 139 of mouse UT-A3, after which it shares 100 % homology and a common C-terminus with mouse UT-A3 [26]. The effect of cyclic AMP on UT-A5 has not been tested.

UT-A6

UT-A6 is expressed in human colon but not in kidney [114]. The effect of cyclic AMP on UT-A6 has not been tested.

References

1. Abdoun K, Stumpff F, Rabbani I, Martens H (2010) Modulation of urea transport across sheep rumen epithelium in vitro by SCFA and CO2. Am J Physiol Gastrointest Liver Physiol 298(2):G190–G202
2. Acher R, Chauvet J, Chauvet MT, Rouille Y (1999) Unique evolution of neurohypophysial hormones in cartilaginous fishes: possible implications for urea-based osmoregulation. J Exp Zool 284(5):475–484

3. Ashkar ZM, Martial S, Isozaki T, Price SR, Sands JM (1995) Urea transport in initial IMCD of rats fed a low-protein diet: functional properties and mRNA abundance. Am J Physiol Renal Physiol 268(6):F1218–F1223
4. Bagnasco SM (2006) The erythrocyte urea transporter UT-B. J Membrane Biol 212(2):133–138
5. Bagnasco SM, Peng T, Janech MG, Karakashian A, Sands JM (2001) Cloning and characterization of the human urea transporter UT-A1 and mapping of the human *Slc14a2* gene. Am J Physiol Renal Physiol 281:F400–F406
6. Bagnasco SM, Peng T, Nakayama Y, Sands JM (2000) Differential expression of individual UT-A urea transporter isoforms in rat kidney. J Am Soc Nephrol 11(11):1980–1986
7. Bagnis C, Chapel S, Chiaroni J, Bailly P (2009) A genetic strategy to control expression of human blood group antigens in red blood cells generated in vitro. Transfusion 49(5):967–976
8. Bankir L, Chen K, Yang B (2004) Lack of UT-B in vasa recta and red blood cells prevents urea-induced improvement of urinary concentrating ability. Am J Physiol Renal Physiol 286(1):F144–F151
9. Berger UV, Tsukaguchi H, Hediger MA (1998) Distribution of mRNA for the facilitated urea transporter UT3 in the rat nervous system. Anat Embryol 197:405–414
10. Birukawa N, Ando H, Goto M, Kanda N, Pastene LA, Urano A (2008) Molecular cloning of urea transporters from the kidneys of baleen and toothed whales. Comp Biochem Physiol B Biochem Mol Bio 149(2):227–235
11. Blount MA, Klein JD, Martin CF, Tchapyjnikov D, Sands JM (2007) Forskolin stimulates phosphorylation and membrane accumulation of UT-A3. Am J Physiol Renal Physiol 293(4):F1308–F1313
12. Blount MA, Sim JH, Zhou R, Martin CF, Lu W, Sands JM, Klein JD (2010) The expression of transporters involved in urine concentration recover differently after ceasing lithium treatment. Am J Physiol Renal Physiol 298:F601–F608
13. Bradford AD, Terris J, Ecelbarger CA, Klein JD, Sands JM, Chou C-L, Knepper MA (2001) 97 and 117 kDa forms of the collecting duct urea transporter UT-A1 are due to different states of glycosylation. Am J Physiol Renal Physiol 281(1):F133–F143
14. Braun MH, Steele SL, Ekker M, Perry SF (2009) Nitrogen excretion in developing zebrafish (Danio rerio): a role for Rh proteins and urea transporters. Am J Physiol Renal Physiol 296(5):F994–F1005
15. Braun MH, Steele SL, Perry SF (2009) The responses of zebrafish (Danio rerio) to high external ammonia and urea transporter inhibition: nitrogen excretion and expression of rhesus glycoproteins and urea transporter proteins. J Exp Biol 212(23):3846–3856
16. Cartron JP, Ripoche P (1995) Urea transport and Kidd blood groups. Transfus Clin Biol 2(4):309–315
17. Chen G, Fröhlich O, Yang Y, Klein JD, Sands JM (2006) Loss of N-linked glycosylation reduces urea transporter UT-A1 response to vasopressin. J Biol Chem 281(37):27436–27442
18. Collins D, Winter DC, Hogan AM, Schirmer L, Baird AW, Stewart GS (2010) Differential protein abundance and function of UT-B transporters in human colon. Am J Physiol Gastrointest Liver Physiol 298(3):G345–G351
19. Couriaud C, Ripoche P, Rousselet G (1996) Cloning and functional characterization of a rat urea transporter: Expression in the brain. Biochim Biophys Acta Gene Struct Expression 1309(3):197–199
20. Doran JJ, Klein JD, Kim Y-H, Smith TD, Kozlowski SD, Gunn RB, Sands JM (2006) Tissue distribution of UT-A and UT-B mRNA and protein in rat. Am J Physiol Regul Integr Comp Physiol 290(5):R1446–R1459
21. Doran JJ, Timmer RT, Sands JM (1999) Accurate mRNA size determination in northern analysis using individual lane size markers. Biotechniques 27:280–282
22. Duchesne R, Klein JD, Velotta JB, Doran JJ, Rouillard P, Roberts BR, McDonough AA, Sands JM (2001) UT-A urea transporter protein in heart: increased abundance during uremia, hypertension, and heart failure. Circ Res 89:139–145

23. Fenton RA, Cooper GJ, Morris ID, Smith CP (2002) Coordinated expression of UT-A and UT-B urea transporters in rat testis. Am J Physiol Cell Physiol 282(6):C1492–C1501

24. Fenton RA, Cottingham CA, Stewart GS, Howorth A, Hewitt JA, Smith CP (2002) Structure and characterization of the mouse UT-A gene (*Slc14a2*). Am J Physiol Renal Physiol 282(4):F630–F638

25. Fenton RA, Hewitt JE, Howorth A, Cottingham CA, Smith CP (1999) The murine urea transporter genes *Slc14a1* and *Slc14a2* occur in tandem on chromosome 18. Cytogenet Cell Genet 87(1–2):95–96

26. Fenton RA, Howorth A, Cooper GJ, Meccariello R, Morris ID, Smith CP (2000) Molecular characterization of a novel UT-A urea transporter isoform (UT-A5) in testis. Am J Physiol Cell Physiol 279(5):C1425–C1431

27. Fenton RA, Shodeinde A, Knepper MA (2006) UT-A urea transporter promoter, UT-Aalpha, targets principal cells of the renal inner medullary collecting duct. Am J Physiol Renal Physiol 290(1):F188–F195

28. Fenton RA, Stewart GS, Carpenter B, Howorth A, Potter EA, Cooper GJ, Smith CP (2002) Characterization of the mouse urea transporters UT-A1 and UT-A2. Am J Physiol Renal Physiol 283(4):F817–F825

29. Fines GA, Ballantyne JS, Wright PA (2001) Active urea transport and an unusual basolateral membrane composition in the gills of a marine elasmobranch. Am J Physiol Regul Integr Comp Physiol 280(1):R16–R24

30. Fröhlich O, Klein JD, Smith PM, Sands JM, Gunn RB (2004) Urea transport in MDCK cells that are stably transfected with UT-A1. Am J Physiol Cell Physiol 286(6):C1264–C1270

31. Fröhlich O, Klein JD, Smith PM, Sands JM, Gunn RB (2006) Regulation of UT-A1-mediated transepithelial urea flux in MDCK cells. Am J Physiol Cell Physiol 291:C600–C606

32. Fröhlich O, Macey RI, Edwards-Moulds J, Gargus JJ, Gunn RB (1991) Urea transport deficiency in Jk(a-b-) erythrocytes. Am J Physiol Cell Physiol 260:C778–C783

33. Hall GD, Smith B, Weeks RJ, Selby PJ, Southgate J, Chester JD (2006) Novel Urothelium specific gene expression identified by differential display reverse transcriptase-polymerase chain reaction. J Urol 175(1):337–342

34. Hill WG, Southern NM, MacIver B, Potter E, Apodaca G, Smith CP, Zeidel ML (2005) Isolation and characterization of the Xenopus oocyte plasma membrane: a new method for studying activity of water and solute transporters. Am J Physiol Renal Physiol 289(1):F217–F224

35. Hong X, Xing H, Yu Y, Wen Y, Zhang Y, Zhang S, Tang G, Xu X (2007) Genetic polymorphisms of the urea transporter gene are associated with antihypertensive response to nifedipine GITS. Methods Find Exp Clin Pharmacol 29(1):3–10

36. Hu MC, Bankir L, Michelet S, Rousselet G, Trinh-Trang-Tan M-M (2000) Massive reduction of urea transporters in remnant kidney and brain of uremic rats. Kidney Int 58(3):1202–1210

37. Hung CC, Nawata CM, Wood CM, Wright PA (2008) Rhesus glycoprotein and urea transporter genes are expressed in early stages of development of rainbow trout (Oncorhynchus mykiss). J Exp ZoolPart A EcolGenetPhysiol 309 (5):262–268. doi:10.1002/jez.456

38. Hung CYC, Galvez F, Ip YK, Wood CM (2009) Increased gene expression of a facilitated diffusion urea transporter in the skin of the African lungfish (Protopterus annectens) during massively elevated post-terrestrialization urea excretion. J Exp Biol 212(8):1202–1211

39. Hyodo S, Katoh F, Kaneko T, Takei Y (2004) A facilitative urea transporter is localized in the renal collecting tubule of the dogfish *Triakis scyllia*. J Exp Biol 207:347–356

40. Inoue H, Jackson SD, Vikulina T, Klein JD, Tomita K, Bagnasco SM (2004) Identification and characterization of a Kidd antigen/UT-B urea transporter expressed in human colon. Am J Physiol Cell Physiol 287(1):C30–C35

41. Inoue H, Kozlowski SD, Klein JD, Bailey JL, Sands JM, Bagnasco SM (2005) Regulated expression of the renal and intestinal UT-B urea transporter in response to varying urea load. Am J Physiol Renal Physiol 289(2):F451–F458

42. Irshaid NM, Eicher NI, Hustinx H, Poole J, Olsson ML (2002) Novel alleles at the JK blood group locus explain the absence of the erythrocyte urea transporter in European families. Br J Haematol 116(2):445–453

43. Irshaid NM, Henry SM, Olsson ML (2000) Genomic characterization of the kidd blood group gene: different molecular basis of the Jk(a-b-) phenotype in Polynesians and Finns. Transfusion 40(1):69–74

44. Jung J-Y, Madsen KM, Han K-H, Yang C-W, Knepper MA, Sands JM, Kim J (2003) Expression of urea transporters in potassium-depleted mouse kidney. Am J Physiol Renal Physiol 285(6):F1210–F1224

45. Kakumura K, Watanabe S, Bell JD, Donald JA, Toop T, Kaneko T, Hyodo S (2009) Multiple urea transporter proteins in the kidney of holocephalan elephant fish (Callorhinchus milii). Comp Biochem Physiol B Biochem Mol Biol 154 (2):239–247

46. Karakashian A, Timmer RT, Klein JD, Gunn RB, Sands JM, Bagnasco SM (1999) Cloning and characterization of two new mRNA isoforms of the rat renal urea transporter: UT-A3 and UT-A4. J Am Soc Nephrol 10(2):230–237

47. Kim D-U, Klein JD, Racine S, Murrell BP, Sands JM (2005) Urea may regulate urea transporter protein abundance during osmotic diuresis. Am J Physiol Renal Physiol 288(1):F188–F197

48. Kim Y-H, Kim D-U, Han K-H, Jung J-Y, Sands JM, Knepper MA, Madsen KM, Kim J (2002) Expression of urea transporters in the developing rat kidney. Am J Physiol Renal Physiol 282(3):F530–F540

49. Kiran D, Mutsvangwa T (2010) Effects of partial ruminal defaunation on urea-nitrogen recycling, nitrogen metabolism, and microbial nitrogen supply in growing lambs fed low or high dietary crude protein concentrations. J Anim Sci 88(3):1034–1047

50. Kishore BK, Terris J, Fernandez-Llama P, Knepper MA (1997) Ultramicro-determination of vasopressin-regulated renal urea transporter protein in microdissected renal tubules. Am J Physiol Renal Physiol 272(4):F531–F537

51. Klein JD, Blount MA, Sands JM (2011) Urea transport in the kidney. Compr Physiol Apr 1(2):699–729

52. Klein JD, Blount MA, Fröhlich O, Denson C, Tan X, Sim J, Martin CF, Sands JM (2010) Phosphorylation of UT-A1 on serine 486 correlates with membrane accumulation and urea transport activity in both rat IMCDs and cultured cells. Am J Physiol Renal Physiol 298(4):F935–F940

53. Klein JD, Sands JM, Qian L, Wang X, Yang B (2004) Upregulation of urea transporter UT-A2 and water channels AQP2 and AQP3 in mice lacking urea transporter UT-B. J Am Soc Nephrol 15(5):1161–1167

54. Klein JD, Timmer RT, Rouillard P, Bailey JL, Sands JM (1999) UT-A urea transporter protein expressed in liver: upregulation by uremia. J Am Soc Nephrol 10(10):2076–2083

55. Konno N, Hyodo S, Matsuda K, Uchiyama M (2006) Arginine vasotocin promotes urea permeability through urea transporter expressed in the toad urinary bladder cells. Gen Comp Endocrinol 152(2–3):281–285

56. Konno N, Hyodo S, Matsuda K, Uchiyama M (2006) Effect of osmotic stress on expression of a putative facilitative urea transporter in the kidney and urinary bladder of the marine toad, Bufo marinus. J Exp Biol 209(7):1207–1216

57. Kwun Y-S, Yeo SW, Ahn Y-H, Lim S-W, Jung J-Y, Kim W-Y, Sands JM, Kim J (2003) Immunohistochemical localization of urea transporters A and B in the rat cochlea. Hearing Res 183:84–96

58. Laurent P, Wood CM, Wang Y, Perry SF, Gilmour KM, Part P, Chevalier C, West M, Walsh PJ (2001) Intracellular vesicular trafficking in the gill epithelium of urea-excreting fish. Cell Tissue Res 303(2):197–210

59. Levin MH, de la Fuente R, Verkman AS (2007) Urearetics: a small molecule screen yields nanomolar potency inhibitors of urea transporter UT-B. FASEB J 21(2):551–563

60. Li C, Klein JD, Wang W, Knepper MA, Nielsen S, Sands JM, Frokiaer J (2004) Altered expression of urea transporters in response to ureteral obstruction. Am J Physiol Renal Physiol 286(6):F1154–F1162

61. Lim S-W, Han K-H, Jung J-Y, Kim W-Y, Yang C-W, Sands JM, Knepper MA, Madsen KM, Kim J (2006) Ultrastructural localization of UT-A and UT-B in rat kidneys with different hydration status. Am J Physiol Regul Integr Comp Physiol 290(2):R479–R492

62. Lucien N, Bruneval P, Lasbennes F, Belair MF, Mandet C, Cartron JP, Bailly P, Trinh-Trang-Tan MM (2005) UT-B1 urea transporter is expressed along the urinary and gastrointestinal tracts of the mouse. Am J Physiol Regul Integr Comp Physiol 288(4):R1046–R1056

63. Lucien N, Sidoux-Walter F, Olivès B, Moulds J, Le Pennec PY, Cartron JP, Bailly P (1998) Characterization of the gene encoding the human Kidd blood group urea transporter protein—evidence for splice site mutations in Jk_{null} individuals. J Biol Chem 273(21):12973–12980

64. Lucien N, Sidoux-Walter F, Roudier N, Ripoche P, Huet M, Trinh-Trang-Tan M-M, Cartron J-P, Bailly P (2002) Antigenic and functional properties of the human red blood cell urea transporter hUT-B1. J Biol Chem 277:34101–34108

65. Ludden PA, Stohrer RM, Austin KJ, Atkinson RL, Belden EL, Harlow HJ (2009) Effect of protein supplementation on expression and distribution of urea transporter-B in lambs fed low-quality forage. J Anim Sci 87(4):1354–1365

66. MacIver B, Smith CP, Hill WG, Zeidel ML (2008) Functional characterization of mouse urea transporters UT-A2 and UT-A3 expressed in purified Xenopus laevis oocyte plasma membranes. Am J Physiol Renal Physiol 294(4):F956–F964

67. Mannuzzu LM, Moronne MM, Macey RI (1993) Estimate of the number of urea transport sites in erythrocyte ghosts using a hydrophobic mercurial. J Membr Biol 133:85–97

68. Marini JC, Klein JD, Sands JM, Van Amburgh ME (2004) Effect of nitrogen intake on nitrogen recycling and urea transporter abundance in lambs. J Anim Sci 82:1157–1164

69. Martial S, Olives B, Abrami L, Couriaud C, Bailly P, You G, Hediger MA, Cartron J-P, Ripoche P, Rousselet G (1996) Functional differentiation of the human red blood cell and kidney urea transporters. Am J Physiol Renal Physiol 271(6):F1264–F1268

70. McDonald MD, Smith CP, Walsh PJ (2006) The physiology and evolution of urea transport in fishes. J Membr Biol 212 (2):93–107

71. McDonald MD, Vulesevic B, Perry SF, Walsh PJ (2009) Urea transporter and glutamine synthetase regulation and localization in gulf toadfish gill. J Exp Biol 212(5):704–712

72. McDonald MD, Walsh PJ, Wood CM (2002) Branchial and renal excretion of urea and urea analogues in the plainfin midshipman, *Porichthys notatus*. J Comp Physiol B Biochem System Environ Physiol 172(8):699–712

73. McDonald MD, Wood CM, Wang YX, Walsh PJ (2000) Differential branchial and renal handling of urea, acetamide and thiourea in the gulf toadfish *Opsanus beta*: evidence for two transporters. J Exp Biol 203(6):1027–1037

74. Minocha R, Studley K, Saier MH Jr (2003) The urea transporter (UT) family: bioinformatic analyses leading to structural, functional, and evolutionary predictions. Receptor Channel 9:345–352

75. Mistry AC, Chen G, Kato A, Nag K, Sands JM, Hirose S (2005) A novel type of urea transporter, UT-C, highly expressed in proximal tubule of seawater eel kidney. Am J Physiol Renal Physiol 288(3):F455–F465

76. Morgan RL, Ballantyne JS, Wright PA (2003) Regulation of a renal urea transporter with reduced salinity in a marine elasmobranch. Raja erinacea. J Exp Biol 206(18):3285–3292

77. Morgan RL, Wright PA, Ballantyne JS (2003) Urea transport in kidney brush-border membrane vesicles from an elasmobranch, *Raja erinacea*. J Exp Biol 206(18):3293–3302

78. Nakayama Y, Naruse M, Karakashian A, Peng T, Sands JM, Bagnasco SM (2001) Cloning of the rat Slc14a2 gene and genomic organization of the UT-A urea transporter. Biochim Biophys Acta 1518:19–26

79. Nakayama Y, Peng T, Sands JM, Bagnasco SM (2000) The TonE/TonEBP pathway mediates tonicity-responsive regulation of UT-A urea transporter expression. J Biol Chem 275(49):38275–38280

80. Naruse M, Klein JD, Ashkar ZM, Jacobs JD, Sands JM (1997) Glucocorticoids downregulate the rat vasopressin-regulated urea transporter in rat terminal inner medullary collecting ducts. J Am Soc Nephrol 8(4):517–523

81. Neau P, Degeilh F, Lamotte H, Rousseau B, Ripoche P (1993) Photoaffinity labeling of the human red-blood-cell urea- transporter polypeptide components–possible homology with the kidd blood group antigen. Eur J Biochem 218:447–455

82. Nielsen S, Terris J, Smith CP, Hediger MA, Ecelbarger CA, Knepper MA (1996) Cellular and subcellular localization of the vasopressin-regulated urea transporter in rat kidney. Proc Natl Acad Sci USA 93:5495–5500

83. Ogami A, Miyazaki H, Niisato N, Sugimoto T, Marunaka Y (2006) UT-B1 urea transporter plays a noble role as active water transporter in C6 glial cells. Biochem Biophys Res Commun 351(3):619–624

84. Olivès B, Martial S, Mattei MG, Matassi G, Rousselet G, Ripoche P, Cartron JP, Bailly P (1996) Molecular characterization of a new urea transporter in the human kidney. FEBS Lett 386(2–3):156–160

85. Olivès B, Mattei M-G, Huet M, Neau P, Martial S, Cartron J-P, Bailly P (1995) Kidd blood group and urea transport function of human erythrocytes are carried by the same protein. J Biol Chem 270:15607–15610

86. Olives B, Merriman M, Bailly P, Bain S, Barnett A, Todd J, Cartron JP, Merriman T (1997) The molecular basis of the Kidd blood group polymorphism and its lack of association with type 1 diabetes susceptibility. Hum Mol Genet 6(7):1017–1020

87. Olives B, Neau P, Bailly P, Hediger MA, Rousselet G, Cartron JP, Ripoche P (1994) Cloning and functional expression of a urea transporter from human bone marrow cells. J Biol Chem 269(50):31649–31652

88. Pallone T, Zhang Z, Rhinehart K (2003) Physiology of the renal medullary microcirculation. Am J Physiol Renal Physiol 284:F253–F266

89. Pannabecker TL, Dahlmann A, Brokl OH, Dantzler WH (2000) Mixed descending- and ascending-type thin limbs of Henle's loop in mammalian renal inner medulla. Am J Physiol Renal Physiol 278(2):F202–F208

90. Pannabecker TL, Dantzler WH, Layton HE, Layton AT (2008) Role of three-dimensional architecture in the urine concentrating mechanism of the rat renal inner medulla. Am J Physiol Renal Physiol 295(5):F1271–F1285

91. Pannabecker TL, Henderson CS, Dantzler WH (2008) Quantitative analysis of functional reconstructions reveals lateral and axial zonation in the renal inner medulla. Am J Physiol Renal Physiol 294(6):F1306–F1314

92. Peng T, Sands JM, Bagnasco SM (2002) Glucocorticoids inhibit transcription and expression of the rat UT-A urea transporter gene. Am J Physiol Renal Physiol 282(5):F853–F858

93. Pilley CM, Wright PA (2000) The mechanisms of urea transport by early life stages of rainbow trout (*Oncorhynchus mykiss*). J Exp Biol 203(20):3199–3207

94. Potter EA, Stewart G, Smith CP (2006) Urea flux across MDCK-mUT-A2 monolayers is acutely sensitive to AVP, cAMP, and $[Ca^{2+}]_i$. Am J Physiol Renal Physiol 291(1):F122–F128

95. Prichett WP, Patton AJ, Field JA, Brun KA, Emery JG, Tan KB, Rieman DJ, McClung HA, Nadeau DP, Mooney JL, Suva LJ, Gowen M, Nuttall ME (2000) Identification and cloning of a human urea transporter HUT11, which is downregulated during adipogenesis of explant cultures of human bone. J Cell Biochem 76(4):639–650

96. Promeneur D, Rousselet G, Bankir L, Bailly P, Cartron JP, Ripoche P, Trinh-Trang-Tan MM (1996) Evidence for distinct vascular and tubular urea transporters in the rat kidney. J Am Soc Nephrol 7(6):852–860

97. Ranade K, Wu KD, Hwu CM, Ting CT, Pei D, Pesich R, Hebert J, Chen YDI, Pratt R, Olshen R, Masaki K, Risch N, Cox DR, Botstein D (2001) Genetic variation in the human urea transporter-2 is associated with variation in blood pressure. Hum Mol Genet 10(19):2157–2164

98. Ritzhaupt A, Wood IS, Jackson AA, Moran BJ, Shirazi-Beechey SP (1998) Isolation of a RT-PCR fragment from human colon and sheep rumen RNA with nucleotide sequence similarity to human and rat urea transporter isoforms. Biochem Soc Trans 26:S122

99. Rodela TM, Gilmour KM, Walsh PJ, McDonald MD (2009) Cortisol-sensitive urea transport across the gill basolateral membrane of the gulf toadfish (Opsanus beta). Am J Physiol Regul Integr Comp Physiol 297(2):R313–R322

100. Rousselet G, Ripoche P, Bailly P (1996) Tandem sequence repeats in urea transporters: Identification, of an urea transporter signature sequence. Am J Physiol Renal Physiol 270(3):F554–F555

101. Sands JM (1999) Regulation of renal urea transporters. J Am Soc Nephrol 10(3):635–646

102. Sands JM (1999) Urea transport: It's not just "freely diffusible" anymore. News Physiol Sci 14(1):46–47

103. Sands JM, Gargus JJ, Fröhlich O, Gunn RB, Kokko JP (1992) Urinary concentrating ability in patients with Jk(a-b-) blood type who lack carrier-mediated urea transport. J Am Soc Nephrol 2:1689–1696

104. Sands JM, Timmer RT, Gunn RB (1997) Urea transporters in kidney and erythrocytes. Am J Physiol Renal Physiol 273(3):F321–F339

105. Schmidt C, Hocherl K, Bucher M (2007) Cytokine-mediated regulation of urea transporters during experimental endotoxemia. Am J Physiol Renal Physiol 292(5):F1479–F1489

106. Shayakul C, Knepper MA, Smith CP, DiGiovanni SR, Hediger MA (1997) Segmental localization of urea transporter mRNAs in rat kidney. Am J Physiol Renal Physiol 272(5):F654–F660

107. Shayakul C, Steel A, Hediger MA (1996) Molecular cloning and characterization of the vasopressin-regulated urea transporter of rat kidney collecting ducts. J Clin Invest 98(11):2580–2587

108. Shayakul C, Tsukaguchi H, Berger UV, Hediger MA (2001) Molecular characterization of a novel urea transporter from kidney inner medullary collecting ducts. Am J Physiol Renal Physiol 280(3):F487–F494

109. Sidoux-Walter F, Lucien N, Nissinen R, Sistonen P, Henry S, Moulds J, Cartron J-P, Bailly P (2000) Molecular heterogeneity of the Jk_{null} phenotype: expression analysis of the Jk(S291P) mutation found in Finns. Blood 96(4):1566–1573

110. Sidoux-Walter F, Lucien N, Olivès B, Gobin R, Rousselet G, Kamsteeg EJ, Ripoche P, Deen PMT, Cartron JP, Bailly P (1999) At physiological expression levels the Kidd blood group/urea transporter protein is not a water channel. J Biol Chem 274(42):30228–30235

111. Simmons NL, Chaudhry AS, Graham C, Scriven ES, Thistlethwaite A, Smith CP, Stewart GS (2009) Dietary regulation of ruminal bUT-B urea transporter expression and localization. J Anim Sci 87(10):3288–3299

112. Smith CP, Fenton RA (2006) Genomic organization of the mammalian SLC14a2 urea transporter genes. J Membr Biol 212(2):109–117

113. Smith CP, Lee W-S, Martial S, Knepper MA, You G, Sands JM, Hediger MA (1995) Cloning and regulation of expression of the rat kidney urea transporter (rUT2). J Clin Invest 96(3):1556–1563

114. Smith CP, Potter EA, Fenton RA, Stewart GS (2004) Characterization of a human colonic cDNA encoding a structurally novel urea transporter, UT-A6. Am J Physiol Cell Physiol 287(4):C1087–C1093

115. Spector DA, Yang Q, Liu J, Wade JB (2004) Expression, localization, and regulation of urea transporter B in rat urothelia. Am J Physiol Renal Physiol 287(1):F102–F108

116. Spector DA, Yang Q, Wade JB (2007) High urea and creatinine concentrations and urea transporter B in mammalian urinary tract tissues. Am J Physiol Renal Physiol 292(1):F467–F474

117. Stewart G (2011) The emerging physiological roles of the *SLC14A* family of urea transporters. Br J Pharmacol 164:1780–1792

118. Stewart GS, Fenton RA, Wang W, Kwon TH, White SJ, Collins VM, Cooper G, Nielsen S, Smith CP (2004) The basolateral expression of mUT-A3 in the mouse kidney. Am J Physiol Renal Physiol 286(5):F979–F987

119. Stewart GS, Graham C, Cattell S, Smith TPL, Simmons NL, Smith CP (2005) UT-B is expressed in bovine rumen: potential role in ruminal urea transport. Am J Physiol Regul Integr Comp Physiol 289(2):R605–R612

120. Stewart GS, King SL, Potter EA, Smith CP (2007) Acute regulation of the urea transporter mUT-A3 expressed in a MDCK cell line. Am J Physiol Renal Physiol 292(4):F1157–F1163

121. Terris J, Ecelbarger CA, Sands JM, Knepper MA (1998) Long-term regulation of collecting duct urea transporter proteins in rat. J Am Soc Nephrol 9(5):729–736

122. Terris JM, Knepper MA, Wade JB (2001) UT-A3: localization and characterization of an additional urea transporter isoform in the IMCD. Am J Physiol Renal Physiol 280(2):F325–F332

123. Tickle P, Thistlethwaite A, Smith CP, Stewart GS (2009) Novel bUT-B2 urea transporter isoform is constitutively activated. Am J Physiol Regul Integr Comp Physiol 297(2):R323–R329

124. Timmer RT, Klein JD, Bagnasco SM, Doran JJ, Verlander JW, Gunn RB, Sands JM (2001) Localization of the urea transporter UT-B protein in human and rat erythrocytes and tissues. Am J Physiol Cell Physiol 281(4):C1318–C1325

125. Trinh-Trang-Tan M-M, Cartron JP, Bankir L (2005) Molecular basis for the dialysis disequilibrium syndrome: altered aquaporin and urea transporter expression in the brain. Nephrol Dial Transplant 20(9):1984–1988

126. Trinh-Trang-Tan M-M, Lasbennes F, Gane P, Roudier N, Ripoche P, Cartron J-P, Bailly P (2002) UT-B1 proteins in rat: tissue distribution and regulation by antidiuretic hormone in kidney. Am J Physiol Renal Physiol 283(5):F912–F922

127. Tsukaguchi H, Shayakul C, Berger UV, Tokui T, Brown D, Hediger MA (1997) Cloning and characterization of the urea transporter UT3. Localization in rat kidney and testis. J Clin Invest 99(7):1506–1515

128. Uchiyama M, Kikuchi R, Konno N, Wakasugi T, Matsuda K (2009) Localization and regulation of a facilitative urea transporter in the kidney of the red-eared slider turtle (Trachemys scripta elegans). J Exp Biol 212(2):249–256

129. Uchiyama M, Konno N (2006) Hormonal regulation of ion and water transport in anuran amphibians. Gen Comp Endocrinol 147(1):54–61

130. Wade JB, Lee AJ, Liu J, Ecelbarger CA, Mitchell C, Bradford AD, Terris J, Kim G-H, Knepper MA (2000) UT-A2: a 55 kDa urea transporter protein in thin descending limb of Henle's loop whose abundance is regulated by vasopressin. Am J Physiol Renal Physiol 278(1):F52–F62

131. Wagner L, Klein JD, Sands JM, Baylis C (2002) Urea transporters are widely distributed in endothelial cells and mediate inhibition of L-arginine transport. Am J Physiol Renal Physiol 283(3):F578–F582

132. Walsh PJ, Grosell M, Goss GG, Bergman HL, Bergman AN, Wilson P, Laurent P, Alper SL, Smith CP, Kamunde C, Wood CM (2001) Physiological and molecular characterization of urea transport by the gills of the Lake Magadi tilapia (*Alcolapia grahami*). J Exp Biol 204(3):509–520

133. Walsh PJ, Wood CM, Perry SF, Thomas S (1994) Urea transport by hepatocytes and red blood cells of selected elasmobrach and teleost fishes. J Exp Med 193:321–335

134. Wester ES, Johnson ST, Copeland T, Malde R, Lee E, Storry JR, Olsson ML (2008) Erythroid urea transporter deficiency due to novel JKnull alleles. Transfusion 48 (2):365–372

135. Wilkie MP (2002) Ammonia excretion and urea handling by fish gills: present understanding and future research challenges. J Exp Zool 293(3):284–301

136. C-á Wood, P-á Walsh, S-á Chew, Y-á Ip (2005) Greatly elevated urea excretion after air exposure appears to be carrier mediated in the slender lungfish (Protopterus dolloi). Physiol Biochem Zool 78(6):893–907

137. Wood CM, McDonald MD, Sundin L, Laurent P, Walsh PJ (2003) Pulsatile urea excretion in the gulf toadfish: mechanisms and controls. Comp Biochem Physiol B: Biochem Mol Biol 136(4):667–684

138. Wood CM, Warne JM, Wang YX, McDonald MD, Balment RJ, Laurent P, Walsh PJ (2001) Do circulating plasma AVT and/or cortisol levels control pulsatile urea excretion in the gulf toadfish (*Opsanus beta*)? Comp Biochem Physiol A: Mol Integr Physiol 129(4):859–872

139. Wright PA, Land MD (1998) Urea production and transport in teleost fishes. Comp Biochem Physiol A Comp Physiol 119A(1):47–54
140. Xu Y, Olives B, Bailly P, Fischer E, Ripoche P, Ronco P, Cartron J-P, Rondeau E (1997) Endothelial cells of the kidney vasa recta express the urea transporter HUT11. Kidney Int 51(1):138–146
141. Yamaguchi Y, Takaki S, Hyodo S (2009) Subcellular distribution of urea transporter in the collecting tubule of shark kidney is dependent on environmental salinity. J Exp Zool A Ecol Genet Physiol 311(9):705–718
142. Yang B, Bankir L, Gillespie A, Epstein CJ, Verkman AS (2002) Urea-selective concentrating defect in transgenic mice lacking urea transporter UT-B. J Biol Chem 277:10633–10637
143. Yang BX, Verkman AS (1998) Urea transporter UT3 functions as an efficient water channel—direct evidence for a common water/urea pathway. J Biol Chem 273(16):9369–9372
144. You G, Smith CP, Kanai Y, Lee W-S, Stelzner M, Hediger MA (1993) Cloning and characterization of the vasopressin-regulated urea transporter. Nature 365:844–s847
145. Yuan J, Pannabecker TL (2010) Architecture of inner medullary descending and ascending vasa recta: pathways for countercurrent exchange. Am J Physiol Renal Physiol 299(1):F265–F272
146. Zhai XY, Fenton RA, Andreasen A, Thomsen JS, Christensen AE (2007) Aquaporin-1 is not expressed in descending thin limbs of short-loop nephrons. J Am Soc Nephrol 18:2937–2944
147. Zhao D, Sonawane ND, Levin MH, Yang B (2007) Comparative transport efficiencies of urea analogues through urea transporter UT-B. Biochim Biophys Acta Biomembranes 1768(7):1815–1821

Chapter 5
Structure of Urea Transporters

Elena J. Levin and Ming Zhou

Abstract Members of the urea transporter (UT) family mediate rapid, selective transport of urea down its concentration gradient. To date, crystal structures of two evolutionarily distant UTs have been solved. These structures reveal a common UT fold involving two structurally homologous domains that encircle a continuous membrane-spanning pore and indicate that UTs transport urea via a channel-like mechanism. Examination of the conserved architecture of the pore, combined with crystal structures of ligand-bound proteins, molecular dynamics simulations, and functional data on permeation and inhibition by a broad range of urea analogs and other small molecules, provides insight into the structural basis of urea permeation and selectivity.

Keywords Urea transporter · Urea channel · Membrane proteins · Crystallography · Permeation

Structural Studies of Urea Transporters

Proteins that mediate the movement of ions and small molecules across the lipid bilayer are typically classified into one of two categories based on their mechanism of transport: channels or transporters. Channels function by transporting the substrate along a continuous, semirigid pore that spans from one side of the bilayer to the other. In contrast, transporters have a central binding site for their substrates that is exposed alternately to one side of the bilayer or the other by a series of conformational changes. These different mechanisms have consequences for the functional properties of the transport protein. Channels are able to mediate extremely rapid flux and can discriminate between different substrates based on their size, shape, and other physical and

E.J. Levin · M. Zhou (✉)
Verna and Marrs McLean Department of Biochemistry and Molecular Biology,
Baylor College of Medicine, 1 Baylor Plaza, Houston TX 77030, USA
e-mail: mzhou@bcm.edu

chemical properties, but can only transport substrates along the direction of their electrochemical gradient; transporters typically have slower rates but are able to mediate "uphill" transport by coupling their conformational changes to an energetic driving force, such as a chemical reaction or the downhill transport of a secondary substrate. An indispensible tool for understanding how the functional properties of membrane transport proteins arise is an atomistic understanding of their three-dimensional structures. In this chapter, the structures of two members of the UT family are discussed and interpreted in terms of their mechanisms of permeation and selectivity.

Primary Structure and Function of UT

The amino acid sequences of members of the urea transporter (UT) family are characterized by a number of shared features. UTs generally contain 10 predicted transmembrane helices or, in the case of the UT-A1 isoform, 20 predicted transmembrane helices from two UT domains in tandem. The regions corresponding to the first and last five transmembrane helices in each UT domain have significant homology to each other, indicating that the protein may have arisen from the duplication of an ancestral five-transmembrane helix protein [1]. Another notable feature determined from comparison of UT sequences is that each five-transmembrane repeat contains a conserved signature motif with the consensus sequence LPXXTXPF, which was proposed to play an important role in urea permeation [2]. Functional studies of UTs revealed that the proteins mediate transport of urea passively down its concentration gradient at estimated single-protein rates in the range of 10^4–10^6 molecules per second, are selective for urea and a small number of urea analogs, and that their rates of transport saturate at high concentrations of urea [3–6]. These properties are consistent with the behavior of a membrane channel.

Determination of UT Structures by X-Ray Crystallography

A high-resolution structure is generally a prerequisite to understanding the mechanistic basis of a protein's function. Since bacterial proteins are typically more stable and easier to crystallize, initial efforts to obtain a UT structure by X-ray crystallography focused on bacterial homologs. Bacteria can utilize urea for two purposes: as a source of nitrogen for building amino acids and nucleotides and, in the case of enteric bacteria, to produce ammonia as a buffer against the highly acidic environment of the gastrointestinal system [7, 8]. In 2002, Sebbane and colleagues cloned and sequenced a UT from the enteric pathogen *Yersinia pseudotuberculosis* and demonstrated that it could complement UreI, a proton-gated urea channel from the ulcer-causing pathogen *Helicobacter pylori* [9]. Surprisingly, yUT possessed no detectable homology to UreI, but instead shared 21–25 % sequence identity to the mammalian UTs. As more bacterial genomes became available, other bacterial UTs were identified and characterized, including ApUT from *Actinobacillus*

pleuropneumoniae [10]. ApUT was the first UT to be purified in detergent and reconstituted into proteoliposomes, which were used in stopped-flow fluorimetry assays of urea permeation [11]. ApUT was shown to mediate rapid, downhill flux of urea and was sensitive to inhibition by phloretin, a characteristic property of mammalian UTs [12]. These results demonstrated that bacterial UTs were suitable model systems for structural studies of the UT family. The first crystal structure of a UT family member was the homolog from the bacterium *Desulfovibrio vulgaris*, dvUT [13]. This structure was later followed by the structure of UT-B from bovines, obtained by overexpressing the mammalian protein in insect cells [14].

Characteristics of the Urea Transporter Fold

Topology and Fold of dvUT and UT-B

The dvUT and bovine UT-B structures are highly similar, and both possess the same overall fold. Both proteins form trimers with parallel orientations in the membrane (Fig. 5.1a), with a large cavity at the trimer interface (Fig. 5.1b). The fold of the individual protomers contains a total of fourteen α-helices, including ten that are transmembrane helices and two short helices in the soluble regions of the N- and C-termini (Fig. 5.2a). The remaining two helices are "re-entrant" helices; that is, they form part of structures that enter the membrane on one side, penetrate only partway into the bilayer, and then re-exit on the same side. The two re-entrant helices in the UT structures extend roughly halfway into the membrane and are tilted at approximately 45° relative to the bilayer plane. Assuming that the UT proteins obey the "positive-inside" rule [15], the N- and C-termini are oriented toward the cytoplasm. This topology is consistent with the location of known sites of post-translational modifications, including N-glycosylation sites on the extracellular loop between the fifth and sixth transmembrane helices of both UT-A and UT-B [16, 17] and phosphorylation sites on the N-terminus of UT-A1 and UT-A3 [18].

The first five and last five transmembrane helices in the UT protomer each form a separate domain with an approximate semicircular shape; the two domains also each
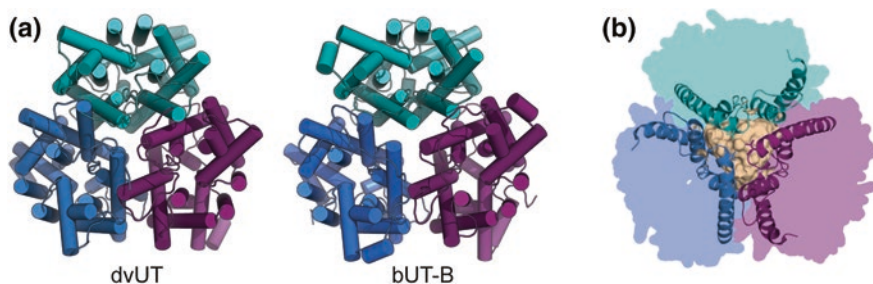

Fig. 5.1 Oligomeric structure of urea transporters. **a** Crystal structures of the dvUT (*left*) and bovine UT-B (*right*) trimers, viewed from the extracellular side. **b** Helices surrounding the cavity at the center of the trimer interface. The surface of the cavity is shown in tan
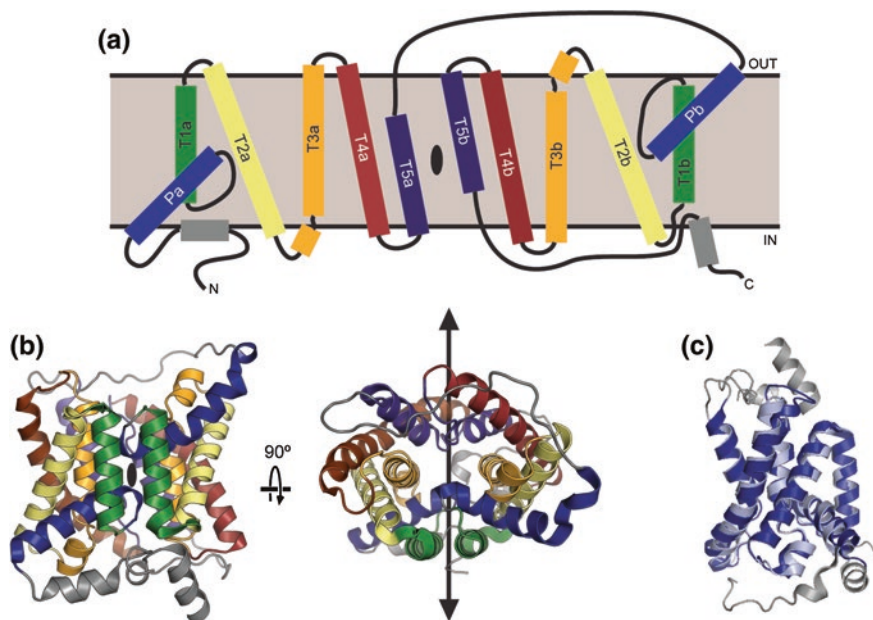
Fig. 5.2 Topology and fold of urea transporters. **a** Topology diagram of a UT protomer. Helices that are equivalent in the inverted repeats are colored in pairs; helices not part of the pseudo-symmetry are *gray*. The location of the pseudosymmetry axis is marked with a *black oval*. **b** Cartoon representation of the bUT-B protomer from two orientations, colored according to the same scheme as in panel **a**. The pseudosymmetry axis is marked with a *black oval* (*left*) or with a *black line* (*right*). **c** The N-(*light blue*) and C-terminal (*dark blue*) halves of bUT-B, comprising the first and last five transmembrane helices, respectively, are shown superposed on each other

contain one re-entrant helix (Fig. 5.2b). Consistent with their sequence homology [1], the two domains are similar and can be aligned with a root mean square deviation (RMSD, a measure of the average distance between equivalent atoms in two structures) of less than 1 Å (Fig. 5.2c). Because their topology is inverted with respect to each other, the two repeats give the UT fold twofold pseudosymmetry along an axis parallel to the plane of the membrane. Inverted internal structural repeats are found frequently in membrane proteins and have been observed previously in a number of channel and transporter folds [19–25]. At the center of the interface between the two domains, intersecting with the pseudosymmetry axis, lies a solvent-accessible pore that spans from one side of the bilayer to the other (Fig. 5.3a).

Conservation with Other UTs

Mammals have two UT genes that, via alternative splicing, are used to construct different proteins with at least five unique transmembrane domains. The bovine UT-B and dvUT have only approximately 33 % sequence identity, and yet the
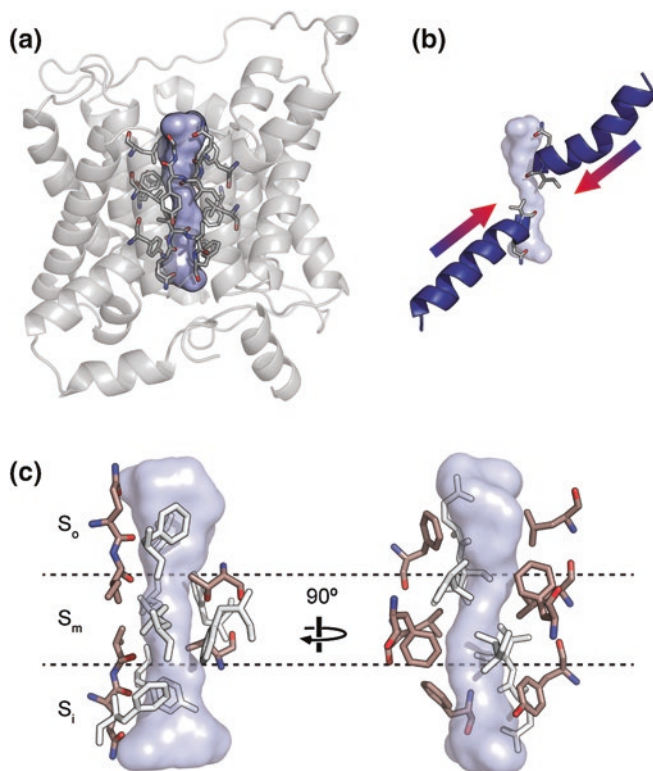
Fig. 5.3 The urea transporter permeation pathway. **a**. The central pore in a bUT-B protomer is shown as a *blue* surface. Residues lining the pore are shown as sticks. **b**. The locations of the pore helices are shown relative to the UT pore. **c**. The UT selectivity filter shown from two orientations, divided into the S_o, S_m, and S_i regions. Conserved residues capable of forming hydrophilic (*left*) or hydrophobic (*right*) interactions with ligands within the filter are highlighted in pink

RMSD between their transmembrane helices is less than 1 Å. It is therefore likely that the basic features of the core hydrophobic regions of UT protomers, including the ten transmembrane helix topology and the location of the permeation pathway, are conserved across the UT family. The soluble regions of the different mammalian UT proteins show more variation: For example, the UT-A isoforms UT-A1 and UT-A3 have an ~90 residue N-terminal domain, predicted to be unstructured, while the N-terminus of UT-B is relatively short, and UT-A1 has an intracellular linker over 100 residues long connecting the two UT domains. Post-translational modifications in these regions likely account for differences in how the mammalian UT isoforms are regulated and trafficked [26].

While the individual subunits of different UT proteins likely have highly similar folds, it is not as clear whether all homologs possess the same oligomeric state. Native gel electrophoresis and a low-resolution projection map from 2D crystals suggested that the bacterial homolog ApUT forms a dimer [11]. Because the UT-A1 isoform contains two tandem UT domains, it cannot form a three-domain

homotrimer similar to UT-B. It is also unlikely that UT-A1 forms a heterotrimer with UT-B or one of the single-domain UT-A isoforms because they are spatially segregated in renal tissues. UT-A3 and UT-A1 are both expressed in the epithelia of the inner medullary collecting ducts, but UT-A1 is localized to the apical membrane [27], while UT-A3 is localized to the basolateral membrane [28]. One possibility is that UT-A forms a higher-order complex than UT-B, such as a hexamer. Because the permeation pathway is enclosed within a single protomer, differences in the number of subunits may not have a significant effect on the function of the protein. Alternatively, urea binding to dvUT was shown to exhibit a Hill coefficient of ~3 [13], which could be indicative of strong positive cooperativity between the different subunits. Additional structural studies on the UT-A homologs will likely be necessary to resolve this issue.

Features of the Permeation Pathway

The UT trimer contains a large cavity at the center of the subunit interface (Fig. 5.1b), but it is blocked from the solvent on both sides of the membrane by hydrophobic residues, and the cavity interior is packed with lipid molecules. It is therefore more likely that the permeation pathway for urea and other solutes is the pore in the middle of each subunit, lined by highly conserved residues (Fig. 5.3a). The structure of this pore is discussed in detail below.

Architecture of the UT Selectivity Filter

The UT pore can be divided into three regions: two hydrophilic vestibules forming the entrances to the pore on either side, which are likely of sufficient width for an entering urea molecule to retain its hydration waters, and a narrower region approximately 15 Å long at the center of the pore, lined with highly conserved residues. This constricted region, referred to as the selectivity filter, ranges in diameter from ~1 to 3 Å across and is roughly rectangular in cross section. The pseudosymmetry axis of the protein runs directly through the center of the pore. The structural elements forming the four walls of the pore are the two pore helices (Fig. 5.3b), the third transmembrane helices from each pseudosymmetry repeat (T3a and T3b), and the fifth transmembrane helices from each repeat (T5a and T5b). These last two helices are actually shorter than the full length of the membrane, so that the regions forming the selectivity filter are unwound and expose backbone elements to the lumen of the pore. This region also corresponds to the location of the conserved signature motifs [2].

    The selectivity filter can be further subdivided into outer, middle, and inner regions, referred to as S_o, S_m, and S_i (Fig. 5.3c). S_o and S_i are related by the pseudosymmetry axis and have a similar architecture. One wall of the pore at these

sites is formed by a row of oxygen atoms contributed by backbone carbonyls and side chains located on the C-terminal ends of the pore helices, which point directly into the selectivity filter. The ability of these atoms to act as hydrogen bond acceptors would therefore likely be strengthened by the helix dipole moments. These oxygen atoms are flanked by hydrophobic residues from T3a and T3b, which form the two perpendicular walls of the selectivity filter. The S_m site is the narrowest region of the pore and is hydrophobic except for a pair of threonine residues from the conserved LPXXTXPF motifs on the N-terminal ends of T5a and T5b. These residues form a hydrogen bond that crosses the center of the selectivity filter.

Comparison with Other Solute Channels

UTs are one of three unrelated families of proteins of known structure that transport urea by a channel-like mechanism. The others are the proton-gated UreI channels [29], most notable for conferring acid resistance to *Helicobacter pylori* [30], and some members of the aquaporin family, often referred to as the aquaglyceroporins, which are capable of transporting urea in addition to water and other small polar molecules such as glycerol [31]. Surprisingly, there is no apparent similarity between the permeation pathways of UTs and UreI, whose selectivity filter is characterized by two constrictions ringed by aromatic residues [29, 32]. In contrast, the permeation pathways of aquaporins show obvious parallels to the UT pore, particularly in the presence of re-entrant helices and exposed backbone carbonyls that stabilize the permeant water molecules through hydrogen bonds. Interestingly, the aquaporins also have a pseudosymmetry axis that intersects the center of the permeation pathway. The center of the pore harbors the NPA motifs, containing two pseudosymmetry-related asparagines that are reminiscent of the central threonines in UT and that contribute to selectivity in aquaporins [33–35].

There are also elements of similarity between the UT pore and the permeation pathways of some ion channels. In tetrameric K^+ channels, the central permeation pathway is encircled by four re-entrant pore helices [36], whose dipole moments are thought to help stabilize K^+ within the hydrophobic core of the membrane [37]. Exposed backbone carbonyls are also key features of the K^+ channel selectivity filter and provide octahedral coordination to replace the hydration sphere on K^+, although these oxygens are located on non-helical segments following the pore helices, rather than being located directly on the helix C-termini. Tilted re-entrant helices also play a role in permeation of chloride ions in the CLC channels [38].

Interestingly, the spatial organization of the ten transmembrane helices in the UT fold is similar to that of the first ten helices in the ammonia transporters of the Amt/Rh family [22, 39, 40]. Because the ammonia transporters lack equivalents to the UT pore helices, their largely hydrophobic pores bear little resemblance to the pores of the UT proteins. However, the similarities in their folds suggest a possible shared evolutionary origin.

Interactions with Ligands and the Structural Basis of Selectivity and Inhibition

The structures of dvUT and bovine UT-B provide a framework for understanding the mechanism of binding and permeation of urea and urea analogs, which, although not naturally occurring compounds, can be useful tools for understanding the structural determinants of selectivity in UTs. The structures may also aid in optimizing the binding of clinically useful UT inhibitors. The structural basis of interactions between UTs and various substrates and inhibitors is discussed below, based on information from crystal structures bound to urea analogs, molecular dynamics simulations, functional studies, and docking models.

Interactions with Urea and Urea Analogs

There are currently no crystal structures available for any UT protein bound to urea, but structures have been solved for dvUT bound to the urea analog 1,3-dimethylurea (DMU) [13] and bovine UT-B bound to selenourea (Fig. 5.4a) [14]. Both structures contain two molecules of the substrate bound to the selectivity filter, one in S_o and the second in S_i (Fig. 5.4b, c). Both DMU and selenourea are oriented with their amide nitrogens positioned to form hydrogen bonds with the oxygen atoms at the ends of the pore helices. In the DMU-bound structure, ordered water molecules are also visible forming hydrogen bonds with the oxygen atoms on both DMU molecules, suggesting that the substrate is not fully desolvated in these regions. Comparison of the binding sites of the two substrates shows that their locations are not exactly equivalent: DMU bound to S_o is positioned to potentially form hydrogen bonds with the first and second oxygen atoms, while selenourea is positioned to interact with the second and third. Similarly, the binding sites are slightly offset in S_i as well. This suggests a mechanism for how the selectivity filter could continuously provide at least two hydrogen bonds to a urea molecule migrating stepwise through the S_o and S_i sites. No electron density corresponding to substrates was observed in the S_m region; however, it remained ambiguous whether this was due to the absence of a stable binding site in this region, or because the larger, impermeable DMU and selenourea analogs could not enter the narrowest region of the pore.

To gain additional information on the interaction between urea and the pore, particularly in the S_m region, molecular dynamics simulations were carried out on bovine UT-B and used to calculate a potential of mean force (PMF) for urea permeation, representing the change in the total energy of the system as a function of the position of urea in the pore [14]. Multiple local energy minima were observed in the S_o and S_i sites, indicating that these regions contain a series of low-affinity urea-binding sites. These minima agree well with the observed positions of urea analogs in the crystal structures. Also, in agreement with the ligand-bound crystal structures, urea in the S_o and S_i sites was still partly solvated and
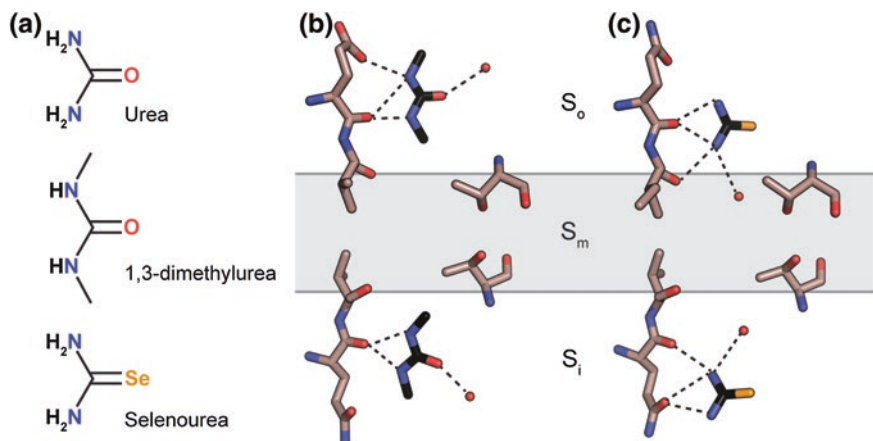
Fig. 5.4 Ligand-binding sites in the urea transporter selectivity filter. **a** The chemical structures of urea, dimethylurea (DMU), and selenourea. **b**, **c** The locations of DMU molecules in the dvUT structure (**a**) and selenourea molecules in the bUT-B structure (**b**) are shown relative to the oxygens lining one side of the selectivity filter. The central threonines in the S_m site and ordered water molecules within hydrogen bonding distance to the bound substrates are shown as well

oriented in alignment to the pore helix dipoles. Upon entering the S_m site, urea was completely stripped of hydration waters and the PMF exhibits a large energy barrier, with a maximal ΔG of ~5 kcal/mol. No conformational changes other than thermal fluctuations were required for urea to pass completely through the pore, confirming that UTs are channels, not transporters.

Of the different UTs, the selectivity of UT-B has been the most thoroughly characterized due in part to the early development of assays for measuring substrate flux through UT-B in erythrocytes [41–43]. This approach has been used to test the selectivity of UT-B with a large number of urea analogues [6]. The channel can permeate formamide and acetamide at rates close to those for urea, indicating that loss or substitution of one amide nitrogen is tolerated. Transport is significantly decreased by changes to the substrate that increase the size and decrease the strength of potential hydrogen bonds, such as substitution of the oxygen atom with sulfur in thiourea, or N-methylation of the amides in DMU; however, both of these compounds are effective inhibitors of UT-B. The structural data discussed above provide a rationale for this behavior: DMU and thiourea are able to compete with urea for binding to the S_o and S_i sites, but have difficulty permeating through the constricted S_m site.

In comparison with UT-B, functional data on UT-A are relatively scarce; however, transport through mouse UT-A2 and UT-A3 has been measured in vesicles derived from oocyte plasma membranes [3]. Both homologs exhibited higher selectivity than UT-B and did not permeate any of the tested urea analogs, including formamide and acetamide. The residues forming the selectivity filter in both UT-A domains and UT-B are similar, and the structural basis for this difference in selectivity is not yet understood.

Interactions with Other Natural Substrates

The permeation of water through UT-B, although initially controversial [44, 45], has since been well established [43, 46, 47]. Recent estimates of the rate of water permeation through UT-B are similar to those measured for aquaporins [48]. Given the similarities between the architecture of the aquaporin and UT pores discussed above, this result is not entirely surprising. Molecular dynamics simulations of water permeation through a homology model of human UT-B, based on the bovine UT-B structure, suggest that the magnitude of the energy barrier for water permeation is similar to that observed for aquaporins [48]. The observation that UT-B is an efficient water channel raises the question of how protons are excluded from leaking through the pore. In aquaporins, proton exclusion has been attributed primarily to two electrostatic barriers: one at a constriction formed by positively charged residues and another at the NPA motifs, where the positive ends of two helix dipoles point into the pore [49, 50]. In contrast, the UT selectivity filter lacks any positively charged side chains, and the orientations of the two pore helices are reversed relative to aquaporins, leading to a negative potential at the S_m site rather than a positive one. Interestingly, molecular dynamics simulations predict that water permeating through UT-B undergoes a reversal of the orientation of its dipole moment correlated with passage through the S_m site [48]. A similar change in orientation was predicted by molecular dynamics simulations in aquaporins [51, 52] and recently gained experimental support from an ultra-high crystal structure of a yeast aquaporin [53]. This re-orientation was proposed to play a role in proton exclusion in aquaporins.

Permeability of human UT-B to ammonia, but not ammonium, has also been reported recently [54]. Molecular dynamics simulations suggest that the ammonia is transported via the same central pore that serves as the urea and water permeation pathway and that the energetics of permeation are similar to those for water, including the location and size of the central energy barrier at the S_m site.

The ability to transport water and ammonia has also been assayed for UT-A. UT-A2 and UT-A3 were found to be impermeable to both compounds [3]. This observation fits with the overall pattern of higher selectivity for the UT-A isoforms. Given that the rate of flux through UT-A is one to two orders of magnitude slower than UT-B [3, 4], the diameter of the S_m site could be smaller, resulting in a higher-energy barrier. However, it is counterintuitive to imagine that a narrower permeation pathway could result in an improved ability of the channel to reject substrates smaller than its native ligand. The residues that line the selectivity filter are well conserved between UT-A2, UT-A3, and UT-B, including at the S_m site, making it difficult to ascertain the basis for these differences without a UT-A crystal structure.

Inhibitors of UT Permeation

In addition to urea analogs, there are a number of organic compounds that are structurally unrelated to urea known to inhibit UTs. The plant flavonoid phloretin was the first compound of this class to be discovered and inhibits UTs with micromolar

affinity [55]. However, phloretin is a relatively non-selective inhibitor of a large number of structurally unrelated transport proteins [56–60] and may modulate transport by directly affecting the physical properties of the lipid bilayer [61, 62]. More recently, the search for novel diuretics has lead to the discovery of multiple classes of high-affinity inhibitors of the mammalian UTs [63–68], including compounds that are selective for UT-B over UT-A [68] and vice versa [64]. Currently, there is no crystal structure available for any of these compounds bound to the protein. Given the large size of the inhibitors relative to the dimensions of the pore, they seem unlikely to bind at the predicted urea-binding sites within the selectivity filter itself, but curiously, the IC_{50}s of the triazolothienopyrimidine UT-B inhibitors were sensitive to the magnitude of the urea gradient, suggesting a competitive mechanism of inhibition involving shared binding sites. In contrast, the UT-A selective compounds exhibited non-competitive inhibition [64]. By measuring the kinetics of inhibition, Yao et al. were able to demonstrate that the triazolothienopyrimidine-derived UT-B selective inhibitors must diffuse through the bilayer and bind to the intracellular side of protein [68]; similar experiments demonstrated that non-selective thienoquinolin inhibitors block from the intracellular side [66], and selective UT-A inhibitors bound to either the intracellular or extracellular side [64]. Computational docking models predict that these compounds block the pores by binding to the vestibules immediately outside of the selectivity filter.

References

1. Minocha R, Studley K, Saier MH Jr (2003) The urea transporter (UT) family: bioinformatic analyses leading to structural, functional, and evolutionary predictions. Receptors Channels 9:345–352
2. Rousselet G, Ripoche P, Bailly P (1996) Tandem sequence repeats in urea transporters: identification of an urea transporter signature sequence. Am J Physiol 270:F554–F555
3. Maciver B, Smith CP, Hill WG, Zeidel ML (2008) Functional characterization of mouse urea transporters UT-A2 and UT-A3 expressed in purified Xenopus laevis oocyte plasma membranes. Am J Physiol Renal Physiol 294:F956–F964
4. Mannuzzu LM, Moronne MM, Macey RI (1993) Estimate of the number of urea transport sites in erythrocyte ghosts using a hydrophobic mercurial. J Membr Biol 133:85–97
5. Mayrand RR, Levitt DG (1983) Urea and ethylene glycol-facilitated transport systems in the human red cell membrane. Saturation, competition, and asymmetry. J Gen Physiol 81:221–237
6. Zhao D, Sonawane ND, Levin MH, Yang B (2007) Comparative transport efficiencies of urea analogues through urea transporter UT-B. Biochim Biophys Acta 1768:1815–1821
7. Marcus EA, Moshfegh AP, Sachs G, Scott DR (2005) The periplasmic alpha-carbonic anhydrase activity of Helicobacter pylori is essential for acid acclimation. J Bacteriol 187:729–738
8. Young GM, Amid D, Miller VL (1996) A bifunctional urease enhances survival of pathogenic *Yersinia enterocolitica* and *Morganella morganii* at low pH. J Bacteriol 178:6487–6495
9. Sebbane F, Bury-Mone S, Cailliau K, Browaeys-Poly E, De Reuse H, Simonet M (2002) The Yersinia pseudotuberculosis Yut protein, a new type of urea transporter homologous to eukaryotic channels and functionally interchangeable in vitro with the Helicobacter pylori UreI protein. Mol Microbiol 45:1165–1174

10. Godara G, Smith C, Bosse J, Zeidel M, Mathai J (2009) Functional characterization of *Actinobacillus pleuropneumoniae* urea transport protein, ApUT. Am J Physiol Regul Integr Comp Physiol 296:R1268–R1273

11. Raunser S, Mathai JC, Abeyrathne PD, Rice AJ, Zeidel ML, Walz T (2009) Oligomeric structure and functional characterization of the urea transporter from Actinobacillus pleuropneumoniae. J Mol Biol 387:619–627

12. Hediger MA, Smith CP, You G, Lee WS, Kanai Y, Shayakul C (1996) Structure, regulation and physiological roles of urea transporters. Kidney Int 49:1615–1623

13. Levin EJ, Quick M, Zhou M (2009) Crystal structure of a bacterial homologue of the kidney urea transporter. Nature 462:757–761

14. Levin EJ, Cao Y, Enkavi G, Quick M, Pan Y, Tajkhorshid E, Zhou M (2012) Structure and permeation mechanism of a mammalian urea transporter. Proc Natl Acad Sci USA 109:11194–11199

15. von Heijne G, Gavel Y (1988) Topogenic signals in integral membrane proteins. Eur J Biochem 174:671–678

16. Tsukaguchi H, Shayakul C, Berger UV, Tokui T, Brown D, Hediger MA (1997) Cloning and characterization of the urea transporter UT3: localization in rat kidney and testis. J Clin Invest 99:1506–1515

17. You G, Smith CP, Kanai Y, Lee WS, Stelzner M, Hediger MA (1993) Cloning and characterization of the vasopressin-regulated urea transporter. Nature 365:844–847

18. Bansal AD, Hoffert JD, Pisitkun T, Hwang S, Chou CL, Boja ES, Wang G, Knepper MA (2010) Phosphoproteomic profiling reveals vasopressin-regulated phosphorylation sites in collecting duct. J Am Soc Nephrol 21:303–315

19. Abramson J, Smirnova I, Kasho V, Verner G, Kaback HR, Iwata S (2003) Structure and mechanism of the lactose permease of Escherichia coli. Science 301:610–615

20. Hu NJ, Iwata S, Cameron AD, Drew D (2011) Crystal structure of a bacterial homologue of the bile acid sodium symporter ASBT. Nature 478:408–411

21. Huang Y, Lemieux MJ, Song J, Auer M, Wang DN (2003) Structure and mechanism of the glycerol-3-phosphate transporter from Escherichia coli. Science 301:616–620

22. Khademi S, O'Connell J 3rd, Remis J, Robles-Colmenares Y, Miercke LJ, Stroud RM (2004) Mechanism of ammonia transport by Amt/MEP/Rh: structure of AmtB at 1.35 A. Science 305:1587–1594

23. Liao J, Li H, Zeng W, Sauer DB, Belmares R, Jiang Y (2012) Structural insight into the ion-exchange mechanism of the sodium/calcium exchanger. Science 335:686–690

24. Yamashita A, Singh SK, Kawate T, Jin Y, Gouaux E (2005) Crystal structure of a bacterial homologue of Na^+/Cl^- dependent neurotransmitter transporters. Nature 437:215–223

25. Yernool D, Boudker O, Jin Y, Gouaux E (2004) Structure of a glutamate transporter homologue from *Pyrococcus horikoshii*. Nature 431:811–818

26. Klein JD, Blount MA, Sands JM (2011) Urea transport in the kidney. Compr Physiol 1:699–729

27. Nielsen S, Terris J, Smith CP, Hediger MA, Ecelbarger CA, Knepper MA (1996) Cellular and subcellular localization of the vasopressin- regulated urea transporter in rat kidney. Proc Natl Acad Sci USA 93:5495–5500

28. Stewart GS, Fenton RA, Wang W, Kwon TH, White SJ, Collins VM, Cooper G, Nielsen S, Smith CP (2004) The basolateral expression of mUT-A3 in the mouse kidney. Am J Physiol Renal Physiol 286:F979–F987

29. Strugatsky D, McNulty R, Munson K, Chen CK, Soltis SM, Sachs G, Luecke H (2013) Structure of the proton-gated urea channel from the gastric pathogen *Helicobacter pylori*. Nature 493:255–258

30. Weeks DL, Eskandari S, Scott DR, Sachs G (2000) A H^+ -gated urea channel: the link between *Helicobacter pylori* urease and gastric colonization. Science 287:482–485

31. Newby ZE, O'Connell J 3rd, Robles-Colmenares Y, Khademi S, Miercke LJ, Stroud RM (2008) Crystal structure of the aquaglyceroporin PfAQP from the malarial parasite Plasmodium falciparum. Nat Struct Mol Biol 15:619–625

32. McNulty R, Ulmschneider JP, Luecke H, Ulmschneider MB (2013) Mechanisms of molecular transport through the urea channel of Helicobacter pylori. Nat Commun 4:2900

33. Murata K, Mitsuoka K, Hirai T, Walz T, Agre P, Heymann JB, Engel A, Fujiyoshi Y (2000) Structural determinants of water permeation through aquaporin-1. Nature 407:599–605

34. Wang Y, Schulten K, Tajkhorshid E (2005) What makes an aquaporin a glycerol channel? A comparative study of AqpZ and GlpF. Structure 13:1107–1118

35. Wree D, Wu B, Zeuthen T, Beitz E (2011) Requirement for asparagine in the aquaporin NPA sequence signature motifs for cation exclusion. FEBS J 278:740–748

36. Doyle DA, Morais Cabral J, Pfuetzner RA, Kuo A, Gulbis JM, Cohen SL, Chait BT, MacKinnon R (1998) The structure of the potassium channel: molecular basis of K$^+$ conduction and selectivity. Science 280:69–77

37. Roux B, MacKinnon R (1999) The cavity and pore helices in the KcsA K$^+$ channel: electrostatic stabilization of monovalent cations. Science 285:100–102

38. Dutzler R, Campbell EB, Cadene M, Chait BT, MacKinnon R (2002) X-ray structure of a ClC chloride channel at 3.0 A reveals the molecular basis of anion selectivity. Nature 415:287–294

39. Gruswitz F, Chaudhary S, Ho JD, Schlessinger A, Pezeshki B, Ho CM, Sali A, Westhoff CM, Stroud RM (2010) Function of human Rh based on structure of RhCG at 2.1 A. Proc Natl Acad Sci USA 107:9638–9643

40. Lupo D, Li XD, Durand A, Tomizaki T, Cherif-Zahar B, Matassi G, Merrick M, Winkler FK (2007) The 1.3-A resolution structure of Nitrosomonas europaea Rh50 and mechanistic implications for NH3 transport by Rhesus family proteins. Proc Natl Acad Sci USA 104:19303–19308

41. Chasan B, Solomon AK (1985) Urea reflection coefficient for the human red cell membrane. Biochim Biophys Acta 821:56–62

42. Levitt DG, Mlekoday HJ (1983) Reflection coefficient and permeability of urea and ethylene glycol in the human red cell membrane. J Gen Physiol 81:239–253

43. Yang B, Verkman AS (1998) Urea transporter UT3 functions as an efficient water channel. Direct evidence for a common water/urea pathway. J Biol Chem 273:9369–9372

44. Martial S, Olives B, Abrami L, Couriaud C, Bailly P, You G, Hediger MA, Cartron JP, Ripoche P, Rousselet G (1996) Functional differentiation of the human red blood cell and kidney urea transporters. Am J Physiol 271:F1264–F1268

45. Sidoux-Walter F, Lucien N, Olives B, Gobin R, Rousselet G, Kamsteeg EJ, Ripoche P, Deen PM, Cartron JP, Bailly P (1999) At physiological expression levels the Kidd blood group/urea transporter protein is not a water channel. J Biol Chem 274:30228–30235

46. Meng Y, Zhou X, Li Y, Zhao D, Liang S, Zhao X, Yang B (2005) A novel mutation at the JK locus causing Jk null phenotype in a Chinese family. Sci China C Life Sci 48:636–640

47. Yang B, Verkman AS (2002) Analysis of double knockout mice lacking aquaporin-1 and urea transporter UT-B. Evidence for UT-B-facilitated water transport in erythrocytes. J Biol Chem 277:36782–36786

48. Azouzi S, Gueroult M, Ripoche P, Genetet S, Aronovicz YC, Le Van Kim C, Etchebest C, Mouro-Chanteloup I (2013) Energetic and molecular water permeation mechanisms of the human red blood cell urea transporter B. PLoS One 8:e82338

49. Beitz E, Wu B, Holm LM, Schultz JE, Zeuthen T (2006) Point mutations in the aromatic/arginine region in aquaporin 1 allow passage of urea, glycerol, ammonia, and protons. Proc Natl Acad Sci USA 103:269–274

50. Wu B, Steinbronn C, Alsterfjord M, Zeuthen T, Beitz E (2009) Concerted action of two cation filters in the aquaporin water channel. EMBO J 28:2188–2194

51. de Groot BL, Grubmuller H (2001) Water permeation across biological membranes: mechanism and dynamics of aquaporin-1 and GlpF. Science 294:2353–2357

52. Tajkhorshid E, Nollert P, Jensen MO, Miercke LJ, O'Connell J, Stroud RM, Schulten K (2002) Control of the selectivity of the aquaporin water channel family by global orientational tuning. Science 296:525–530

53. Kosinska Eriksson U, Fischer G, Friemann R, Enkavi G, Tajkhorshid E, Neutze R (2013) Subangstrom resolution X-ray structure details aquaporin-water interactions. Science 340:1346–1349

54. Geyer RR, Musa-Aziz R, Enkavi G, Mahinthichaichan P, Tajkhorshid E, Boron WF (2013) Movement of NH(3) through the human urea transporter B: a new gas channel. Am J Physiol Renal Physiol 304:F1447–F1457

55. Chou CL, Knepper MA (1989) Inhibition of urea transport in inner medullary collecting duct by phloretin and urea analogues. Am J Physiol 257:F359–F365

56. Fan HT, Morishima S, Kida H, Okada Y (2001) Phloretin differentially inhibits volume-sensitive and cyclic AMP-activated, but not Ca-activated, Cl(−) channels. Br J Pharmacol 133:1096–1106

57. Tsukaguchi H, Shayakul C, Berger UV, Mackenzie B, Devidas S, Guggino WB, van Hoek AN, Hediger MA (1998) Molecular characterization of a broad selectivity neutral solute channel. J Biol Chem 273:24737–24743

58. Wang Y, Mackenzie B, Tsukaguchi H, Weremowicz S, Morton CC, Hediger MA (2000) Human vitamin C (L-ascorbic acid) transporter SVCT1. Biochem Biophys Res Commun 267:488–494

59. Wheeler TJ, Hinkle PC (1981) Kinetic properties of the reconstituted glucose transporter from human erythrocytes. J Biol Chem 256:8907–8914

60. Xiang M, Feng M, Muend S, Rao R (2007) A human Na^+/H^+ antiporter sharing evolutionary origins with bacterial NhaA may be a candidate gene for essential hypertension. Proc Natl Acad Sci USA 104:18677–18681

61. Andersen OS, Finkelstein A, Katz I, Cass A (1976) Effect of phloretin on the permeability of thin lipid membranes. J Gen Physiol 67:749–771

62. Cseh R, Benz R (1999) Interaction of phloretin with lipid monolayers: relationship between structural changes and dipole potential change. Biophys J 77:1477–1488

63. Anderson MO, Zhang J, Liu Y, Yao C, Phuan PW, Verkman AS (2012) Nanomolar potency and metabolically stable inhibitors of kidney urea transporter UT-B. J Med Chem 55:5942–5950

64. Esteva-Font C, Phuan PW, Anderson MO, Verkman AS (2013) A small molecule screen identifies selective inhibitors of urea transporter UT-A. Chem Biol 20:1235–1244

65. Levin MH, de la Fuente R, Verkman AS (2007) Urearetics: a small molecule screen yields nanomolar potency inhibitors of urea transporter UT-B. FASEB J 21:551–563

66. Li F, Lei T, Zhu J, Wang W, Sun Y, Chen J, Dong Z, Zhou H, Yang B (2013) A novel small-molecule thienoquinolin urea transporter inhibitor acts as a potential diuretic. Kidney Int 83:1076–1086

67. Liu Y, Esteva-Font C, Yao C, Phuan PW, Verkman AS, Anderson MO (2013) 1,1-Difluoroethyl-substituted triazolothienopyrimidines as inhibitors of a human urea transport protein (UT-B): new analogs and binding model. Bioorg Med Chem Lett 23:3338–3341

68. Yao C, Anderson MO, Zhang J, Yang B, Phuan PW, Verkman AS (2012) Triazolothien-opyrimidine inhibitors of urea transporter UT-B reduce urine concentration. J Am Soc Nephrol 23:1210–1220

Chapter 6
Expression of Urea Transporters and Their Regulation

Janet D. Klein

Abstract UT-A and UT-B families of urea transporters consist of multiple isoforms that are subject to regulation of both acutely and by long-term measures. This chapter provides a brief overview of the expression of the urea transporter forms and their locations in the kidney. Rapid regulation of UT-A1 results from the combination of phosphorylation and membrane accumulation. Phosphorylation of UT-A1 has been linked to vasopressin and hyperosmolality, although through different kinases. Other acute influences on urea transporter activity are ubiquitination and glycosylation, both of which influence the membrane association of the urea transporter, again through different mechanisms. Long-term regulation of urea transport is most closely associated with the environment that the kidney experiences. Low-protein diets may influence the amount of urea transporter available. Conditions of osmotic diuresis, where urea concentrations are low, will prompt an increase in urea transporter abundance. Although adrenal steroids affect urea transporter abundance, conflicting reports make conclusions tenuous. Urea transporters are upregulated when P2Y2 purinergic receptors are decreased, suggesting a role for these receptors in UT regulation. Hypercalcemia and hypokalemia both cause urine concentration deficiencies. Urea transporter abundances are reduced in aging animals and animals with angiotensin-converting enzyme deficiencies. This chapter will provide information about both rapid and long-term regulation of urea transporters and provide an introduction into the literature.

Keywords Urea · Urea transporter · Vasopressin · dDAVP · Osmolality · Phosphorylation

—————————————
J.D. Klein (✉)
Renal Division, Department of Medicine and Department of Physiology, Emory University School of Medicine, WMB Room 3319B, 1639 Pierce Drive, NE, Atlanta, GA 30322, USA
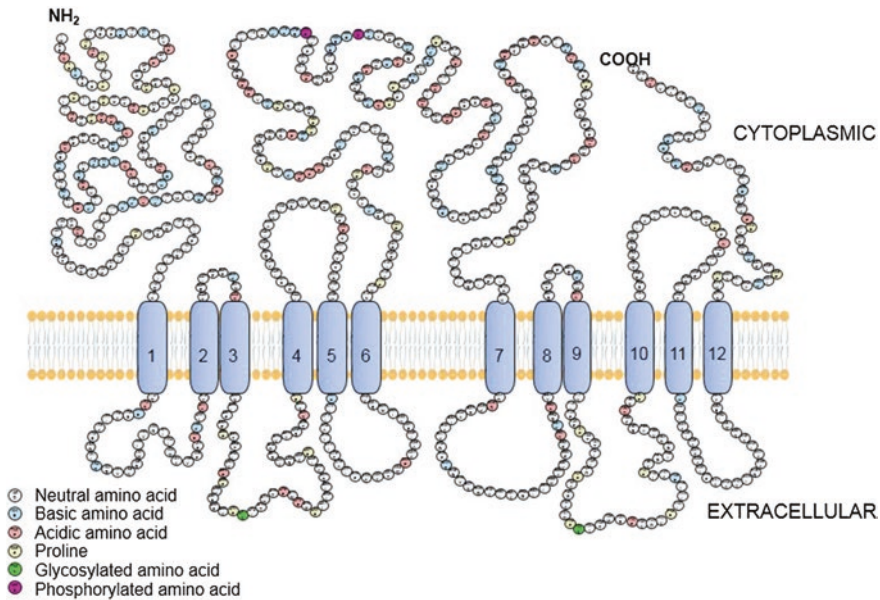e-mail: janet.klein@emory.edu

Fig. 6.1 Schematic representation of the amino acid sequence and primary structure of UT-A1. Reproduced courtesy of comprehensive physiology [92]

Tissue Distribution of Urea Transporters

The urea transporters are grouped into two families, SLC14a1 and SLC14a2 that are more commonly known as the UT-B and UT-A urea transporters, respectively. The urea transporter genes and proteins are described in Chap. 5 of this book. Both of these families have multiple isoforms and all of these forms are regulated both acutely and under long-term control. In this chapter, we will examine the tissue and intracellular localization and regulation of these transporter proteins.

A brief recap: UT-A1 protein is expressed in the apical plasma membrane and intracellularly in the terminal IMCD in rats [16, 35, 88, 91, 114, 132] and humans [7]. The full length UT-A1 has a base molecular weight about 88 kDa and exists as two major glycoprotein forms that migrate at 97 and 117 kDa on denaturing polyacrylamide electrophoresis gels. The primary sequence and proposed secondary sequence are provided in Fig. 6.1. Polyclonal antibodies have been raised against three portions of UT-A1: the c-terminus (which identifies UT-A1, UT-A2, and UT-A4, based on molecular weight) [125, 132, 181, 193], the N-terminal region (which identifies UT-A1, UT-A3, and UT-A4); and an intracellular loop region which identifies only UT-A1 [45, 80, 146, 181, 182]. All of these antibodies identify both the 117 and 97 kDa glycoprotein forms of UT-A1. UT-A3 is essentially the NH$_2$ terminal half of UT-A1 (Fig. 6.2). Like UT-A1, UT-A3 is expressed only in the IMCD [44, 80, 164]. UT-A2 consists of the carboxy terminal half of UT-A1

Fig. 6.2 Schematic representation of the general structure of UT-A3. Ball and line drawing referable to Fig. 6.1 for UT-A1
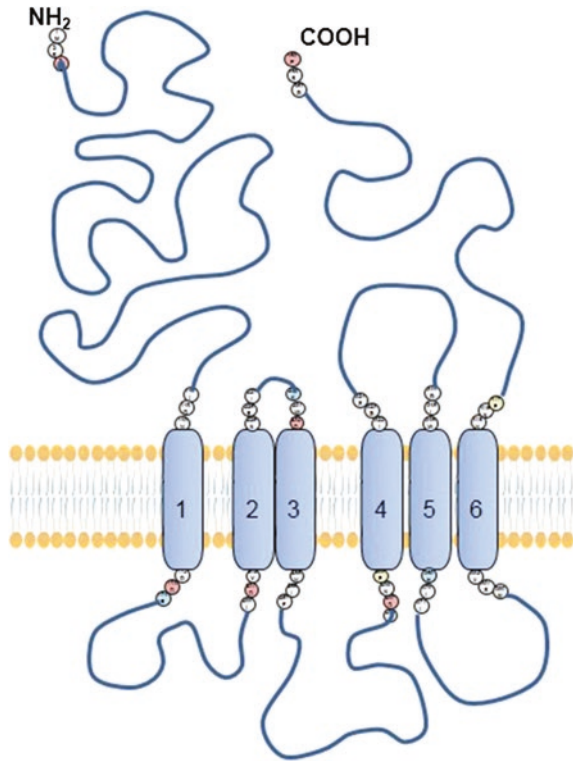
from amino acids 533–929 (Fig. 6.3) and is found mainly in the thin descending limb of the loop of Henle. The C-terminal antibody to UT-A1 also detects UT-A2 as a 55 kDa protein band on Western blot of inner medullary proteins. UT-A2 is also detected in liver and heart as 55 and 39 kDa proteins bands. Immunohistochemistry shows that UT-A2 is expressed in tDLs. UT-A2 is confined to the last 28–44 % of the tDL of short-looped nephrons. UT-A4 consists of the N-terminal quarter of UT-A1 spliced into the C-terminal quarter of UT-A1 [80]. UT-A4 mRNA is expressed in rat kidney medulla but endogenous expression of UT-A4 protein in the kidney has not been verified. UT-A5 and UT-A6 are expressed in mouse testis and human colon, respectively, and have not been detected in kidney [45, 168].

UT-B1 protein is detected on Western blot as a broadband between 45 and 65 kDa in human red blood cells and 37–51 kDa in rat or mouse red blood cells [186, 203]. UT-B1 is detected in kidney medulla as a broadband between 41 and 54 kDa [186]. Immunohistological analysis of human and rodent kidneys show UT-B1 in endothelial cells (non-fenestrated) that identify descending vasa recta [60, 135, 186, 188, 201, 203]. In particular, UT-B1 is found in descending vasa recta external to collecting duct clusters [136]. UT-B1 protein is also present in rat testis, brain, colon, heart, liver, lung, aorta, cochlea, muscle, mesenteric artery, and urothelia [30, 35, 41, 60, 67, 105, 115, 169, 186, 187, 194]. UT-B2, a second
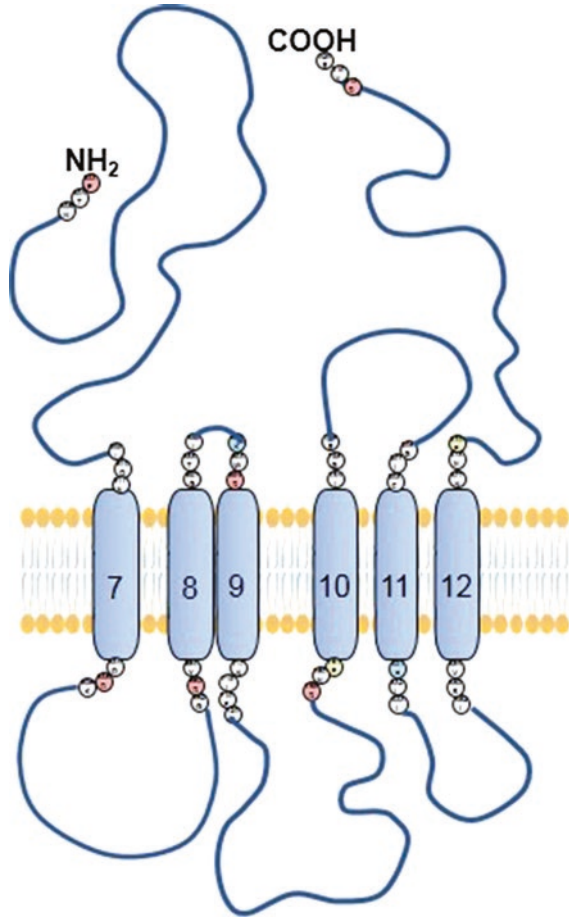
Fig. 6.3 Schematic representation of the general structure of UT-A2. Ball and line drawing referable to Fig. 6.1 for UT-A1

isoform, is expressed in the rumen of sheep and cows and in bovine parotid salivary gland [34]. This UT-B isoform is sensitive to pH environments [1, 90, 116, 119, 166, 173]. Recently, UT-A1 but not UT-A2 or UT-B1 was shown to be affected to dietary nitrogen in goat kidney [172].

The reduction of urine concentrating ability in mice lacking UT-B [10] is consistent with decreased concentrating ability in animal models, where UT-B1 protein abundance is decreased, such as with potassium deprivation [77], ureteral obstruction [110], water loading [114], and severe inflammation [158]. In addition to having a role in urine concentration, studies of UT-B knockout mice suggest that this protein is important in cardiac conduction, since deletion of UT-B results in altered development of troponin T and atrial natriuretic peptide, as well as progressive heart block in these mice [120, 212]. A recent report suggests that UT-B1 can transport both water and NH_3 gas as well as urea presenting some new regulatory possibilities for function of this transporter [51].

Rapid Regulation of Urea Transport

The isolated perfused tubule technique has been the primary method for investigating the rapid regulation of urea transport [153, 155]. This approach provides functional information that is physiologically relevant. However, in the IMCD, it cannot determine which urea transporter is responsible for a functional effect since it expresses both UT-A1 and UT-A3. Functional studies show that phloretin-inhibitable urea transport is present in both the apical and basolateral plasma membranes of rat terminal IMCDs with the apical membrane being the rate-limiting barrier for vasopressin-stimulated urea transport [170]. The availability of antibodies that detect specific urea transporters and their localization and the generation of stably transfected cell lines expressing a single urea transporter have provided the opportunity to assess the roles of UT-A1 and UT-A3 in the rapid regulation of urea transport in the IMCD. The UT-A1/UT-A3 double knockout mouse is not able to concentrate urea [43, 65]. Figure 6.4 shows the urine osmolalities of wild-type and UT-A1/UT-A3 knockout mice. Under baseline conditions, the knockout mice produce urine that is much more dilute than the wild-type mice, and even when stimulated to concentrate with vasopressin, the knockout mice are unable to improve their urine osmolality (Fig. 6.4). Recently, a mouse that expresses UT-A1 but lacks UT-A3 (UT-A1$^{+/+}$/UT-A3$^{-/-}$) has been generated [93]. This is the first mouse model that contains only one of the UT-A urea transporters and it is capable of concentrating urine to levels that are close to those in control animals. Treatment of UT-A1$^{+/+}$/UT-A3$^{-/-}$ mice with vasopressin increases urine osmolality. In order to better understand the separate roles for

Fig. 6.4 Animals lacking UT-A1 and UT-A3 are unable to concentrate their urine. Shown are average urine osmolalities from wild-type mice and UT-A1/A3 knockout (KO) mice. The number of animals per group varied from 8 to 14. Mice were treated with arginine vasopressin (+AVP) or vehicle (−AVP) for 7 days before urine was collected, and osmolality measured using a vapor pressure osmometer. * = significantly different
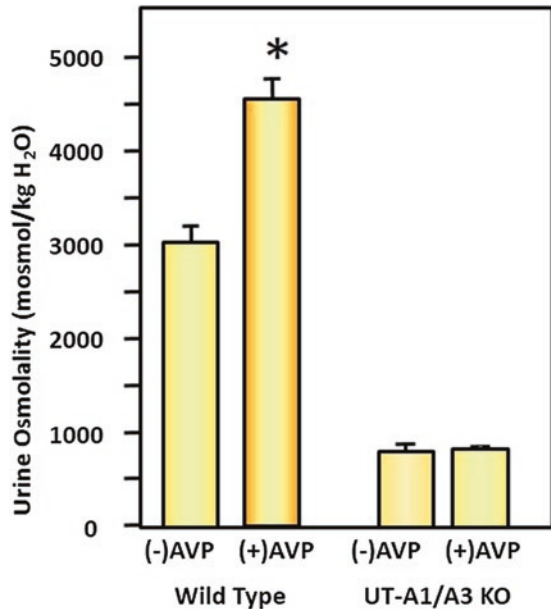
UT-A1 and UT-A3 in the vasopressin response, the next step will be to characterize these animals using perfusion techniques with isolated inner medullary collecting ducts. This will help us understand the rapid response of the single urea transporter to vasopressin. The concept that urea enters the cell apically through UT-A1 and exits the cell by UT-A3 at the basolateral surface suggests that the basolateral localization of UT-A3 may have great practical appeal.

Vasopressin

Isolated perfused tubule studies show that addition of vasopressin to the basolateral membrane of the rat terminal IMCD results in increased facilitated urea permeability [102, 123, 124, 130, 155, 156, 171]. This is believed to occur through the canonical vasopressin stimulatory pathway; that is, by binding of vasopressin to V2 receptors, stimulating adenylyl cyclase (AC), generating cAMP, and ultimately stimulating cyclic AMP-dependent protein kinase (PKA) (Fig. 6.5). The effect occurs within minutes of adding vasopressin to the bath [195]. Vasopressin also increases urea flux in freshly isolated IMCD cell suspensions, UT-A1-MDCK cells (Fröhlich et al. [47, 48], UT-A1-mIMCD3 cells [91], and mUT-A3-MDCK cells [176]. The urea reflection coefficient in the rat terminal IMCD is unity [27, 100], demonstrating that there is no solvent drag of urea in this nephron segment.

Vasopressin thus exerts its effects through manipulation of cAMP levels that then impact transporter activity. UT-A1 is phosphorylated and activated by cyclic AMP-dependent protein kinase, PKA [151]. This is discussed more thoroughly below. UT-A2 is not stimulated by cAMP analogs when expressed in
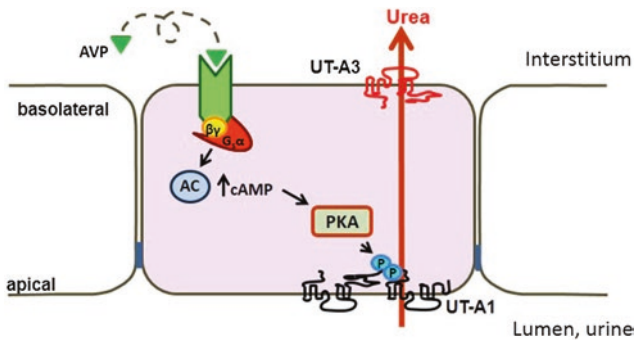
Fig. 6.5 A mechanistic diagram showing the classic regulatory pathway mediated by vasopressin. Protein Kinase A (PKA), which is stimulated by vasopressin-mediated increases in adenylyl cyclase (AC), and subsequent increases in cAMP, phosphorylates UT-A1 promoting its trafficking to the apical plasma membrane. UT-A3 is located basolaterally based on immunohistochemical evidence. The large arrow shows that urea enters the cell through UT-A1 at the apical surface and exits through UT-A3 at the basolateral surface, resulting in increased interstitial urea concentrations. (*diagram courtesy of Dr. M. Blount, Emory University*)

either *Xenopus* oocytes or human embryonic kidney (HEK) cells [6, 80, 142, 161, 163, 167, 211]. However, in MDCK cells that are stably transfected with mouse UT-A2, vasopressin does increase urea flux [139]. Forskolin and increased intracellular calcium also increase urea flux in mUT-A2-MDCK cells; however, the PKA inhibitor H-89 had no effect on forskolin-stimulated urea flux in the mUT-A2-MDCK cells. Urea transport by UT-A3 is stimulated by cAMP analogs when expressed in Xenopus oocytes or HEK293 cells [46, 80, 168] except in one study [164]. Urea transport is also stimulated by vasopressin via a PKA-mediated pathway in cells that are stably transfected with mouse UT-A3, mUT-A3-MDCK cells [174]. The effect of cAMP on UT-A5 and UT-A6 has not been tested.

Phosphorylation

The deduced amino acid sequences for UT-A1 and UT-A3 contain several consensus PKA phosphorylation sites [80]. Proteomic and cDNA array approaches have identified UT-A1 and UT-A3 as proteins that are phosphorylated by vasopressin in the inner medulla [11, 18, 57, 59, 190, 213, 214]. Incubating freshly isolated suspensions of rat IMCDs with vasopressin increases the phosphorylation of both the 117 and 97 kDa UT-A1 glycoproteins within 2 min [215] and of the 67 and 44 kDa UT-A3 proteins [14]. Vasopressin also increases the phosphorylation of UT-A1 in UT-A1 MDCK cells [47, 48] and UT-A1 mIMCD3 cells [91]. The time course and dose response for vasopressin-stimulated increases in UT-A1 phosphorylation are consistent with the time course and dose response for vasopressin-stimulated increases in urea permeability in perfused rat terminal IMCDs [131, 171, 195, 215]. cAMP, forskolin, and dDAVP (a V2-selective agonist) also increase UT-A1 phosphorylation, and PKA inhibitors block vasopressin- or forskolin-stimulated phosphorylation of UT-A1 in rat IMCD suspensions [215] and UT-A1 MDCK cells [48, 178]. In addition to stimulating PKA, vasopressin/cAMP can stimulate Epac (exchange protein activated by cAMP) [17, 56, 58, 107, 113, 205, 210]. Activating Epac increases urea permeability in perfused rat terminal IMCDs and increases UT-A1 phosphorylation in IMCD suspensions [198].

A phosphoproteomic analysis identified serine 486 as a potential vasopressin-stimulated phosphorylation site in UT-A1 [57]. This same serine was identified in a second study that also identified serine 499 as a second potential PKA phosphorylation site [15]. Using site-directed mutagenesis and transient transfection in heterologous expression systems, PKA was shown to phosphorylate UT-A1 at Ser 486 and Ser 499 [15]. Chimera proteins of UT-A that attached the loop region of UT-A1 (aa 460–532) containing Ser 486 and Ser 499 to the UT-A2 protein, which normally lacks this region, showed that this section conferred vasopressin sensitivity to UT-A2 [122]. Ser 486-phosphorylated UT-A1 is detected primarily in the apical plasma membrane in rat IMCDs [91]. A subsequent phosphoproteomic screen showed that Ser 84, which is present in both UT-A1 and UT-A3, could be phosphorylated by PKA [11]. Vasopressin was shown to increase phosphorylation
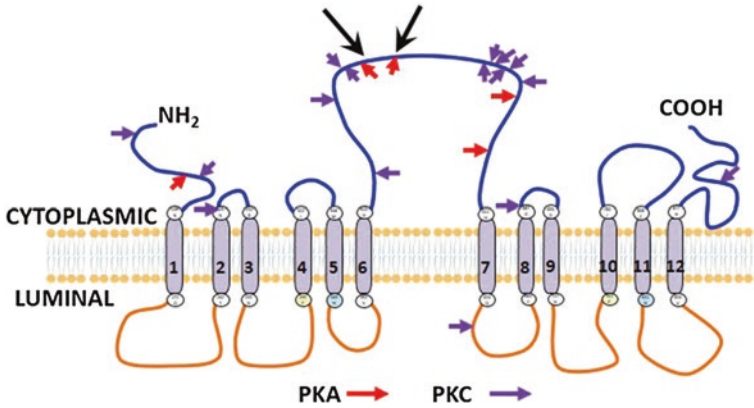
Fig. 6.6 This schematic representation of UT-A1 shows the locations of consensus sequences for PKA and PKC phosphorylation sites. The large black arrows show the confirmed PKA sites that are necessary for UT-A1 accumulation in the apical plasma membrane

at Ser 84 in rat UT-A1 and UT-A3 [63]; however, the vasopressin-stimulated phosphorylation site in human or mouse UT-A3 has not been determined, since Ser 84 is not conserved in the human sequence and neither of the two PKA consensus sites in mouse (Ser 85 or Ser 92) are phosphorylated [168]. There is currently no explanation for the species variation in sites that are phosphorylated.

As well as the PKA-mediated phosphorylation of UT-A1, there are other consensus kinase sites on this urea transporter. Recently, PKC has been shown to stimulate urea permeability and the phosphorylation of UT-A1 [95, 183, 199, 200]. PKCα in particular appears to be involved in the phosphorylation of UT-A1 under hypertonic conditions [199]. Figure 6.6 shows the consensus phosphorylation sites for PKA and PKC in UT-A1, UT-A2, UT-A3, and UT-A4.

Stimulation by phosphorylation suggests the importance of dephosphorylation in the regulation of urea transporters; however, there are very limited studies analyzing the dephosphorylation of urea transporters. Ilori et al. have reported that the phosphorylation level of UT-A1 is effected by inhibition of calcineurin suggesting that protein phosphatase 2B may be responsible for dephosphorylation of UT-A1, but this account also suggests the possibility that other phosphatases may be involved [66].

Plasma Membrane Accumulation

Vasopressin increases the plasma membrane accumulation of UT-A1 and UT-A3 in freshly isolated suspensions of IMCDs from normal rats [14, 94]. However, vasopressin does not increase the plasma membrane accumulation of UT-A1 in IMCDs from Brattleboro rats or 2-week water diuretic rats [68, 94]. Brattleboro rats are a naturally

occurring strain that congenitally lack vasopressin in the CNS, thus are a model for central diabetes insipidus. When forskolin is used as an agonist, instead of vasopressin, it does increase the plasma membrane accumulation of UT-A1 in IMCDs from 2-week water diuretic rats [94]. One possible explanation is that chronically diuretic animals have a blunted cAMP response to vasopressin [33, 86, 160]. Directly stimulating AC with forskolin [160] may result in higher levels of cAMP production and an increase in UT-A1 accumulation in the plasma membrane [94]. Activating Epac increases UT-A1 plasma membrane accumulation in rat IMCD suspensions [198]. Confirming the importance of cAMP in the regulation of urea transport, Sanches et al. have shown that inhibition of phosphodiesterase 5 with sildenafil causes an upregulation of renal UT-A1 and a decrease in lithium-related polyuria [145].

Vasopressin or forskolin also increases UT-A1 apical plasma membrane accumulation in UT-A1-MDCK cells [91]. Mutations of both Ser 486 and Ser 499, but not either one alone, eliminates vasopressin stimulation of UT-A1 apical plasma membrane accumulation and urea transport, indicating that at least one of these serines must be phosphorylated to increase apical plasma membrane accumulation and urea flux [15]. A phospho-specific antibody to pSer486-UT-A1 confirmed that vasopressin increases UT-A1 accumulation in the apical plasma membrane and that the pSer486-UT-A1 form is primarily detected in the apical plasma membrane [91].

Vasopressin also increases plasma membrane accumulation of UT-A3 in rat IMCDs, both in the basolateral and apical membranes [14]. In mUT-A3-MDCK cells, 10 min of vasopressin stimulates urea flux through transporters already in the basolateral plasma membrane [176]. The basal expression of UT-A3 in the basolateral plasma membrane involves protein kinase C (PKC) and calmodulin, while its regulation by vasopressin involves a casein-kinase II-dependent pathway [176].

In rat IMCDs, UT-A1 is linked to the SNARE machinery via snapin, suggesting that SNARE-SNAP vesicle trafficking mechanism may be functionally important for regulating urea transport [121]. UT-A1 also interacts with caveolin-1 in lipid rafts, which provides another mechanism for the regulation of UT-A1 activity within the plasma membrane [40]. UT-A1 is endocytosed by a dynamin-dependent process that is mediated by both caveolae and clathrin-coated pit pathways [62, 179].

Ubiquitination

Both UT-A1 and UT-A3 proteins can be ubiquitinated based on studies showing that abundance of these proteins is increased when ubiquitin proteasome proteolytic pathways have been inhibited. [22, 175]. Only UT-A1, however, has been rigorously shown to have ubiquitinated high-molecular weight forms by immunoprecipitation and Western analysis [22]. The ubiquitin ligase MDM2 mediates UT-A1 ubiquitination and degradation, which may contribute to the regulation of UT-A1 [22]. Figure 6.7 shows the possible ramifications of UT-A1 ubiquitination.
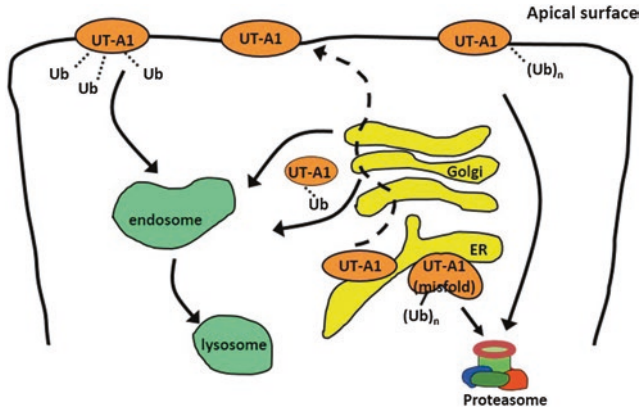
Fig. 6.7 This illustration shows the possible consequences of UT-A1 ubiquitination. Ubiquitination prior to membrane insertion or polyubiquitination at the membrane could lead to protosomal degradation. Monoubiquitination at the membrane could lead to endosome insertion and potentially lysosomal degradation as could monoubiquitination prior to membrane insertion
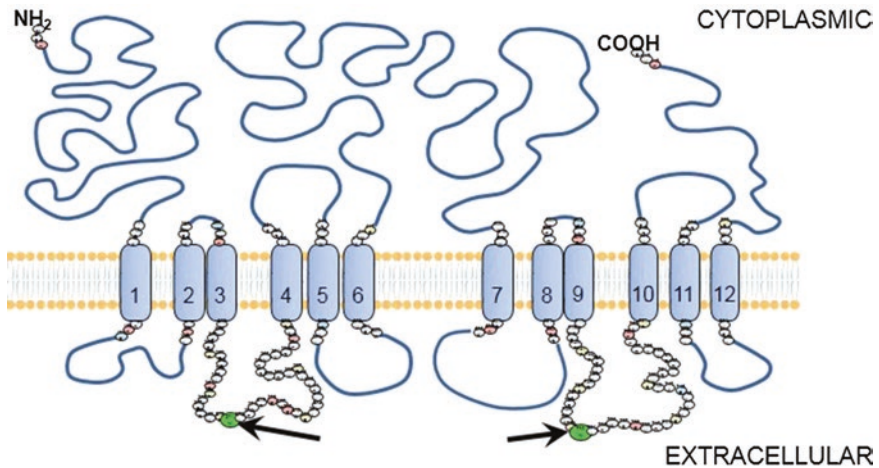
Fig. 6.8 Illustration showing the glycosylation sites on UT-A1. Provided is a ball and line cartoon of UT-A1 with the extracellular amino acids identified and the known glycosylated residues identified with *arrows*

Glycosylation

UT-A1 has four consensus N-linked glycosylation sites, but only Asn 279 and Asn 742 in the rodent (Asn 271 and Asn 733 in humans) are predicted to reside in extracellular domains of UT-A1 [20] (Fig. 6.8). Mutation of either these Asn residues reduces urea flux by reducing UT-A1 half-life and apical plasma membrane

accumulation in MDCK cells [20]. Glycosylation is reported to be linked to UT-A1 lipid raft localization within the membrane [21]. Recent accounts suggest that glycosylation is important to the transport activity of UT-A3 [177]. Another chapter in this book will be devoted to the regulation of urea transport by glycosylation-mediated mechanisms.

Hyperosmolality

The osmolality of the renal medulla varies over a wide range, depending on the hydration status of the animal. Increasing the osmolality, either by adding NaCl (as occurs during transition to an antidiuretic state) or mannitol, rapidly increases urea permeability in rat terminal IMCDs, even in the absence of vasopressin [49, 103, 156]. These findings suggest that hyperosmolality is an independent regulator of urea transport. When vasopressin is present, increasing osmolality has an additive stimulatory effect on urea permeability [24, 52, 103, 156]. Hyperosmolality-stimulated urea permeability is inhibited by phloretin and thiourea [52]. Kinetic studies show that hyperosmolality, similar to vasopressin, increases urea permeability by increasing V_{max} rather than K_m [26, 52]. However, hyperosmolality stimulates urea permeability via increases in PKC activation and intracellular calcium [53, 81, 95, 200], while vasopressin stimulates urea permeability via increases in AC [171]. Hyperosmolality, similar to vasopressin, increases phosphorylation and plasma membrane accumulation both UT-A1 and UT-A3 [13, 14, 94, 215]. Thus, both hyperosmolality and vasopressin rapidly increase urea permeability, but they do so via different signaling pathways with vasopressin dependent on the second messenger cAMP and hypertonicity dependent on intracellular calcium. In a recent study, treatment of patients with hypertonic saline solution resulted in increased expression of UT-A1, confirming responsiveness in human subjects [71]. Hyperosmolality has also been shown to induce expression of UT-A2 in mouse medullary collecting duct [76].

The collecting duct of the houndshark, Triakis scyllium expresses a urea transporter [202]. Transfer of the shark from 30 % sea water to 100 % sea water results in a progressive increase in the apical plasma membrane accumulation of its urea transporter in the collecting duct [202].

Other Agents that Acutely Regulate Urea Transporters

The mRNA for the type 1 angiotensin II (AT1) receptor is present in rat IMCDs [78, 157, 180], and radioligand-binding studies show that AT1 receptors are expressed [126]. Angiotensin II does not affect basal (no vasopressin) urea permeability in rat terminal IMCDs [81]. However, it increases both vasopressin-stimulated urea permeability and UT-A1 phosphorylation via PKC-mediated effects [81]. By augmenting the maximal urea permeability response to vasopressin, angiotensin II may play a physiologic role in the urinary concentrating mechanism.

Glucagon increases the fractional excretion of urea [2, 3, 98]. However, the effects of glucagon on urea transport in the IMCD have varied between studies. In one study, glucagon decreased urea permeability in perfused rat terminal IMCDs and UT-A1 abundance in rat IMCD suspensions [207]. These effects of glucagon occur by stimulating a PKC-signaling pathway [207]. In other studies, glucagon did not alter the basal- or vasopressin-stimulated urea permeability in perfused rat IMCDs. Neither did it alter cAMP production in any segment of the IMCD [69, 117].

Oxytocin increases urea permeability by binding to the V2-receptors and increasing cAMP production [24, 25]. Oxytocin-stimulated urea permeability is inhibited by phloretin [24]. Chlorpropamide increases basal urea permeability in the rat terminal IMCD [143]. Alpha-2-adrenergic agonists, such as epinephrine and clonidine, inhibit vasopressin-stimulated urea permeability in the rat terminal IMCD [117, 144]. Furosemide inhibits vasopressin-stimulated urea permeability in the rat terminal IMCD [104]. Chronic use of chloroquine downregulates cAMP levels and inhibits urea transport [192]. Amphotericin B also inhibits vasopressin-stimulated urea permeability, but not cAMP-stimulated urea permeability, in the rat terminal IMCD [206]. Neither atrial natriuretic peptide [133] nor insulin [118] alters urea permeability in rat terminal IMCDs.

Recent and ongoing investigations have targeted small urea analogs as potential new diuretics. These small molecules have been designed to inhibit both UT-B and UT-A urea transporters by binding at vulnerable key residues in the projected channel portion of the transporters [4, 28, 36, 99, 112, 150, 208].

There are some initial investigations suggesting a possible role for reactive oxygen species in the control of urea transporters and urine concentration. To date, these have concentrated on the effects of nitric oxide (NO) in a setting of diabetes mellitus suggesting that NO supports the increased transporter protein levels that are the response to that disease state [29].

Long-term Regulation of Urea Transporters

In addition to the rapid regulation of urea transport by phosphorylation and other post-translational modifications of urea transporters and reagents that alter the membrane accumulation of the urea transporters, there are various long-term effects of vasopressin and other agents that can change urea transporter protein abundance. Experimentally, there have been two methods used to alter the vasopressin levels in animal models: alteration of the hydration state through water loading or water restriction to alter endogenous vasopressin levels; or administering exogenous vasopressin to stimulate both V2 and V1 receptors or dDAVP to stimulate only the V2 receptor. The administration of vasopressin or dDAVP to achieve consistently high levels of the agonists is routinely accomplished through a sustained release mini-pump, although serial injections have been used. While both vasopressin and dDAVP induce antidiuresis, there are differences in their quantitative and temporal effects on urine flow rate and urine concentration [9].

UT-A1

Administering vasopressin to Brattleboro rats for 5 days decreases UT-A1 protein abundance in the inner medulla [87, 181]. Consistent with this change in UT-A1 protein abundance, perfused terminal IMCDs from rats that were water loaded for 3 days have higher basal- and higher vasopressin-stimulated urea permeabilities than terminal IMCDs from rats given water ad libitum [82]. Histochemistry also shows increased UT-A1 expression in 3-day water-loaded rats without a change in UT-A1's subcellular distribution [114]. This increase in urea transport and UT-A1 protein abundance does not result from a decrease in UT-A1 or UT-A1b mRNA abundances since Northern blot analysis shows no change in abundance of either mRNA in response to changes in hydration state in most studies [8, 42, 141, 142, 161, 167], although one study does report that UT-A1 mRNA abundance is decreased in water restricted or vasopressin-treated Brattleboro rats [162]. Overall, changes in UT-A1 protein abundance in response to changes in vasopressin levels or hydration state do not appear to be regulated by transcription. In rats with chronic primary polydipsia, 36 h of water deprivation caused no change in UT-A1 protein abundance [19].

When vasopressin is administered for a longer period of time, 12 days instead of 5 days as in the preceding studies, UT-A1 protein abundance is significantly increased [87]. Similarly, water loading rats for 14 days (instead of 3 days) significantly decreased UT-A1 protein abundance [87]. The exact timing of the initiation of UT-A1 increases is unknown since a careful time course between 3 and 14 days has not been performed; however, the timing responses that have been observed are consistent with the time course for increases in inner medullary urea content when Brattleboro rats are treated with vasopressin [55].

Analysis of the UT-A promoter I may explain this time course since there is no CRE in the 1.3 kb that has been cloned and cAMP does not increase promoter I activity [127, 128]. However, a TonE element is present in promoter I, and hyperosmolality increases promoter activity [127, 128]. Thus, vasopressin administration may initially increase the transcription of the Na–K–2Cl cotransporter in the thick ascending limb; the increase in NaCl reabsorption will in turn increase inner medullary osmolality, which will then increase UT-A1 transcription through TonE [64, 127, 128, 209]. Since the inner medullary interstitium becomes hypertonic sooner than the 12 days of vasopressin administration, additional mechanisms may also be involved in increasing UT-A1 abundance. In particular, there may be a role for PKC in a long-term as well as a short-term regulation given that hypertonicity results in UT-A1 membrane accumulation in response to a PKC-mediated pathway.

UT-A2 and UT-A3

The mRNA abundances of UT-A2, UT-A2b, UT-A3, and UT-A3b are reduced in the inner medulla of 3-day water-loaded rats. Under antidiuretic conditions, however, they are increased. For example, levels rise in rats and mice that are water restricted

for 3 days, rats receiving dDAVP for 3 weeks and Brattleboro rats treated with vasopressin for 1 week [8, 46, 101, 141, 142, 162, 167]. The protein expression of UT-A2 and UT-A3 are also decreased in water-loaded animals as determined by immunohistology. Although decreased in abundance, there is no apparent change in the subcellular distribution of either urea transporter [114]. During antidiuresis, UT-A2 protein is increased within 7 days of dDAVP administration to Brattleboro rats [193] and decreased by 7 days of furosemide (an inhibitor of NKCC2) administration [108]. A transcriptional mechanism could be involved in the UT-A2 response since this transporter is under the control of the UT-A promoter II, which contains a CRE element and is increased by cAMP and by extension, vasopressin [127]. UT-A2 expression is also increased in mIMCD3 cells that are grown in hypertonic medium-containing urea and NaCl. In isotonic medium, mIMCD3 cells do not express any UT-A isoform [108, 128]. UT-A3 is under the control of the UT-A promoter I that contains a TonE and could be mediated by tonicity-responsive transcription [128].

UT-B

UT-B1 mRNA abundance in both the outer and inner medulla is reduced after administering dDAVP or vasopressin to Brattleboro rats for 6 hours. Upon longer treatment with vasopressin or dDAVP (5 days), the UT-B1 mRNA abundance was increased in the outer medulla and the inner medullary base, but remained decreased in the inner medullary tip [141]. One study reports an increased expression of UT-B1 protein was observed by immunohistochemistry in rats that had been water loaded for 3 days. Subcellular distribution of UT-B1 was unaltered in the water-loaded animals [114]. Another study reports that UT-B1 protein was substantially downregulated by long-term dDAVP infusion [188]. The response of UT-B1 to vasopressin is unclear. Expression of UT-B2 protein is not affected by vasopressin [185].

Low-protein Diets

The fractional excretion of urea is decreased in rats fed a low-protein diet for at least 2 weeks [137]. In contrast to the terminal IMCD, the initial IMCD has a low basal urea permeability that is not increased by vasopressin [153, 155]. However, 2 weeks of a low-protein diet induces the functional expression of vasopressin-stimulated urea permeability in the initial IMCD [6, 69, 70]. The low-protein diet-induced vasopressin-stimulated urea permeability in the initial IMCD is stimulated by hyperosmolality and inhibited by phloretin and thiourea [6, 70]. Thus, it has the same functional characteristics as the vasopressin-stimulated urea permeability that is normally expressed in the terminal IMCD [6]. A low-protein diet also increases basal urea permeability in the deepest third of the IMCD, the IMCD3 [83], and increases UT-A1 protein abundance in the inner medulla [181].

The sensitivity of inner medullary mRNA for UT-A1 and UT-A2 to low-protein conditions is controversial [6, 61, 167]. Feeding normal rats a low-, normal-, or high-protein diet (10, 20, or 40 % protein, respectively) for 1 week resulted in no change in the mRNA for either UT-A1or UT-A2. Feeding Brattleboro rats with a low-protein diet resulted in decreased UT-A1 mRNA, suggesting that vasopressin and dietary protein may cross talk in the regulation of urea transporter abundance. Although Sprague-Dawley or Brattleboro rats did not show any change in their UT-A2 mRNA upon low-protein (10 %) feeding, rats that were fed an 8 % low-protein diet for 1 week showed an increased UT-A2 mRNA in the inner medullary base [6]. Thus, conflicting accounts in the literature exist and a definitive study has not yet been reported. UT-B1 mRNA abundance is unaffected by a change in dietary protein from 10 to 40 % in either normal or Brattleboro rats [61]. In sheep, UT-A mRNA abundances in pelvic epithelium lining and outer medulla were decreased by a low-protein diet [5], which may be important for renal conservation of nitrogen during protein restriction.

Osmotic Diuresis

In the normal kidney, the inner medulla vacillates between diuresis and antidiuresis with urea and NaCl being the predominant solutes contributing to inner medullary osmolality. There are some excellent reviews on the urea-specific signaling pathways that have been explored in mIMCD3 cells [12, 184]. In situations where the urea content of the urinary solute is low, UT-A1 protein abundance increases [85, 106, 108, 114]. This increase in UT-A1 may be an effort to restore the hyperosmolality of the medullary interstitium to promote urine concentrating ability. When the medullary interstitial urea concentration is high, UT-A2 and UT-B1 in the outer medulla increase in abundance, as one might see with a urea-induced osmotic diuresis. However, during a NaCl- or glucose-induced osmotic diuresis, the same increase is not seen [85, 106, 114]. The urea-induced osmotic diuresis alters both UT-A1 and UT-A3 protein abundances, but UT-A1 is increased while UT-A3 decreases, which suggests that the tonicity enhancer binding protein (TonEBP) is attempting to minimize changes in plasma osmolality and maintain water homeostasis [89]. TonEBP is also known as NFAT5 or the osmotic response element binding protein (OREBP). This element is an important regulator of urine concentrating ability [74, 106]. Transgenic mice that overexpress a dominant negative form of TonEBP have reduced urine concentrating ability, reduced urine osmolality, and reduced UT-A1 and UT-A2 mRNA abundances [106]. When these mice are deprived of water or given vasopressin, they increase urine osmolality and UT-A1 mRNA, but not UT-A2 mRNA abundance. The inability of UT-A2 to respond under conditions where TonEBP is downregulated sheds light on the mechanism of the change in UT-A2 during urea-induced osmotic diuresis. TonEBP also stimulates mRNAs for proteins that cause accumulation of organic osmolytes, i.e., aldose reductase [75]. Mice lacking aldose reductase cannot

effectively concentrate their urine. Knock-in of the aldose reductase transgene mostly corrected their urine concentrating ability, and this was accompanied by an increase in UT-A1, suggesting a further link between osmolality and urea transport regulation [204].

Adrenal Steroids

Adrenalectomy produces a urine concentrating defect although the mechanism is unclear [23, 73, 79, 159]. Glucocorticoids such as dexamethasone increase the fractional excretion of urea in rats [97]. Two studies have examined the effect of glucocorticoids on UT-A1 protein abundance and obtained opposite results. In one study, rats were adrenalectomized and compared to sham-operated rats or adrenalectomized rats receiving a stress dose of dexamethasone [129]. Compared to sham-operated rats, adrenalectomy increased urea permeability in terminal IMCDs and UT-A1 protein abundance in the inner medullary tip [129]. The second study used a somewhat different model: All rats were adrenalectomized and given aldosterone replacement, and half of the animals were also given dexamethasone [23, 111]. The rats lacking glucocorticoid had a decrease in UT-A1 and UT-A3 protein abundances [23, 111]. The reason for the different findings regarding UT-A1 between these studies is unclear, but may be due to the different treatment protocols.

Administering dexamethasone at stress levels to normal rats decreased UT-A1 and UT-A3 mRNA abundances in the inner medullary tip but does not change UT-A2 mRNA abundance [138]. Dexamethasone also decreases UT-A promoter I activity [138], suggesting that the decrease in UT-A1 and UT-A3 mRNA abundance is transcriptionally regulated. When rats received dexamethasone treatment for 14 days, both UT-A1 and UT-A3 protein abundance decreased with an associated increase in urea excretion [111].

Mineralocorticoids (aldosterone) also decrease UT-A1 protein abundance in the inner medulla of adrenalectomized rats [50]. This decrease can be blocked by the mineralocorticoid receptor antagonist, spironolactone [50]. Spironolactone does not block the decrease due to dexamethasone [50], indicating that each adrenal steroid hormone works through its own receptor. Aldosterone-induced volume expansion with a high-NaCl diet decreased both UT-A1 and UT-A3 protein abundances [196].

Purinergic Receptor P2Y2

Activation of $P2Y_2$ purinergic (G-protein coupled) receptor in the IMCD tends to oppose the action of vasopressin [216]. $P2Y_2$-receptor knockout mice have increased urine concentrating ability, and UT-A1 and UT-A2 protein abundances, when compared to wild-type mice [216]. Administering vasopressin for 45 min or 5 days increases UT-A1 protein abundance in $P2Y_2$-receptor knockout mice [216].

UT-A2 protein abundance increases in both control and $P2Y_2$-receptor-null mice given vasopressin for 5 days [216], suggesting a role for cAMP in the regulation of UT-A2. Acute treatment with PKA agonists failed to cause an increase in UT-A2 [46]. However, longer treatment times resulted in the upregulation of UT-A2 protein abundance [191, 193], suggesting that cAMP may be involved in the long-term regulation of UT-A2, but not the acute response.

Electrolyte Abnormalities that Reduce Urine Concentrating Ability

Both hypercalcemia and hypokalemia cause reductions in urine concentrating ability [49, 77, 109, 152]. Surprisingly, rats made hypercalcemic for 3 or 4 days by administering vitamin D have an increase in basal urea permeability in their terminal IMCDs compared to normocalcemic control rats [152]. UT-A1 protein abundance is also increased [152]. This response is similar to the decrease in UT-A1 protein abundance following 3 days of vasopressin administration or water restriction [82, 87, 181]. It is not known whether a longer period of hypercalcemia would result in the downregulation of UT-A1, similar to what is observed following longer periods of water diuresis [87]. These changes may be regulated by the calcium-sensing receptor in the apical plasma membrane of the terminal IMCD [154]. Treatment of mice that model autosomal dominant polycystic kidney disease (ADPKD) or rats that model autosomal recessive polycystic kidney disease (ARPKD) with R-568, a type 2 calcimimetic, results in hypocalcemia and polyuria in both animal models. Low-dose R-568 treatment resulted in minimal changes in UT-A1 protein abundance, with significant increases seen in female ARPKD rats, but not in males [197].

Hypokalemia reduces TonEBP protein abundance and nuclear distribution in the medulla [74]. Downregulation of TonEBP contributed to reduced expression of UT-A1 and UT-A2, although UT-A2 expression was transcriptionally reduced while UT-A1 was reduced post-transcriptionally [74]. In addition, UT-B1 expression was reduced with a concomitant decrease in mRNA abundance in response to hypokalemia [74]. Another study also showed that feeding rats with low-potassium diet reduces the abundance of UT-A1, UT-A3, and UT-B1 proteins in the inner medulla [77]. However, this study found that hypokalemia increases UT-A2 protein abundance in the outer medulla [77]. The reason for the different findings regarding UT-A2 between these studies is unclear.

Aging

Normal aging results in a decrease in urine concentrating ability (reviews: (Sands [147–149]. UT-A1, UT-A3, and UT-B1 protein abundances are reduced in kidneys of aged rats [32, 140, 189]. A supra-physiologic dose of dDAVP increases urine

osmolality and UT-A1, UT-A2, and UT-B1 protein abundances, but not to the levels observed in younger rats [31]. Recently, N-acetylcysteine has been linked to beneficial effects on renal function in aging animals involving increased levels of NKCC2, AQP2, and UT-A1 [165].

Angiotensin II

In addition to its well-recognized role in blood pressure regulation and sodium homeostasis, the renin–angiotensin system may play an important role in the urinary concentrating mechanism. Infusing angiotensin II into the renal artery increases urine osmolality [39], whereas knockout of the gene for angiotensin-converting enzyme (ACE) or angiotensinogen, or treatment of neonatal rats with an ACE inhibitor impairs urine concentrating ability [37, 38, 54, 72, 84, 96, 134]. Mice that lack tissue ACE have a normal appearing medulla, but still have a urine concentrating defect [38] and UT-A1 protein abundance is decreased to 25 % of the level seen in wild-type mice [96]. Administering angiotensin II to these mice for 2 weeks does not correct either the urine concentrating defect or the reduction of UT-A1 protein abundance [96].

References

1. Abdoun K, Stumpff F, Rabbani I, Martens H (2010) Modulation of urea transport across sheep rumen epithelium in vitro by SCFA and CO_2. Am J Physiol Gastrointest Liver Physiol 298:G190–G202
2. Ahloulay M, Bouby N, Machet F, Kubrusly M, Coutaud C, Bankir L (1992) Effects of glucagon on glomerular filtration rate and urea and water excretion. Am J Physiol Renal Physiol 263:F24–F36
3. Ahloulay M, Déchaux M, Laborde K, Bankir L (1995) Influence of glucagon on GFR and on urea and electrolyte excretion: direct and indirect effects. Am J Physiol Renal Physiol 269:F225–F235
4. Anderson MO, Zhang J, Liu Y, Yao C, Phuan PW, Verkman AS (2012) Nanomolar potency and metabolically stable inhibitors of kidney urea transporter UT-B. J Med Chem 55:5942–5950
5. Artagaveytia N, Elalouf JM, De RC, Boivin R, Cirio A (2005) Expression of urea transporter (UT-A) mRNA in papilla and pelvic epithelium of kidney in normal and low protein fed sheep. Comp Biochem Physiol B: Biochem Mol Biol 140:279–285
6. Ashkar ZM, Martial S, Isozaki T, Price SR, Sands JM (1995) Urea transport in initial IMCD of rats fed a low-protein diet: functional properties and mRNA abundance. Am J Physiol Renal Physiol 268:F1218–F1223
7. Bagnasco SM, Peng T, Janech MG, Karakashian A, Sands JM (2001) Cloning and characterization of the human urea transporter UT-A1 and mapping of the human Slc14a2 gene. Am J Physiol Renal Physiol 281:F400–F406
8. Bagnasco SM, Peng T, Nakayama Y, Sands JM (2000) Differential expression of individual UT-A urea transporter isoforms in rat kidney. J Am Soc Nephrol 11:1980–1986

9. Bankir L (2001) Antidiuretic action of vasopressin: quantitative aspects and interaction between V_{1a} and V_2 receptor-mediated effects. Cardiovasc Res 51:372–390

10. Bankir L, Chen K, Yang B (2004) Lack of UT-B in vasa recta and red blood cells prevents urea-induced improvement of urinary concentrating ability. Am J Physiol Renal Physiol 286:F144–F151

11. Bansal AD, Hoffert JD, Pisitkun T, Hwang S, Chou CL, Boja ES, Wang G, Knepper MA (2010) Phosphoproteomic profiling reveals vasopressin-regulated phosphorylation sites in collecting duct. J Am Soc Nephrol 21:303–315

12. Berl T (2000) On the adaptation of renal cells to hypertonicity. Am J of Kidney Dis 35:XLVII–XLVIL

13. Blessing NW, Blount MA, Sands JM, Martin CF, Klein JD (2008) Urea transporters UT-A1 and UT-A3 accumulate in the plasma membrane in response to increased hypertonicity. Am J Physiol Renal Physiol 295:F1336–F1341

14. Blount MA, Klein JD, Martin CF, Tchapyjnikov D, Sands JM (2007) Forskolin stimulates phosphorylation and membrane accumulation of UT-A3. Am J Physiol Renal Physiol 293:F1308–F1313

15. Blount MA, Mistry AC, Fröhlich O, Price SR, Chen G, Sands JM, Klein JD (2008) Phosphorylation of UT-A1 urea transporter at serines 486 and 499 is important for vasopressin-regulated activity and membrane accumulation. Am J Physiol Renal Physiol 295:F295–F299

16. Blount MA, Sim JH, Zhou R, Martin CF, Lu W, Sands JM, Klein JD (2010) The expression of transporters involved in urine concentration recover differently after ceasing lithium treatment. Am J Physiol Renal Physiol 298:F601–F608

17. Bos JL (2003) Epac: a new cAMP target and new avenues in cAMP research. Nat Rev Mol Cell Biol 4:733–738

18. Brooks HL, Ageloff S, Kwon TH, Brandt W, Terris JM, Seth A, Michea L, Nielsen S, Fenton R, Knepper MA (2003) cDNA array identification of genes regulated in rat renal medulla in response to vasopressin infusion. Am J Physiol Renal Physiol 284:F218–F228

19. Cadnapaphornchai MA, Summer SN, Falk S, Thurman JM, Knepper MA, Schrier RW (2003) Effect of primary polydipsia on aquaporin and sodium transporter abundance. Am J Physiol Renal Physiol 285:F965–F971

20. Chen G, Fröhlich O, Yang Y, Klein JD, Sands JM (2006) Loss of N-linked glycosylation reduces urea transporter UT-A1 response to vasopressin. J Biol Chem 281:27436–27442

21. Chen G, Howe AG, Xu G, Frohlich O, Klein JD, Sands JM (2011) Mature N-linked glycans facilitate UT-A1 urea transporter lipid raft compartmentalization. FASEB J 25:4531–4539

22. Chen G, Huang H, Fröhlich O, Yang Y, Klein JD, Price SR, Sands JM (2008) MDM2 E3 ubiquitin ligase mediates UT-A1 urea transporter ubiquitination and degradation. Am J Physiol Renal Physiol 295:F1528–F1534

23. Chen YC, Cadnapaphornchai MA, Summer SN, Falk S, Li C, Wang W, Schrier RW (2005) Molecular mechanisms of impaired urinary concentrating ability in glucocorticoid-deficient rats. J Am Soc Nephrol 16:2864–2871

24. Chou C-L, DiGiovanni SR, Luther A, Lolait SJ, Knepper MA (1995) Oxytocin as an antidiuretic hormone. II Role of V_2 vasopressin receptor. Am J Physiol Renal Physiol 269:F78–F85

25. Chou C-L, DiGiovanni SR, Mejia R, Nielsen S, Knepper MA (1995) Oxytocin as an antidiuretic hormone. I. Concentration dependence of action. Am J Physiol Renal Physiol 269:F70–F77

26. Chou C-L, Knepper MA (1989) Inhibition of urea transport in inner medullary collecting duct by phloretin and urea analogues. Am J Physiol Renal Physiol 257:F359–F365

27. Chou C-L, Sands JM, Nonoguchi H, Knepper MA (1990) Urea-gradient associated fluid absorption with $\sigma_{urea} = 1$ in rat terminal collecting duct. Am J Physiol Renal Physiol 258:F1173–F1180

28. Cil O, Ertunc M, Onur R (2012) The diuretic effect of urea analog dimethylthiourea in female Wistar rats. Hum Exp Toxicol 31:1050–1055

29. Cipriani P, Kim SL, Klein JD, Sim JH, von Bergen TN, Blount MA (2012) The role of nitric oxide in the dysregulation of the urine concentration mechanism in diabetes mellitus. Front Physiol 3:176

30. Collins D, Winter DC, Hogan AM, Schirmer L, Baird AW, Stewart GS (2010) Differential protein abundance and function of UT-B transporters in human colon. Am J Physiol Gastrointest Liver Physiol 298:G345–G351

31. Combet S, Geffroy N, Berthonaud V, Dick B, Teillet L, Verbavatz J-M, Corman B, Trinh-Trang-Tan M-M (2003) Correction of age-related polyuria by dDAVP: molecular analysis of aquaporins and urea transporters. Am J Physiol Renal Physiol 284:F199–F208

32. Combet S, Teillet L, Geelen G, Pitrat B, Gobin R, Nielsen S, Trinh-Trang-Tan MM, Corman B, Verbavatz JM (2001) Food restriction prevents age-related polyuria by vasopressin-dependent recruitment of aquaporin-2. Am J Physiol Renal Physiol 281:F1123–F1131

33. Cotte N, Balestre MN, Phalipou S, Hibert M, Manning M, Barberis C, Mouillac B (1998) Identification of residues responsible for the selective binding of peptide antagonists and agonists in the V2 vasopressin receptor. J Biol Chem 273:9462–29468

34. Dix L, Ward DT, Stewart GS (2013) Short communication: urea transporter protein UT-B in the bovine parotid gland. J Dairy Sci 96:1685–1690

35. Doran JJ, Klein JD, Kim Y-H, Smith TD, Kozlowski SD, Gunn RB, Sands JM (2006) Tissue distribution of UT-A and UT-B mRNA and protein in rat. Am J Physiol Regul Integr Comp Physiol 290:R1446–R1459

36. Esteva-Font C, Phuan P-W, Anderson MO, Verkman AS (2013) A small molecule screen identifies selective inhibitors of urea transporter UT-A. Chem Biol 20 (in press)

37. Esther CR Jr, Howard TE, Marino EM, Goddard JM, Capecchi MR, Bernstein KE (1996) Mice lacking angiotensin-converting enzyme have low blood pressure, renal pathology, and reduced male fertility. Lab Invest 74:953–965

38. Esther CR Jr, Marrero MB, Howard TE, Machaud A, Corvol P, Capecchi MR, Bernstein KE (1997) The critical role of tissue angiotensin-converting enzyme as revealed by gene targeting in mice. J Clin Invest 99:2375–2385

39. Faubert PF, Chou SY, Porush JG, Byrd R (1987) Regulation of papillary plasma flow by angiotensin II. Kidney Int 32:472–478

40. Feng X, Huang H, Yang Y, Fröhlich O, Klein JD, Sands JM, Chen G (2009) Caveolin-1 directly interacts with UT-A1 urea transporter: the role of caveolae/lipid rafts in UT-A1 regulation at the cell membrane. Am J Physiol Renal Physiol 296:F1514–F1520

41. Fenton RA, Cooper GJ, Morris ID, Smith CP (2002) Coordinated expression of UT-A and UT-B urea transporters in rat testis. Am J Physiol Cell Physiol 282:C1492–C1501

42. Fenton RA, Cottingham CA, Stewart GS, Howorth A, Hewitt JA, Smith CP (2002) Structure and characterization of the mouse UT-A gene (Slc14a2). Am J Physiol Renal Physiol 282:F630–F638

43. Fenton RA, Flynn A, Shodeinde A, Smith CP, Schnermann J, Knepper MA (2005) Renal phenotype of UT-A urea transporter knockout mice. J Am Soc Nephrol 16:1583–1592

44. Fenton RA, Hewitt JE, Howorth A, Cottingham CA, Smith CP (1999) The murine urea transporter genes Slc14a1 and Slc14a2 occur in tandem on chromosome 18. Cytogen Cell Gen 87:95–96

45. Fenton RA, Howorth A, Cooper GJ, Meccariello R, Morris ID, Smith CP (2000) Molecular characterization of a novel UT-A urea transporter isoform (UT-A5) in testis. Am J Physiol Cell Physiol 279:C1425–C1431

46. Fenton RA, Stewart GS, Carpenter B, Howorth A, Potter EA, Cooper GJ, Smith CP (2002) Characterization of the mouse urea transporters UT-A1 and UT-A2. Am J Physiol Renal Physiol 283:F817–F825

47. Fröhlich O, Klein JD, Smith PM, Sands JM, Gunn RB (2004) Urea transport in MDCK cells that are stably transfected with UT-A1. Am J Physiol Cell Physiol 286:C1264–C1270

48. Fröhlich O, Klein JD, Smith PM, Sands JM, Gunn RB (2006) Regulation of UT-A1-mediated transepithelial urea flux in MDCK cells. Am J Physiol Cell Physiol 291:C600–C606

49. Galla JH, Booker BB, Luke RG (1986) Role of the loop segment in the urinary concentrating defect of hypercalcemia. Kidney Int 29:977–982

50. Gertner R, Klein JD, Bailey JL, Kim D-U, Luo X, Bagnasco SM, Sands JM (2004) Aldosterone decreases UT-A1 urea transporter expression via the mineralocorticoid receptor. J Am Soc Nephrol 15:558–565

51. Geyer RR, Musa-Aziz R, Enkavi G, Mahinthichaichan P, Tajkhorshid E, Boron WF (2013) Movement of NH3 through the human urea transporter B: a new gas channel. Am J Physiol Renal Physiol 304:F1447–F1457

52. Gillin AG, Sands JM (1992) Characteristics of osmolarity-stimulated urea transport in rat IMCD. Am J Physiol Renal Physiol 262:F1061–F1067

53. Gillin AG, Star RA, Sands JM (1993) Osmolarity-stimulated urea transport in rat terminal IMCD: role of intracellular calcium. Am J Physiol Renal Physiol 265:F272–F277

54. Guron G, Nilsson A, Nitescu N, Nielsen S, Sundelin B, Frokiaer J, Friberg P (1999) Mechanisms of impaired urinary concentrating ability in adult rats treated neonatally with enalapril. Acta Physiol Scand 165:103–112

55. Harrington AR, Valtin H (1968) Impaired urinary concentration after vasopressin and its gradual correction in hypothalamic diabetes insipidus. J Clin Invest 47:502–510

56. Helms MN, Chen X-J, Ramosevac S, Eaton DC, Jain L (2006) Dopamine regulation of amiloride-sensitive sodium channels in lung cells. Am J Physiol Lung Cell Mol Physiol 291:L610–L618

57. Hoffert JD, Pisitkun T, Wang G, Shen RF, Knepper MA (2006) Quantitative phosphoproteomics of vasopressin-sensitive renal cells: regulation of aquaporin-2 phosphorylation at two sites. Proc Natl Acad Sci USA 103:7159–7164

58. Honegger KJ, Capuano P, Winter C, Bacic D, Stange G, Wagner CA, Biber J, Murer H, Hernando N (2006) Regulation of sodium-proton exchanger isoform 3 (NHE3) by PKA and exchange protein directly activated by cAMP (EPAC). Proc Natl Acad Sci USA 103:803–808

59. Hoorn EJ, Hoffert JD, Knepper MA (2005) Combined proteomics and pathways analysis of collecting duct reveals a protein regulatory network activated in vasopressin escape. J Am Soc Nephrol 16:2852–2863

60. Hu MC, Bankir L, Michelet S, Rousselet G, Trinh-Trang-Tan M-M (2000) Massive reduction of urea transporters in remnant kidney and brain of uremic rats. Kidney Int 58:1202–1210

61. Hu MC, Bankir L, Trinh-Trang-Tan MM (1999) mRNA expression of renal urea transporters in normal and Brattleboro rats: effect of dietary protein intake. Exp Nephrol 7:44–51

62. Huang H, Feng X, Zhuang J, Froehlich O, Klein JD, Cai H, Sands JM, Chen G (2010) Internalization of UT-A1 urea transporter is dynamin dependent and mediated by both caveolae and clathrin coated pit pathways. Am J Physiol Renal Physiol 299:F1389–F1395

63. Hwang S, Gunaratne R, Rinschen MM, Yu M-J, Pisitkun T, Hoffert JD, Fenton RA, Knepper MA, Chou C-L (2010) Vasporessin increases phosphorylation of ser84 and ser486 in Slc14a2 collecting duct urea transporters. Am J Physiol Renal Physiol 299:F559–F567

64. Igarashi P, Whyte DA, Nagami GT (1996) Cloning and kidney cell-specific activity of the promoter of the murine renal Na-K-Cl cotransporter gene. J Biol Chem 271:9666–9674

65. Ilori TO, Blount MA, Martin CF, Sands JM, Klein JD (2013) Urine concentration in the diabetic mouse requires both water and urea transporters. Am J Physiol Renal Physiol 304:F103–F111

66. Ilori TO, Wang Y, Blount MA, Martin CF, Sands JM, Klein JD (2012) Acute calcineurin inhibition with tacrolimus increases phosphorylated UT-A1. Am J Physiol Renal Physiol 302:F998–F1004

67. Inoue H, Jackson SD, Vikulina T, Klein JD, Tomita K, Bagnasco SM (2004) Identification and characterization of a Kidd antigen/UT-B urea transporter expressed in human colon. Am J Physiol Cell Physiol 287:C30–C35

68. Inoue T, Terris J, Ecelbarger CA, Chou C-L, Nielsen S, Knepper MA (1999) Vasopressin regulates apical targeting of aquaporin-2 but not of UT1 urea transporter in renal collecting duct. Am J Physiol 276:F559–F566

69. Isozaki T, Gillin AG, Swanson CE, Sands JM (1994) Protein restriction sequentially induces new urea transport processes in rat initial IMCDs. Am J Physiol 266:F756–F761

70. Isozaki T, Verlander JW, Sands JM (1993) Low protein diet alters urea transport and cell structure in rat initial inner medullary collecting duct. J Clin Invest 92:2448–2457

71. Issa VS, Andrade L, Ayub-Ferreira SM, Bacal F, de Bragança AC, Guimarães GV, Marcondes-Braga FG, Cruz FD, Chizzola PR, Conceição-Souza GE, Velasco IT, Bocchi EA (2013) Hypertonic saline solution for prevention of renal dysfunction in patients with decompensated heart failure. Int J Cardiol 167:34–40

72. Ito M, Oliverio MI, Mannon PJ, Best CF, Maeda N, Smithies O, Coffman TM (1995) Regulation of blood pressure by the type 1A angiotensin II receptor gene. Proc Natl Acad Sci USA 92:3521–3525

73. Jackson BA, Braun-Werness JL, Kusano E, Dousa TP (1983) Concentrating defect in the adrenalectomized rat. Abnormal vasopressin-sensitive cyclic adenosine monophosphate metabolism in the papillary collecting duct. J Clin Invest 72:997–1004

74. Jeon US, Han K-H, Park S-H, Lee SD, Sheen MR, Jung J-Y, Kim WY, Sands JM, Kim J, Kwon HM (2007) Downregulation of renal TonEBP in hypokalemic rats. Am J Physiol Renal Physiol 293:F408–F415

75. Jeon US, Kim JA, Sheen MR, Kwon HM (2006) How tonicity regulates genes: story of TonEBP transcriptional activator. Acta Physiol Scand 187:241–247

76. Jin W, Yao X, Wang T, Ji Q, Li Y, Yang X, Yao L (2012) Effects of hyperosmolality on expression of urea transporter A2 and aquaporin 2 in mouse medullary collecting duct cells. J Huazhong Univ Sci Technol [Med Sci] 32:59–64

77. Jung J-Y, Madsen KM, Han K-H, Yang C-W, Knepper MA, Sands JM, Kim J (2003) Expression of urea transporters in potassium-depleted mouse kidney. Am J Physiol Renal Physiol 285:F1210–F1224

78. Kakinuma Y, Fogo A, Inagami T, Ichikawa I (1993) Intrarenal localization of angiotensin II type 1 receptor mRNA in the rat. Kidney Int 43:1229–1235

79. Kamoi K, Tamura T, Tanaka K, Ishikashi M, Yamagi T (1993) Hyponatremia and osmoregulation of thirst and vasopressin secretion in patients with adrenal insufficiency. J Clin Endocrin Metab 77:1584–1588

80. Karakashian A, Timmer RT, Klein JD, Gunn RB, Sands JM, Bagnasco SM (1999) Cloning and characterization of two new mRNA isoforms of the rat renal urea transporter: UT-A3 and UT-A4. J Am Soc Nephrol 10:230–237

81. Kato A, Klein JD, Zhang C, Sands JM (2000) Angiotensin II increases vasopressin-stimulated facilitated urea permeability in rat terminal IMCDs. Am J Physiol Renal Physiol 279:F835–F840

82. Kato A, Naruse M, Knepper MA, Sands JM (1998) Long-term regulation of inner medullary collecting duct urea transport in rat. J Am Soc Nephrol 9:737–745

83. Kato A, Sands JM (1999) Urea transport processes are induced in rat IMCD subsegments when urine concentrating ability is reduced. Am J Physiol Renal Physiol 276:F62–F71

84. Kihara M, Umemura S, Sumida Y, Yokoyama N, Yabana M, Nyui N, Tamura K, Murakami K, Fukamizu A, Ishii M (1998) Genetic deficiency of angiotensinogen produces an impaired urine concentrating ability in mice. Kidney Int 53:548–555

85. Kim D-U, Klein JD, Racine S, Murrell BP, Sands JM (2005) Urea may regulate urea transporter protein abundance during osmotic diuresis. Am J Physiol Renal Physiol 288:F188–F197

86. Kim D-U, Sands JM, Klein JD (2003) Changes in renal medullary transport proteins during uncontrolled diabetes mellitus in rats. Am J Physiol Renal Physiol 285:F303–F309

87. Kim D-U, Sands JM, Klein JD (2004) Role of vasopressin in diabetes mellitus-induced changes in medullary transport proteins involved in urine concentration in Brattleboro rats. Am J Physiol Renal Physiol 286:F760–F766

88. Kim Y-H, Kim D-U, Han K-H, Jung J-Y, Sands JM, Knepper MA, Madsen KM, Kim J (2002) Expression of urea transporters in the developing rat kidney. Am J Physiol Renal Physiol 282:F530–F540

89. Kim YM, Kim WY, Lee HW, Kim J, Kwon HM, Klein JD, Sands JM, Kim D (2009) Urea and NaCl regulate UT-A1 urea transporter in opposing directions via TonEBP pathway during osmotic diuresis. Am J Physiol Renal Physiol 296:F67–F77

90. Kiran D, Mutsvangwa T (2010) Effects of partial ruminal defaunation on urea-nitrogen recycling, nitrogen metabolism, and microbial nitrogen supply in growing lambs fed low or high dietary crude protein concentrations. J Anim Sci 88:1034–1047

91. Klein JD, Blount MA, Fröhlich O, Denson C, Tan X, Sim J, Martin CF, Sands JM (2010) Phosphorylation of UT-A1 on serine 486 correlates with membrane accumulation and urea transport activity in both rat IMCDs and cultured cells. Am J Physiol Renal Physiol 298:F935–F940

92. Klein JD, Blount MA, Sands JM (2011) Urea transport in the kidney. Compr Physiol 1:699–729

93. Klein JD, Froehlich O, Mistry AC, Kent KJ, Martin CF, Sands JM (2013) Transgenic mice expressing UT-A1, but lacking UT-A3, have intact urine concentrating ability. FASEB J 27(1111):17

94. Klein JD, Fröhlich O, Blount MA, Martin CF, Smith TD, Sands JM (2006) Vasopressin increases plasma membrane accumulation of urea transporter UT-A1 in rat inner medullary collecting ducts. J Am Soc Nephrol 17:2680–2686

95. Klein JD, Martin CF, Kent KJ, Sands JM (2012) Protein kinase C alpha mediates hypertonicity-stimulated increase in urea transporter phosphorylation in the inner medullary collecting duct. Am J Physiol Renal Physiol 302:F1098–F1103

96. Klein JD, Quach DL, Cole JM, Disher K, Mongiu AK, Wang X, Bernstein KE, Sands JM (2002) Impaired urine concentration and the absence of tissue ACE: the involvement of medullary transport proteins. Am J Physiol Renal Physiol 283:F517–F524

97. Knepper MA, Danielson RA, Saidel GM, Johnston KH (1975) Effects of dietary protein restriction and glucocorticoid administration on urea excretion in rats. Kidney Int 8:303–315

98. Knepper MA, Gunter CV, Danielson RA (1976) Effects of glucagon on renal function in protein-deprived rats. Surg Forum 27:29–31

99. Knepper MA, Miranda CA (2013) Urea channel inhibitors: a new functional class of aquaretics. Kidney Int 83:991–993

100. Knepper MA, Sands JM, Chou C-L (1989) Independence of urea and water transport in rat inner medullary collecting duct. Am J Physiol Renal Physiol 256:F610–F621

101. Knox FG, Burnett JC Jr, Kohan DE, Spielman WS, Strand JC (1980) Escape from the sodium-retaining effects of mineralocorticoids. Kidney Int 17:263–276

102. Kondo Y, Imai M (1987) Effects of glutaraldehyde fixation on renal tubular function. I. Preservation of vasopressin-stimulated water and urea pathways in rat papillary collecting duct. Pfluegers Arch 408:479–483

103. Kudo LH, César KR, Ping WC, Rocha AS (1992) Effect of peritubular hypertonicity on water and urea transport of inner medullary collecting duct. Am J Physiol Renal, Fluid Electrolyte Physiol 262:F338–F347

104. Kudo LH, Van Baak AA, Rocha AS (1990) Effect of vasopressin on sodium transport across inner medullary collecting duct. Am J Physiol Renal Physiol 258:F1438–F1447

105. Kwun Y-S, Yeo SW, Ahn Y-H, Lim S-W, Jung J-Y, Kim W-Y, Sands JM, Kim J (2003) Immunohistochemical localization of urea transporters A and B in the rat cochlea. Hearing Res 183:84–96

106. Lam AK, Ko BC, Tam S, Morris R, Yang JY, Chung SK, Chung SS (2004) Osmotic response element-binding protein (OREBP) is an essential regulator of the urine concentrating mechanism. J Biol Chem 279:48048–48054

107. Laroche-Joubert N, Marsy S, Michelet S, Imbert-Teboul M, Doucet A (2002) Protein kinase A-independent activation of ERK and H, K-ATPase by cAMP in native kidney cells. Role of Epac I. J Biol Chem 277:18598–18604

108. Leroy C, Basset G, Gruel G, Ripoche P, Trinh-Trang-Tan M-M, Rousselet G (2000) Hyperosmotic NaCl and urea synergistically regulate the expression of the UT-A2 urea transporter in vitro and in vivo. Biochem Biophys Res Commun 271:368–373

109. Levi M, Peterson L, Berl T (1983) Mechanism of concentrating defect in hypercalcemia. Role of polydipsia and prostaglandins. Kidney Int 23:489–497

110. Li C, Klein JD, Wang W, Knepper MA, Nielsen S, Sands JM, Frokiaer J (2004) Altered expression of urea transporters in response to ureteral obstruction. Am J Physiol Renal Physiol 286:F1154–F1162

111. Li C, Wang W, Summer SN, Falk S, Schrier RW (2008) Downregulation of UT-A1/UT-A3 is associated with urinary concentrating defect in glucocorticoid-excess state. J Am Soc Nephrol 19:1975–1981

112. Li F, Lei T, Zhu J, Wang W, Sun Y, Chen J, Dong Z, Zhou H, Yang B (2013) A novel small-molecule thienoquinolin urea transporter inhibitor acts as a potential diuretic. Kidney Int 83:1076–1086

113. Li Y, Konings IBM, Zhao J, Price LS, de Heer E, Deen PMT (2008) Renal expression of exchange protein directly activated by cAMP (Epac) 1 and 2. Am J Physiol Renal Physiol 295:F525–F533

114. Lim S-W, Han K-H, Jung J-Y, Kim W-Y, Yang C-W, Sands JM, Knepper MA, Madsen KM, Kim J (2006) Ultrastructural localization of UT-A and UT-B in rat kidneys with different hydration status. Am J Physiol Regul Integr Comp Physiol 290:R479–R492

115. Lucien N, Bruneval P, Lasbennes F, Belair MF, Mandet C, Cartron JP, Bailly P, Trinh-Trang-Tan MM (2005) UT-B1 urea transporter is expressed along the urinary and gastrointestinal tracts of the mouse. Am J Physiol Regul Integr Comp Physiol 288:R1046–R1056

116. Ludden PA, Stohrer RM, Austin KJ, Atkinson RL, Belden EL, Harlow HJ (2009) Effect of protein supplementation on expression and distribution of urea transporter-B in lambs fed low-quality forage. J Anim Sci 87:1354–1365

117. Maeda Y, Terada Y, Nonoguchi H, Knepper MA (1992) Hormone and autocoid regulation of cAMP production in rat IMCD subsegments. Am J Physiol Renal Physiol 263:F319–F327

118. Magaldi AJ, Cesar KR, Yano Y (1994) Effect of insulin on water and urea transport in the inner medullary collecting duct. Am J Physiol Renal Physiol 266:F394–F399

119. Marini JC, Klein JD, Sands JM, Van Amburgh ME (2004) Effect of nitrogen intake on nitrogen recycling and urea transporter abundance in lambs. J Anim Sci 82:1157–1164

120. Meng Y, Zhao C, Zhang X, Zhao H, Guo L, Lu B, Zhao X, Yang B (2009) Surface electrocardiogram and action potential in mice lacking urea transporter UT-B. Sci China C Life Sci 52:474–478

121. Mistry AC, Mallick R, Fröhlich O, Klein JD, Rehm A, Chen G, Sands JM (2007) The UT-A1 urea transporter interacts with snapin, a snare-associated protein. J Biol Chem 282:30097–30106

122. Mistry AC, Mallick R, Klein JD, Sands JM, Froehlich O (2010) Functional characterization of the central hydrophilic linker region of the urea transporter UT-A1: cAMP activation and snapin binding. Am J Physiol Cell Physiol 298:C1431–C1437

123. Morgan T, Berliner RW (1968) Permeability of the loop of Henle, vasa recta, and collecting duct to water, urea, and sodium. Am J Physiol 215:108–115

124. Morgan T, Sakai F, Berliner RW (1968) In vitro permeability of medullary collecting duct to water and urea. Am J Physiol 214:574–581

125. Morris RG, Uchida S, Brooks H, Knepper MA, Chou CL (2005) Altered expression profile of transporters in the inner medullary collecting duct of aquaporin-1 knockout mice. Am J Physiol Renal Physiol 289:F194–F199

126. Mujais SK, Kauffman S, Katz AI (1986) Angiotensin II binding sites in individual segments of the rat nephron. J Clin Invest 77:315–318

127. Nakayama Y, Naruse M, Karakashian A, Peng T, Sands JM, Bagnasco SM (2001) Cloning of the rat Slc14a2 gene and genomic organization of the UT-A urea transporter. Biochim Biophys Acta 1518:19–26

128. Nakayama Y, Peng T, Sands JM, Bagnasco SM (2000) The TonE/TonEBP pathway mediates tonicity-responsive regulation of UT-A urea transporter expression. J Biol Chem 275:38275–38280

129. Naruse M, Klein JD, Ashkar ZM, Jacobs JD, Sands JM (1997) Glucocorticoids downregulate the rat vasopressin-regulated urea transporter in rat terminal inner medullary collecting ducts. J Am Soc Nephrol 8:517–523

130. Nielsen S, DiGiovanni SR, Christensen EI, Knepper MA, Harris HW (1993) Cellular and subcellular immunolocalization of vasopressin-regulated water channel in rat kidney. Proc Natl Acad Sci USA 90:11663–11667

131. Nielsen S, Knepper MA (1993) Vasopressin activates collecting duct urea transporters and water channels by distinct physical processes. Am J Physiol Renal Physiol 265:F204–F213

132. Nielsen S, Terris J, Smith CP, Hediger MA, Ecelbarger CA, Knepper MA (1996) Cellular and subcellular localization of the vasopressin-regulated urea transporter in rat kidney. Proc Natl Acad Sci USA 93:5495–5500

133. Nonoguchi H, Sands JM, Knepper MA (1988) Atrial natriuretic factor inhibits vasopressin-stimulated osmotic water permeability in rat inner medullary collecting duct. J Clin Invest 82:1383–1390

134. Okubo S, Niimura F, Matsusaka T, Fogo A, Hogan BLM, Ichikawa I (1998) Angiotensinogen gene null-mutant mice lack homeostatic regulation of glomerular filtration and tubular reabsorption. Kidney Int 53:617–625

135. Pallone T, Zhang Z, Rhinehart K (2003) Physiology of the renal medullary microcirculation. Am J Physiol Renal Physiol 284:F253–F266

136. Pannabecker TL, Dantzler WH, Layton HE, Layton AT (2008) Role of three-dimensional architecture in the urine concentrating mechanism of the rat renal inner medulla. Am J Physiol Renal Physiol 295:F1271–F1285

137. Peil AE, Stolte H, Schmidt-Nielsen B (1990) Uncoupling of glomerular and tubular regulations of urea excretion in rat. Am J Physiol Renal Physiol 258:F1666–F1674

138. Peng T, Sands JM, Bagnasco SM (2002) Glucocorticoids inhibit transcription and expression of the rat UT-A urea transporter gene. Am J Physiol Renal Physiol 282:F853–F858

139. Potter EA, Stewart G, Smith CP (2006) Urea flux across MDCK-mUT-A2 monolayers is acutely sensitive to AVP, cAMP, and $[Ca^{2+}]_i$. Am J Physiol Renal Physiol 291:F122–F128

140. Preisser L, Teillet L, Aliotti S, Gobin R, Berthonaud V, Chevalier J, Corman B, Verbavatz JM (2000) Downregulation of aquaporin-2 and -3 in aging kidney is independent of V_2 vasopressin receptor. Am J Physiol Renal Physiol 279:F144–F152

141. Promeneur D, Bankir L, Hu MC, Trinh-Trang-Tan M-M (1998) Renal tubular and vascular urea transporters: influence of antidiuretic hormone on messenger RNA expression in Brattleboro rats. J Am Soc Nephrol 9:1359–1366

142. Promeneur D, Rousselet G, Bankir L, Bailly P, Cartron JP, Ripoche P, Trinh-Trang-Tan MM (1996) Evidence for distinct vascular and tubular urea transporters in the rat kidney. J Am Soc Nephrol 7:852–860

143. Rocha AS, Ping WC, Kudo LH (1991) Effect of chlorpropamide on water and urea transport in the inner medullary collecting duct. Kidney Int 39:79–86

144. Rouch AJ, Kudo LH (1996) α₂-Adrenergic-mediated inhibition of water and urea permeability in the rat IMCD. Am J Physiol Renal Physiol 271:F150–F157

145. Sanches TR, Volpini RA, Massola Shimizu MH, Braganca AC, Oshiro-Monreal F, Seguro AC, Andrade L (2012) Sildenafil reduces polyuria in rats with lithium-induced NDI. Am J Physiol Renal Physiol 302:F216–F225

146. Sands JM (1999) Regulation of renal urea transporters. J Am Soc Nephrol 10:635–646

147. Sands JM (2003) Urine-concentrating ability in the aging kidney. Sci Aging Knowledge Environ 24:pe15

148. Sands JM (2009) Urinary concentration and dilution in the aging kidney. Semin Nephrol 29:579–586

149. Sands JM (2012) Urine concentrating and diluting ability during aging. J Gerontol A Biol Sci Med Sci 67:1352–1357

150. Sands Jeff M (2013) Urea transporter inhibitors: en route to new diuretics. Chem Biol 20:1201–1202

151. Sands JM, Blount MA, Klein JD (2011) Regulation of renal urea transport by vasopressin. Trans Am Clin Climatol Assoc 122:82–92

152. Sands JM, Flores FX, Kato A, Baum MA, Brown EM, Ward DT, Hebert SC, Harris HW (1998) Vasopressin-elicited water and urea permeabilities are altered in the inner medullary collecting duct in hypercalcemic rats. Am J Physiol Renal Physiol 274:F978–F985

153. Sands JM, Knepper MA (1987) Urea permeability of mammalian inner medullary collecting duct system and papillary surface epithelium. J Clin Invest 79:138–147

154. Sands JM, Naruse M, Baum M, Jo I, Hebert SC, Brown EM, Harris HW (1997) Apical extracellular calcium/polyvalent cation-sensing receptor regulates vasopressin-elicited water permeability in rat kidney inner medullary collecting duct. J Clin Invest 99:1399–1405

155. Sands JM, Nonoguchi H, Knepper MA (1987) Vasopressin effects on urea and H_2O transport in inner medullary collecting duct subsegments. Am J Physiol Renal Physiol 253:F823–F832

156. Sands JM, Schrader DC (1991) An independent effect of osmolality on urea transport in rat terminal IMCDs. J Clin Invest 88:137–142

157. Sasaki A, Kida O, Kita T, Kato J, Nakamura S, Kodama K, Miyata A, Kangawa K, Matsuo H, Tanaka K (1989) Effects of antiserum against α-rat atrial natriuretic polypeptide in spontaneously hypertensive rats. Am J Physiol Heart Circ Physiol 257:H1104–H1109

158. Schmidt C, Hocherl K, Bucher M (2007) Cytokine-mediated regulation of urea transporters during experimental endotoxemia. Am J Physiol Renal Physiol 292:F1479–F1489

159. Schwartz MJ, Kokko JP (1980) Urinary concentrating defect of adrenal insufficiency. Permissive role of adrenal steroids on the hydroosmotic response across the rabbit cortical collecting duct. J Clin Invest 66:234–242

160. Seamon KB, Padgett W, Daly JW (1981) Forskolin—unique diterpene activator of adenylate cyclase in membranes and intact cells. Proc Natl Acad Sci USA 87:3363–3367

161. Shayakul C, Knepper MA, Smith CP, DiGiovanni SR, Hediger MA (1997) Segmental localization of urea transporter mRNAs in rat kidney. Am J Physiol 272:F654–F660

162. Shayakul C, Smith CP, Mackenzie HS, Lee W-S, Brown D, Hediger MA (2000) Long-term regulation of urea transporter expression by vasopressin in Brattleboro rats. Am J Physiol Renal Physiol 278:F620–F627

163. Shayakul C, Steel A, Hediger MA (1996) Molecular cloning and characterization of the vasopressin-regulated urea transporter of rat kidney collecting ducts. J Clin Invest 98:2580–2587

164. Shayakul C, Tsukaguchi H, Berger UV, Hediger MA (2001) Molecular characterization of a novel urea transporter from kidney inner medullary collecting ducts. Am J Physiol Renal Physiol 280:F487–F494

165. Shimizu MHM, Volpini RA, de Bragança AC, Campos R, Canale D, Sanches TR, Andrade L, Seguro AC (2013) N-acetylcysteine attenuates renal alterations induced by senescence in the rat. Exp Gerontol 48:298–303

166. Simmons NL, Chaudhry AS, Graham C, Scriven ES, Thistlethwaite A, Smith CP, Stewart GS (2009) Dietary regulation of ruminal bovine UT-B urea transporter expression and localization. J Anim Sci 87:3288–3299

167. Smith CP, Lee W-S, Martial S, Knepper MA, You G, Sands JM, Hediger MA (1995) Cloning and regulation of expression of the rat kidney urea transporter (rUT2). J Clin Invest 96:1556–1563

168. Smith CP, Potter EA, Fenton RA, Stewart GS (2004) Characterization of a human colonic cDNA encoding a structurally novel urea transporter, UT-A6. Am J Physiol Cell Physiol 287:C1087–C1093

169. Spector DA, Yang Q, Liu J, Wade JB (2004) Expression, localization, and regulation of urea transporter B in rat urothelia. Am J Physiol Renal Physiol 287:F102–F108

170. Star RA (1990) Apical membrane limits urea permeation across the rat inner medullary collecting duct. J Clin Invest 86:1172–1178

171. Star RA, Nonoguchi H, Balaban R, Knepper MA (1988) Calcium and cyclic adenosine monophosphate as second messengers for vasopressin in the rat inner medullary collecting duct. J Clin Invest 81:1879–1888

172. Starke S, Muscher AS, Hirschhausen N, Pfeffer E, Breves G, Huber K (2012) Expression of urea transporters is affected by dietary nitrogen restriction in goat kidney. J Anim Sci 90:3889–3897

173. Stewart GS, Graham C, Cattell S, Smith TPL, Simmons NL, Smith CP (2005) UT-B is expressed in bovine rumen: potential role in ruminal urea transport. Am J Physiol Regul Integr Comp Physiol 289:R605–R612

174. Stewart GS, King SL, Potter EA, Smith CP (2007) Acute regulation of the urea transporter mUT-A3 expressed in a MDCK cell line. Am J Physiol Renal Physiol 292:F1157–F1163

175. Stewart GS, O'Brien JH, Smith CP (2008) Ubiquitination regulates the plasma membrane expression of renal UT-A urea transporters. Am J Physiol Cell Physiol 295:C121–C129

176. Stewart GS, Thistlethwaite A, Lees H, Cooper GJ, Smith C (2009) Vasopressin regulation of the renal UT-A3 urea transporter. Am J Physiol Renal Physiol 296:F642–F649

177. Su H, Carter CB, Frohlich O, Cummings RD, Chen G (2012) Glycoforms of UT-A3 urea transporter with poly-N-acetyllactosamine glycosylation have enhanced transport activity. Am J Physiol Renal Physiol 303:F201–F208

178. Su H, Carter CB, Laur O, Sands JM, Chen G (2012) Forskolin stimulation promotes urea transporter UT-A1 ubiquitination, endocytosis, and degradation in MDCK cells. Am J Physiol Renal Physiol 303:F1325–F1332

179. Su H, Liu B, Frohlich O, Ma H, Sands JM, Chen G (2013) Small GTPase Rab14 down-regulates UT-A1 urea transport activity through enhanced clathrin-dependent endocytosis. FASEB J 27:4100–4107

180. Terada Y, Tomita K, Nonoguchi H, Marumo F (1993) PCR localization of angiotensin II receptor and angiotensin mRNAs in rat kidney. Kidney Int 43:1251–1259

181. Terris J, Ecelbarger CA, Sands JM, Knepper MA (1998) Long-term regulation of collecting duct urea transporter proteins in rat. J Am Soc Nephrol 9:729–736

182. Terris JM, Knepper MA, Wade JB (2001) UT-A3: localization and characterization of an additional urea transporter isoform in the IMCD. Am J Physiol Renal Physiol 280:F325–F332

183. Thai TL, Blount MA, Klein JD, Sands JM (2012) Lack of protein kinase C-α leads to impaired urine concentrating ability and decreased aquaporin-2 in angiotensin II-induced hypertension. Am J Physiol Renal Physiol 303:F37–F44

184. Tian W, Cohen DM (2001) Signaling and gene regulation by urea in cells of the mammalian kidney medulla. Comp Biochem Physiol A: Mol Integr Physiol 130:429–436

185. Tickle P, Thistlethwaite A, Smith CP, Stewart GS (2009) Novel bUT-B2 urea transporter isoform is constitutively activated. Am J Physiol Regul Integr Comp Physiol 297:R323–R329

186. Timmer RT, Klein JD, Bagnasco SM, Doran JJ, Verlander JW, Gunn RB, Sands JM (2001) Localization of the urea transporter UT-B protein in human and rat erythrocytes and tissues. Am J Physiol Cell Physiol 281:C1318–C1325

187. Trinh-Trang-Tan M-M, Cartron JP, Bankir L (2005) Molecular basis for the dialysis disequilibrium syndrome: altered aquaporin and urea transporter expression in the brain. Nephrol Dial Transplant 20:1984–1988

188. Trinh-Trang-Tan M-M, Lasbennes F, Gane P, Roudier N, Ripoche P, Cartron J-P, Bailly P (2002) UT-B1 proteins in rat: tissue distribution and regulation by antidiuretic hormone in kidney. Am J Physiol Renal Physiol 283:F912–F922

189. Trinh-Trang-Tan MM, Geelen G, Teillet L, Corman B (2003) Urea transporter expression in aging kidney and brain during dehydration. Am J Physiol Regul Integr Comp Physiol 285:R1355–R1365

190. Uawithya P, Pisitkun T, Ruttenberg BE, Knepper MA (2008) Transcriptional profiling of native inner medullary collecting duct cells from rat kidney. Physiol Genomics 32:229–253

191. Verkman AS, Yang BX, Song YL, Manley GT, Ma TH (2000) Role of water channels in fluid transport studied by phenotype analysis of aquaporin knockout mice. Exp Physiol 85:233S–241S

192. von Bergen TN, Blount MA (2012) Chronic use of chloroquine disrupts the urine concentration mechanism by lowering cAMP levels in the inner medulla. Am J Physiol Renal Physiol 303:F900–F905

193. Wade JB, Lee AJ, Liu J, Ecelbarger CA, Mitchell C, Bradford AD, Terris J, Kim G-H, Knepper MA (2000) UT-A2: a 55 kDa urea transporter protein in thin descending limb of Henle's loop whose abundance is regulated by vasopressin. Am J Physiol Renal Physiol 278:F52–F62

194. Wagner L, Klein JD, Sands JM, Baylis C (2002) Urea transporters are widely distributed in endothelial cells and mediate inhibition of L-arginine transport. Am J Physiol Renal Physiol 283:F578–F582

195. Wall SM, Suk Han J, Chou C-L, Knepper MA (1992) Kinetics of urea and water permeability activation by vasopressin in rat terminal IMCD. Am J Physiol Renal Physiol 262:F989–F998

196. Wang X-Y, Beutler K, Nielsen J, Nielsen S, Knepper MA, Masilamani S (2002) Decreased abundance of collecting duct urea transporters UT-A1 and UT-A3 with ECF volume expansion. Am J Physiol Renal Physiol 282:F577–F584

197. Wang X, Harris PC, Somlo S, Batlle D, Torres VE (2009) Effect of calcium-sensing receptor activation in models of autosomal recessive or dominant polycystic kidney disease. Nephrol Dial Transplant 24:526–534

198. Wang Y, Klein JD, Blount MA, Martin CF, Kent KJ, Pech V, Wall SM, Sands JM (2009) Epac regulation of the UT-A1 urea transporter in rat IMCDs. J Am Soc Nephrol 20:2018–2024

199. Wang Y, Klein JD, Fröhlich O, Sands JM (2013) Role of protein kinase C-a in hypertonicity-stimulated urea permeability in mouse inner medullary collecting ducts. Am J Physiol Renal Physiol 304:F233–F238

200. Wang Y, Liedtke CM, Klein JD, Sands JM (2010) Protein kinase C regulates urea permeability in the rat inner medullary collecting duct. Am J Physiol Renal Physiol 299:F1401–F1406

201. Xu Y, Olives B, Bailly P, Fischer E, Ripoche P, Ronco P, Cartron J-P, Rondeau E (1997) Endothelial cells of the kidney vasa recta express the urea transporter HUT11. Kidney Int 51:138–146

202. Yamaguchi Y, Takaki S, Hyodo S (2009) Subcellular distribution of urea transporter in the collecting tubule of shark kidney is dependent on environmental salinity. J Exp Zool Part A Ecol Genet Physiol 311:705–718

203. Yang B, Bankir L, Gillespie A, Epstein CJ, Verkman AS (2002) Urea-selective concentrating defect in transgenic mice lacking urea transporter UT-B. J Biol Chem 277:10633–10637

204. Yang JY, Tam WY, Tam S, Guo H, Wu X, Li G, Chau JFL, Klein JD, Chung SK, Sands JM, Chung SS (2006) Genetic restoration of aldose reductase to the collecting tubules restores maturation of the urine concentrating mechanism. Am J Physiol Renal Physiol 291:F186–F195

205. S-k Yang, Xiao L, Li J, Liu F, Sun L, Kanwar YS (2013) Role of guanine-nucleotide exchange factor Epac in renal physiology and pathophysiology. Am J Physiol Renal Physiol 304:F831–F839

206. Yano Y, Monteiro JL, Seguro AC (1994) Effect of amphotericin B on water and urea transport in the inner medullary collecting duct. J Am Soc Nephrol 5:68–74

207. Yano Y, Rodrigues AC Jr, deBraganca AC, Andrade LC, Magaldi AJ (2008) PKC stimulated by glucagon decreases UT-A1 urea transporter expression in rat IMCD. Pflugers Arch 456:1229–1237

208. Yao C, Anderson MO, Zhang J, Yang B, Phuan PW, Verkman AS (2012) Triazolothienopyrimidine inhibitors of urea transporter ut-b reduce urine concentration. J Am Soc Nephrol 23:1210–1220

209. Yasui M, Zelenin SM, Celsi G, Aperia A (1997) Adenylate cyclase-coupled vasopressin receptor activates AQP2 promoter via a dual effect on CRE and AP1 elements. Am J Physiol Renal Physiol 272:F443–F450

210. Yip KP (2008) Epac-mediated Ca^{2+} mobilization and exocytosis in inner medullary collecting duct. Am J Physiol Renal Physiol 291:F882–F890

211. You G, Smith CP, Kanai Y, Lee W-S, Stelzner M, Hediger MA (1993) Cloning and characterization of the vasopressin-regulated urea transporter. Nature 365:844–847
212. Yu H, Meng Y, Wang LS, Jin X, Gao LF, Zhou L, Ji K, Li Y, Zhao LJ, Chen GQ, Zhao XJ, Yang B (2009) Differential protein expression in heart in UT-B null mice with cardiac conduction defects. Proteomics 9:504–511
213. Yu MJ, Pisitkun T, Wang G, Aranda JF, Gonzales PA, Tchapyjnikov D, Shen RF, Alonso MA, Knepper MA (2008) Large-scale quantitative LC-MS/MS analysis of detergent-resistant membrane proteins from rat renal collecting duct. Am J Physiol Cell Physiol 295:C661–C678
214. Yu MJ, Pisitkun T, Wang G, Shen RF, Knepper MA (2006) LC-MS/MS analysis of apical and basolateral plasma membranes of rat renal collecting duct cells. Mol Cell Proteom 5:2131–2145
215. Zhang C, Sands JM, Klein JD (2002) Vasopressin rapidly increases the phosphorylation of the UT-A1 urea transporter activity in rat IMCDs through PKA. Am J Physiol Renal Physiol 282:F85–F90
216. Zhang Y, Sands JM, Kohan DE, Nelson RD, Martin CF, Carlson NG, Kamerath CD, Ge Y, Klein JD, Kishore BK (2008) Potential role of purinergic signaling in urinary concentration in inner medulla: insights from P2Y2 receptor gene knockout mice. Am J Physiol Renal Physiol 295:F1715–F1724

Chapter 7
Biochemical Properties of Urea Transporters

Guangping Chen

Abstract Urea and urea transporters (UT) are critical to the production of concentrated urine and hence in maintaining body fluid balance. The UT-A1 urea transporter is the major and most important UT isoform in the kidney. Native UT-A1, expressed in the terminal inner medullary collecting duct (IMCD) epithelial cells, is a glycosylated protein with two glycoforms of 117 and 97 kDa. Vasopressin is the major hormone in vivo that rapidly increases urea permeability in the IMCD through increases in phosphorylation and apical plasma-membrane accumulation of UT-A1. The cell signaling pathway for vasopressin-mediated UT-A1 phosphorylation and activity involves two cAMP-dependent signaling pathways: protein kinase A (PKA) and exchange protein activated by cAMP (Epac). In this chapter, we will discuss UT-A1 regulation by phosphorylation, ubiquitination, and glycosylation.

Keywords Urinary concentration · Vasopressin · Protein kinase A · Phosphorylation · Membrane trafficking · Ubiquitination · Protein degradation · N-linked glycosylation

Phosphorylation of Urea Transporters

A tubular perfusion study by Sands et al. [57] in 1987 first demonstrated that the terminal IMCD exhibits a high basal urea permeability. This activity is dramatically increased in the presence of the hormone vasopressin. The first UT-A urea transporter, UT-A2, was cloned by You et al. [81] in 1991 and was characterized as

G. Chen (✉)
Department of Physiology, and Renal Division Department of Medicine,
Emory University School of Medicine, Whitehead Research Building Room 605N,
615 Michael Street, Atlanta, GA 30322, USA
e-mail: gchen3@emory.edu

the vasopressin-regulated urea transporter. Vasopressin [AVP; also known as anti-diuretic hormone (ADH)], synthesized in the hypothalamus and stored in vesicles in the posterior pituitary, is the major hormone regulating urine-concentrating ability. Vasopressin increases both osmotic water and urea permeabilities in principal cells in the kidney collecting duct [51, 54, 56, 73]. Using [^{32}P] radioisotope labeling techniques in IMCD suspensions, Zhang et al. [83] in 2002 provided the first experimental evidence that UT-A1 is directly phosphorylated by vasopressin. Subsequently, new technologies, such as proteomic and cDNA array, have identified UT-A1, as well as UT-A3, as the phosphorylated proteins stimulated by vasopressin in the inner medulla [2, 6, 25, 27, 70, 82]. Adding vasopressin (or the cAMP stimulator forskolin) to IMCD suspensions rapidly increases the abundance of phosphorylated UT-A1 at 2 min, which peaks at 5–10 min and remains elevated for up to 30 min [83]. The time course and dose response of UT-A1 phosphorylation are identical to vasopressin-induced stimulation of urea permeability observed by Wall et al. [73] in 1992 in perfused rat terminal IMCDs. Vasopressin also increases the phosphorylation of UT-A1 in UT-A1-MDCK cells [18, 19] and UT-A1-mIMCD3 cells [37]. The role of UT-A1 phosphorylation for vasopressin-stimulated activity and trafficking to the IMCD apical plasma membrane was further emphasized by Blount et al. [3] using phosphomutant forms of UT-A1 heterologously expressed in cultured cells.

Vasopressin Signaling Pathway Mediating UT-A1 Phosphorylation

Star et al. [62] in 1988 used isolated perfused tubules to demonstrate that both vasopressin-regulated urea transport and vasopressin-regulated water transport are dependent on a rise in intracellular cyclic AMP. The addition of vasopressin to the basolateral membrane of a rat terminal IMCD stimulates kidney urea permeability via the V$_2$ vasopressin receptor. This is mimicked by a selective V$_2$ agonist, dDAVP, in perfused terminal IMCDs [62]. Vasopressin binds to the IMCD cell V$_2$ receptor in the basolateral plasma membrane, activates the heterotrimeric G protein Gαs, and results in an increased generation of cAMP by at least two adenylyl cyclase isoforms, III and VI [50, 57, 73, 83]. Rat, mouse, and human UT-A1 are stimulated by cAMP when expressed in Xenopus oocytes [1, 17, 59, 60]. One important downstream kinase activated by increased cAMP is PKA. A study by Zhang et al. [83] showed that the PKA inhibitor H89 significantly suppresses vasopressin-stimulated UT-A1 phosphorylation. These studies indicate that UT-A1 is phosphorylated, possibly by PKA directly. In vitro assays using synthetic UT-A1 peptides showed that purified PKA can directly phosphorylate UT-A1 [2]. Inhibitors of PKA reduce both the vasopressin-stimulated and basal levels of UT-A1 phosphorylation, showing that PKA can phosphorylate UT-A1, both basally and in response to vasopressin stimulation [83].

Though cyclic AMP is traditionally believed to act through PKA, a study by Fröhlich et al. [19] noticed that the PKA inhibitor H-89 could not completely inhibit forskolin-induced urea flux in UT-A1-MDCK cells. The portion of the non-PKA effect caused by elevated cAMP raises the possibility that vasopressin may have a second cAMP-dependent, but non-PKA-mediated, signaling pathway in rat IMCDs. In addition to acting through PKA, cAMP can activate Epac (exchange protein activated by cAMP) [4, 26, 40, 44, 74]. There are two closely related Epac proteins, Epac1 and Epac2, and both have been detected in rat IMCDs [40, 44]. Functional analysis showed that incubation of rat IMCD suspensions with the Epac activator Sp-8-pCPT-2′-O-Me-cAMPS causes an increase in UT-A1 phosphorylation and its accumulation in the plasma membrane [74]. Epac activates Rap1, a Ras-related small molecular weight G protein, which in turn signals through mitogen-activated protein kinase (MEK) and extracellular signal-related kinase (ERK). Inhibition of MEK 1/2 phosphorylation by U0126 decreased the forskolin-stimulated UT-A1 phosphorylation [74]. Thus, as illustrated in Fig. 7.1, UT-A1 phosphorylation is stimulated by vasopressin in the IMCD through at least two cAMP-dependent signaling pathways: PKA-dependent and Epac-MEK-dependent pathways.
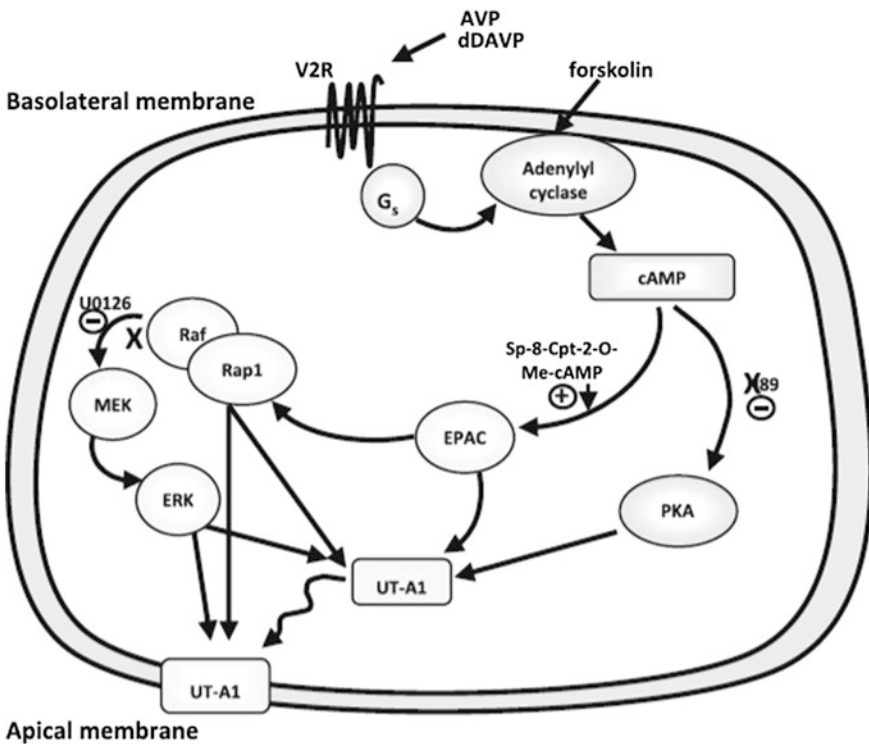

Fig. 7.1 UT-A1 phosphorylation signaling pathways mediated by vasopressin: protein kinase A (PKA)-dependent and exchange protein activated by cAMP (Epac)-mitogen-activated protein kinase (MEK)-dependent pathways [74]

UT-A1 Phosphorylation by PKA

The rat UT-A1 amino acid sequence contains multiple consensus PKA phosphorylation motifs (x-(R/K)-(R/K)-x-(S/T)-(^P): 3 phosphorylation sites in the N-terminus, 6 in the large intracellular loop, and 1 in the C-terminus. Mass spectrometry-based phosphoproteomic analysis of rat collecting ducts by Hoffert [25] and later by Bansal [2] suggested several cAMP-PKA sites including Ser10, Ser62, Ser63, Ser84, Ser486, and Ser499. Among these sites, three are highly demonstrated by mass spectrometry to be regulated by vasopressin: Ser84, Ser486, and Ser499 [2]. Although the UT-A1 amino acid sequence possesses many potential PKA phosphorylation sites, including both serine and threonine residues, phosphoproteomic analysis [2, 25] only shows phosphorylation of serine residues. This is in agreement with an early observation by Zhang et al. [83] that vasopressin does not phosphorylate the UT-A1 tyrosine residue. The anti-phosphotyrosine antibody (PY-20) did not recognize any proteins from UT-A1 immunoprecipitated samples from IMCD suspensions.

Serine 486 and serine 499 in the central intracellular loop of UT-A1 have been experimentally reported to serve as cAMP-PKA phosphorylation sites by two independent laboratories [2, 3, 25, 37]. Ser499 is highly evolutionary conserved across rat, mouse, horse, cow, and human UT-A1. Ser486 is also conserved in all of these species except for cows, where it is an asparagine residue. Mutation of both Ser486 and Ser499, but not either one alone, eliminates forskolin's ability to stimulate UT-A1 accumulation in the apical plasma membrane and urea transport, indicating that at least one of these serines must be phosphorylated [3]. The double mutant was unable to traffic to the plasma membrane, showing that phosphorylation of UT-A1 at these sites is critical to urea transport and trafficking [3]. A phospho-specific antibody to Ser486 UT-A1 shows that Ser486-phosphorylated UT-A1 is primarily expressed in the apical plasma membrane in rat IMCDs [37].

A third vasopressin-stimulated phosphorylation site in rat UT-A1 at Ser84 has been suggested by phosphoproteomic analysis [2, 25] and confirmed by Hwang et al. [31]. Ser84 is present in both UT-A1 and UT-A3. However, Ser84 is less conserved among species. In human UT-A1, Ser84 is not preserved but substituted by aspartic acid. Interestingly, the aspartic acid in humans has the same charge (-1) as a phosphorylated serine; therefore, it probably represents a constitutively activated form [2].

UT-A1 Phosphorylation by PKC and Other Kinases

It is well documented that urea permeability is regulated by vasopressin via cAMP-dependent signaling pathways. The PKA activated by cAMP is the most important kinase responsible for UT-A1 phosphorylation, particularly in the presence of vasopressin; however, other kinases may also phosphorylate UT-A1. Several early observations demonstrate that urea permeability in perfused IMCDs is activated by hypertonicity (adding NaCl or mannitol) in the absence of vasopressin [20, 39, 58].

Interestingly, hypertonicity does not increase intracellular cAMP levels in the IMCD, but it does increase intracellular calcium [21]. Hypertonicity increases urea permeability via changes in intracellular calcium, suggesting involvement of a calcium-dependent protein kinase in the urea transport response [76]. Subsequent studies showed that hypertonicity mediates urea permeability through a calcium-dependent PKC signaling pathway independently of vasopressin [21, 38, 58, 75].

PKC is a family of serine/threonine-related protein kinases that play a key role in many cellular functions and affect many signal transduction pathways. PKC isoforms can be subclassified into three groups: conventional PKC (cPKC) isoforms (PKCα, βI, βII, and λ); novel PKC isoforms (nPKCs) (PKCδ, ε, η, θ, μ); and atypical PKC isoforms (aPKCs) (PKCι/λ and ζ) [75]. Seven PKC isoforms are present in rat inner medulla, including PKC α, β, γ, δ, ε, θ, τ, and λ [76]. Consistent with putative PKC phosphorylation sites in UT-A1's amino acid sequence, PKC does phosphorylate UT-A1 [38].

The role of PKC in UT-A1 phosphorylation and urea transport activity regulation has been extensively investigated in PKCα knockout mice [38, 69, 75]. PKCα is a calcium-dependent PKC isoform and PKCα-deficient mice have a urine-concentrating defect [38, 79]. Direct evidence using metabolic labeling with ^{32}P-orthophosphate shows that inhibiting PKC prevents the hypertonicity-mediated stimulation of UT-A1 phosphorylation. In IMCD suspensions from PKCα-deficient mice, hypertonicity fails to induce UT-A1 phosphorylation [38, 75]. Although there are a number of potential PKC phosphorylation sites in UT-A1, the exact sites phosphorylated by PKC have not been identified yet. Klein et al. [38] showed that in response to hypertonicity, UT-A1 phosphorylation was increased; however, phosphorylation at serine 486 was not increased, indicating that PKC does not phosphorylate UT-A1 at the same residue as PKA [38]. Further investigation is required to detail the exact PKC phosphorylation sites in UT-A1.

In addition to being phosphorylated by PKA and PKC, analysis of the UT-A1 amino acid sequence reveals various other potential phosphorylation consensus sites, suggesting that UT-A1 may also be susceptible to other kinases. These phosphorylation recognition sites include: casein kinase I, II (CK1, CK2), GSK3, never in mitosis A (NimA)-related kinase (NEK) 2, phosphoinositide-3-OH-kinase-related kinases (PIKKs), and phosphorylase kinase (PK). Proteomic studies by Knepper's group identified over 200 serine/threonine protein kinases in native collecting duct cells [2, 70]. Rinschen et al. [53] reported that vasopressin activates CaM kinase II in collecting duct cells.

Regulation of UT-A1 Phosphorylation by Dephosphorylation Enzymes

Phosphatases act in an opposite way to kinase/phosphorylases. Undoubtedly, the level of protein phosphorylation is also controlled by dephosphorylation enzymes that catalyze the dephosphorylation of UT-A1. Compared to UT-A1

phosphorylation, the specific phosphatases that act on UT-A1 and the role of dephosphorylation in the activation and transport activity of the urea transporter UT-A1 is relatively less explored. Early studies by Zhang et al. in 2002 [83] showed that treatment of IMCD suspensions with the phosphatase inhibitors calyculin or okadaic acid could increase the level of phosphorylated UT-A1.

Calcineurin is a calcium-calmodulin-dependent serine threonine phosphatase, also known as protein phosphatase 3 (PPP3CA). It was previously referred to as protein phosphatase 2B (PP2B) [32]. Calcineurin activity is detected in the kidney inner medulla. Ilori et al. [32] recently investigated the effect of calcineurin and protein phosphatase PP1 and PP2A on the dephosphorylation of UT-A1. Inhibition of these two phosphatases increases phosphorylation of the UT-A1 urea transporter without the use of vasopressin. In vitro perfusion of IMCDs showed that incubation with the calcineurin inhibitor tacrolimus increases urea permeability [32]. Interestingly, inhibition of calcineurin by tacrolimus showed an increase in UT-A1 phosphorylation at serine 486, while inhibition of PP1 and PP2A with calyculin increases total phosphorylated UT-A1 but does not increase Ser486-phosphorylated UT-A1. These results suggest that UT-A1 might be dephosphorylated by multiple phosphatases (like PP2A and calcineurin) and that the PKA-mediated phosphorylation at serine 486 is dephosphorylated by calcineurin.

Ubiquitination of Urea Transporters

Protein degradation is an important mechanism by which cells control the levels of cellular proteins. Eukaryotic cells contain two major proteolytic systems, the lysosome and the 26S proteasome systems, which mediate protein degradation. Membrane proteins are capable of being degraded by the proteasomal and/or lysosomal pathways, depending on the type of ubiquitination (i.e., monoubiquitin vs. polyubiquitin) and the state of the protein complex (e.g., phosphorylation). Different types of ubiquitin modification of proteins often yield different consequences. Monoubiquitination, which chiefly occurs on the plasma membrane, often involves the trafficking and lysosomal degradation of membrane proteins. In contrast, polyubiquitinated proteins in the cytosol are usually targeted to the proteasome for degradation. Evidence indicates that the ubiquitination process plays an important role in regulating renal transepithelial urea transport [11, 63, 65, 66].

UT-A1 Degradation by the Ubiquitin-Proteasome Pathway

An in silico analysis of UT-A1 reveals a consensus MDM2-binding sequence in the intracellular loop, suggesting that ubiquitination/degradation may serve as an important mechanism for UT-A1 regulation. Indeed, studies from Smith's group and our group [11, 63] showed that inhibition of ubiquitin-proteasome activity by MG132 or lactacystin decreases UT-A degradation and increases cell-surface

expression, with a concurrent rise in urea transport activity [11, 63]. Inhibition of the lysosome pathway, however, does not affect UT-A1 degradation [11]. These findings demonstrate that UT-A1 undergoes ubiquitination and is degraded through the proteasome but not the lysosomal proteolytic pathway. Stewart et al. [63] reported that inhibition of the ubiquitin-proteasome pathway also increased urea transport activity of mouse (m) UT-A2 and mUT-A3, heterologously expressed in MDCK cells, in a concentration-dependent manner [63], indicating that UT-A2 and UT-A3 are regulated by the ubiquitin-proteasome pathway as well.

Activation of PKA/cAMP Promotes UT-A1 Ubiquitination and Degradation

Vasopressin regulates urea permeability in the IMCD through increases in UT-A1 phosphorylation and apical plasma-membrane accumulation [3, 37, 83]. Interestingly, forskolin treatment also promotes UT-A1 ubiquitination in UT-A1-MDCK cells [65]. In freshly isolated IMCD suspensions, extended vasopressin treatment (4h) stimulates UT-A1 ubiquitination and protein degradation [66]. Pretreatment with the PKA inhibitor H89 significantly inhibits forskolin-induced UT-A1 ubiquitination [66]. This indicates that activation of the cAMP/PKA pathway, resulting in UT-A1 phosphorylation, may also trigger the ubiquitination and protein degradation machinery for UT-A1. The resulting ubiquitination of membrane proteins after activation by PKA eventually leads to the attenuation of signaling processes. This could be the general mechanism for many membrane protein ubiquitination processes, particularly for ligand-induced tyrosine kinase receptor ubiquitination [29, 47, 71]. Upon epidermal growth factor (EGF) stimulation, the EGF receptor (EGFR) undergoes rapid dimerization, activation of its intrinsic tyrosine kinase activity, and autophosphorylation at multiple tyrosine sites within its cytoplasmic tail. Tyrosine phosphorylation then recruits ubiquitin ligase C-Cbl to EGFR and results in ubiquitination of EGFR. The ubiquitinated EGFR is then rapidly internalized and degraded [71]. In fact, early studies by Kim [36] and Terris [34] have noted that administering vasopressin to Brattleboro rats (which lack vasopressin) for 5 days decreases UT-A1 protein abundance in the inner medulla. The negative feedback loop of UT-A1 activation and ubiquitination acts as an important mechanism in vivo to attenuate the hormonal response by promoting UT-A1 ubiquitination and endocytosis, and facilitating protein degradation, thereby allowing the cell to return to the basal condition.

UT-A1 Monoubiquitination and Lysosomal Degradation

Mature membrane proteins on the cell surface can be modified by the addition of either monoubiquitin or polyubiquitin chains. Interestingly, when compared to ubiquitinated UT-A1 induced by proteasome inhibitor treatment, we observed the

much smaller size of ubiquitinated UT-A1 induced by forskolin treatment. This encouraged us to investigate whether forskolin-induced UT-A1 ubiquitination is different. We took the advantage of two specific ubiquitin antibodies for this study: FK1 recognizes only polyubiquitinated proteins, while FK2 detects both monoubiquitinated and polyubiquitinated proteins [66]. Forskolin stimulation induces UT-A1 ubiquitination [65]. However, forskolin-induced UT-A1 ubiquitination is not detected by the FK1 antibody (which only recognizes polyubiquitin) but by the FK2 antibody (which recognizes both mono- and polyubiquitin). This indicates that forskolin-induced UT-A1 ubiquitination is monoubiquitination. Further study showed that the two major PKA phosphorylation sites of UT-A1, at Ser486 and Ser499, are required for forskolin-induced UT-A1 monoubiquitination, since the double mutation of Ser486 and Ser499 reduces forskolin-induced UT-A1 ubiquitination [66]. In contrast, the two PKA phosphorylation sites do not influence UT-A1 ubiquitination caused by the proteasome inhibitor MG132 [66].

By isolating cell plasma membranes using a sucrose-gradient ultracentrifugation or by immune-labeling cell-surface UT-A1, we found that forskolin-induced UT-A1 monoubiquitination mainly occurs on the cell membrane [66]. Early studies [11, 63] showed that UT-A1 is ubiquitinated and degraded by the proteasome but not the lysosome proteolytic pathway. However, the proteasome inhibitor MG132 and lactacystin do not block forskolin-induced UT-A1 degradation; on the contrary, forskolin-induced UT-A1 degradation is prevented by the lysosome inhibitor chloroquine [66]. Double immunostaining of UT-A1 and a lysosomal marker confirms that forskolin-induced UT-A1 enters the lysosome compartment for degradation, which is different from the degradation of non-stimulated UT-A1.

Ubiquitination Regulates UT-A1 Membrane Expression

As a membrane protein, UT-A1 transport activity relies on its presence in the plasma membrane, which is determined by both endocytosis and exocytosis. The importance of ubiquitination in the endocytosis of various membrane proteins has been appreciated in recent years [13, 33, 45]. Both monoubiquitination and polyubiquitination can serve as efficient internalization signals [13, 33, 45]. Under non-stimulated conditions, inhibition of proteasome activity increases the amount of UT-A1 protein on the cell surface, as reported by Smith et al. [63] and by us [11], indicating that polyubiquitination affects UT-A1 membrane expression.

Although some membrane protein endocytosis is mediated by polyubiquitination or even in an ubiquitination independent manner [15, 72, 80], a body of evidence shows that monoubiquitin is an efficient signal for the internalization of membrane proteins such as GPCR, RTKs, hERG, and skAE1 [22, 49, 67, 68]. UT-A1 internalization occurs through both caveolae- and clathrin-coated pits (CCP) under non-stimulated conditions [30]. Forskolin-induced UT-A1 monoubiquitination and its endocytosis are blocked by chlorpromazine, as well as K^+ depletion, but not by filipin and nystatin [66]. This indicates that the monoubiquitination-induced UT-A1

internalization is predominantly through a clathrin-mediated route and is subsequently targeted to the lysosome for degradation.

MDM2-mediated UT-A1 Ubiquitination

Ubiquitination is a posttranslational modification carried out by a cascade of three enzymes: an E1, ubiquitin-activating enzyme, which binds to ubiquitin to generate a high-energy E1-ubiquitin intermediate; an E2, ubiquitin-conjugating enzyme, which is a ubiquitin carrier protein; and an E3, ubiquitin ligase, which transfers ubiquitin to a target protein [14]. UT-A1 has a consensus binding site (FxxxWxx[LIV]) in its intracellular loop for MDM2, a RING finger E3 ligase that ubiquitinates p53 and many other proteins [42]. This sequence is highly conserved among rats, humans, mice, dogs, cattle, and platypuses. Protein binding experiments confirm that UT-A1 can directly interact with MDM2; the binding site is located in the NH_2-terminal p53-binding region of MDM2 (30). Functionally, MDM2 mediates UT-A1 ubiquitination in an in vitro ubiquitination assay. Overexpression of MDM2 promotes UT-A1 ubiquitination and increases the degradation of UT-A1 protein in HEK 293 cells (30). However, all of these data come from in vitro studies. It is not clear whether UT-A1 ubiquitination is mediated by MDM2 in tissue and whether other E3 ligases are also involved in UT-A1 ubiquitination. Another important unsolved issue is determining the ubiquitin conjugation sites. UT-A1 possesses a number of lysines dispersed in the intracellular N-terminus, intracellular C-terminus, and the large intracellular loop. However, the lysines that could serve as ubiquitin conjugation sites in UT-A1 have not yet been determined. Further studies are required to identify which lysines are ubiquitinated and whether mutation of these residues affects UT-A1 ubiquitination, protein stability, and membrane accumulation.

In summary, UT-A1 can be polyubiquitinated and degraded through a proteasome pathway and can also be monoubiquitinated and degraded in a lysosome system. The different pathways of UT-A1 ubiquitination and degradation depend on the state of the protein and play distinct roles in response to different physiological situations. Figure 7.2 illustrates UT-A1 ubiquitination, endocytosis, and protein degradation under basal and stimulated conditions. UT-A1 has two endocytic pathways [30] and two protein degradation pathways [11, 63, 66]. The detailed regulatory mechanisms of how UT-A1 is routed to these two different endocytic pathways and the two different degradation systems could be very complicated; however, ubiquitination could be a key regulator of UT-A1 sorting, trafficking, and protein turnover. The caveolin-mediated pathway is responsible for constitutive UT-A1 internalization, whereas the clathrin-coated pit pathway may regulate UT-A1 endocytosis stimulated by vasopressin in vivo (by forskolin in vitro), and the latter pathway is accelerated by monoubiquitination. The monoubiquitinated UT-A1 is trafficked to the lysosome for degradation. In contrast, cytosolic UT-A1, misfolded UT-A1 from the endoplasmic reticulum, and constitutively internalized cell-surface UT-A1 (mostly from the caveolae-mediated endocytic pathway) is polyubiquitinated and
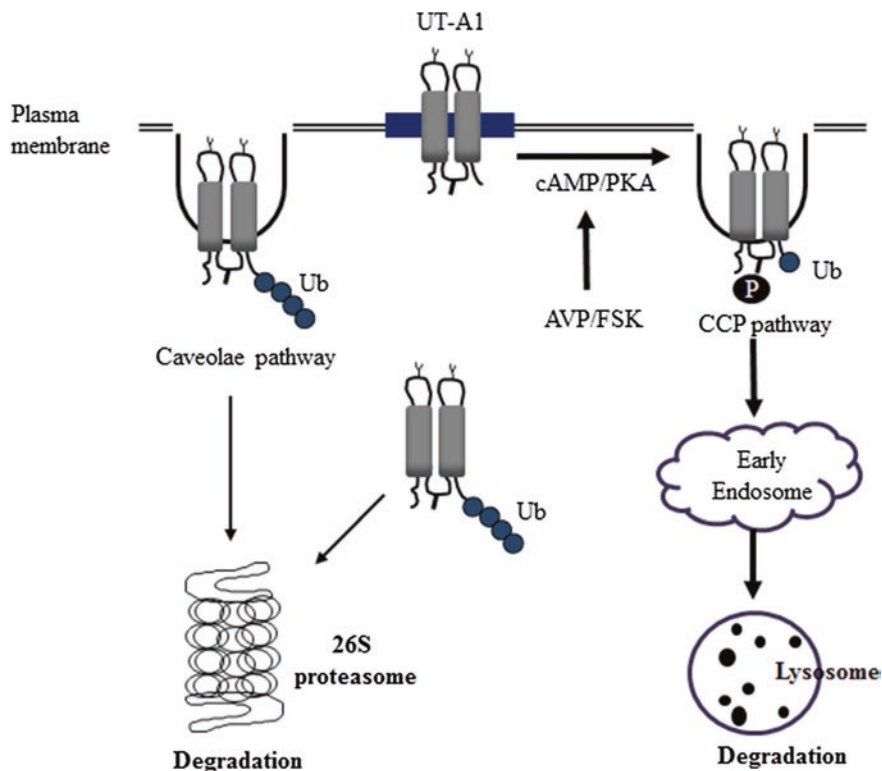
Fig. 7.2 UT-A1 ubiquitination, internalization, and degradation. Under normal conditions, cyto-solic UT-A1 (including misfolded UT-A1 from the ER) and constitutively internalized cell-surface UT-A1 (mostly from the caveolae-mediated endocytic pathway) are polyubiquitinated and degraded in the 26S proteasome system. However, upon AVP/FSK stimulation, UT-A1 is phos-phorylated and processed for monoubiquitination at the cell surface and internalized via a CCP pathway. The internalized monoubiquitinated UT-A1 is trafficked to the early endosome, then targeted to the lysosome for degradation. *CCP* clathrin-coated pits, *AVP* arginine vasopressin, *FSK* forskolin, *PKA* protein kinase A

targeted to the proteasome for degradation. Needless to say, both endocytic path-ways, both ubiquitination processes, and both protein degradation systems are important and required for proper cell functions. They cooperate in concert to main-tain the cell in perfect homeostasis under both normal and stimulated conditions.

Glycosylation of Urea Transporters

UT-A1 Is a Highly Glycosylated Protein

Immunoblotting studies of normal rat renal inner medulla (IM) demonstrate that the native UT-A1 urea transporter is a glycoprotein with two glycoforms of 117 and 97 kDa [5, 35]. These two forms are not caused by gene splicing but by

Fig. 7.3 Glycosylation analysis of 97- and 117-kDa UT-A1 by lectin pull-down assay. Normal rat kidney inner medullary lysates were incubated with the indicated agarose bound lectins at 4 °C overnight. The lectin precipitated samples were analyzed by immunoblotting with UT-A1 antibody
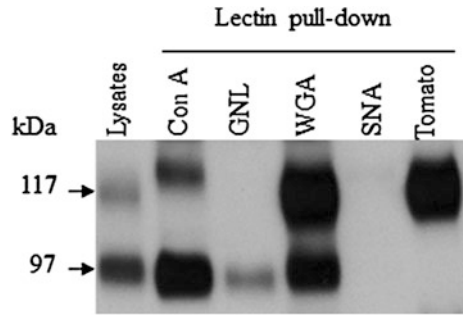
different degrees of posttranslational glycosylation. Both of the 97- and 117-kDa bands disappear and yield a single 88-kDa deglycosylated UT-A1 after deglycosylation treatment by PNGase F [5].

It has been believed that the two glycoforms of UT-A1 are the mature glycosylation forms, since they are both insensitive to endoglycosidase H treatment [5]. Experiments using differential centrifugation to fractionate inner medullary membranes also show that both the 97- and 117-kDa glycoforms of UT-A1 are expressed in the cell plasma membrane [5]. Furthermore, both of the two UT-A1 glycoforms are phosphorylated in response to vasopressin stimulation [31, 37, 83]. However, by using different lectins that recognize different structural determinants in glycans, we recently clarified the difference in glycosylation structure between 97- and 117-kDa forms of UT-A1 [10]. Tomato lectin, which is specific for poly-N-acetyllactosamine (poly-LacNAc) on the terminal ends of glycans, only binds to the 117-kDa UT-A1. Conversely, GNL, which binds to mannose, only pulled down the 97-kDa UT-A1. Therefore, the higher molecular mass form, the 117-kDa UT-A1, is a complex N-glycan with heavier glycosylation. The 97-kDa UT-A1 is a hybrid glycan form with low content of terminal N-acetylglucosamine (GlcNAc) residues but high content of mannose glycans (Fig. 7.3).

Interestingly, the relative protein abundance of the two forms varies under different conditions. The 117-kDa form increases dramatically in several states associated with decreased urine concentration, such as streptozotocin (STZ)-induced diabetes mellitus (DM) [35], a low-protein diet [34], hypercalcemia [55], water diuresis [34], and furosemide administration [34]. A tubule perfusion study of initial IMCDs from rats with STZ-induced DM shows that the appearance of the 117-kDa form in the inner medullary base is associated with increased urea transport activity [52]. Therefore, changes in the relative abundance of the 97- and 117-kDa forms of UT-A1 may have important roles in regulating UT-A1 function.

Role of Glycosylation in UT-A1 Membrane Expression and Protein Stability

N-Glycosylation is a key posttranslational modification and is required for the functional activity of many membrane transporters. N-Glycosylation can play an

important role in modulating protein biological activity, directing protein folding, regulating cell-surface expression and membrane localization, or increasing protein stability. The amino acid sequence of rat UT-A1 contains four consensus N-linked glycosylation sites (NX(S/T), where X $\neq$ proline) at Asn-13, $-279, -544$, and -742. By site-directed mutagenesis, we determined that two sites (Asn-279 and Asn-742) are involved in N-linked glycosylation of UT-A1. Interestingly, these two sites make different contributions to the glycosylation of UT-A1. The Asn-742 site in the second extracellular loop appears to have a greater extent of glycosylation than the Asn-279 site in the first extracellular loop, suggesting differential glycan synthesis and trimming among these two sites [9]. It is not clear whether and how the two glycosylation sites play different roles in urea transport activity.

In MDCK cells expressing wild-type UT-A1, urea flux was stimulated by either vasopressin or forskolin. However, the cells expressing mutant forms of UT-A1 lacking these two N-glycosylation sites had a delayed and significantly reduced maximal urea flux [9]. In many cases, N-linked glycosylation is critical for membrane protein intracellular movement and its eventual delivery to the cell surface. Indeed, most membrane proteins targeted to the plasma membrane possess N-linked glycosylation. Hendriks et al. [24] reported that the glycan mutant of AQP2 was unable to exit the Golgi apparatus and failed to be delivered to the cell membrane. By fractional ultracentrifugation, we found that unglycosylated UT-A1 is mainly trapped in the Golgi apparatus, and it significantly lost its ability to move to the cell surface in response to vasopressin and forskolin. This indicates that loss of glycosylation affects UT-A1 exiting both the ER and Golgi, especially when moving from the Golgi to the cell surface.

For many glycoproteins, deletion of glycosylation increases protein turnover. Removal of the glycosylation site in AQP2 produces a protein with a reduced half-life [24]. Pulse-chase experiments show that UT-A1 half-life is reduced when the two glycosylation sites are eliminated. Immature unglycosylated proteins often stay longer in the ER [9]. The prolonged residence may facilitate UT-A1 breakdown by the ER quality control mechanisms. Additionally, even when an unglycosylated protein escapes from the ER, it is more susceptible to proteolytic attack and has a greater chance of being degraded before being inserted into the plasma membrane [41]. Thus, by affecting UT-A1 trafficking to the plasma membrane and protein stability, glycosylation actively participates in the regulation of UT-A1 function.

Role of Glycosylation in UT-A1 Lipid Raft Targeting

The cell plasma membrane contains many specialized microdomains, referred to as lipid rafts, floating in the membrane. The lipid raft is a highly ordered membrane structure enriched in cholesterol and sphingolipids [61]. The activity of many membrane proteins can be modulated by its specific localization within different microdomains at the plasma membrane [12]. Being associated with lipid

rafts becomes an important regulatory mechanism for some proteins. Some membrane protein (channel) activity is higher outside of lipid raft microdomains, as seen in TRPM8 [48]. However, NKCC1 is strongly activated when it is moved into lipid rafts [77].

Protein partitioning to membrane rafts occurs either via protein–protein interactions or by a variety of posttranslational modifications, such as palmitoylation, myristoylation, acylation, or glycosylphosphatidylinositol modification [7, 23, 46, 77]. Glycosylation serves as an important apical plasma-membrane trafficking signal that has been well acknowledged [9, 24, 28]. The role for glycosylation as a lipid raft sorting signal has been appreciated in several reports. Xiong et al. [78] reported that differential partitioning in lipid raft microdomains determines the apical versus basolateral localization of the PMCA2w and 2z splice variants. Therefore, directing membrane protein into lipid rafts by glycosylation is of particular importance in the control of membrane protein apical trafficking.

The UT-A1 urea transporter is associated with lipid rafts, both in stably expressing UT-A1-HEK-293 cells [16, 30] and in freshly isolated rat kidney IMCD suspensions [10, 30]. The highly glycosylated 117-kDa form of UT-A1 prefers to reside in less buoyant lipid rafts (fractions 1–3). Loss of glycosylation impairs UT-A1 trafficking to lipid rafts [10]. Interestingly, unlike in IMCD and HEK293 cells, UT-A1 in transfected MDCK cells has a much wider distribution, both in the lipid raft fractions and in the non-raft fractions. By using sugar-specific binding lectins, we compared UT-A1 trafficking to lipid raft versus non-raft subdomains and found that the UT-A1 in non-lipid rafts contains a higher amount of mannose, as detected by concanavalin A. In contrast, UT-A1 in lipid rafts is the mature N-acetylglucosamine-containing form, as detected by wheat germ agglutinin. Differential N-glycosylation influences UT-A1 distribution in lipid rafts. The mature glycosylation acts as a targeting signal, facilitating UT-A1 trafficking into membrane lipid raft subdomains. In polarized epithelial cells, lipid rafts are believed to be in the apical membrane [61]. Thus, association with lipid rafts mediated by glycosylation represents an important mechanism for UT-A1 targeting to the apical plasma membrane in polarized epithelial cells.

UT-A1 Glycosylation in Streptozotocin-Induced Diabetic Rats

Diabetes is a metabolic disease characterized by increased blood glucose. The elevated glucose and its metabolic derivatives affect many aspects of cellular function including the sophisticated protein glycosylation mechanisms. In diabetes, the kidney has elevated urea reabsorption activity, which plays a critical role in ameliorating the osmotic diuresis caused by glucosuria [35, 36]. In STZ-induced diabetic rats, which have uncontrolled type 1 DM, UT-A1 urea transporter protein abundance in the inner medullary (IM) tip was 55 % of control in 5-day diabetic rats but increased to 170, 220, and 280 % at 10, 14, and 20 days of DM,

respectively. Interestingly, the two glycosylated UT-A1 forms increase differentially. Diabetes causes an increase in the 117-kDa rather than 97-kDa glycoprotein in both the IM tip and base [35]. Analysis of the lipid rafts shows an increase of 117-kDa UT-A1 in lipid rafts in STZ diabetic rat IM. The increased 117-kDa UT-A1 in lipid rafts may contribute to the enhanced urea permeability in IMCDs in diabetic rats [35, 36].

Glycosylation, an extremely complicated posttranslational process, is initially started in the ER, as early as during protein synthesis. The maturation of a glycan is mainly processed in the Golgi complex by trimming and adding different sugars, such as fucose, sialic acid, iduronic acid, xylose, etc. More recently, studies are examining the structural change of glycan sugars on UT-A1 [10, 64]. These new studies demonstrate that diabetes not only causes an increase of UT-A1 protein abundance, but also results in UT-A1 glycan changes, including an increase of sialic acid content [10]. Since sialic acid (N-acetylneuraminic acid) is a negatively charged large sugar that caps the terminal galactose in the carbohydrate chains on the cell surface, sialylation modification often affects glycoproteins in many aspects, like changing the proteins overall conformation, ligand binding, and galectin binding [8, 84]. We found that increased sialylation, reflecting glycan maturation, is linked to an increase in UT-A1 urea transport activity [43]. In addition, we found that the amount of fucose content in UT-A1 is increased and the glycan becomes more branched under diabetic conditions (unpublished observation). Future studies should investigate more deeply the structural features of UT-A1 N-glycosylation, particularly under diabetic conditions. In terms of this question, the new technology of glycomics will be helpful to decipher the specific oligosaccharide structures and this information will be helpful to dissect how glycan changes regulate UT-A1 apical membrane trafficking, lipid raft association, protein stability, and functional activity.

References

1. Bagnasco SM, Peng T, Nakayama Y, Sands JM (2000) Differential expression of individual UT-A urea transporter isoforms in rat kidney. J Am Soc Nephrol 11(11):1980–1986
2. Bansal AD, Hoffert JD, Pisitkun T, Hwang S, Chou CL, Boja ES et al (2010) Phosphoproteomic profiling reveals vasopressin-regulated phosphorylation sites in collecting duct. J Am Soc Nephrol 21(2):303–315
3. Blount MA, Mistry AC, Frohlich O, Price SR, Chen G, Sands JM et al (2008) Phosphorylation of UT-A1 urea transporter at serines 486 and 499 is important for vasopressin-regulated activity and membrane accumulation. Am J Physiol Renal Physiol 295(1):F295–F299
4. Bos JL (2003) Epac: a new cAMP target and new avenues in cAMP research. Nat Rev Mol Cell Biol 4(9):733–738
5. Bradford AD, Terris JM, Ecelbarger CA, Klein JD, Sands JM, Chou CL et al (2001) 97- and 117-kDa forms of collecting duct urea transporter UT-A1 are due to different states of glycosylation. Am J Physiol Renal Physiol 281(1):F133–F143

6. Brooks HL, Ageloff S, Kwon TH, Brandt W, Terris JM, Seth A et al (2003) cDNA array identification of genes regulated in rat renal medulla in response to vasopressin infusion. Am J Physiol Renal Physiol 284(1):F218–F228

7. Brown DA, London E (1998) Functions of lipid rafts in biological membranes. Annu Rev Cell Dev Biol 14:111–136

8. Cha SK, Ortega B, Kurosu H, Rosenblatt KP, Kuro OM, Huang CL (2008) Removal of sialic acid involving Klotho causes cell-surface retention of TRPV5 channel via binding to galectin-1. Proc Natl Acad Sci USA 105(28):9805–9810

9. Chen G, Frohlich O, Yang Y, Klein JD, Sands JM (2006) Loss of N-linked glycosylation reduces urea transporter UT-A1 response to vasopressin. J Biol Chem 281(37):27436–27442

10. Chen G, Howe AG, Xu G, Frohlich O, Klein JD, Sands JM (2011) Mature N-linked glycans facilitate UT-A1 urea transporter lipid raft compartmentalization. FASEB J 25(12):4531–4539

11. Chen G, Huang H, Frohlich O, Yang Y, Klein JD, Price SR et al (2008) MDM2 E3 ubiquitin ligase mediates UT-A1 urea transporter ubiquitination and degradation. Am J Physiol Renal Physiol 295(5):F1528–F1534

12. Dart C (2010) Lipid microdomains and the regulation of ion channel function. J Physiol 588(Pt 17):3169–3178

13. de Juan-Sanz J, Zafra F, Lopez-Corcuera B, Aragon C (2011) Endocytosis of the neuronal glycine transporter GLYT2: role of membrane rafts and protein kinase C-dependent ubiquitination. Traffic 12(12):1850–1867

14. Debigare R, Price SR (2003) Proteolysis, the ubiquitin-proteasome system, and renal diseases. Am J Physiol Renal Physiol 285(1):F1–F8

15. Eriksen J, Bjorn-Yoshimoto WE, Jorgensen TN, Newman AH, Gether U (2010) Postendocytic sorting of constitutively internalized dopamine transporter in cell lines and dopaminergic neurons. J Biol Chem 285(35):27289–27301

16. Feng X, Huang H, Yang Y, Frohlich O, Klein JD, Sands JM et al (2009) Caveolin-1 directly interacts with UT-A1 urea transporter: the role of caveolae/lipid rafts in UT-A1 regulation at the cell membrane. Am J Physiol Renal Physiol 296(6):F1514–F1520

17. Fenton RA, Stewart GS, Carpenter B, Howorth A, Potter EA, Cooper GJ et al (2002) Characterization of mouse urea transporters UT-A1 and UT-A2. Am J Physiol Renal Physiol 283(4):F817–F825

18. Frohlich O, Klein JD, Smith PM, Sands JM, Gunn RB (2004) Urea transport in MDCK cells that are stably transfected with UT-A1. Am J Physiol Cell Physiol 286(6):C1264–C1270

19. Frohlich O, Klein JD, Smith PM, Sands JM, Gunn RB (2006) Regulation of UT-A1-mediated transepithelial urea flux in MDCK cells. Am J Physiol Cell Physiol 291(4):C600–C606

20. Gillin AG, Sands JM (1992) Characteristics of osmolarity-stimulated urea transport in rat IMCD. Am J Physiol 262(6 Pt 2):F1061–F1067

21. Gillin AG, Star RA, Sands JM (1993) Osmolarity-stimulated urea transport in rat terminal IMCD: role of intracellular calcium. Am J Physiol 265(2 Pt 2):F272–F277

22. Haglund K, Sigismund S, Polo S, Szymkiewicz I, Di Fiore PP, Dikic I (2003) Multiple mono-oubiquitination of RTKs is sufficient for their endocytosis and degradation. Nat Cell Biol 5(5):461–466

23. Hartmann AM, Blaesse P, Kranz T, Wenz M, Schindler J, Kaila K et al (2009) Opposite effect of membrane raft perturbation on transport activity of KCC2 and NKCC1. J Neurochem 111(2):321–331

24. Hendriks G, Koudijs M, van Balkom BW, Oorschot V, Klumperman J, Deen PM et al (2004) Glycosylation is important for cell surface expression of the water channel aquaporin-2 but is not essential for tetramerization in the endoplasmic reticulum. J Biol Chem 279(4):2975–2983

25. Hoffert JD, Pisitkun T, Wang G, Shen RF, Knepper MA (2006) Quantitative phosphoproteomics of vasopressin-sensitive renal cells: regulation of aquaporin-2 phosphorylation at two sites. Proc Natl Acad Sci USA 103(18):7159–7164

26. Honegger KJ, Capuano P, Winter C, Bacic D, Stange G, Wagner CA et al (2006) Regulation of sodium-proton exchanger isoform 3 (NHE3) by PKA and exchange protein directly activated by cAMP (EPAC). Proc Natl Acad Sci USA 103(3):803–808

27. Hoorn EJ, Hoffert JD, Knepper MA (2005) Combined proteomics and pathways analysis of collecting duct reveals a protein regulatory network activated in vasopressin escape. J Am Soc Nephrol 16(10):2852–2863

28. Hoover RS, Poch E, Monroy A, Vazquez N, Nishio T, Gamba G et al (2003) N-Glycosylation at two sites critically alters thiazide binding and activity of the rat thiazide-sensitive Na(+):Cl(−) cotransporter. J Am Soc Nephrol 14(2):271–282

29. Huang F, Kirkpatrick D, Jiang X, Gygi S, Sorkin A (2006) Differential regulation of EGF receptor internalization and degradation by multiubiquitination within the kinase domain. Mol Cell 21(6):737–748

30. Huang H, Feng X, Zhuang J, Frohlich O, Klein JD, Cai H et al (2010) Internalization of UT-A1 urea transporter is dynamin dependent and mediated by both caveolae- and clathrin-coated pit pathways. Am J Physiol Renal Physiol 299(6):F1389–F1395

31. Hwang S, Gunaratne R, Rinschen MM, Yu MJ, Pisitkun T, Hoffert JD et al (2010) Vasopressin increases phosphorylation of Ser84 and Ser486 in Slc14a2 collecting duct urea transporters. Am J Physiol Renal Physiol 299(3):F559–F567

32. Ilori TO, Wang Y, Blount MA, Martin CF, Sands JM, Klein JD (2012) Acute calcineurin inhibition with tacrolimus increases phosphorylated UT-A1. Am J Physiol Renal Physiol 302(8):F998–F1004

33. Kamsteeg EJ, Hendriks G, Boone M, Konings IB, Oorschot V, van der Sluijs P et al (2006) Short-chain ubiquitination mediates the regulated endocytosis of the aquaporin-2 water channel. Proc Natl Acad Sci USA 103(48):18344–18349

34. Kato A, Naruse M, Knepper MA, Sands JM (1998) Long-term regulation of inner medullary collecting duct urea transport in rat. J Am Soc Nephrol 9(5):737–745

35. Kim D, Sands JM, Klein JD (2003) Changes in renal medullary transport proteins during uncontrolled diabetes mellitus in rats. Am J Physiol Renal Physiol 285(2):F303–F309

36. Kim D, Sands JM, Klein JD (2004) Role of vasopressin in diabetes mellitus-induced changes in medullary transport proteins involved in urine concentration in Brattleboro rats. Am J Physiol Renal Physiol 286(4):F760–F766

37. Klein JD, Blount MA, Frohlich O, Denson CE, Tan X, Sim JH et al (2010) Phosphorylation of UT-A1 on serine 486 correlates with membrane accumulation and urea transport activity in both rat IMCDs and cultured cells. Am J Physiol Renal Physiol 298(4):F935–F940

38. Klein JD, Martin CF, Kent KJ, Sands JM (2012) Protein kinase C-alpha mediates hypertonicity-stimulated increase in urea transporter phosphorylation in the inner medullary collecting duct. Am J Physiol Renal Physiol 302(9):F1098–F1103

39. Kudo LH, Cesar KR, Ping WC, Rocha AS (1992) Effect of peritubular hypertonicity on water and urea transport of inner medullary collecting duct. Am J Physiol 262(3 Pt 2): F338–F347

40. Laroche-Joubert N, Marsy S, Michelet S, Imbert-Teboul M, Doucet A (2002) Protein kinase A-independent activation of ERK and H, K-ATPase by cAMP in native kidney cells: role of Epac I. J Biol Chem 277(21):18598–18604

41. Li LB, Chen N, Ramamoorthy S, Chi L, Cui XN, Wang LC et al (2004) The role of N-glycosylation in function and surface trafficking of the human dopamine transporter. J Biol Chem 279(20):21012–21020

42. Li M, Chen D, Shiloh A, Luo J, Nikolaev AY, Qin J et al (2002) Deubiquitination of p53 by HAUSP is an important pathway for p53 stabilization. Nature 416(6881):648–653

43. Li X, Yang B, Chen M, Klein JD, Sands JM, Chen G (2014) Activation of PKC-α and Src increases UT-A1 α-2, 6 sialylation. J Am Soc Nephrol 25 (in press)

44. Li Y, Konings IB, Zhao J, Price LS, de Heer E, Deen PM (2008) Renal expression of exchange protein directly activated by cAMP (Epac) 1 and 2. Am J Physiol Renal Physiol 295(2):F525–F533

45. Lin DH, Yue P, Pan CY, Sun P, Zhang X, Han Z et al (2009) POSH stimulates the ubiquitination and the clathrin-independent endocytosis of ROMK1 channels. J Biol Chem 284(43):29614–29624

46. Lingwood D, Simons K (2010) Lipid rafts as a membrane-organizing principle. Science 327(5961):46–50

47. Mao Y, Shang Y, Pham VC, Ernst JA, Lill JR, Scales SJ et al (2011) Polyubiquitination of insulin-like growth factor I receptor (IGF-IR) activation loop promotes antibody-induced receptor internalization and down-regulation. J Biol Chem 286(48):41852–41861

48. Morenilla-Palao C, Pertusa M, Meseguer V, Cabedo H, Viana F (2009) Lipid raft segregation modulates TRPM8 channel activity. J Biol Chem 284(14):9215–9224

49. Musch MW, Puffer AB, Goldstein L (2008) Volume expansion stimulates monoubiquitina-tion and endocytosis of surface-expressed skate anion-exchanger isoform. Am J Physiol Regul Integr Comp Physiol 294(5):R1657–R1665

50. Nielsen S, Knepper MA (1993) Vasopressin activates collecting duct urea transporters and water channels by distinct physical processes. Am J Physiol 265(2 Pt 2):F204–F213

51. Nielsen S, Terris J, Smith CP, Hediger MA, Ecelbarger CA, Knepper MA (1996) Cellular and subcellular localization of the vasopressin-regulated urea transporter in rat kidney. Proc Natl Acad Sci USA 93(11):5495–5500

52. Pech V, Klein JD, Kozlowski SD, Wall SM, Sands JM (2005) Vasopressin increases urea permeability in the initial IMCD from diabetic rats. Am J Physiol Renal Physiol 289(3):F531–F535

53. Rinschen MM, Yu MJ, Wang G, Boja ES, Hoffert JD, Pisitkun T et al (2010) Quantitative phosphoproteomic analysis reveals vasopressin V2-receptor-dependent signaling pathways in renal collecting duct cells. Proc Natl Acad Sci USA 107(8):3882–3887

54. Sands JM, Blount MA, Klein JD (2011) Regulation of renal urea transport by vasopressin. Trans Am Clin Climatol Assoc 122:82–92

55. Sands JM, Flores FX, Kato A, Baum MA, Brown EM, Ward DT et al (1998) Vasopressin-elicited water and urea permeabilities are altered in IMCD in hypercalcemic rats. Am J Physiol 274(5 Pt 2):F978–F985

56. Sands JM, Layton HE (2014) Advances in understanding the urine-concentrating mechanism. Annu Rev Physiol 76:387–409

57. Sands JM, Nonoguchi H, Knepper MA (1987) Vasopressin effects on urea and H_2O transport in inner medullary collecting duct subsegments. Am J Physiol 253(5 Pt 2):F823–F832

58. Sands JM, Schrader DC (1991) An independent effect of osmolality on urea transport in rat terminal inner medullary collecting ducts. J Clin Invest 88(1):137–142

59. Shayakul C, Knepper MA, Smith CP, DiGiovanni SR, Hediger MA (1997) Segmental locali-zation of urea transporter mRNAs in rat kidney. Am J Physiol 272(5 Pt 2):F654–F660

60. Shayakul C, Steel A, Hediger MA (1996) Molecular cloning and characterization of the vasopressin-regulated urea transporter of rat kidney collecting ducts. J Clin Invest 98(11):2580–2587

61. Simons K, Gerl MJ (2010) Revitalizing membrane rafts: new tools and insights. Nat Rev Mol Cell Biol 11(10):688–699

62. Star RA, Nonoguchi H, Balaban R, Knepper MA (1988) Calcium and cyclic adenosine monophosphate as second messengers for vasopressin in the rat inner medullary collecting duct. J Clin Invest 81(6):1879–1888

63. Stewart GS, O'Brien JH, Smith CP (2008) Ubiquitination regulates the plasma membrane expression of renal UT-A urea transporters. Am J Physiol Cell Physiol 295(1):C121–C129

64. Su H, Carter CB, Frohlich O, Cummings RD, Chen G (2012) Glycoforms of UT-A3 urea transporter with poly-N-acetyllactosamine glycosylation have enhanced transport activity. Am J Physiol Renal Physiol 303(2):F201–F208

65. Su H, Carter CB, Laur O, Sands JM, Chen G (2012) Forskolin stimulation promotes urea transporter UT-A1 ubiquitination, endocytosis, and degradation in MDCK cells. Am J Physiol Renal Physiol 303(9):F1325–F1332

66. Su H, Chen M, Sands JM, Chen G (2013) Activation of the cAMP/PKA pathway induces UT-A1 urea transporter monoubiquitination and targets it for lysosomal degradation. Am J Physiol Renal Physiol 305(12):F1775–F1782

67. Sun T, Guo J, Shallow H, Yang T, Xu J, Li W et al (2011) The role of monoubiquitination in endocytic degradation of human ether-a-go-go-related gene (hERG) channels under low K+ conditions. J Biol Chem 286(8):6751–6759

68. Terrell J, Shih S, Dunn R, Hicke L (1998) A function for monoubiquitination in the internalization of a G protein-coupled receptor. Mol Cell 1(2):193–202

69. Thai TL, Blount MA, Klein JD, Sands JM (2012) Lack of protein kinase C-alpha leads to impaired urine concentrating ability and decreased aquaporin-2 in angiotensin II-induced hypertension. Am J Physiol Renal Physiol 303(1):F37–F44

70. Uawithya P, Pisitkun T, Ruttenberg BE, Knepper MA (2008) Transcriptional profiling of native inner medullary collecting duct cells from rat kidney. Physiol Genomics 32(2):229–253

71. Umebayashi K, Stenmark H, Yoshimori T (2008) Ubc4/5 and c-Cbl continue to ubiquitinate EGF receptor after internalization to facilitate polyubiquitination and degradation. Mol Biol Cell 19(8):3454–3462

72. Varghese B, Barriere H, Carbone CJ, Banerjee A, Swaminathan G, Plotnikov A et al (2008) Polyubiquitination of prolactin receptor stimulates its internalization, postinternalization sorting, and degradation via the lysosomal pathway. Mol Cell Biol 28(17):5275–5287

73. Wall SM, Han JS, Chou CL, Knepper MA (1992) Kinetics of urea and water permeability activation by vasopressin in rat terminal IMCD. Am J Physiol 262(6 Pt 2):F989–F998

74. Wang Y, Klein JD, Blount MA, Martin CF, Kent KJ, Pech V et al (2009) Epac regulates UT-A1 to increase urea transport in inner medullary collecting ducts. J Am Soc Nephrol 20(9):2018–2024

75. Wang Y, Klein JD, Froehlich O, Sands JM (2013) Role of protein kinase C-alpha in hypertonicity-stimulated urea permeability in mouse inner medullary collecting ducts. Am J Physiol Renal Physiol 304(2):F233–F238

76. Wang Y, Klein JD, Liedtke CM, Sands JM (2010) Protein kinase C regulates urea permeability in the rat inner medullary collecting duct. Am J Physiol Renal Physiol 299(6):F1401–F1406

77. Welker P, Bohlick A, Mutig K, Salanova M, Kahl T, Schluter H et al (2008) Renal Na+-K+-Cl- cotransporter activity and vasopressin-induced trafficking are lipid raft-dependent. Am J Physiol Renal Physiol 295(3):F789–F802

78. Xiong Y, Antalffy G, Enyedi A, Strehler EE (2009) Apical localization of PMCA2w/b is lipid raft-dependent. Biochem Biophys Res Commun 384(1):32–36

79. Yao L, Huang DY, Pfaff IL, Nie X, Leitges M, Vallon V (2004) Evidence for a role of protein kinase C-alpha in urine concentration. Am J Physiol Renal Physiol 287(2):F299–F304

80. Ye S, Cihil K, Stolz DB, Pilewski JM, Stanton BA, Swiatecka-Urban A (2010) c-Cbl facilitates endocytosis and lysosomal degradation of cystic fibrosis transmembrane conductance regulator in human airway epithelial cells. J Biol Chem 285(35):27008–27018

81. You G, Smith CP, Kanai Y, Lee WS, Stelzner M, Hediger MA (1993) Cloning and characterization of the vasopressin-regulated urea transporter. Nature 365(6449):844–847

82. Yu MJ, Pisitkun T, Wang G, Shen RF, Knepper MA (2006) LC-MS/MS analysis of apical and basolateral plasma membranes of rat renal collecting duct cells. Mol Cell Proteomics 5(11):2131–2145

83. Zhang C, Sands JM, Klein JD (2002) Vasopressin rapidly increases phosphorylation of UT-A1 urea transporter in rat IMCDs through PKA. Am J Physiol Renal Physiol 282(1):F85–F90

84. Zhuo Y, Bellis SL (2011) Emerging role of alpha2,6-sialic acid as a negative regulator of galectin binding and function. J Biol Chem 286(8):5935–5941

Chapter 8
Transport Characteristics of Urea Transporter-B

Baoxue Yang

Abstract UT-B represents the major urea transporter in erythrocytes, in addition to being expressed in kidney descending vasa recta, brain, spleen, ureter, bladder, and testis. Expression of urea transporter UT-B confers high urea permeability to mammalian erythrocytes. Erythrocyte membranes are also permeable to various urea analogues, suggesting common transport pathways for urea and structurally similar solutes. UT-B is highly permeable to urea and the chemical analogues formamide, acetamide, methylurea, methylformamide, ammonium carbamate, and acrylamide, each with a $P_s > 5.0 \times 10^{-6}$ cm/s at 10 °C. The amides formamide, acetamide, acrylamide, and butyramide efficiently diffuse across lipid bilayers. The urea analogues dimethylurea, acrylamide, methylurea, thiourea, and methylformamide inhibit UT-B-mediated urea transport by >60 % by a pore-blocking mechanism. UT-B is also a water channel in erythrocytes and has a single-channel water permeability that is similar to aquaporin-1. Whether UT-B is an NH_3 channel still needs further study. Urea permeability (P_{urea}) in erythrocytes differs between different mammals. Carnivores (dog, fox, cat) exhibit high P_{urea}. In contrast, herbivores (cow, donkey, sheep) show much lower P_{urea}. Erythrocyte P_{urea} in human and pig (omnivores) was intermediate. Rodents and lagomorphs (mouse, rat, rabbit) have P_{urea} intermediate between carnivores and omnivores. Birds that do not excrete urea and do not express UT-B in their erythrocytes have very low values. In contrast to P_{urea}, water permeability is relatively similar in all mammals studied. This chapter will provide information about the transporter characteristics of UT-B.

Keywords UT-B · Water transport · Urea analogues · Ammonia · Species

B. Yang (✉)
State Key Laboratory of Natural and Biomimetic Drugs, Key Laboratory of Molecular Cardiovascular Sciences, Ministry of Education, Department of Pharmacology, School of Basic Medical Sciences, Peking University, Beijing 100191, China
e-mail: baoxue@bjmu.edu.cn

Fig. 8.1 Chemical structures of urea analogues that are inhibitors of UT-B [24]

dimethylurea   acrylamide   methylurea

thiourea   methylformamide
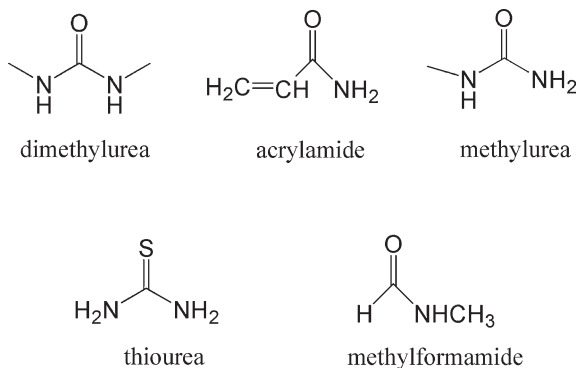
Urea Transport Mediated by Urea Transporters

Studies in the 1970s [13, 18] demonstrated the permeability of mammalian erythrocyte membranes to urea and some other solutes. Presently, it is clear that UT-B is highly expressed in mammalian erythrocytes [4, 14] and represents the major urea transporter in erythrocytes [15, 20, 21]. Measurements comparing the properties of wild-type and UT-B-null erythrocytes provide evidence for UT-B as a transporter that selectively transports urea [21]. Humans lacking UT-B have low erythrocyte urea permeability. From the number of UT-B proteins per erythrocyte and the erythrocyte urea permeability, it was estimated that the UT-B turnover rate is $2–15 \times 10^6$ urea molecules/s [10, 16].

Urea is a polar, highly water soluble, and charge neutral molecule, with an oxygen and two nitrogen atoms serving as hydrogen-bond acceptors, and two amino functional groups providing a total of four hydrogen bonds for donation. High polarity and water solubility necessitates a polar-hydrophilic pathway(s) for efficient transmembrane transport through UT-B [24].

UT-B-mediated urea transport is strongly inhibited by urea analogues (Fig. 8.1). Urea flux was inhibited 98 % by dimethylurea, 93 % by acrylamide, 87 % by methylurea, 72 % by thiourea, and 64 % by methylformamide. The tenfold greater erythrocyte binding affinity of thiourea compared to urea suggests a pore-blocking mechanism of inhibition. Inhibition of UT-B by all these solutes is reversible. Butyramide, acrylamide, acetamide, and formamide did not appreciably inhibit urea permeability in erythrocytes. Phloretin significantly inhibits UT-B-mediated urea transport. However, phloretin also affects other membrane transporter proteins non-specifically [24].

Transport of Urea Analogues Is Mediated by UT-B

The mechanism of small solute transport in erythrocytes has been a subject of long-standing interest [5, 12, 13]. It was previously reported that human erythrocytes are highly permeable to small non-electrolytes such as formamide and acetamide,
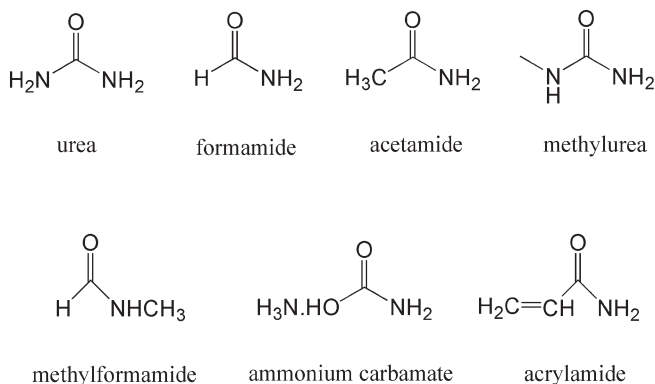
Fig. 8.2 Chemical structures of urea analogues that are transported by UT-B [24]

implying the presence of a hydrophilic pathway(s) [13, 17]. The UT-B knockout mouse model makes it possible to determine transport rates of urea analogues [24]. Formamide, acetamide, and urea permeabilities were inhibited >80 % by UT-B deletion or 0.7 mM phloretin in wild-type erythrocytes. These solutes showed identical permeabilities in UT-B-null and wild-type erythrocytes, both in the absence and presence of phloretin. UT-B-attributable P_s (solute permeability) for urea, formamide, acetamide, methylurea, methylformamide, ammonium carbamate, and acrylamide (Fig. 8.2) ranged from 0.5 to 3.2×10^{-5} cm/s. UT-B had a lower permeability to glycolamide, hydroxyurea, and carbohydrazide (P_s of 0.6–1.5×10^{-6} cm/s). Phloretin treatment did not reduce butyramide or isobutyramide permeabilities in both wild-type and UT-B-null erythrocytes (P_s of 9×10^{-6} cm/s and 6×10^{-6} cm/s, respectively), demonstrating that UT-B does not transport butyramide or isobutyramide. In contrast, UT-B conferred >70 % of total erythrocyte urea, formamide, acetamide, methylurea, hydroxyurea, and ammonium carbamate transport.

Measurements of solute permeabilities across UT-B-null erythrocytes showed that urea, methylurea, dimethylurea, hydroxyurea, and thiourea permeabilities were low (<8×10^{-7} cm/s) at temperatures between 10 °C and 37 °C, and weakly temperature dependent, which suggests that UT-B is the specific transporter for these solutes. In contrast, formamide, acetamide, acrylamide, and butyramide permeabilities were strongly temperature dependent, ninefold, 11-fold, sevenfold, and sevenfold higher, respectively, at 37 °C compared to 10 °C. Transport of the amides formamide, acetamide, methylformamide, acrylamide, butyramide, and isobutyramide was strongly temperature dependent, indicative of diffusion across the erythrocyte lipid bilayer.

UT-B-mediated transport requires at least one primary amide, i.e. carbonyl function, attached to a primary unsubstituted amino group. Indeed, UT-B mediates efficient transport of formamide, acetamide, carbamate, and acrylamide, all of which contain primary amide functions. N-methylated amides are poorly transported by UT-B, as evidenced by the relative threefold and 15-fold lower transmembrane flux of methylurea and dimethylurea, respectively. Methylation

decreases amide hydrogen-bond capacity and increases lipophilicity and molecular size. Compounds lacking amide functionalities altogether, such as glycine and acetic acid, are not transported by UT-B.

Acetamide and urea have similar molecular sizes, with both also possessing an oxygen to accept hydrogen bonding. Replacement of this oxygen by sulphur, as in thioacetamide and thiourea, results in reduced UT-B-facilitated transport. This could be attributed to loss of hydrogen-bonding capacity of sulphur versus oxygen. In addition, molecular volumes and polar surface are as large or greater as in sulphur-containing compounds compared to their oxygen-containing counterparts. Similarly, guanidine, which has comparable physicochemical properties as urea, was not transported by UT-B, as it replaces urea carbonyl byimine function $(C{=}N{-}H)$. More lipophilic, less polar analogues such as butyramide, isobutyramide, and acetone tend to rely upon membrane diffusion rather than UT-B facilitated transport. In hydrophilic transport pathways, hydrogen-bond formation is one of the essential processes conferring transport specificity.

Urea is a highly polar molecule with significant hydrogen-bonding capacity, and it seems likely that UT-B-facilitated transport relies on hydrogen bonding. UT-B prefers to transport neutral, more hydrophilic, urea and primary amides that have more H-bonding capacity and selectively retard transport of lipophilic molecules. Large analogues with less hydrogen-bonding capacity tend to have less permeability. This suggests that UT-B provides a unique type of narrow hydrophilic pathway for transport of urea and that transport specificity/selectivity may largely be governed by H-bonding capacity, size, and the hydrophilic nature of solute. Since urea analogues such as thiourea and acetamide are similar to urea in structure, they were suggested to inhibit urea transport by interacting competitively at transport sites [2, 11].

Water Transport Mediated by Urea Transporters

By measuring osmotic water permeability in *Xenopus* oocytes expressing UTs, it was found that UT-B functions as an efficient water channel [22]. Quantitative measurement of single-channel osmotic water permeability (P_f) of UT-B gives a value of 1.4 cm^3/s. UT-B-mediated water permeability is weakly temperature dependent (activation energy <4 kcal/mol), inhibited >75 % by the urea transport inhibitor 1,3-dimethylthiourea, but not inhibited by the water channel (aquaporin) inhibitor $HgCl_2$. These results indicate that UT-B functions as a urea/water channel utilizing a common aqueous pathway (Fig. 8.3).

The significant intrinsic water permeability of UT-B suggests the existence of a continuous aqueous channel through the UT-B protein that permits passage of both water and urea. A study of temperature dependence shows a weak temperature dependence for UT-B-mediated transport of both water and urea. The low Arrhenius activation energy (<4 kcal/mol) is consistent with an aqueous pore pathway and is in agreement with the low activation energies found for several of the

Fig. 8.3 Schematic diagram of UT-B as a urea/water channel utilizing a common aqueous pathway
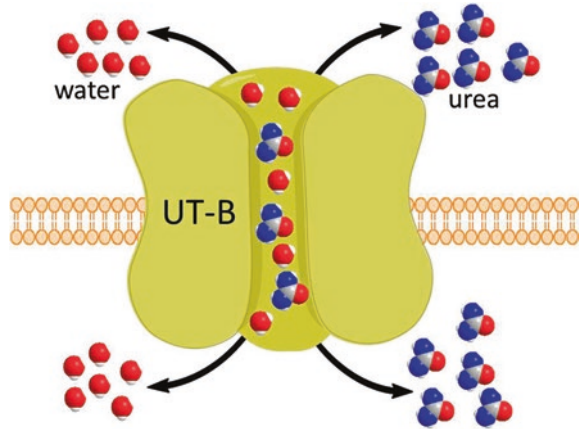
aquaporin-type water channels. UT-B-mediated water and urea transports were each strongly inhibited by the urea analogue 1,3-dimethylthiourea and by phloretin. Neither water nor urea transport was inhibited by $HgCl_2$, a potent inhibitor of most aquaporin-type water channels. $HgCl_2$, but not the urea transport inhibitors, strongly inhibit water permeability in oocytes expressing water channel AQP1. These results support a common aqueous route for water and urea transport through UT-B.

Increased water permeability in *Xenopus* oocytes expressing UT-B was subsequently confirmed by Sidoux-Walter et al. [19]. However, they concluded that UT-B-facilitated water transport does not occur under physiological conditions. They proposed, based on water versus urea permeability measurements in oocytes expressing different levels of UT-B, that UT-B-associated water permeability occurs only when UT-B expressed at non-physiological, high levels.

To quantify UT-B-mediated water transport, Yang et al. generated double knockout mice lacking UT-B and the major erythrocyte water channel AQP1 [21]. Osmotic water permeability in erythrocytes from mice lacking both AQP1 and UT-B is 4.2-fold lower in the double knockout mice than in erythrocytes from mice lacking AQP1 alone. A similar low water permeability was found in erythrocytes from AQP1 null mice after UT-B inhibition by phloretin and in erythrocytes from UT-B null mice after inhibition of AQP1 by $HgCl_2$. UT-B-facilitated water transport was weakly temperature dependent. These results explain why the activation energy of erythrocyte water transport after mercurial inhibition or AQP1 deletion is substantially lower than expected for lipid-mediated water transport [9]. The experimental results also provide a molecular basis for the conclusion of Dix and Solomon [3], which were based on studies of membrane perturbing agents, showing that the mercurial-insensitive water permeability in erythrocytes involves, in large part, a protein pathway.

Figure 8.4 summarizes the contributions of protein and lipid pathways for water and urea transport in mouse erythrocytes. At 10 °C, ~90 % of water is transported through
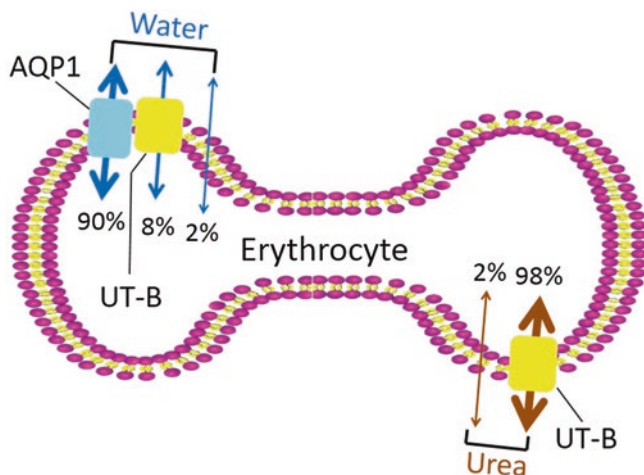
Fig. 8.4 Schematic diagram of relative contributions of AQP1, UT-B, and the lipid bilayer to erythrocyte water and urea permeability (reproduced from [23])

AQP1, 8 % through UT-B, and the remainder through the lipid membrane. The vast majority of urea is transported through UT-B. At 37 °C, ~79 % of water is transported through AQP1, 6 % through UT-B, and the remainder through the lipid membrane.

It is interesting to compare the intrinsic (single channel) water permeabilities of AQP1 versus UT-B. Assuming, as in human erythrocytes, that there are 14,000 copies of UT-B and 200,000 copies of AQP1 [8] per mouse erythrocyte plasma membrane, then there is ~1 UT-B molecule per 14 AQP1 molecules. Yang and Verkman [23] showed that AQP1 contributes 13 times more than UT-B to erythrocyte water permeability. Thus, the single-channel (per molecule) water permeability of UT-B in erythrocytes is very similar to that of AQP1 (7.5×10^{-14} cm^3/s). The presence of a continuous aqueous pathway through UT-B that efficiently facilitates osmosis is an interesting observation that may account for the exceptionally high transport turnover rate of UT-B (2–6×10^6 molecules/s) [10], as high as that of ion channels and >2–3 orders of magnitude greater than that of classic carriers and active transporters. A recent functional study of human erythrocyte variants and MD simulations clearly demonstrates that urea and water share the same pathway through the pore of UT-B [1]. Geyer et al. [6] also confirmed that human UT-B is a water channel in Xenopus oocytes.

Ammonia Transport Mediated by Urea Transporters

Geyer et al. explored the NH$_3$ permeability of human UT-B expressed in Xenopus oocytes [6]. They monitored gas permeability using microelectrodes to record the maximum transient change in surface pH (ΔpHS) caused by exposing oocytes to

5 % CO_2/33 mM HCO_3^- (pHS increase) or 0.5 mM NH_3/NH_4^+ (pHS decrease). UT-B expression had no effect on the CO_2-induced ΔpHS but doubled the NH_3-induced ΔpHS. Phloretin reduced UT-B-dependent ($-\Delta pHS*$) NH_3 by 70 %. p-Chloromercuribenzenesulphonate (pCMBS) reduced ($\Delta pHS*$) NH_3 by 100 %. Molecular dynamics (MD) simulations of membrane-embedded models of UT-B identified the monomeric UT-B pores as the main conduction pathway for NH_3. These data suggest that UT-B has significant NH_3 permeability.

However, a subsequent study showed that UT-B seems not to be involved in NH_3 transport in human erythrocytes, although the erythrocyte variants used in the same study gave evidence of water permeation through UT-B [1]. These authors think that the measurement of ammonia transport across UT-B might be limited by the high erythrocyte lipid ammonia diffusion and/or by the weak NH_3 unit permeability of UT-B. Thus, the permeability of UT-B to NH_3 needs further studies.

UT-B-Mediated Urea Transport in Different Species

Urea permeability was measured in erythrocytes from 11 mammals using the stopped flow technique. The results show that P_{urea} of erythrocytes differs greatly among species. Erythrocytes from dog exhibited the highest P_{urea} (5.3×10^{-5} cm/s), followed by that from fox (3.8×10^{-5} cm/s) > mouse (3.3×10^{-5} cm/s) > cat (2.8×10^{-5} cm/s) > rat (2.5×10^{-5} cm/s) > rabbit (2.4×10^{-5} cm/s) > pig (1.5×10^{-5} cm/s) > human (1.1×10^{-5} cm/s) > sheep (1.0×10^{-5} cm/s) > cow (0.8×10^{-5} cm/s) > donkey (0.7×10^{-5} cm/s). The range of variation of P_{urea} among species spans more than a 7.5-fold difference between the donkey and the dog. P_{urea} was significantly inhibited by 0.7 mM phloretin in all species indicating that urea transport through the erythrocyte membrane is mediated by selective urea transporter proteins.

Osmotic water permeability was measured in erythrocytes from the same 11 mammals. The lowest value was observed in the human (in $\times 10^{-3}$ cm/s, 2.9 ± 0.4) and the highest value in the rabbit (5.2 ± 0.3), only 1.8-fold higher than that in human. Water permeability in erythrocytes is thus relatively similar in all species tested.

Cell membrane urea permeability resulting from simple diffusion across the lipid bilayer is strongly temperature dependent, contrary to that occurring through facilitated transporters. Comparing P_{urea} observed at different temperatures (10, 22, and 27 °C) thus provides information about how much urea transport occurs by simple diffusion. In cat, fox, dog, rat, and mouse, P_{urea} was high at all three temperatures, and only weakly temperature dependent. In contrast, there was a stronger influence of temperature on P_{urea} in cow, donkey, sheep, human, pig, and rabbit. The high activation energy (E_a) of urea transport in herbivores and omnivores suggests that most of the urea transported through the erythrocyte membrane moves through the lipid bilayer by simple diffusion, with only a moderate amount of urea transported through UT-B. In contrast, in three carnivores and two rodents,

only a small fraction of the total urea transport occurs by simple diffusion, and the majority occurs through UT-B. A very significant inverse relationship was observed between E_a and P_{urea}. Only the rabbit departs somewhat from the general trend. It exhibits the same P_{urea} as that of the rat and mouse while its E_a is similar to that of the other herbivores. The urea flux through UT-B in the rabbit is probably much smaller than the UT-B-mediated urea flux in rat and mouse.

The urea and water (P_f) permeabilities were also measured in erythrocytes from 5 species of birds. In goose, duck, pigeon, and quail, P_{urea} ranged from 0.04 to 0.07×10^{-5} cm/s, i.e. 10–20-fold lower than in mammals. In chicken, the value of P_{urea} was not available due to P_f (0.05×10^{-3} cm/s) is too low to measure urea flux-driven volume change in erythrocytes with stopped flow technique. In goose, duck, pigeon, and quail, erythrocytes showed an osmotic water permeability that was modestly higher than that observed in mammals ($6.1–7.3 \times 10^{-3}$ cm/s).

The urea permeability of erythrocytes in mammals is obviously related to their ability to concentrate urea. The high P_{urea} allows fast equilibration of urea in erythrocytes during their transit in the renal medulla, where the urea concentration may reach values 50–200-fold higher than in peripheral blood. Because of their high (AQP1-dependent) water permeability, erythrocytes would undergo severe shrinkage when exposed to the high urea concentration of the inner medulla, where their membrane is not also highly permeable to urea. They would shrink during their transit in the hyperosmotic medulla and subsequently swell on leaving the medulla if they did not possess a high urea permeability [9]. Birds, which concentrate urine to some extent (up to 2.5 times more than plasma in the quail) but excrete their nitrogen wastes as uric acid rather than as urea, do not exhibit facilitated urea transport in their erythrocytes and show a very low P_{urea}, as already described in the literature [7, 9], and as shown in five different birds [24].

References

1. Azouzi S, Gueroult M, Ripoche P, Genetet S, Colin Aronovicz Y, Le Van Kim C, Etchebest C, Mouro-Chanteloup (2013) Energetic and molecular water permeation mechanisms of the human red blood cell urea transporter B. PLoS One 8:e82338
2. Chou CL, Knepper MA (1989) Inhibition of urea transport in inner medullary collecting duct by phloretin and urea analogues. Am J Physiol 257:F359–F365
3. Dix JA, Solomon AK (1984) Role of membrane proteins and lipids in water diffusion across red cell membranes. Biochim Biophys Acta 773:219–230
4. Frohlich O, Macey RI, Edwards-Moulds J, Gargus JJ, Gunn RB (1991) Urea transport deficiency in Jk(a-b-) erythrocytes. Am J Physiol 260:F778–C783
5. Galey WR, Owen JD, Solomon AK (1973) Temperature dependence of nonelectrolyte permeation across red cell membranes. J Gen Physiol 61:727–746

6. Geyer RR, Musa-Aziz R, Enkavi G, Mahinthichaichan P, Tajkhorshid E, Boron WF (2013) Movement of NH3 through the human urea transporter B (UT-B): a new gas channel. Am J Physiol Renal Physiol 304:F1447–F1457
7. Hunter FR (1970) Facilitated diffusion in pigeon erythrocytes. Am J Physiol 218:1765–1770
8. Lucien N, Sidoux-Walter F, Roudier N, Ripoche P, Huet M, Trinh-Trang-Tan MM, Cartron JP, Bailly P (2002) Antigenic and functional properties of the human red blood cell urea transporter hUT-B1. J Biol Chem 277:34101–34108
9. Macey RI (1984) Transport of water and urea in red blood cells. Am J Physiol 246:C195–C203
10. Mannuzzu LM, Moronne MM, Macey RI (1993) Estimate of the number of urea transport sites in erythrocyte ghosts using a hydrophobic mercurial. J Membr Biol 133:85–97
11. Martial S, Neau P, Degeilh F, Lamotte H, Rousseau B, Ripoche P (1993) Urea derivatives as tools for studying the urea-facilitated transport system. Pflugers Arch 423:51–58
12. Mayrand RR, Levitt DG (1983) Urea and ethylene glycol-facilitated transport systems in the human red cell membrane. Saturation, competition, and asymmetry. J Gen Physiol 81:221–237
13. Naccache P, Sha'afi RI (1973) Patterns of nonelectrolyte permeability in human red blood cell membrane. J Gen Physiol 62:714–736
14. Olives B, Mattei MG, Huet M, Neau P, Martial S, Cartron JP, Bailly P (1995) Kidd blood group and urea transport function of human erythrocytes are carried by the same protein. J Biol Chem 270:15607–15610
15. Olives B, Neau P, Bailly P, Hediger MA, Rousselet G, Cartron JP, Ripoche P (1994) Cloning and functional expression of a urea transporter from human bone marrow cells. J Biol Chem 269:31649–31652
16. Sands JM, Timmer RT, Gunn RB (1997) Urea transporters in kidney and erythrocytes. Am J Physiol 273:F321–F339
17. Sha'afi RI, Dakkuri A, To'mey G (1971) Solute and solvent flow across mammalian red cell membrane. How to test for Onsager reciprocal relation. Biochim Biophys Acta 249:260–265
18. Sha'afi RI, Gary-Bobo CM (1973) Water and nonelectrolytes permeability in mammalian red cell membranes. Prog Biophys Mol Biol 26:103–146
19. Sidoux-Walter F, Lucien N, Olives B, Gobin R, Rousselet G, Kamsteeg EJ, Ripoche P, Deen PM, Cartron JP, Bailly P (1999) At physiological expression levels the Kidd blood group/urea transporter protein is not a water channel. J Biol Chem 274:30228–30235
20. Tsukaguchi HI, Shayakul C, Berger UV, Tokui T, Brown D, Hediger MA (1997) Cloning and characterization of the urea transporter UT3: localization in rat kidney and testis. J Clin Invest 99:1506–1515
21. Yang B, Bankir L, Gillepsie A, Epstein CJ, Verkman AS (2002) Urea-selective concentrating defect in transgenic mice lacking urea transporter UT-B. J Biol Chem 277:10633–10637
22. Yang B, Verkman AS (1998) Urea transporter UT3 functions as an efficient water channel. Direct evidence for a common water/urea pathway. J Biol Chem 273:9369–9372
23. Yang B, Verkman AS (2002) Analysis of double knockout mice lacking aquaporin-1 and urea transporter UT-B: evidence for UT-B facilitated water transport in erythrocytes. J Biol Chem 277:36782–36786
24. Zhao D, Sonawane ND, Levin MH, Yang B (2007) Comparative transport efficiencies of urea analogues through urea transporter UT-B. Biochim Biophys Acta 1768:1815–1821

Chapter 9
Urea Transporter Knockout Mice and Their Renal Phenotypes

Robert A. Fenton and Baoxue Yang

Abstract Urea transporter gene knockout mice have been created for the study of the urine-concentrating mechanism. The major findings in studies of the renal phenotype of these mice are as follows: (1) Urea accumulation in the inner medullary interstitium is dependent on intrarenal urea recycling mediated by urea transporters; (2) urea transporters are essential for preventing urea-induced osmotic diuresis and thus for water conservation; (3) NaCl concentration in the inner medullary interstitium is not significantly affected by the absence of IMCD, descending limb of Henle and descending vasa recta urea transporters. Studies in urea transporter knockout mouse models have highlighted the essential role of urea for producing maximally concentrated urine.

Keywords Urea transporters · Urea · Knockout mouse · Urine-concentrating mechanism · Intrarenal urea recycling

Introduction

Over 70 years ago, Gamble and colleagues proposed that the kidney possesses specialized mechanisms that allow large amounts of urea to be excreted without obligating water excretion [19]. Shannon et al. built on these observations and demonstrated that the rate of urea excretion by the kidney is determined by its

Baoxue Yang—Co-corresponding author.

R.A. Fenton (✉)
Department of Biomedicine, Interpret Center, Aarhus University, Aarhus, Building 233/234, 8000 Aarhus, Denmark
e-mail: rofe@ana.au.dk

B. Yang
State Key Laboratory of Natural and Biomimetic Drugs, Key Laboratory of Molecular Cardiovascular Sciences, Ministry of Education, Department of Pharmacology, School of Basic Medical Sciences, Peking University, Beijing 100191, China
e-mail: baoxue@bjmu.edu.cn

rate of filtration and its tubular reabsorption [45, 46]. Further functional studies of urea transport mechanisms have highlighted that urea reabsorption occurs by two distinct mechanisms: a constitutive process that occurs in the proximal nephron accounting for reabsorption of 40 % of the filtered load of urea and a regulated process in the distal nephron that is dependent on the level of antidiuresis [45, 46]. Although the cortical collecting ducts have a low urea permeability [20], the terminal IMCD possesses an extremely high urea permeability that increases after vasopressin (AVP) exposure [41, 42]. Furthermore, the urea transport process in the IMCD is saturable [9, 10]. Based on these functional studies, almost 20 years ago, the first urea transport protein was isolated and characterized [59].

Two urea transporter genes have been cloned: UT-A (*Slc14a2*) and UT-B (*Slc14a1*) [33, 35], Fenton et al. [14]. *Slc14a2* encodes several mRNA transcripts via the use of alternative splicing and alternative promoters, and several of these have been isolated as cDNA and characterized (see other sections and [14, 17, 16, 37, 47, 48]. UT-A1 is expressed in IMCD cells [36], Fenton et al. [14]) (Fig. 9.1), and its transport activity is acutely regulated by AVP [18]. UT-A2 is localized to the lower portions of the thin descending limbs (TDL) of short loops of Henle in the inner stripe of the outer medulla [14, 17, 55] and under prolonged antidiuretic conditions in TDL of long loops of Henle in the inner medulla [55]. UT-A2-mediated urea transport can be acutely regulated by cAMP [38]. UT-A3 expression is restricted to the basolateral membrane domains of the terminal IMCD [8, 50], and its mRNA abundance increases with chronic AVP stimulation [14, 17]. The *Slc14a1* gene encodes a protein, UT-B, that is expressed in descending vasa recta [57]. The data from studies of UT gene knockout mouse models suggest that UTs play important roles in intrarenal urea recycling (Fig. 9.1).

UT-A1 and UT-A3 Knockout Mice

Generation of UT-A1/3$^{-/-}$ Mice

In 2004, a mouse model that allowed a specific assessment of the role of inner medullary urea transport in kidney function was generated [13]. UT-A1/UT-A3 knockout mice (termed *UT-A1/3$^{-/-}$* mice from this point) were produced by standard gene-targeting techniques by deletion of 3 kb of the UT-A gene containing a single 148-bp exon, exon 10. Exon 10 is predicted to lie in a large hydrophobic region of UT-A1 and is putatively membrane spanning [40]. Due to the complex differential splicing of the UT-A gene (see earlier chapter), deletion of exon 10 would be predicted to completely disrupt the UT-A1 and UT-A3 proteins, but also delete a testis-specific isoform UT-A5 [14, 17]. Successful deletion of the UT-A1 and UT-A3 urea transporters from the IMCD was confirmed using immunohistochemistry and immunoblotting. Importantly, the expression of the thin descending limb urea transporter UT-A2 was unaffected. A functional assessment of *UT-A1/3$^{-/-}$* mice using isolated perfused tubules highlighted a complete absence of phloretin-sensitive and AVP-regulated urea transport in IMCD segments (Fig. 9.2).
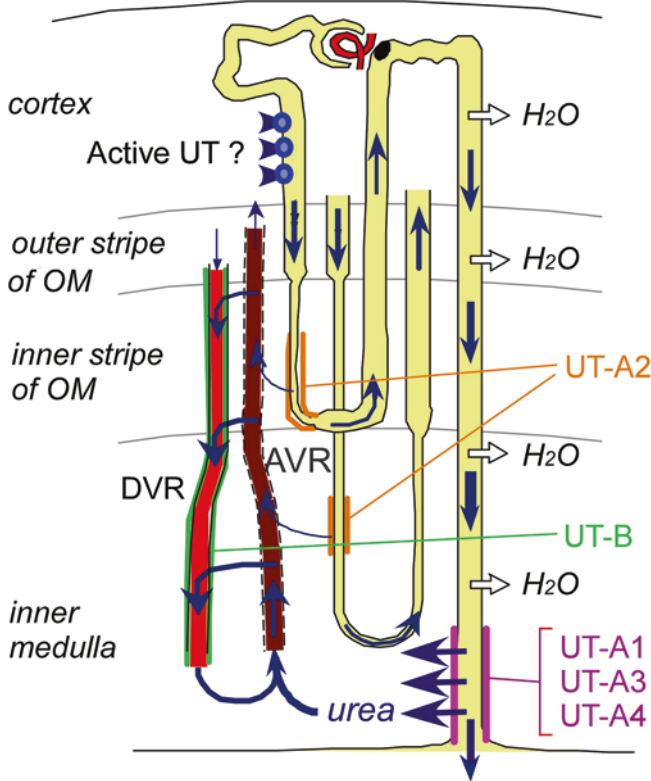
Fig. 9.1 Schematic diagram of intrarenal urea recycling pathways and UT localization. A short loop and a long loop of Henle are depicted within the four kidney zones, along with an arterial (descending) and a venous (ascending) vasa recta (DVR and AVR, respectively). UT-B is expressed in DVR, UT-A2 in descending limb of loops of Henle, and UT-A1, UT-A3, and possibly UT-A4 in inner medullary collecting ducts. The pathways allowing urea to recycle are indicated by *blue arrows*. In normal mice, concentrated urea is delivered to the tip of the papilla by the terminal part of the collecting ducts expressing the vasopressin-regulated urea transporters UT-A1/3. Urea is taken up by ascending blood (plasma and red blood cells) in AVR, and a significant fraction of it is returned to the inner medulla by being reintroduced in the DVR (expressing UT-B). Reproduced from [32]

Phenotype of UT-A1/3$^{-/-}$ Mice

Compared to wild-type mice, *UT-A1/3*$^{-/-}$ mice have no apparent differences in appearance, body weight, behavior, sensory function, or physical attributes. A comprehensive pathological and histological survey of different tissues isolated from *UT-A1/3*$^{-/-}$ mice determined that apart from kidneys and testis, no abnormalities were detectable [15]. The kidneys of knockout mice were significantly smaller and the testes significantly larger compared to controls. An unexpected
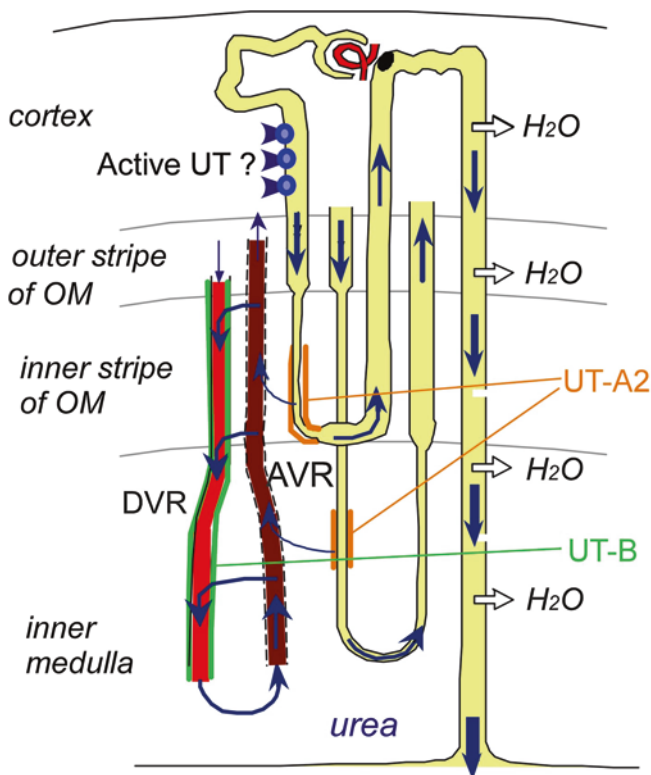
Fig. 9.2 Schematic diagram of intrarenal urea flows in UT-A1/3$^{-/-}$ mice. The urea flows are indicated by *blue arrows*. In UT-A1/3$^{-/-}$ mice, dramatically less urea is reabsorbed in the papilla, leading to greater urea excretion in the urine

phenotype of *UT-A1/3$^{-/-}$* mice was prominent blood congestion in the renal medulla of the kidneys, but with no significant difference in total renal blood flow. Excretion of nitrates and nitrites (products of nitric oxide metabolism) was markedly increased in the *UT-A1/3$^{-/-}$* mice relative to controls, which may partly be responsible for the observed blood congestion.

Role of Collecting Duct Urea Transport in the Urinary Concentrating Mechanism

A proportion of our fundamental understanding of urea transporters in the urinary concentrating mechanism is based on a model of urea handling proposed by Robert Berliner [7]. During antidiuresis, water is osmotically absorbed from the urea-impermeable parts of the collecting ducts via aquaporins, resulting in a

progressive increase in the luminal urea concentration along the collecting duct system. When this fluid reaches the urea-permeable IMCD, urea exits from the tubule lumen to the interstitium and is trapped by countercurrent exchange [6, 23]. In the presence of AVP, urea concentrations in the interstitium nearly equilibrate across the IMCD epithelium, which allows an almost complete osmotic balance between the collecting duct lumen and the interstitium. This process prevents osmotic diuresis due to urea. To directly examine this hypothesis, the urinary concentrating ability of *UT-A1/3*$^{-/-}$ mice on different amounts of dietary protein intake was examined [13, 15]. *UT-A1/3*$^{-/-}$ mice fed either a normal (20 % protein by weight) or high-protein (40 %) diet had a significantly greater water intake, urine flow, and reduced urine osmolality compared to controls. *UT-A1/3*$^{-/-}$ mice fed a low-protein diet (4 % protein) did not show these differences compared to wild-type mice. After an 18-h water restriction, *UT-A1/3*$^{-/-}$ mice on a normal or high-protein diet were unable to reduce their urine flow to levels below those observed under basal conditions, resulting in volume depletion and loss of body weight. *UT-A1/3*$^{-/-}$ mice on a 4 % protein diet were able to maintain fluid balance without alterations in body weight. These studies provide direct evidence that the concentrating defect in *UT-A1/3*$^{-/-}$ mice is due to a urea-dependent osmotic diuresis. During consumption of low-protein diets, hepatic urea production is low and urea delivery to the IMCD is low, rendering the absence or presence of IMCD urea transport immaterial with regard to water balance, i.e., greater urea delivery to the IMCD results in greater water excretion. In conclusion, the results are consistent with a role for IMCD urea transporters in the maintenance of water balance through their ability to prevent a urea-induced osmotic diuresis.

Role of Collecting Duct Urea Transport in NaCl Accumulation in the Inner Medulla

In 1959, the widely accepted classical countercurrent multiplier model was proposed by Kuhn and Ramel [30]. They proposed that the concentration gradient that drives the countercurrent multiplier system in the outer medulla and concentrates interstitial NaCl relies on active reabsorption of NaCl in the water-impermeable thick ascending limb of the loop of Henle (TAL). In contrast, the mechanism that concentrates NaCl in the inner medullary interstitium and contributes to passive water reabsorption from the IMCD remains controversial. As the thin ascending limbs of Henle's loop, unlike the TAL, are incapable of active NaCl transport [22, 28], a variety of mechanisms have been suggested to explain NaCl accumulation in the inner medulla [24, 25, 51]. The most widely recognized accepted model is the "passive" mechanism of NaCl accumulation [26]; Kokko and Rector [27, 49], proposed in similar formats by both Kokko and Rector and Stephenson. In this model, rapid urea reabsorption from the IMCD generates and maintains a high urea concentration in the inner medullary interstitium, resulting in a transepithelial gradient favoring the passive reabsorption of NaCl from the thin ascending limb of Henle's loop. With a low urea permeability

in the thin ascending limbs, any reabsorbed NaCl from the thin ascending limb will not be replaced by urea, making the ascending limb fluid dilute relative to the fluid in other nephron segments and generating a "single effect" analogous to that in the outer medulla. Counterflow between the ascending and descending limbs of Henle's loops will multiply this single effect, with the end effect similar to countercurrent multiplication in the outer medulla TALs. Since the passive mechanism relies on rapid urea transport out of the IMCD lumen, it would be expected that the lack of urea transport in the IMCDs of *UT-A1/3*$^{-/-}$ mice would impair the ability to concentrate NaCl in the inner medulla. However, experimental studies were unable to prove this hypothesis correct. In an initial study, in water-restricted *UT-A1/3*$^{-/-}$ mice, there was a significantly reduced concentration of urea in the inner medullary interstitium compared to controls [13], but no reduction in the mean Na^+, Cl^-, or K^+ concentrations. In a second study, urea and Na^+ concentrations and osmolality were measured in the cortex, outer medulla, and the inner medulla isolated from *UT-A1/3*$^{-/-}$ or wild-type mice fed a low- (4 %) or high (40 %)-protein diet [15]. Although increasing the dietary protein intake resulted in a greater tissue osmolality, due predominantly to a greater accumulation of urea in the inner medulla in wild-type mice, sodium concentrations were unaffected at all levels of the corticomedullary axis. *UT-A1/3*$^{-/-}$ mice had a substantially attenuated corticomedullary osmolality gradient and no urea gradient on either diet, yet the corticomedullary sodium gradients were almost identical to wild-type mice. The conclusion from these studies in *UT-A1/3*$^{-/-}$ mice is that NaCl accumulation in the inner medulla is not reliant on either IMCD urea transport or the accumulation of urea in the IMCD interstitium, contradicting the passive concentrating model in the form originally proposed.

An Economy of Water in Renal Function Referable to Urea

A hypothesis regarding urea and renal function was described nearly 75 years ago as "an economy of water in renal function referable to urea" or the "Gamble phenomenon" [19]. Gamble determined that the water requirement for excretion of urea was less than for excretion of an osmotically equivalent amount of NaCl and that less water was required for the excretion of urea and NaCl together than the water needed to excrete an osmotically equivalent amount of either urea or NaCl alone. These results suggested a specialized role of IMCD urea transporters, which was directly tested using *UT-A1/3*$^{-/-}$ mice [12]. Both elements of the Gamble phenomenon were absent in *UT-A1/3*$^{-/-}$ mice. Giving wild-type mice progressively increasing quantities of urea or NaCl in the diet induced osmotic diuresis when excretion levels were high (6,000 μosmol/day for urea; 3,500 μosmol/day for NaCl). Interestingly, mice were unable to increase urinary NaCl concentrations above 420 mM. Thus, one aspect of the Gamble phenomenon derives from an ability of both urea and NaCl excretions to be saturable, presumably a result of an exceeded reabsorptive capacity for urea and NaCl in the renal tubule. Additionally, conservation of water with mixtures of NaCl and urea versus NaCl or urea alone

occurs by lowering the concentration of each to levels that avoid osmotic diuresis, rather than a specific interaction between urea transport and NaCl transport at an epithelial level.

Role of IMCD Urea Transporters in the Regulation of Glomerular Filtration Rate

High-protein diet consumption results in an increase in whole kidney glomerular filtration rate (GFR) [11, 34], potentially a result of changes in the tubuloglomerular feedback (TGF) system [43]. Feeding a high-protein diet to rats increases GFR by approximately 30 % and increases single-nephron GFR (SNGFR) in the distal tubule by 20 %, due to reduced suppression of SNGFR by TG feedback [43]. Based on these studies, it was apparent that the sensing mechanism of the TG feedback system was rendered less responsive by a high protein intake. This diminished TGF response was caused, at least in part, by a reduced early distal NaCl concentration, without a change in early distal tubule osmolality [44]. These observations prompted Bankir et al. [2, 3] to suggest that the increased concentrations of urea in the early distal tubule resulting from the high-protein intake allowed the concentration of NaCl to be lower in the early distal tubule, without rendering an osmotic effect. This increased urea concentration in the late TAL and early distal tubule would be dependent both on the urea concentration of the glomerular filtrate and on the extent of urea recycling, a result of passive urea secretion into the loop of Henle from urea reabsorption in the IMCD. This hypothesis was directly tested in *UT-A1/3$^{-/-}$* mice, where urea recycling is likely to be eliminated (Fig. 9.2). However, no significant differences were observed in FITC-inulin clearance between *UT-A1/3$^{-/-}$* and wild-type mice under either a low- or a high-protein diet, suggesting that GFR in the knockout mice is not significantly affected. Therefore, these studies indicate that urea reabsorption from the IMCD, and more specifically the process of urea recycling, is not an important determinant of protein-induced increases in GFR.

UT-A2 Knockout Mice

Urea transporter UT-A2 is a major urea transporter of the thin descending limb of the loop of Henle in short-looped nephrons [1, 14, 17, 47, 59] (Fig. 9.1). To investigate the physiological role of UT-A2 in vivo, Uchida et al. generated UT-A2-selective knockout mice by deleting 3 kb of the mouse UT-A2 promoter by gene targeting [54]. Deletion of this segment selectively disrupted expression of UT-A2 (Fig. 9.3), while sparing the expression of other kidney UT-A transporters. UT-A2 null mice exhibited normal growth and no physiological abnormalities. Under basal conditions (free access to food and water), plasma urea, sodium, and chloride concentrations were not changed in UT-A2 null mice.
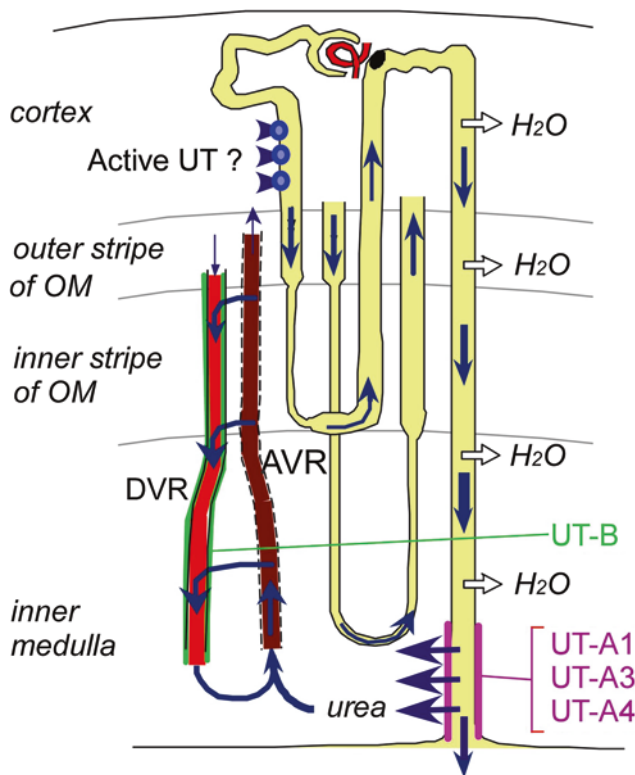
Fig. 9.3 Schematic diagram of intrarenal urea flows in UT-A2$^{-/-}$ mice. The urea flows are indicated by *blue arrows*. In UT-A2$^{-/-}$ mice, there is no urea permeability in short and long loops of Henle. A complete intrarenal urea recycling pathway exists in UT-A2$^{-/-}$ mice

The daily urine output and urine osmolality were similar in UT-A2 null mice and wild-type mice. It was found that UT-A2 null mice had only a mild deficit in urine-concentrating ability in the context of limited urea supply to the kidney due to consumption of a low-protein diet (4 % protein). The study on UT-A2 null mice suggests that UT-A2 makes a minimal contribution to urea accumulation in the inner medulla under basal conditions. UT-A2 might play a role in maintaining a high urea concentration within the inner medulla, with inadequate daily protein intake.

UT-B Knockout Mice

Generation and General Phenotype of UT-B Knockout Mice

UT-B is expressed in endothelia of renal descending vasa recta [21, 52, 53, 56] (Fig. 9.1). UT-B knockout mice were generated by a gene-targeting strategy [57]
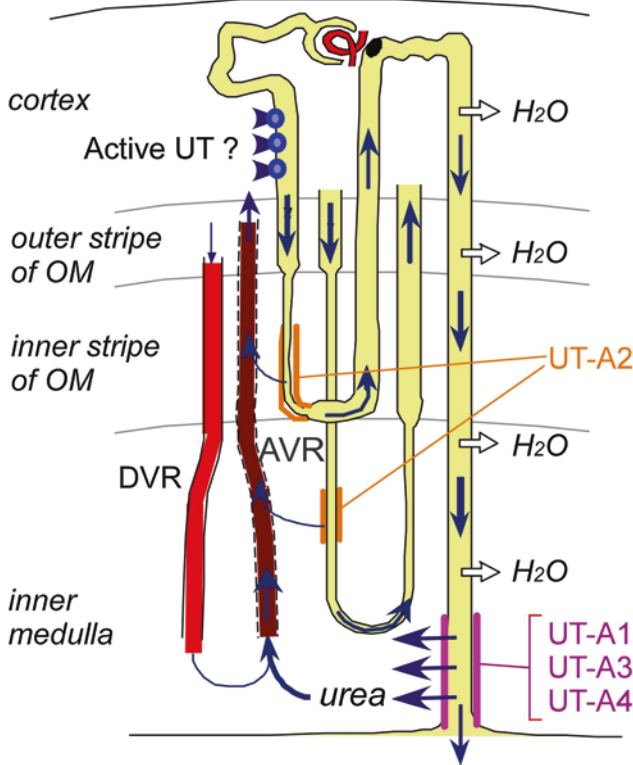
Fig. 9.4 Schematic diagram of intrarenal urea flows in UT-B$^{-/-}$ mice. The urea flows are indicated by *blue arrows*. In UT-B$^{-/-}$ mice, there is no urea permeability in descending vasa recta (DVR). More urea is taken up by ascending vasa recta (AVR) into circulation, and less urea is returned to the IM by DVR (without UT-B) in UT-B$^{-/-}$ mice than in wild-type mice. Reproduced from [32]

that resulted in only truncated UT-B transcripts and no UT-B protein in kidney in the UT-B knockout mice (Fig. 9.4).

UT-B null mice exhibited normal growth and no overt abnormalities in their main biological functions, behavior, and sensory activity. The sex and genotype ratios were normally distributed, suggesting no influence of UT-B gene deletion on survival or development. The UT-B null mice had normal plasma sodium, potassium, chloride, bicarbonate, and creatinine concentrations.

Role of Descending Vasa Recta Urea Transport in the Urinary Concentrating Mechanism

The UT-B null mice were moderately polyuric, consuming and excreting approximately 50 % more fluid than litter-matched heterozygous and wild-type mice. The average urine osmolality in UT-B null mice was significantly lower than that in wild-type mice.

In response to a 24-h water deprivation, urine osmolality in the UT-B null mice increased significantly, although to a significantly lesser extent than in wild-type mice. Plasma osmolality was slightly but not significantly higher in UT-B null mice than in wild-type mice. The urine-to-plasma ratio for osmolality, an index of overall concentrating capacity of the kidney, was lower by one-third in UT-B null mice compared with wild-type mice. Plasma urea concentration was significantly higher, and urinary urea concentration was significantly lower in the UT-B null mice. These opposing changes suggest that plasma urea increased because the kidney was less able to recycle urea and concentrate urea in the urine. The urine-to-plasma ratio of urea concentration reflects the capacity of the kidney to concentrate urea above its level in body fluids. This ratio was markedly decreased in UT-B null mice. The composition of the aqueous component of the inner medulla suggests that the significantly reduced inner medullary osmolality resulted primarily from a decrease in inner medulla urea concentration.

The kidney transforms large amounts of urea-poor plasma into a small volume of urea-rich urine. Thus, besides the overall urinary concentrating defect in UT-B null mice, we investigated the possibility of a selective defect in urea-concentrating capacity by measurement of the urine-to-plasma urea concentration ratio and inner medullary composition. UT-B deficiency in the kidney resulted in decreased urinary urea and increased plasma urea concentrations, producing a 2-fold decrease in the urine-to-plasma urea concentration ratio.

UT-B deficiency also produced a 2-fold reduction in inner medullary urea concentration with little effect on inner medullary chloride (salt) concentration. These observations suggest that some of the urea delivered to the tip of the papilla from the IMCD by UT-A1/UT-A3 and carried up by the blood through the venous ascending vasa recta is not recycled into UT-B-deficient arterial descending vasa recta and thus is returned to the general circulation (Fig. 9.4). In contrast to the remarkably reduced urea-concentrating ability in the UT-B null mice, the defect in the concentration of all solutes as assessed by the urine-to-plasma osmolality ratio (lower by only one-third) was more modest, suggesting that UT-B plays a greater role in enabling the kidney to concentrate urea than other solutes in the urine. The selective reduction in inner medullary urea concentration supports this conclusion.

UT-A2/B Knockout Mice

Generation of UT-A2 and UT-B Double Knockout Mice

UT-A2 and UT-B are expressed in the thin descending limb of the loop of Henle and descending vasa recta, respectively [39] (Fig. 9.1). UT-B deletion alone caused a significant urea-selective urine-concentrating defect [57], but UT-A2 deletion alone did not significantly change urine-concentrating ability [54]. To further evaluate the contribution of UT-A2 and UT-B to the urine-concentrating mechanism and their possible interaction, it was necessary to generate a mouse model in which urea recycling through both the vasa recta and the thin limbs would be impaired, with the maintenance of normal urea delivery to the inner medulla (via UT-A1/A3). For
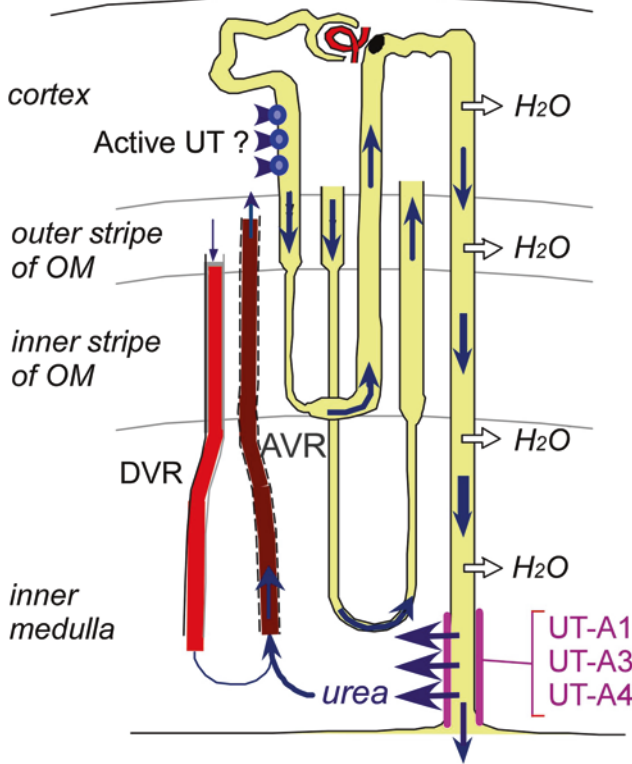
Fig. 9.5 Schematic diagram of intrarenal urea flows in UT-A2/B$^{-/-}$ mice. The urea flows are indicated by *blue arrows*. In UT-A2/B$^{-/-}$ mice, there is no urea permeability in short and long loops of Henle and in descending vasa recta (DVR). The intrarenal urea recycling pathway is deficient in UT-A2/B$^{-/-}$ mice. Less urea is taken up by the ascending vasa recta (AVR) and returned to the blood in UT-A2/B$^{-/-}$ mice than in UT-B$^{-/-}$ mice, and less urea is returned to the inner medulla in UT-A2/B$^{-/-}$ mice than in wild-type mice. Reproduced from [32]

this purpose, a double UT-A2 and UT-B knockout mice (UT-A2/B$^{-/-}$) were generated with gene targeting of UT-A2 in UT-B gene-targeted ES cells [32]. There was no specific UT-A2 and UT-B expression in TDL and descending vasa recta, respectively, in homozygous UT-A2/B$^{-/-}$ mice (Fig. 9.5). Body weight and kidney weight were not influenced by combined UT-A2 and UT-B deletions.

UT-A2 Deletion Partially Remedies the Urine-Concentrating Defect Caused by UT-B Deletion

Daily urine volume in UT-A2/B$^{-/-}$ mice significantly exceeded that in litter-matched wild-type mice but was distinctly lower than that in UT-B knockout mice. Urine osmolality in UT-A2/B$^{-/-}$ mice was lower than that in wild-type mice, but

significantly exceeded that in UT-B null mice. In response to an 18-h water depriva-
tion, urine osmolality increased by 50 ~ 60 % in all three genotypes, reaching 2,900,
2,000, and 3,300 mosmol/kg H_2O in UT-A2/B$^{-/-}$, UT-B null, and wild-type mice,
respectively. Plasma osmolality was similar in mice of all three genotypes. However,
both plasma urea concentration and urinary urea concentration in UT-A2/B$^{-/-}$ mice
were between those in UT-B null and wild-type mice. The urine-to-plasma ratio of
urea concentration in UT-A2/B$^{-/-}$ was also intermediate. In contrast, there was no
significant difference in sodium, potassium, and chloride concentrations among the
three genotypes. Plasma creatinine and creatinine clearance (an index of glomerular
filtration rate) were similar in the three groups, suggesting that UT-A2 and UT-B
deletions do not influence glomerular hemodynamics. The inner medullary urea con-
centration in UT-A2/B$^{-/-}$ was between those in wild-type and UT-B null mice.

UT-A2 Plays a Role in the Long-Term Accumulation of Urea in the Inner Medulla

To evaluate the contribution of UT-A2 to the urea-dependent enhancement of urine-
concentrating capacity, UT-A2/B$^{-/-}$, UT-B null, and wild-type mice were subjected
to an acute modest hyperosmotic urea load (0.3 ml of 1 M urea ip, an amount equal to
1/10 of their daily urea excretion). After administration of the urea load, urea excretion
increased abruptly during the first 2 h in all three groups and decreased progressively
thereafter, with a similar time course and intensity in mice of the three genotypes.
However, this increase resulted from a very different pattern of changes in urine con-
centration and urine flow rate in UT-A2/B$^{-/-}$, UT-B null, and wild-type mice.

During the early phase (0–4 h), urine osmolality rose more in UT-A2/B$^{-/-}$ than
in UT-B null mice, and urine flow rate rose only modestly, as in wild-type mice. In
contrast, UT-B null mice exhibited a much higher increase in urine flow rate. During
the late phase (6–10 h), neither the UT-A2/B$^{-/-}$ mice nor the UT-B null mice were
able to raise urea concentration in the urine, contrary to wild-type mice. Thus, even if
UT-A2 deletion on top of UT-B deletion restored a close-to-normal urine osmolality
and flow rate in the 24-h urine collection, UT-A2 deletion did not allow the kidney to
progressively accumulate urea in the medulla after an acute urea load. This suggests
that UT-A2 plays a role in the long-term accumulation of urea in the inner medulla.

In the early phase, the large rise in urine flow rate seen in UT-B null mice drove
an increase in the excretion of urea and nonurea solutes that was greater than in the
two other mouse models. This was followed by a fall in the excretion of nonurea
solutes in the late phase for UT-B knockout mice. In contrast, during this late phase,
the concentration of nonurea solutes rose continuously in UT-A2/B$^{-/-}$ mice so that
the excretion of these solutes remained stable and similar to that in wild-type mice.

After the urea load, plasma urea rose promptly, reached a peak at 30 min in all
groups, and then returned to almost basal values after 8 h. The magnitude of the
rise from basal to peak level was different in the three groups. Plasma urea con-
centration in UT-B null mice was the highest compared with UT-A2/B$^{-/-}$ mice

and wild-type mice. However, the plasma creatinine level was similar in the three groups, suggesting that the GFR was roughly similar in all genotypes in the basal condition and after the urea load. Taken together, these results suggest that in wild-type mice, UT-B (in vasa recta) and UT-A2 (in thin limbs) contribute to the intra-renal cycling of urea and to the generation of concentrated urine in different ways because the deletion of one or both of the transporters induced opposite changes.

To explain the milder urine-concentrating defect induced by the deletion of UT-A2 on top of UT-B, we postulate that when UT-A2 is normally expressed in the TDL, a significant amount of urea is added to the descending vasa recta, i.e., that urea is reabsorbed rather than secreted (as previously assumed) through UT-A2. In rats, and even more so in mice, TDL of short-looped nephrons are in close proximity to AVR in the vascular bundles throughout the inner stripe of the outer medulla [29]. A passive diffusion of urea from TDL to AVR could take place only if there is an outward-directed urea concentration gradient across the TDL epithelium (Fig. 9.1). Such a gradient can be generated by an active urea secretion into the pars recta, as previously proposed [5, 58]. Urea secretion has been postulated recently because of the high fractional excretion of urea observed in wild-type mice [13, 58].

The defect in the urine-concentrating ability of UT-B null mice is most likely due to the dramatic reduction in countercurrent exchange of urea from ascending to DVR [4, 58]. The impaired vascular countercurrent exchange compromises urea delivery to the inner medulla via the DVR, augments the lag in the vascular urea concentration and osmolality of the interstitial fluid, and increases vascular flow in the deep inner medulla, thus resulting in a decrease in urine osmolality. This interpretation is consistent with simulation results in a modeling study [31].

The simultaneous deletion of both the vasa recta and the TDL urea transporters resulted in a significantly milder defect than the deletion of either urea transporter alone. In the UT-A2/B$^{-/-}$ mice, substantially less urea is reabsorbed from the short TDL in the inner stripe, compared with wild-type or UT-B null mice. Instead, that urea is delivered, via the ascending limb and distal tubule, into the collecting duct and returned to the inner medulla. Taken together, these results suggest a novel role for UT-A2 in the concentrating mechanism. UT-A2 might contribute to the accumulation of urea in the inner medulla during transition from diuresis to antidiuresis rather than to maintenance of a high urea concentration during steady state.

Conclusions

The creation of urea transporter knockout mice has allowed us to address several long-standing hypotheses for the role of urea in kidney function and as such redefined the role of urea in the urinary concentrating mechanism. Whether studies of urea transport processes in the mouse kidney can be directly compared to urea-handling mechanisms in other species remains to be determined.

References

1. Bagnasco SM, Peng T, Nakayama Y, Sands JM (2000) Differential expression of individual UT-A urea transporter isoforms in rat kidney. J Am Soc Nephrol 11:1980–1986
2. Bankir L, Ahloulay M, Bouby N, Trinh-Trang-Tan MM, Machet F, Lacour B, Jungers P (1993) Is the process of urinary urea concentration responsible for a high glomerular filtration rate? Am J Soc Nephrol 4:1091–1103
3. Bankir L, Bouby N, Trinh-Trang-Tan MM (1991) Vasopressin-dependent kidney hypertrophy: role of urinary concentration in protein-induced hypertrophy and in the progression of chronic renal failure. Am J Kidney Dis 17:661–665
4. Bankir L, Chen K, Yang B (2004) Lack of UT-B in vasa recta and red blood cells prevents the urea-induced improvement in urinary concentrating ability. Am J Physiol Renal Physiol 286:F144–F151
5. Bankir L, Trinh-Trang-Tan MM (2000) Urea and the kidney. In: Brenner BM (ed) The kidney, 6th edn. Saunders, Philadelphia, p 637–679
6. Berliner RW, Bennett CM (1967) Concentration of urine in the mammalian kidney. Am J Med 42(5):777–789
7. Berliner RW, Levinsky NG, Davidson DG, Eden M (1958) Dilution and concentration of the urine and the action of antidiuretic hormone. Am J Med 24:730–744
8. Blount MA, Klein JD, Martin CF, Tchapyjnikov D, Sands JM (2007) Forskolin stimulates phosphorylation and membrane accumulation of UT-A3. Am J Physiol Renal Physiol 293:F1308–F1313
9. Chou CL, Sands JM, Nonoguchi H, Knepper MA (1990) Concentration dependence of urea and thiourea transport in rat inner medullary collecting duct. Am J Physiol 258(3 Pt 2):F486–F494
10. Chou CL, Knepper MA (1989) Inhibition of urea transport in inner medullary collecting duct by phloretin and urea analogues. Am J Physiol 257:F359–F365
11. Dicker SE (1949) Effect of the protein content of the diet on the glomerular filtration rate of young and adult rats. J Physiol 108:197–202
12. Fenton RA, Chou CL, Sowersby H, Smith CP, Knepper MA (2006) Gamble's 'economy of water' revisited: studies in urea transporter knockout mice. Am J Physiol Renal Physiol 291:148–154
13. Fenton RA, Chou CL, Stewart GS, Smith CP, Knepper MA (2004) Urinary concentrating defect in mice with selective deletion of phloretin sensitive urea transporters in the renal collecting duct. Proc Natl Acad Sci USA 101:7469–7474
14. Fenton RA, Cottingham CA, Stewart GS, Howorth A, Hewitt JA, Smith CP (2002) Structure and characterization of the mouse UT-A gene (Slc14a2). Am J Physiol Renal Physiol 282:F630–F638
15. Fenton RA, Flynn A, Shodeinde A, Smith CP, Schnermann J, Knepper MA (2005) Renal phenotype of UT-A urea transporter knockout mice. J Am Soc Nephrol 16(6):1583–1592
16. Fenton RA, Howorth A, Cooper GJ, Meccariello R, Morris ID, Smith CP (2000) Molecular characterization of a novel UT-A urea transporter isoform (UT- A5) in testis. Am J Physiol Cell Physiol 279:C1425–C1431

17. Fenton RA, Stewart GS, Carpenter B, Howorth A, Potter EA, Cooper GJ, Smith CP (2002) Characterization of mouse urea transporters UT-A1 and UT-A2. Am J Physiol Renal Physiol 283:F817–F825
18. Froehlich O, Klein JD, Smith PM, Sands JM, Gunn RB (2006) Regulation of UT-A1-mediated transepithelial urea flux in MDCK cells. Am J Physiol Cell Physiol 291:600–606
19. Gamble JL, Chou CL, Sowersby H, Smith CP, Knepper MA (1934) An economy of water in renal function referable to urea. Am J Physiol 109:139–154
20. Grantham JJ, Burg MB (1966) Effect of vasopressin and cyclic AMP on permeability of isolated collecting tubules. Am J Physiol 211:255–259
21. Hu MC, Bankir L, Michelet S, Rousselet G, Trinh-Trang-Tan MM (2000) Massive reduction of urea transporters in remnant kidney and brain of uremic rats. Kidney Int 58:1202–1210
22. Imai M (1979) The connecting tubule: a functional subdivision of the rabbit distal nephron segments. Kidney Int 15:346–356
23. Jamison RL, Bennett CM, Berliner RW (1967) Countercurrent multiplication by the thin loops of Henle. Am J Physiol 212:357–366
24. Knepper MA, Chou CL, Layton HE (1993) How is urine concentrated by the renal inner medulla? Contrib Nephrol 102:144–160
25. Knepper MA, Saidel GM, Hascall VC, Dwyer T (2003) Concentration of solutes in the renal inner medulla: interstitial hyaluronan as a mechano-osmotic transducer. Am J Physiol Renal Physiol 284:F433–F446
26. Kokko JP (1970) Sodium chloride and water transport in the descending limb of Henle. J Clin Invest 49:1838–1846
27. Kokko JP, Rector FC Jr (1972) Countercurrent multiplication system without active transport in inner medulla. Kidney Int 2:214–223
28. Kondo Y, Abe K, Igarashi Y, Kudo K, Tada K, Yoshinaga K (1993) Direct evidence for the absence of active Na^+ reabsorption in hamster ascending thin limb of Henle's loop. J Clin Invest 91:5–11
29. Kriz W (1981) Structural organisation of the renal medulla: comparative and functional aspects. Am J Physiol Regul Integr Comp Physiol 241:R3–R16
30. Kuhn W, Ramel A (1959) Activer Salztransport als moeglicher (und wahrscheinlicher) Einzeleffekt bei der Harnkonzentrierung in der Niere. Helv Chim Acta 42:628–660
31. Layton AT (2007) Role of UT-B urea transporters in the urine concentrating mechanism of the rat kidney. Bull Math Biol 69:887–929
32. Lei T, Zhou L, Layton AT, Zhou H, Zhou X, Bankir L, Yang B (2011) Role of thin descending limb urea transport in renal urea handling and the urine concentrating mechanism. Am J Physiol Renal Physiol 301:F1251–F1259
33. Lucien N, Sidoux-Walter F, Olivès B, Moulds J, Le Pennec PY, Cartron JP, Bailly P (1998) Characterization of the gene encoding the human Kidd blood group/urea transporter protein. Evidence for splice site mutations in Jknull individuals. J Biol Chem 273:12973–12980
34. Mackay EM, Mackay LL, Addis T (1928) Factors which determine renal weight. V. The protein intake. Am J Physiol 86:459–465
35. Nakayama Y, Naruse M, Karakashian A, Peng T, Sands JM, Bagnasco SM (2001) Cloning of the rat Slc14a2 gene and genomic organization of the UT-A urea transporter. Biochim Biophys Acta 1518:19–26
36. Nielsen S, Terris J, Smith CP, Hediger MA, Ecelbarger CA, Knepper MA (1996) Cellular and subcellular localization of the vasopressin-regulated urea transporter in rat kidney. Proc Natl Acad Sci USA 93:5495–5500
37. Olives B, Neau P, Bailly P, Hediger MA, Rousselet G, Cartron JP, Ripoche P (1994) Cloning and functional expression of a urea transporter from human bone marrow cells. J Biol Chem 269:31649–31652
38. Potter EA, Stewert G, Smith CP (2006) Urea flux across MDCK-mUT-A2 monolayers is acutely sensitive to AVP, cAMP and [Ca2 +]i. Am J Physiol Renal Physiol 291:F122–F128
39. Promeneur D, Rousselet G, Bankir L, Bailly P, Cartron JP, Ripoche P, Trinh-Trang-Tan MM (1996) Evidence for distinct vascular and tubular urea transporters in the rat kidney. Am J Soc Nephrol 7:852–860

40. Sands JM (2003) Mammalian urea transporters. Annu Rev Physiol 65:543–566
41. Sands JM, Knepper MA (1987) Urea permeability of mammalian inner medullary collecting duct system and papillary surface epithelium. J Clin Invest 79(1):138–147
42. Sands JM, Nonoguchi H, Knepper MA (1987) Vasopressin effects on urea and H_2O transport in inner medullary collecting duct subsegments. Am J Physiol 253:F823–F832
43. Seney FD Jr, Persson EG, Wright FS (1987) Modification of tubuloglomerular feedback signal by dietary protein. Am J Physiol 252(1 Pt 2):F83–F90
44. Seney FD Jr, Wright FS (1985) Dietary protein suppresses feedback control of glomerular filtration in rats. J Clin Invest 75:558–568
45. Shannon JA (1936) Glomerular filtration and urea excretion in relation to urine flow in the dog. Am J Physiol 117:206–225
46. Shannon JA (1938) Urea excretion in the normal dog during forced diuresis. Am J Physiol 122:782–787
47. Smith CP, Lee WS, Martial S, Knepper MA, You G, Sands JM, Hediger MA (1995) Cloning and regulation of expression of the rat kidney urea transporter (rUT2). J Clin Invest 96:1556–1563
48. Smith CP, Potter EA, Fenton RA, Stewart GS (2004) Characterization of a human colonic cDNA encoding a structurally novel urea transporter, hUT-A6. Am J Physiol Cell Physiol 287:C1087–C1093
49. Stephenson JL (1972) Concentration of urine in a central core model of the renal counterflow system. Kidney Int 2:85–94
50. Stewart GS, Fenton RA, Wang W, Kwon TH, White SJ, Collins VM, Cooper G, Nielsen S, Smith CP (2004) The basolateral expression of mUT-A3 in the mouse kidney. Am J Physiol Renal Physiol 286:F979–F987
51. Thomas SR (2000) Inner medullary lactate production and accumulation: a vasa recta model. Am J Physiol Renal Physiol 279:F468–F481
52. Timmer RT, Klein JD, Bagnasco SM, Doran JJ, Verlander JW, Gunn RB, Sands JM (2001) Localization of the urea transporter UT-B protein in human and rat erythrocytes and tissues. Am J Physiol Cell Physiol 281:C1318–C1325
53. Trinh-Trang-Tan MM, Lasbennes F, Gane P, Roudier N, Ripoche P, Cartron JP, Bailly P (2002) UT-B1 proteins in rat: tissue distribution and regulation by antidiuretic hormone in kidney. Am J Physiol Renal Physiol 283:F912–F922
54. Uchida S, Sohara E, Rai T, Ikawa M, Okabe M, Sasaki S (2005) Impaired urea accumulation in the inner medulla of mice lacking the urea transporter UT-A2. Mol Cell Biol 25:7357–7363
55. Wade JB, Lee AJ, Liu J, Ecelbarger CA, Mitchell C, Bradford AD, Terris J, Kim GH, Knepper MA (2000) UT-A2: a 55-kDa urea transporter in thin descending limb whose abundance is regulated by vasopressin. Am J Physiol Renal Physiol 278:F52–F62
56. Xu Y, Olives B, Bailly P, Ripoche P, Fisher E, Ronco P, Cartron JP, Rondeau E (1997) Endothelial cells of the kidney vasa recta express the urea transporter HUT11. Kidney Int 51:138–146
57. Yang B, Bankir L, Gillespie A, Epstein CJ, Verkman AS (2002) Urea-selective concentrating defect in transgenic mice lacking urea transporter UT-B. J Biol Chem 277:10633–10637
58. Yang B, Bankir L (2005) Urea and urine concentrating ability: new insights from studies on mice. Am J Physiol Renal Physiol 288:F881–F896
59. You G, Smith CP, Kanai Y, Lee WS, Stelzner M, Hediger MA (1993) Cloning and characterization of the vasopressin-regulated urea transporter. Nature 365:844–847

Chapter 10
Extrarenal Phenotypes of the UT-B Knockout Mouse

Baoxue Yang, Xin Li, Lirong Guo, Yan Meng, Zixun Dong and Xuejian Zhao

Abstract The urea transporter UT-B is expressed in multiple tissues including erythrocytes, kidney, brain, heart, liver, colon, bone marrow, spleen, lung, skeletal muscle, bladder, prostate, and testis in mammals. Phenotype analysis of UT-B-null mice has confirmed that UT-B deletion results in a urea-selective urine-concentrating defect (see Chap. 9). The functional significance of UT-B in extrarenal tissues studied in the UT-B-null mouse is discussed in this chapter. UT-B-null mice present depression-like behavior with urea accumulation and nitric oxide reduction in the hippocampus. UT-B deletion causes a cardiac conduction defect, and TNNT2 and ANP expression changes in the aged UT-B-null heart. UT-B also plays a very important role in protecting bladder urothelium from DNA damage and apoptosis by regulating the urea concentration in urothelial cells. UT-B functional deficiency results in urea accumulation in the testis and early maturation of the male reproductive system. These results show that UT-B is an indispensable transporter involved in maintaining physiological functions in different tissues.

Keywords Urea transporters · Urea · Knockout mouse · Erythrocytes · Brain · Heart · Testes

B. Yang (✉)
State Key Laboratory of Natural and Biomimetic Drugs, Key Laboratory of Molecular Cardiovascular Sciences, Ministry of Education, Peking University, Beijing 100191, China
e-mail: baoxue@bjmu.edu.cn

B. Yang · X. Li · Z. Dong
Department of Pharmacology, School of Basic Medical Sciences, Peking University, Beijing 100191, China

L. Guo · Y. Meng · X. Zhao
Department of Pathophysiology, Norman Bethune College of Medicine of Jilin University, Changchun 130021, China

Erythrocyte

Mammalian erythrocytes have long been known to have a high permeability to urea [31, 36]. This is due to a high level of expression of UT-B in the erythrocyte plasma membrane [37, 40]. Urea permeability (P_{urea}) in UT-B-null erythrocytes is 45-fold lower than that in wild-type ones (1.1×10^{-6} cm/s, [48]). UT-B also transports water with a single channel water permeability of 7.5×10^{-14} cm^3/s, similar to that of aquaporin-1 (AQP1) [49, 50].

UT-B in erythrocytes has been proposed to potentially serve two different physiological functions in mammals [27]. First, it protects these cells from repeated osmotic stresses when they flow through the vasa recta in the renal medulla, where urea accumulates to concentrations 50- to 200-fold higher than that in peripheral plasma. With a high permeability to water mainly mediated by the water channel AQP1, erythrocytes would shrink dramatically when they penetrate in the inner medulla if their membrane were not also permeable to urea. Rapid urea transport helps preserve the osmotic stability and deformability of the erythrocytes [11, 30]. Second, it may also contribute to efficient urine concentration [2, 48]. Urine cannot be highly concentrated in the isolated kidney perfused without erythrocytes, which is restored by adding erythrocytes in the perfusate [25]. Rapid urea transport through UT-B in erythrocytes may help build the urine concentration gradient. The erythrocytes offer urea for countercurrent exchange between ascending vasa recta and arterial descending vasa recta through UT-B.

Erythrocyte number and hematocrit are similar in UT-B-null mice and wild-type mice. The mean size of erythrocytes is not significantly different between UT-B-null and wild-type mice. The morphology is also similar in erythrocytes from mice of the two genotypes [50]. However, the physiological significance of UT-B in erythrocytes still needs further experimental studies.

Brain

UT-B mRNA is transcribed in olfactory bulb, cortex, caudate nucleus, hippocampus, and hypothalamus [26]. UT-B is mainly expressed in astrocytes and ependymal cells. Other types of brain cells, including oligodendrocytes, microglia, and endothelial cells of blood vessels in the blood–brain barrier (BBB) are devoid of UT-B [3]. There is no UT-B mRNA or protein expression in the brain of UT-B knockout mice.

Urea is a by-product during polyamine synthesis in the brain [1, 34]. UT-B deletion induces urea levels significantly higher in some regions than those in UT-B heterozygous mice including cortex and hypothalamus, except for the olfactory bulb. Hippocampus, one of the several limbic brain structures implicated in the pathophysiology of mood disorders, presents high urea concentration. There may be two sources for the high level of urea in the UT-B-null hippocampus: diffusion of blood urea and urea synthesis in the brain.

Open field test, in which locomotor activity was recorded for 30 min, showed that UT-B-null mice exhibited lower central/peripheral locomotion ratio than heterozygous mice. UT-B-null mice exhibited longer duration of passive immobility than heterozygous mice in a forced swim test. Sucrose preference was significantly lower in UT-B-null mice than that in heterozygous mice by 20 %. These results suggest that UT-B deletion caused depression-like behavior [26]. Experiments show no difference in latency between UT-B-null mice and heterozygous mice in both buried food pellet discovery and olfaction maze test, which indicates that no abnormal olfaction is found in UT-B-null mice. UT-B-null mice have a normal urea level in the olfactory bulb.

The hippocampus is observed to have a normal structure and morphology, except for a lower cell density in CA3 and CA4 regions in UT-B-null mice, by Nissl-stained sections and electron microscopy. Electron microscopy shows that the UT-B-null hippocampus has markedly sparse regions with vacuolar changes, as well as membranous myelin-like structure formation within myelinated and unmyelinated fibers, which implicates swelling of the fibers and degeneration of membrane structures (Fig. 10.1). Nuclear dissolution in neurons with normal perikaryon and swelling of astrocytes occasionally appeared in UT-B-null mice. The micromorphologic changes indicate the degeneration of membrane structures, especially mitochondria, and defective axoplasmic transport in the nerve fibers that influenced the conduction velocity. Alterations in white matter structure have been observed in a wide range of psychiatric disorders. White matter is considered as a contributing cause of many disorders affecting mood or cognition due to disruptions in functional connectivity between distant brain regions [12]. The ultrastructural defects of the fibers may cause depression in UT-B-null mice.

The molecular mechanism, in which UT-B deletion causes depression-like behavior, may be correlative with the NOS/NO system. Urea has been reported to regulate the NOS/NO system. In the central nervous system, NO plays an important role in schizophrenia, major depression, and bipolar disorders. A nearly 73 % decrease in nitrite content is present in the brain of schizophrenic patients

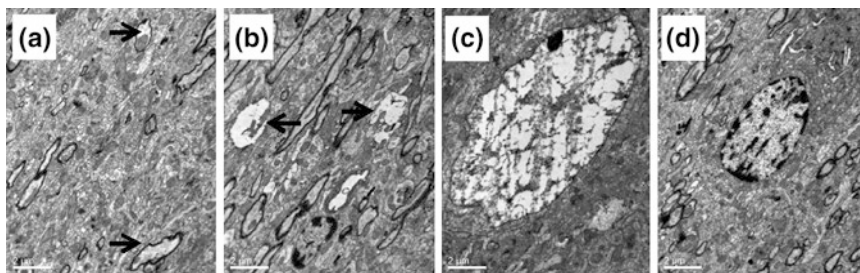**Fig. 10.1** Subcellular structures of hippocampus observed in UT-B-null mice by transmission electron microscope. **a** Swelling of myelinated fibers with myelin figure (*arrowhead*). **b** Swelling of unmyelinated fibers with myelin figure (*arrowhead*). **c** Nuclear dissolution of neuron with normal perikaryons. **d** Slight swelling of astrocyte presented in UT-B-null mice. Scale bars, 2 μm. Adapted from [26]

compared with the healthy controls [43]. NO production in the hippocampus was inhibited by the antidepressant fluoxetine in an animal model of chronic mild stress that mimics human depression [28]. Furthermore, nNOS reduces 5-HT transporter activity in vivo, while 5-HT uptake stimulates nNOS activity and NO production [5, 13]. Uremic levels of urea entering cells via the urea transporter can inhibit L-Arginine (L-Arg) transport into endothelial cells [47], while this effect can be abolished by the urea transporter inhibitor phloretin [46]. Lower NO production in the hippocampus was observed after an acute urea load in both UT-B-null and heterozygous mice. There was no difference in NO content in blood, cortex, and hypothalamus between UT-B-null mice and heterozygous mice. nNOS protein expression increases significantly in the hippocampus from UT-B-null mice, but no difference was detected in eNOS and iNOS expression. These results reveal that up-regulation of nNOS induced by long-term high urea levels in the UT-B-null hippocampus may contribute to the feedback effect of NO reduction caused by L-Arg transport inhibition, which may be related to depression-like behavior (Fig. 10.2).

NO is also an important factor regulating cerebral blood flow (rCBF) and cell viability. Decreased NO production could contribute to the reduced prefrontal blood flow in schizophrenia and depressed patients [20]. rCBF is an important index of the neural basis of schizophrenia. Depressed patients showed significantly lower rCBF values in the left and right superior frontal cortex and left anterior cingulate cortex [16]. UT-B-null mice show a long-lasting significant decrease in rCBF by ~20 % compared with heterozygous mice, which corresponds to the "vascular depression" hypothesis [44].
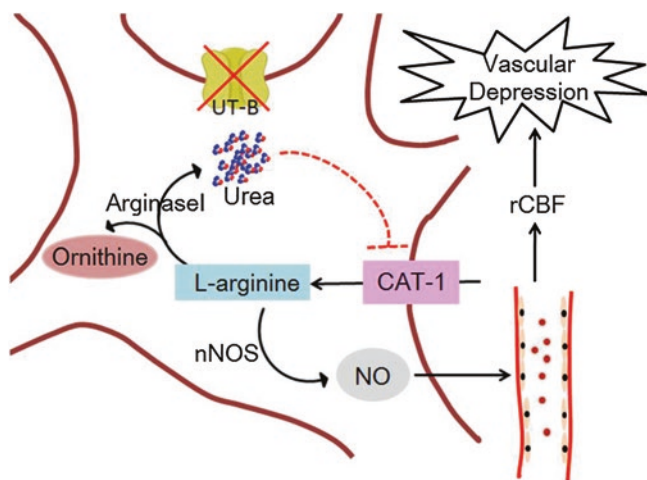

Fig. 10.2 Proposed mechanism of urea/L-Arg/NO pathway for depression-like behavior in UT-B-null mice. Urea accumulation in hippocampus due to UT-B deficiency probably decreases NO production, which causes depression-like behavior

Heart

UT-B is expressed in the heart. Surface electrocardiogram (ECG) recording shows that UT-B-null mice have a significantly prolonged P-R interval at 6–52 weeks of age [32], suggesting that the impetus of atrium cordis spread through the atrioventricular junction to the ventricles is delayed. Some aged UT-B-null mice (52 weeks old) develop atrial ventricular heart block types II and III, which indicates that UT-B deletion can induce progressive heart block. About 20 % of UT-B-null mice have a second-degree cardiac conduction block at 52 weeks of age.

Comparative proteomic analysis of the myocardial proteins showed that nine proteins were up-regulated, and one protein was down-regulated from UT-B-null mice compared to wild-type mice [51]. These proteins are mainly involved in cardiac muscle function, cellular energy metabolism, ion channel function, and oxidative stress.

Proteomic analysis shows that the expression of TNNT2 is significantly up-regulated in 16-week-old UT-B-null mice but down-regulated in 52-week-old UT-B-null mice compared to the same-aged wild-type mice. Intriguingly, the level of TNNT2 in 52-week-old UT-B-null mice is similar to that in 16-week-old wild-type mice. These data indicate that TNNT2 may be involved in the development of cardiac conduction defects. TNNT2 is a subunit of cardiac troponin that plays an important role in many heart diseases and renal diseases, which acts as a Ca^{2+} sensor and affects the contractility of myocardium [15, 38]. However, the mechanism how TNNT2 is involved in the cardiac conduction block remains to be studied.

Natriuretic peptides, a group of naturally occurring substances, act in the body to oppose the activity of the renin–angiotensin system and regulate cardiovascular homeostasis through diuretic, natriuretic, and vasodilatory properties. Three endogenous ligands are involved in the natriuretic peptide system including brain natriuretic peptide (BNP) and C-type natriuretic peptide (CNP). A-type natriuretic peptide (ANP) is synthesized in the atria [6] and has drawn particular attention because of its effects on blood pressure regulation, cardiac function, and cardiovascular risk [35]. ANP is also analyzed as the gold standard of cardiac hypertrophy. No difference is detected in the expression level of ANP between the 16-week-old and 52-week-old wild-type mice. Interestingly, the ANP is especially up-regulated in 52-week-old UT-B-null mice (with the second-degree cardiac conduction block) compared to 16-week-old UT-B-null mice (with the first-degree cardiac conduction block) and 52-week-old wild-type mice (without cardiac conduction block), which suggests that the change in ANP level might be associated with the late cardiac conduction block. Therefore, the modulation of ANP in UT-B-null mice indicates that cardiac hypertrophy may be involved in the mechanism of heart block in mice.

Bladder

UT-B is abundantly expressed in bladder urothelium. As bladder is a transit and storage organ for urine in mammals, bladder urothelial cells are exposed to high osmolality and high urea concentrations all the time. Urea is highly concentrated

within the urine that is stored in bladder. It was hard to understand why UT-B is highly expressed in urothelium [41] since it should be a barrier to keep concentrated urea in the bladder. The specific presence of UT-B may indicate urea is transported through bladder urothelium [42].

The tissue architecture of bladder urothelium appears the same in UT-B-null bladder as that in wide-type bladder under light microscopy. However, transmission electron microscope (TEM) analysis shows an increased myelin figure formation, mitochondrial swelling, and lysosome formation in UT-B-null urothelium, which may result from non-specific injuries (Fig. 10.3). Scattered shrunken urothelial cells with abnormally increased cytoplasmic electron density and chromatin condensation in UT-B-null bladder urothelium suggests an early stage of apoptosis.

Microarray assay of urothelium shows that 69 genes are significantly altered at the mRNA level in UT-B-null mice when contrasted with wild-type mice [7]. Among the genes, DDB1- and CUL4-associated factor 11 (Dcaf11) and minichromosome maintenance 2–4 (MCM2–4) were significantly up-regulated, and ubiquitin carboxy-terminal hydrolase L1 (Uch-L1), adenovirus E1B-19 K/Bcl-2 interacting protein 3 (Bnip3), and 45 S pre rRNA were down-regulated, which are related to apoptosis and DNA damage.

A TUNEL staining assay of bladder urothelium shows more TUNEL-positive cells from UT-B-null mice than wild-type mice. Apoptosis-related protein analysis demonstrates less Bcl-2, more Bax, and cleaved caspase-3 expression in UT-B-null bladder urothelium. Uch-L1, which encourages cell proliferation and boosts signaling pathways against apoptosis, is down-regulated in UT-B-null bladder urothelium. The results indicate that more apoptosis occurs in UT-B-null urothelium than in wild type.

Urea concentration in UT-B-null bladder urothelium is almost ninefold higher than in wild type. Acute urea loading can induce cell cycle delay and apoptosis [21]. Urea also leads oxidative stress in several cell types by the appearance of 8-oxoguanine lesions and single-strand breaks in genomic DNA [33]. In vitro study shows that urea induces apoptosis in T24 cells (a human urinary bladder
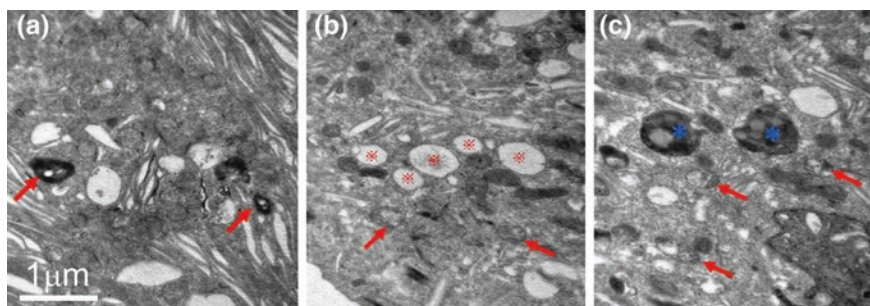

Fig. 10.3 Subcellular structures of urothelial cells in UT-B-null bladder observed by transmission electron microscopy. **a** Discoidal or fusiform-shaped vesicles and heavily stained myelin figure (*arrows*). **b** Swollen mitochondria (*arrows*) in cytoplasm. **c** Swollen mitochondria (*arrows*) and lysosomes (*asterisk*) in cytoplasm. Adapted from [7]

epithelial cell line) as demonstrated by the decreased number of annexin V−/PI− cells (live cells) and the increased number of annexin V+/PI+ cells (late apoptotic cells). Urea significantly induced cell apoptosis in a dose-dependent manner.

Urea is generated from arginine by arginase catalyses. Arginase also provides ornithine, the substrate for polyamine synthesis [9, 52]. Arginase I expression is remarkably decreased, whereas arginase II expression is unchanged in UT-B-null urothelium. This change may result from high urea concentrations in the UT-B-null urothelium. Arginase I colocalizes with ornithine decarboxylase (ODC) in the cytosol, which may preferentially direct ornithine to the polyamine pathway. The down-regulation of arginase I indicates that the formation of the downstream products, ornithine and polyamines, may be reduced. Some studies have found that polyamines, particularly spermine, are involved in the regulation of gene expression, the stabilization of chromatin, and the protection from endonuclease-mediated DNA fragmentation [9, 18, 19]. The level of NO is significantly higher in UT-B-null mouse bladder urothelium compared to wild type [7]. iNOS protein expression is dramatically induced in UT-B-null urothelium, while the expression of eNOS and nNOS is hardly detectable in the urothelium of both genotypes. NO is involved in collateral reactions and leads to DNA damage and cell death in both NO-generating and neighboring cells [29], and the mechanism may be the inhibition of ODC, which then reduces polyamine production. Arginase competes with NOS for the common substrate L-Arg, therefore, regulating and competitively inhibiting each other [9].These results indicate that the high urea concentration in UT-B-null bladder urothelium may lead to unbalanced arginine metabolism. Accumulation of urea induces a shift from the polyamine pathway to the NO pathway, which causes DNA damage and apoptosis (Fig. 10.4).
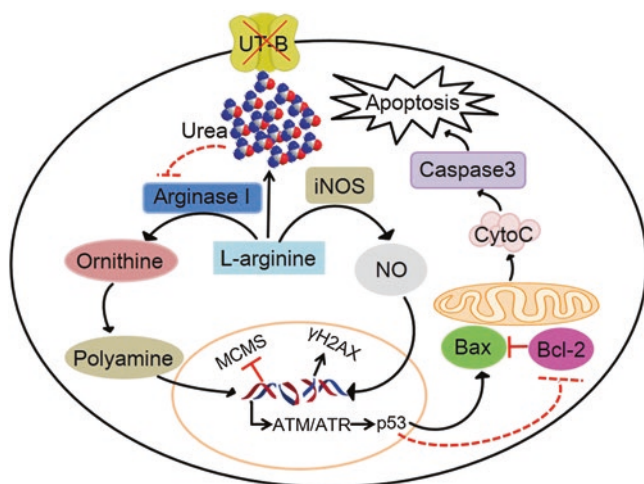

Fig. 10.4 The hypothesis of DNA damage and apoptosis in UT-B-null bladder epithelial cells. High urea concentrations may lead to unbalanced arginine metabolism. Accumulation of urea induces a shift from the polyamine pathway to the NO pathway, which causes DNA damage and apoptosis

UT-B deletion induces bladder urothelium DNA damage with up-regulation of phosphorylation of histone (H2AX), one of the earliest indicators of DNA damage, and down-regulation of MCM2, an important component of the MCM2-7 complex that functions at the DNA replication fork in response to single/double-stranded breaks after DNA damage. Moreover, phosphorylation of ataxia telangiectasia mutated (ATM) kinase at Ser1981 and both p53 expression and phosphorylation at Ser15 were significantly elevated in UT-B-null urothelium. These results demonstrate that functional loss of UT-B in bladder urothelium causing DNA damage and apoptosis depends on ATM-p53 pathway.

DNA damage and apoptosis induced by UT-B deletion are not related to ERK signaling and autophagy in bladder urothelial cells. There is no difference in ERK protein expression and phosphorylation levels between UT-B-null urothelium and wild-type urothelium. No conversion from LC3A to LC3B was detected, which is the characteristic of autophagosome.

Multiple factors could independently or together account for DNA damage and apoptosis of bladder urothelial cells. High urea concentrations induced by UT-B deletion may change multiple biological activities by destroying hydrophobic bonds of protein structure or causing protein carbamylation [4, 39, 53].

Testis

UT-B is expressed in Sertoli cells from stage II–III seminiferous tubules [10, 45]. UT-B in cells locates at the periphery of seminiferous tubules, with expression diminished toward the center of the lumen, indicating that these cells lose UT-B protein as they mature [8]. Sertoli cells in seminiferous tubules have high arginase activity to hydrolyze arginine into urea and ornithine. Thus, a large amount of urea is produced by Sertoli cells. Sertoli cells also form a blood–seminiferous tubule barrier to keep the unique microenvironment for spermatogenesis. UT-B is responsible for transporting urea across the seminiferous tubules in order to facilitate the exit of urea [10, 45].

The urea concentration in testis tissue is significantly higher in UT-B-null mice than wild-type mice under basal conditions, which may result from inhibition of urea exit from Sertoli cells in UT-B-null mice. The difference in testis urea concentration between genotypes becomes more significant with older age. UT-B-null mice also have greater testis weight than wild-type mice from 17 days of age. The time to first appearance of elongated sperm in the testis and the first breeding episode in a competing mate test show that spermatogenesis and fertilizing ability occur 8 days earlier in UT-B-null male mice than in wild-type male mice (Fig. 10.5), which suggests UT-B deletion results in early maturation in the male reproductive system [17].

To determine the velocity of urea distribution, [14C] urea was injected intravenously into both wild-type and UT-B-null mice, and [14C] urea radioactivity in the serum, brain, liver, spleen, and testis was measured 5 min after injection. [14C] urea in testes

Fig. 10.5 Breeding performance of maturing male mice. Male mice at 35 days of age were housed with 70-day-old wild-type female mice. Data are shown for 7 pairs of competing mates (*left*) and 7 pairs of wild-type controls (*right*) and are means $\pm$SE. *M* male; *F* female. Adapted from [17]

from UT-B-null mice is significantly lower than that from wild-type mice, which indicates that UT-B deletion blocks urea transport through the blood–testis barrier.

Histological examination of the testis shows no significant differences in the morphology or distribution of stages of spermatogenesis in all seminiferous tubules of adult UT-B-null mice and adult wild-type mice. The cellular integrity of the seminiferous epithelium also appears normal in UT-B-null mice. Tubular and luminal diameters of seminiferous tubules were similar in UT-B-null and wild-type males. No obvious difference is detected in sperm numbers in cauda epididymis from UT-B-null mice and wild-type mice.

Follicle-stimulating hormone receptor (FSHR) and androgen-binding protein (ABP) expressed in testis are related to Sertoli cell development and function [14, 22]. FSHR is specifically expressed in testicular Sertoli cells and ovarian granulose cells. FSH binds to FSHR on Sertoli cells and stimulates Sertoli cells to produce ABP. FSHR signaling pathways are required for Sertoli cell function and testicular development [22, 23]. Decreases in testicular weight have been reported in FSH-β-deficient mice and FSHR knockout mice [23, 24]. ABP produced by Sertoli cells is considered to be essential for maintaining qualitative and quantitative spermatogenesis. Both FSHR and ABP mRNA expression levels are significantly higher in testis from UT-B-null mice than wild-type mice at 10 days of age and then decrease subsequently. Peak values of FSHR and ABP mRNA expression occur in UT-B-null mice at 10 days of age, 1 week earlier than wild-type mice, which indicates earlier Sertoli cell development in UT-B-null mice.

References

1. Arnt-Ramos LR, O'Brien WE, Vincent SR (1992) Immunohistochemical localization of argininosuccinate synthetase in the rat brain in relation to nitric oxide synthase-containing neurons. Neuroscience 51:773–789

2. Bankir L, Chen K, Yang B (2004) Lack of UT-B in vasa recta and red blood cells prevents urea-induced improvement of urinary concentrating ability. Am J Physiol Renal Physiol 286:F144–F151

3. Berger UV, Tsukaguchi H, Hediger MA (1998) Distribution of mRNA for the facilitated urea transporter UT3 in the rat nervous system. Anat Embryol (Berl) 197:405–414

4. Bheda A, Shackelford J, Pagano JS (2009) Expression and functional studies of ubiquitin C-terminal hydrolase L1 regulated genes. PLoS ONE 4:e6764

5. Chanrion B, Mannoury la Cour C, Bertaso F, Lerner-Natoli M, Freissmuth M, Millan MJ, Bockaert J, Marin P (2007) Physical interaction between the serotonin transporter and neuronal nitric oxide synthase underlies reciprocal modulation of their activity. Proc Natl Acad Sci USA 104:8119–8812

6. Cho Y, Somer BG, Amatya A (1999) Natriuretic peptides and their therapeutic potential. Heart Dis 1:305–328

7. Dong Z, Ran J, Zhou H, Chen J, Lei T, Wang W, Sun Y, Lin G, Bankir L, Yang B (2013) Urea transporter UT-B deletion induces DNA damage and apoptosis in mouse bladder urothelium. PLoS ONE 8:e76952

8. Doran JJ, Klein JD, Kim YH, Smith TD, Kozlowski SD, Gunn RB (2006) Tissue distribution of UT-A and UT-B mRNA and protein in rat. Am J Physiol Regul Integr Comp Physiol 290:R1446–R1459

9. Durante W, Johnson FK, Johnson RA (2007) Arginase: a critical regulator of nitric oxide synthesis and vascular function. Clin Exp Pharmacol Physiol 34:906–911

10. Fenton RA, Cooper GJ, Morris ID, Smith CP (2002) Coordinated expression of UT-A and UT-B urea transporters in rat testis. Am J Physiol Cell Physiol 282:C1492–C1501

11. Fenton RA, Flynn A, Shodeinde A, Smith CP, Schnermann J, Knepper MA (2005) Renal phenotype of UT-A urea transporter knockout mice. J Am Soc Nephrol 16:1583–1592

12. Fields RD (2008) White matter in learning, cognition and psychiatric disorders trends. Neuroscience 31:361–370

13. Garthwaite J (2007) Neuronal nitric oxide synthase and the serotonin transporter get harmonious. Proc Natl Acad Sci USA 104:7739–7740

14. Gerard A (1995) Endocytosis of androgen-binding protein (ABP) by spermatogenic cells. J Steroid Biochem Mol Biol 53:533–542

15. Gomes AV, Potter JD (2004) Molecular and cellular aspects of troponin cardiomyopathies. Ann NY Acad Sci 1015:214–224

16. Gonul AS, Kula M, Bilgin AG, Tutus A, Oguz A (2004) The regional cerebral blood flow changes in major depressive disorder with and without psychotic features. Prog Neuropsychopharmacol Biol Psychiatry 28:1015–1021

17. Guo L, Zhao D, Song Y, Meng Y, Zhao H, Zhao X, Yang B (2007) Reduced urea flux across the blood-testis barrier and early maturation in the male reproductive system in UT-B-null mice. Am J Physiol Cell Physiol 293:C305–C312

18. Khan AU, Di Mascio P, Medeiros MH, Wilson T (1992) Spermine and spermidine protection of plasmid DNA against single-strand breaks induced by singlet oxygen. Proc Natl Acad Sci USA 89:11428–11430

19. Khan AU, Mei YH, Wilson T (1992) A proposed function for spermine and spermidine: protection of replicating DNA against damage by singlet oxygen. Proc Natl Acad Sci USA 89:11426–11427

20. Kim JJ, Mohamed S, Andreasen NC, O'Leary DS, Watkins GL, Boles Ponto LL, Hichwa RD (2000) Regional neural dysfunctions in chronic schizophrenia studied with positron emission tomography. Am J Psychiatry 157:542–548

21. Kraus LM, Kraus AP Jr (2001) Carbamoylation of amino acids and proteins in uremia. Kidney Int Suppl 78:S102–S107
22. Krishnamurthy H, Babu PS, Morales CR, Sairam MR (2001) Delay in sexual maturity of the follicle-stimulating hormone receptor knockout male mouse. Biol Reprod 65:522–531
23. Krishnamurthy H, Danilovich N, Morales CR, Sairam MR (2000) Qualitative and quantitative decline in spermatogenesis of the follicle-stimulating hormone receptor knockout (FORKO) mouse. Biol Reprod 62:1146–1159
24. Kumar TR, Low MJ, Matzuk MM (1998) Genetic rescue of follicle-stimulating hormone beta-deficient mice. Endocrinology 139:3289–3295
25. Lieberthal W, Stephens GW, Wolf EF, Rennke HG, Vasilevsky ML, Valeri CR, Levinsky NG (1987) Effect of erythrocytes on the function and morphology of the isolated perfused rat kidney. Ren Physiol 10:14–24
26. Li X, Ran J, Zhou H, Lei T, Zhou L, Han J, Yang B (2012) Mice lacking urea transporter UT-B display depression-like behavior. J Mol Neurosci 46:362–372
27. Liu L, Lei T, Bankir L, Zhao D, Gai X, Zhao X, Yang B (2011) Erythrocyte permeability to urea and water: comparative study in rodents, ruminants, carnivores, humans, and birds. J Comp Physiol B 181:65–72
28. Luo L, Tan RX (2001) Fluoxetine inhibits dendrite atrophy of hippocampal neurons by decreasing nitric oxide synthase expression in rat depression model. Acta Pharmacol Sin 22:865–870
29. Luperchio S, Tamir S, Tannenbaum SR (1996) NO-induced oxidative stress and glutathione metabolism in rodent and human cells. Free Radic Biol Med 21:513–519
30. Macey RI, Yousef LW (1988) Osmotic stability of red cells in renal circulation requires rapid urea transport. Am J Physiol 254:C669–C674
31. Mayrand RR, Levitt DF (1983) Urea and ethylene glycol-facilitated transport systems in the human red cell membrane saturation, competition, and asymmetry. J Gen Physiol 81:221–237
32. Meng Y, Zhao C, Zhang X, Zhao H, Guo L, Lu B, Zhao X, Yang B (2009) Surface electrocardiogram and action potential in mice lacking urea transporter UT-B. Sci China C Life Sci 52:474–478
33. Michea L, Ferguson DR, Peters EM, Andrews PM, Kirby MR, Burg MB (2000) Cell cycle delay and apoptosis are induced by high salt and urea in renal medullary cells. Am J Physiol Renal Physiol 278:F209–F218
34. Ratner S, Morell H, Carvalho E (1960) Enzymes of arginine metabolism in brain. Arch Biochem Biophys 91:280–289
35. Rubattu S, Sciarretta S, Valenti V, Stanzione R, Volpe M (2008) Natriuretic peptides: an update on bioactivity, potential therapeutic use, and implication in cardiovascular diseases. Am J Hypertens 21:733–741
36. Sha'afi RI, Gary-Bobo CM (1973) Water and nonelectrolytes permeability in mammalian red cell membranes. Prog Biophys Mol Biol 26:103–146
37. Sands JM (2002) Molecular approaches to urea transporters. J Am Soc Nephrol 13:2795–2806
38. Sehnert AJ, Huq A, Weinstein BM, Walker C, Fishman M, Stainier DY (2002) Cardiac troponin T is essential in sarcomere assembly and cardiac contractility. Nat Genet 31:106–110
39. Singh R, Ali Dar T, Ahmad S, Moosavi-Movahedi AA, Ahmad F (2008) A new method for determining the constant-pressure heat capacity change associated with the protein denaturation induced by guanidinium chloride (or urea). Biophys Chem 133:81–89
40. Smith CP, Rousselet G (2001) Facilitative urea transporters. J Membr Biol 183:1–14
41. Spector DA, Yang Q, Liu J, Wade JB (2004) Expression, localization, and regulation of urea transporter B in rat urothelia. Am J Physiol Renal Physiol 287:F102–F108
42. Spector DA, Yang Q, Wade JB (2007) High urea and creatinine concentrations and urea transporter B in mammalian urinary tract tissues. Am J Physiol Renal Physiol 292:F467–F474

43. Srivastava N, Barthwal MK, Dalal PK, Agarwal AK, Nag D, Seth PK, Srimal RC, Dikshit M (2002) A study on nitric oxide, beta-adrenergic receptors and antioxidant status in the poly-morphonuclear leukocytes from the patients of depression. J Affect Disord 72:45–52

44. Thomas AJ, O'Brien JT, Davis S, Ballard C, Barber R, Kalaria RN, Perry RH (2002) Ischemic basis for deep white matter hyperintensities in major depression: a neuropathological study. Arch Gen Psychiatry 59:785–792

45. Tsukaguchi H, Shayakul C, Berger UV, Tokui T, Brown D, Hediger MA (1997) Cloning and characterization of the urea transporter UT3: localization in rat kidney and testis. J Clin Invest 99:1506–1515

46. Wagner L, Klein JD, Sands JM, Baylis C (2002) Urea transporters are distributed in endothelial cells and mediate inhibition of L-arginine transport. Am J Physiol Renal Physiol 283:F578–F582

47. Xiao S, Wagner L, Mahaney J, Baylis C (2001) Uremic levels of urea inhibit L-arginine transport in cultured endothelial cells. Am J Physiol Renal Physiol 280:F989–F995

48. Yang B, Bankir L, Gillepsie A, Epstein CJ, Verkman AS (2002) Urea-selective concentrating defect in transgenic mice lacking urea transporter UT-B. J Biol Chem 277:10633–10637

49. Yang B, Ma T, Verkman AS (2001) Erythrocyte water permeability and renal function in double knockout mice lacking aquaporin-1 and aquaporin-3. J Biol Chem 276:624–628

50. Yang B, Verkman AS (2002) Analysis of double knockout mice lacking aquaporin-1 and urea transporter UT-B: evidence for UT-B facilitated water transport in erythrocytes. J Biol Chem 277:36782–36786

51. Yu H, Meng Y, Wang LS, Jin X, Gao LF, Zhou L, Ji K, Li Y, Zhao LJ, Chen GQ, Zhao XJ, Yang B (2009) Differential protein expression in heart in UT-B null mice with cardiac conduction defects. Proteomics 9:504–511

52. Zhang Z, Dmitrieva NI, Park JH, Levine RL, Burg MB (2004) High urea and NaCl carbonylate proteins in renal cells in culture and in vivo, and high urea causes 8-oxoguanine lesions in their DNA. Proc Natl Acad Sci USA 101:9491–9496

53. Zou Q, Habermann-Rottinghaus SM, Murphy KP (1998) Urea effects on protein stability: hydrogen bonding and the hydrophobic effect. Proteins 31:107–115

Chapter 11
Small-Molecule Inhibitors of Urea Transporters

Alan S. Verkman, Cristina Esteva-Font, Onur Cil, Marc O. Anderson, Fei Li, Min Li, Tianluo Lei, Huiwen Ren and Baoxue Yang

Abstract Urea transporter (UT) proteins, which include isoforms of UT-A in kidney tubule epithelia and UT-B in vasa recta endothelia and erythrocytes, facilitate urinary concentrating function. Inhibitors of urea transporter function have potential clinical applications as sodium-sparing diuretics, or 'urearetics,' in edema from different etiologies, such as congestive heart failure and cirrhosis, as well as in syndrome of inappropriate antidiuretic hormone (SIADH). High-throughput screening of drug-like small molecules has identified UT-A and UT-B inhibitors with nanomolar potency. Inhibitors have been identified with different UT-A versus UT-B selectivity profiles and putative binding sites on UT proteins. Studies in rodent models support the utility of UT inhibitors in reducing urinary concentration, though testing in clinically relevant animal models of edema has not yet been done.

Keywords Urea transporters · Diuretic · Kidney · High-throughput screening

Baoxue Yang—Co-corresponding author.

A.S. Verkman (✉) · C. Esteva-Font · O. Cil
Departments of Medicine and Physiology, University of California, San Francisco, CA 94143-0521, USA
e-mail: alan.verkman@ucsf.edu

M.O. Anderson
Department of Chemistry and Biochemistry, San Francisco State University, San Francisco, CA, USA

F. Li · M. Li · T. Lei · H. Ren · B. Yang
Department of Pharmacology, School of Basic Medical Sciences, Peking University, Beijing 100191, China

B. Yang
State Key Laboratory of Natural and Biomimetic Drugs, Key Laboratory of Molecular Cardiovascular Sciences, Ministry of Education, Peking University, Beijing 100191, China
e-mail: baoxue@bjmu.edu.cn

Introduction

Urea transporter (UT) proteins facilitate the passive transport of urea across the plasma membrane in certain cell types. The involvement of UTs in the generation of concentrated urine by the kidney is the major role of UTs [3, 6, 7, 22, 30]. Urinary concentration involves a countercurrent multiplication mechanism, which is facilitated by aquaporins, the NKCC2 ($Na^+/K^+/2Cl^-$ cotransporter) in the thick ascending limb of the loop of Henle, and urea transporters in tubule epithelia and vasa recta endothelia [20, 24]. On theoretical grounds, loss of UT function is predicted to disrupt urinary concentrating ability [3, 30]

As reviewed in Chap. 5, epithelial cells in kidney tubules express isoforms of UT-A, encoded by the SLc14A2 gene, and endothelial cells in vasa recta express UT-B, encoded by the SLc14A1 gene [4, 10, 21, 25–28]. As diagrammed in Fig. 9.1, UT-A1 and UT-A3 are expressed in kidney inner medullary collecting duct, with UT-A1 at the luminal membrane and UT-A3 at the basolateral membrane [10]. UT-A2 is expressed in thin descending limb of the loop of Henle [10]. Knockout mice lacking both UT-A1 and UT-A3 manifest a marked urinary concentrating defect, in large part because of impaired urea transport from tubular fluid in the inner medullary collecting duct to the medullary interstitium [8, 9]. Interestingly, urinary concentrating function is unimpaired in UT-A2 knockout mice [29] and in UT-A1/A3 knockout mice after transgenic replacement of UT-A1 [14]. Knockout mice lacking UT-B [2, 15, 31], and rare humans with loss of function mutations in UT-B [13, 23], which is the erythrocyte Jk antigen, manifest a relatively mild urinary concentrating defect.

This chapter is focused on small-molecule UT inhibitors. Applications of UT inhibitors include research tools and potential drug development candidates. Selective, potent UT inhibitors can be advantageous over gene knockout to study UT functions because of potential confounding compensatory in knockout mice, such as changes in expression of non-UT proteins. As discussed further below, UT inhibitors have potential clinical applications in edema and syndrome of inappropriate antidiuretic hormone (SIADH). Until recently, available UT inhibitors included the non-selective membrane-intercalating agent phloretin and chemical analogs of urea, such as dimethylthiourea, which have millimolar potency [19, 35]. The discovery and characterization of nanomolar-potency small-molecule UT inhibitors is reviewed in this chapter.

Methods to Assay Urea Transport

Older Assays of Urea Transport

Assays of urea transport rely on measurements of urea movement across cell membranes or cell layers, or secondary effects of urea movement on water transport and hence on cell or vesicle/liposome volume. For example, transport of urea

across an epithelial cell monolayer grown on a porous filter has been measured from the kinetics of urea appearance on the trans-side of the filter following addition of urea to one side of the filter [11]. Urea concentration measurement requires fluid sampling and an enzymatic, urease-based colorimetic assay, as to date there is no optical indicator of urea concentration. Radiolabeled urea (^{14}C-urea) can be used in place of chemical urea, as used in some older measurements [19, 32]. A similar approach can be used to measure urea transport across cell plasma membranes; however, the rapid urea equilibration time makes the separation of cells from the extracellular solution very challenging. Measurement of secondary cell volume changes in response to urea movement in water-permeable cells can be accomplished by a variety of methods [33], volume-dependent light scattering of small cells such as erythrocytes or membrane vesicles/liposomes being the most popular [11, 33]. Though some of these methods are quite accurate and quantitative, they are technically tedious and hence not suitable for automated high-throughput screening.

High-Throughput Assay of Urea Transport for UT-B Inhibitor Identification

The first high-throughput screening assay for identification of UT inhibitors utilized erythrocytes, which natively express UT-B [16]. The assay, as diagramed in Fig. 11.1a, involves a single-time-point readout of erythrocyte lysis by near-infrared light absorbance. Erythrocytes are preloaded with the urea analog acetamide, which is transported by UT-B at a rate such that the equilibration time for acetamide transport is comparable to that of osmotic water transport [35]. In the assay, imposing a large, outwardly directed gradient of acetamide causes cell swelling, which is limited by UT-B-facilitated acetamide efflux. UT-B inhibition slows acetamide efflux and increases cell lysis. However, the I_{max} values from the erythrocyte lysis assay are not absolute inhibition rates of urea transport, because of nonlinearity between acetamide permeability and percentage erythrocyte lysis rate, and differences between acetamide and urea in their transport by UT-B [35].

Conditions were optimized for high-throughput screening to give a robust assay with high sensitivity and a low false-positive rate, including empirical selection of the optimal acetamide loading concentration, mixing conditions, and wavelength for absorbance readout. Greater erythrocyte lysis is seen as reduced optical density at 710 nm (O.D.$_{710}$). The goodness of the optimized assay was evaluated by screening plates containing positive and negative controls (0 and 100 % lysis), which gave a good statistical Z'-factor of ~0.6 for the screen. As discussed further below, the erythrocyte lysis assay has been used successfully to identify inhibitors of human and rodent UT-B.

Stopped-flow light scattering is the gold standard for secondary analysis of UT-B inhibition and quantitative determination of IC$_{50}$ values. A suspension of erythrocytes is mixed rapidly (<1 ms) with a urea-containing solution to create
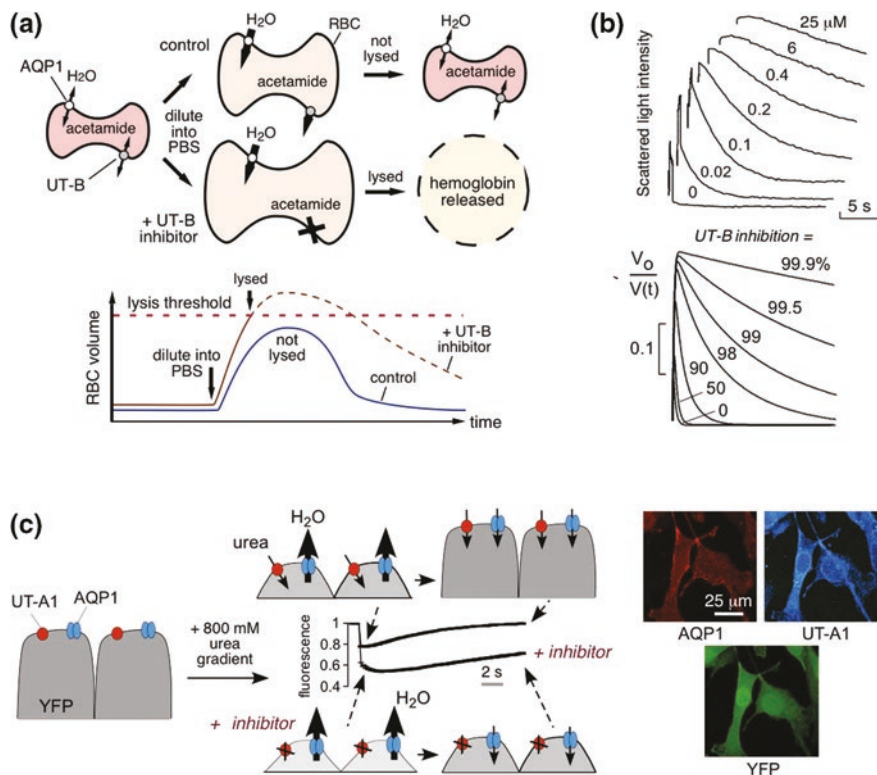
Fig. 11.1 Assays for high-throughput identification of small-molecule UT inhibitors. **a** Erythrocyte osmotic lysis assay for UT-B inhibitor discovery. Erythrocytes expressing water and urea channels (AQP1 and UT-B) are preloaded with the urea analog acetamide. Following replacement of the external buffer with urea/acetamide-free isomolar solution, water entry results in cell swelling, which is limited by UT-B-mediated urea/acetamide efflux. Under optimized assay conditions, UT-B-facilitated urea/acetamide prevents osmotic lysis, whereas UT-B inhibition impairs urea/acetamide exit resulting in substantial lysis. (*Bottom*) Biphasic cell volume changes in the lysis assay. Increased erythrocyte volume beyond a threshold results in lysis. The *dashed curve* shows the hypothetical time course of erythrocyte volume if lysis had not occurred. **b** (*Top*) Stopped-flow measurements of urea transport in human erythrocytes. Concentration–inhibition curves for indicated compounds determined by light scattering in response to a 100 mM inwardly directed urea gradient. (*Bottom*) Numerically simulated inhibitor concentration dependence used to determine IC_{50} from stopped-flow experiments. The inverse of normalized cell volume, $V_o/V(t)$, is plotted to approximate light scattering data at indicated percentages of urea transport inhibition. **c** (*Left*) Assay for UT-A1 inhibitors. MDCK cells stably expressing UT-A1, AQP1, and YFP-H148Q/V163S were subjected to an 800 mM inwardly directed urea gradient. A rapid decrease in cell volume (reduced fluorescence) due to the water efflux through AQP1 is followed by cell reswelling (increased fluorescence) due to urea and water influx. The UT-A1 inhibitor phloretin alters curve shape. (*Right*) UT-A1 and AQP1 immunofluorescence of the triply transfected cells, shown with YFP fluorescence. Adapted from [5, 16]

an inwardly directed urea gradient. A non-saturating concentration of urea is used to minimize competitive effects that would confound IC_{50} interpretation. The inwardly directed urea gradient causes initial osmotic water efflux and erythrocyte

cell shrinking, which is followed by coupled urea and water influx. Scattered light intensity at 90° provides a quantitative measure of cell volume. Figure 11.1b (top) shows light scattering curves for different concentrations of a UT-B inhibitor, showing progressive slowing of the phase of decreasing light scattering with increased inhibitor concentration. To deduce the percentage inhibition from the light scattering data, the results are compared with computational prediction that involves numerical integration of the Kedem–Katchalsky flux equations for coupled erythrocyte water and urea transport (Fig. 11.1b, bottom), as described [33].

High-Throughput Assay of Urea Transport for UT-A Inhibitor Identification

The challenges in the development of a high-throughput assay to identify UT-A inhibitors included the lack of easily obtained cell lines that natively express UT-A, the rapidity of UT-A-facilitated urea equilibration across cell membranes, and the difficulty in robust measurement of cell volume using an automated screening platform. As diagramed in Fig. 11.1c, our assay for identification of UT-A1 inhibitors involved measurement of cell volume changes in response to a rapidly imposed gradient of urea in MDCK cells stably expressing UT-A1 [5, 11]. Cell volume was followed using the chloride-sensing, genetically encoded fluorescent protein YFP-H148Q/V163S, which was developed previously for chloride channel screening [12]. Reduced cell volume concentrates intracellular chloride, producing a near-instantaneous reduction in YFP fluorescence. The cells also stably express a water channel (AQP1), so that osmotic water equilibration time is much faster than urea equilibration time. Figure 11.1c (right) shows fluorescence micrographs of the triply transfected cells used for screening, showing plasma membrane expression of AQP1 (red) and UT-A1 (blue), and cytoplasmic YFP expression (green). Addition of urea to the extracellular solution in a platereader format drives osmotic water efflux and cell shrinking, which is followed by urea (and water) entry with return to the original cell volume. A urea concentration gradient of 800 mM was chosen empirically to produce a robust fluorescence signal for screening. Original data from 96-well plates in Fig. 11.1c (center) show a robust difference in fluorescence curve shape with UT-A1 inhibition by phloretin. The same assay paradigm can be used for other UT isoforms, and because the fluorescence signal comes only from transfected cells, a transient transfection approach can be used in which AQP1-expressing cells are costably transfected with vectors encoding UT and YFP.

UT-B Inhibitors

An initial screen of 50,000 diverse, small-molecule drug-like compounds was done using human erythrocytes based on UT-B-facilitated acetamide transport as described in Fig. 11.1a. Primary screening yielded ~30 UT-B inhibitors belonging

to the phenylsulfoxyoxozole (Fig. 11.2a), benzenesulfonanilide, phthalazinamine, and aminobenzimidazole chemical classes [16]. Analysis of ~700 chemical analogs of these four scaffolds gave many active compounds, the most potent of which inhibited UT-B urea transport with IC_{50} ~10 nM, with ~100 % inhibition at higher concentrations. The compounds were characterized and used to confirm water transport through UT-B, which was reported in our earlier studies using erythrocytes from UT-B and UT-B/AQP1 knockout mice [33]. Though the potency of the best compound was excellent, it was not further developed because of its (i) relatively low potency for rodent UT-B, precluding testing in rodent models; (ii) high UT-B versus UT-A specificity, which is predicted to produce relatively minor benefit in vivo; and (iii) its rapid metabolism in hepatic microsomes, making it difficult to maintain therapeutic concentrations in vivo.

In a follow-on study, 100,000 compounds were screened using mouse erythrocytes with the goal of identifying potent inhibitors of rodent (and human) UT-B [34]. The screen produced triazolothienopyrimidine UT-B inhibitors, with the most potent
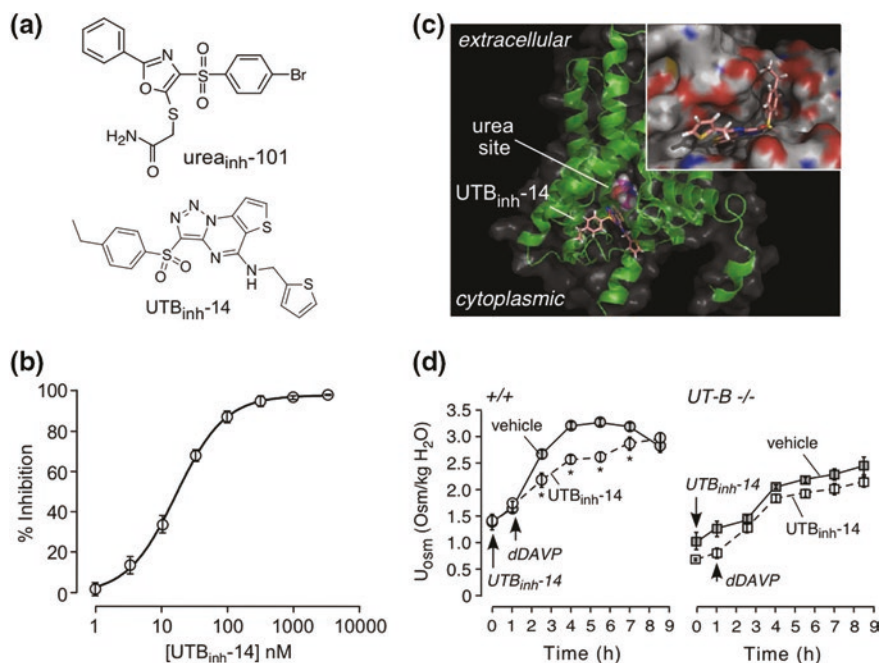
Fig. 11.2 UT-B inhibitor identification by high-throughput screening. **a** Chemical structures of two classes of UT-B inhibitors identified from screens. **b** Concentration–inhibition data with fit to single-site inhibition model. **c** Docking of UTB_{inh}-14 in a homology structural model of human UT-B showing UTB_{inh}-14 binding at the cytoplasmic surface. The computed site of urea analog methylurea (a urea analog) is shown. (*Inset*) Zoomed-in view of UTB_{inh}-14 bound in a groove at the UT-B channel region. **d** Urine osmolality in wild-type mice following dDAVP (1 μg/kg) and UTB_{inh}-14 (300 μg) (or vehicle) (mean ± S.E., 6 mice per group, * $P < 0.01$). Same protocol as in B, but in UT-B knockout mice. Adapted from [1, 34]

compound being 3-(4-ethyl-benzenesulfonyl)-thieno[2,3-e][1,2,3]triazolo[1,5-a]pyrimidin-5-yl]-thiophen-2-ylmethylamine (UTB$_{inh}$-14, Fig. 11.2a). A 5-step synthesis procedure for UTB$_{inh}$-14 was developed to generate highly pure compound for analytical and in vivo studies. UTB$_{inh}$-14 fully and reversibly inhibited urea transport with IC$_{50}$ of ~10 nM for human UT-B and ~25 nM for mouse UT-B (Fig. 11.2b). UTB$_{inh}$-14 was highly selective against UT-B versus UT-A isoforms. Competition studies showed reduced inhibition potency with increasing urea concentration, suggesting that UTB$_{inh}$-14 bound to the UT-B protein near the urea binding site, which was supported by homology modeling and molecular docking computations (Fig. 11.2c).

To study in vivo effects of UTB$_{inh}$-14 on urinary concentrating function, compound administration dose, route, and timing were established, from liquid chromatography/mass spectrometry assays, to maintain predicted therapeutic compound concentrations in blood, kidney, and urine [34]. Following intraperitoneal administration of UTB$_{inh}$-14 in mice to achieve therapeutic concentrations in kidney, urine osmolality following dDAVP in UTB$_{inh}$-14-treated mice was ~700 mosm/kg H$_2$O lower than in vehicle-treated mice (Fig. 11.2d). UTB$_{inh}$-14 did not significantly reduce urine osmolality in UT-B knockout mice, as expected. UTB$_{inh}$-14 also increased urine output and reduced osmolality in mice given free access to water. Though these data provided proof of concept for the potential utility of UT-B inhibition to reduce urinary concentration in a high-vasopressin state, the reduction in urine osmolality was relatively modest and similar to that conferred by UT-B gene deletion, supporting the greater importance of UT-A versus UT-B in urinary concentrating function.

Two medicinal chemistry studies were done to further optimize UTB$_{inh}$-14 properties, with focused investigation of structure–activity relationships with the goal of increasing UTB$_{inh}$-14 metabolic stability [1, 18]. Systematic chemical analysis indicated a major role of CH$_2$ hydroxylation in the ethyl substituent in UTB$_{inh}$-14 metabolic stability. By replacing the CH$_2$ hydrogens with fluorines in {3-[4-(1,1-difluoroethyl)-benzenesulfonyl]-thieno[2,3-e][1,2,3]triazolo[1,5-a]pyrimidin-5-yl}-thiophen-2-ylmethylamine, metabolic stability was ~40-fold improved with little effect on UT-B inhibition potency. The optimized UT-B inhibitor accumulated in kidney and urine in mice, and reduced maximum urinary concentration.

UT-A Inhibitors

The UT-A inhibition assay described in Fig. 11.1c was used to screen 100,000 synthetic small molecules for UT-A1 inhibition [5]. The screen was done on UT-A1 because it is predicted that this UT-A isoform is of the greatest importance for urinary concentration as it is the rate-limiting step in apical membrane urea transport in the inner medullary collecting duct and hence required to establish the hypermolar renal medullary interstitium. The initial screen produced four classes of compounds with low micromolar IC$_{50}$, with an example of a dose–response

study in Fig. 11.3a and chemical structures shown in Fig. 11.3b. Interestingly, the class D compounds have the same triazolothienopyrimidine scaffold as in UTB$_{inh}$-14. Approximately 500 analogs were tested to establish structure–activity relationships.

Each of the four chemical classes contained multiple active compounds with drug-like properties, including the presence of multiple hydrogen bond acceptors, as well as favorable molecular weight, aLogP, and topological polar surface areas. UT-A1 inhibition by each of the compound classes was reversible. Inhibition by compounds of classes A, B, and C was non-competitive, as judged from the minimal effect of urea concentration on apparent IC$_{50}$, whereas class D compounds showed partial competition with urea. Inhibition by compounds of classes A, B, and D occurred over several minutes, suggesting an intracellular site of action on UT-A1, whereas inhibition by class C compounds was very rapid, suggesting an extracellular site of action. An interesting finding was the identification of compounds with a wide range of UT-A1 versus UT-B selectivities, as shown in Fig. 11.3c. Even in the same chemical class, relatively minor chemical modifications produced compounds with very high selectivity and others with little UT-A1 versus UT-B selectivity.

Homology modeling and computational docking was done to investigate potential inhibitor binding sites and selectivity mechanisms. UT-A homology modeling was
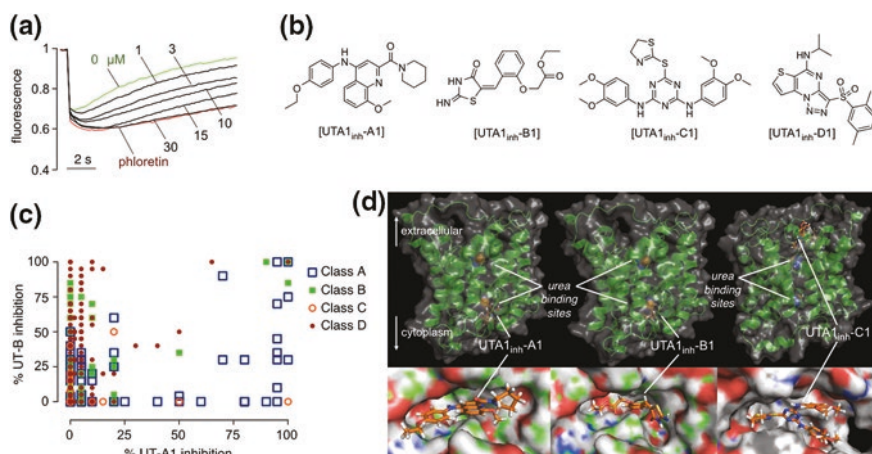
Fig. 11.3 UT-A1 inhibitor identification by high-throughput screening. **a** Concentration-dependent inhibition of UT-A1 urea transport by compound UTA1$_{inh}$-A1, using the primary screening assay described in Fig. 13.2c. **b** Chemical structures of UT-A1 inhibitors of four chemical classes. **c** UT-A1/UT-B selectivity. Percentage UT-B inhibition (*y*-axis) and UT-A1 inhibition (*x*-axis) for active compounds of four chemical classes tested at 25 μM. **d** Computational modeling of urea transporter—inhibitor interaction. Putative inhibitor binding sites in rat UT-A1 showing zoomed-in and zoomed-out representations of UTA1$_{inh}$-A1 (*left*) and UTA1$_{inh}$-B1 (*center*) bound to the UT-A1 cytoplasmic domain, and UTA1$_{inh}$-C1 (*right*) bound to the extracellular domain. Positions of putative urea binding sites deduced from homology modeling are indicated. Adapted from [5]

done using the homologous bovine UT-B bound to selenourea that was solved at 2.5 Å solution (PDB = 4EZD) [5]. Fig. 11.3d shows putative intracellular binding sites of class A and B inhibitors and an extracellular binding site for the class C inhibitors. While binding information based on homology models should be interpreted with caution, we note that docking computations were successful in identifying the most active inhibitors (comparing to tested analogs) for each of the class A, B, and D compounds, and the predicted order of class B compounds for UT-A1 inhibition potency from computation was in reasonable agreement with experimental data.

In Vivo Rat Studies

A compound (called PU-14) with thienoquinolin core structure was found to have inhibition activity on both UT-A and UT-B [17]. Figure 11.4a shows the chemical structure of the compound PU-14, 1-(3-amino-6-methylthieno [2, 3-b] quinolin-2-yl) ethanone. PU-14 inhibited human, rat, and mouse UT-B (Fig. 11.4b) as determined by the erythrocyte lysis assay. PU-14 did not change erythrocyte lysis rate in UT-B null mouse erythrocytes, as expected. PU-14 also inhibited UT-A1 (Fig. 11.4c) in an MDCK cell assay [11].
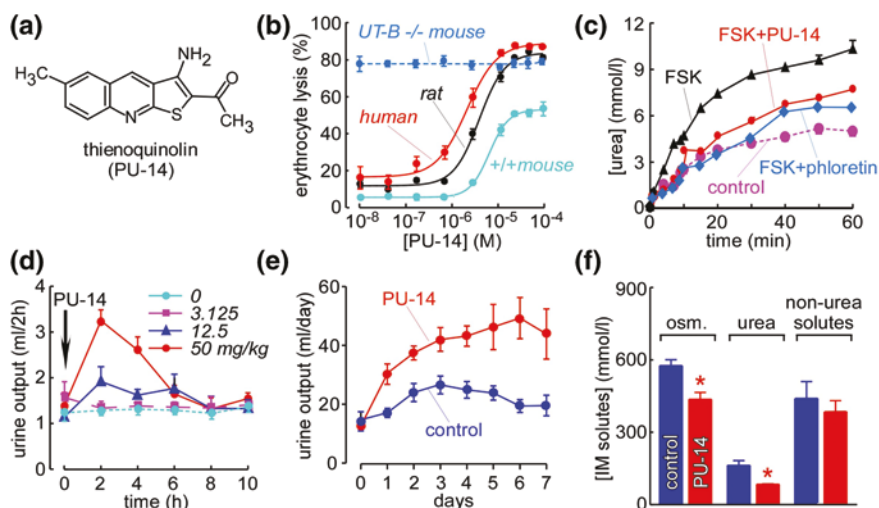
Fig. 11.4 Urea transporter inhibition and diuretic activity of thienoquinolin (PU-14). **a** Chemical structure of PU-14. **b** Dose-dependent UT-B inhibition of PU-14, determined by the erythrocyte osmotic lysis assay. **c** PU-14 of rat UT-A1 measured in stably transfected MDCK cells. Where indicated, phloretin (0.7 mM) or PU-14 (4 μM) was present. **d** Diuretic activity of PU-14. Rats were subcutaneously injected with indicated amounts of PU-14 just after a 2-h urine collection (time 0). Urine samples were collected every 2 h. **e** Long-term diuretic effect of PU-14. Rats were subcutaneously injected with PU-14 at 50 mg/kg for 7 days. **f** Concentration of osmoles, urea, and non-urea solutes in the inner medulla of rats without (control) or with PU-14 treatment fed water ad libitum. Adapted from [17]

To evaluate in vivo activity of PU-14 on urinary concentrating function, rats fed ad libitum were studied in metabolic cages. Urine output significantly increased in a dose-dependent manner in rats subcutaneously administered PU-14 at 12.5, 50, and 100 mg/kg (Fig. 11.4d). Urinary osmolality and urea concentration were significantly decreased. The peak changes of urine output, urinary osmolality, and urinary urea concentration occurred between 2 and 4 h after PU-14 administration, with values returning to baseline by 10 h.

The long-term effect of PU-14 on urinary concentrating ability was also studied. PU-14 at 50 mg/kg was subcutaneously injected every 6 h. As shown in Fig. 11.4e, the 24-h urine output in PU-14-treated rats was significantly higher than that in vehicle control rats. Urinary osmolality and urea concentration in PU-14-treated rats were significantly lower than in vehicle control rats. However, the excretion of osmoles, urea, and non-urea solutes was similar in PU-14-treated and vehicle control rats, suggesting that PU-14 caused a urea-selective diuresis without disturbing electrolyte metabolism. The progressively greater diuretic effect of PU-14 over days may be due to PU-14 accumulation in kidney.

Figure 11.4f shows the compositions of the aqueous component of the inner medulla as measured on supernatants of centrifuged homogenates. Total osmolalities were significantly lower in inner medullary tissue of PU-14-treated rats than those in vehicle control rats, which was primarily because of the reduced inner medullary urea concentration. The concentration of non-urea solutes was similar with those in vehicle control rats. There was no significant difference in blood Na^+, K^+, Cl^-, urea, glucose, total cholesterol, and triglyceride after 7-day treatment with PU-14. These data suggest that PU-14 produces urea-selective diuresis without disturbing electrolyte excretion and metabolism.

Potential Clinical Indicators of Urea Transport Inhibitors

UT inhibitors, particularly of UT-A1, have several potential clinical indications. Urea transport inhibitors have a different mechanism of action from conventional diuretics, which block salt transport across kidney tubule epithelial cells. Diuretics such as furosemide are used widely to increase renal salt and water clearance in conditions associated with total body fluid overload, including congestive heart failure, cirrhosis, and nephrotic syndrome. By disrupting countercurrent mechanisms and intrarenal urea recycling, urea transport inhibitors, alone or in combination with conventional diuretics, may induce a diuresis in states of refractory edema where conventional diuretics are ineffective.

Summary and Future Directions

High-throughput screening has produced multiple chemical classes of small-molecule inhibitors of mammalian UTs, some with low nanomolar potency and UT-isoform selectivity. The UT inhibitors that have emerged from screening have many orders of magnitude greater inhibition potency than prior inhibitors. They should be useful as research tools to study the role of UTs in urinary concentrating function and in extrarenal tissues where they are expressed, and as drug development candidates. However, many challenges remain in the clinical development of UT inhibitors, including demonstration of efficacy in clinically relevant models of refractory edema and SIADH, and in medical chemistry in the selection of inhibitors with appropriate pharmacological properties.

References

1. Anderson MO, Zhang J, Liu Y, Yao C, Phuan PW, Verkman AS (2012) Nanomolar potency and metabolically stable inhibitors of kidney urea transporter UT-B. J Med Chem 55:5942–5950
2. Bankir L, Chen K, Yang B (2004) Lack of UT-B in vasa recta and red blood cells prevents urea-induced improvement of urinary concentrating ability. Am J Physiol Renal Physiol 286:F144–F151
3. Bankir L, Yang B (2012) New insights into urea and glucose handling by the kidney, and the urine concentrating mechanism. Kidney Int 81:1179–1198
4. Doran JJ, Klein JD, Kim YH, Smith TD, Kozlowski SD, Gunn RB, Sands JM (2006) Tissue distribution of UT-A and UT-B mRNA and protein in rat. Am J Physiol Regul Integr Comp Physiol 290:R1446–R1459
5. Esteva-Font C, Phuan PW, Anderson MO, Verkman AS (2013) A small molecule screen identifies selective inhibitors of urea transporter UT-A. Chem Biol 20:1235–1244
6. Fenton RA (2008) Urea transporters and renal function: lessons from knockout mice. Curr Opin Nephrol Hypertens 17:513–518
7. Fenton RA (2009) Essential role of vasopressin-regulated urea transport processes in the mammalian kidney. Pflugers Arch 458:169–177
8. Fenton RA, Chou CL, Stewart GS, Smith CP, Knepper MA (2004) Urinary concentrating defect in mice with selective deletion of phloretin-sensitive urea transporters in the renal collecting duct. Proc Natl Acad Sci USA 101:7469–7474
9. Fenton RA, Flynn A, Shodeinde A, Smith CP, Schnermann J, Knepper MA (2005) Renal phenotype of UT-A urea transporter knockout mice. J Am Soc Nephrol 16:1583–1592
10. Fenton RA, Stewart GS, Carpenter B, Howorth A, Potter EA, Cooper GJ, Smith CP (2002) Characterization of mouse urea transporters UT-A1 and UT-A2. Am J Physiol Renal Physiol 283:F817–F825

11. Frohlich O, Klein JD, Smith PM, Sands JM, Gunn RB (2006) Regulation of UT-A1-mediated transepithelial urea flux in MDCK cells. Am J Physiol Cell Physiol 291:C600–C606

12. Galietta LJ, Haggie PM, Verkman AS (2001) Green fluorescent protein-based halide indicators with improved chloride and iodide affinities. FEBS Lett 499:220–224

13. Klein JD, Blount MA, Sands JM (2012) Molecular mechanisms of urea transport in health and disease. Pflugers Arch 464:561–572

14. Klein JD, Frohlich O, Mistry AC, Kent KJ, Martin CF, Sands JM (2013) Transgenic mice expressing UT-A1, but lacking UT-A3, have intact urine concentration ability. FASEB J 27:1111.17 (Experimental Biology abstract)

15. Lei T, Zhou L, Layton AT, Zhou H, Zhao X, Bankir L, Yang B (2011) Role of thin descending limb urea transport in renal urea handling and the urine concentrating mechanism. Am J Physiol Renal Physiol 301:F1251–F1259

16. Levin MH, de la Fuente R, Verkman AS (2007) Urearetics: a small molecule screen yields nanomolar potency inhibitors of urea transporter UT-B. FASEB J 21:551–563

17. Li F, Lei T, Zhu J, Wang W, Sun Y, Chen J, Dong Z, Zhou H, Yang B (2013) A novel small-molecule thienoquinolin urea transporter inhibitor acts as a potential diuretic. Kidney Int 83:1076–1086

18. Liu Y, Esteva-Font C, Yao C, Phuan PW, Verkman AS, Anderson MO (2013) 1,1-Difluoroethyl-substituted triazolothienopyrimidines as inhibitors of a human urea transport protein (UT-B): new analogs and binding model. Bioorg Med Chem Lett 23:3338–3341

19. Mayrand RR, Levitt DG (1983) Urea and ethylene glycol-facilitated transport systems in the human red cell membrane. Saturation, competition, and asymmetry. J Gen Physiol 81:221–237

20. Pannabecker TL (2013) Comparative physiology and architecture associated with the mammalian urine concentrating mechanism: role of inner medullary water and urea transport pathways in the rodent medulla. Am J Physiol Regul Integr Comp Physiol 304:R488–R503

21. Sands JM (2004) Renal urea transporters. Curr Opin Nephrol Hypertens 13:525–532

22. Sands JM (2007) Critical role of urea in the urine-concentrating mechanism. J Am Soc Nephrol 18:670–671

23. Sands JM, Gargus JJ, Frohlich O, Gunn RB, Kokko JP (1992) Urinary concentrating ability in patients with Jk(a-b-) blood type who lack carrier-mediated urea transport. J Am Soc Nephrol 2:1689–1696

24. Sands JM, Layton HE (2009) The physiology of urinary concentration: an update. Semin Nephrol 29:178–195

25. Shayakul C, Clémençon B, Hediger MA (2013) The urea transporter family (SLC14): physiological, pathological and structural aspects. Mol Aspects Med 34:313–322

26. Shayakul C, Hediger MA (2004) The SLC14 gene family of urea transporters. Pflugers Arch 447:603–609

27. Smith CP (2009) Mammalian urea transporters. Exp Physiol 94:180–185

28. Tsukaguchi H, Shayakul C, Berger UV, Tokui T, Brown D, Hediger MA (1997) Cloning and characterization of the urea transporter UT3: localization in rat kidney and testis. J Clin Invest 99:1506–1515

29. Uchida S, Sohara E, Rai T, Ikawa M, Okabe M, Sasaki S (2005) Impaired urea accumulation in the inner medulla of mice lacking the urea transporter UT-A2. Mol Cell Biol 25:7357–7363

30. Yang B, Bankir L (2005) Urea and urine concentrating ability: new insights from studies on mice. Am J Physiol Renal Physiol 288:F881–F896

31. Yang B, Bankir L, Gillespie A, Epstein CJ, Verkman AS (2002) Urea-selective concentrating defect in transgenic mice lacking urea transporter UT-B. J Biol Chem 277:10633–10637

32. Yang B, Verkman AS (1998) Urea transporter UT3 functions as an efficient water channel. Direct evidence for a common water/urea pathway. J Biol Chem 273:9369–9372

33. Yang B, Verkman AS (2002) Analysis of double knockout mice lacking aquaporin-1 and urea transporter UT-B. Evidence for UT-B-facilitated water transport in erythrocytes. J Biol Chem 277:36782–36786

34. Yao C, Anderson MO, Zhang J, Yang B, Phuan PW, Verkman AS (2012) Triazolothienopyrimidine inhibitors of urea transporter UT-B reduce urine concentration. J Am Soc Nephrol 23:1210–1220
35. Zhao D, Sonawane ND, Levin MH, Yang B (2007) Comparative transport efficiencies of urea analogues through urea transporter UT-B. Biochim Biophys Acta 1768:1815–1821

Chapter 12
Clinical Aspects of Urea Transporters

Jianhua Ran, Hongkai Wang and Tinghai Hu

Abstract Jk antigens, which were identified as urea transporter B (UT-B) in the plasma membrane of erythrocytes, and which determine the Kidd blood type in humans, are involved in transfusion medicine, and even in organ transplantation. The Jk(a-b-) blood type is a consequence of a silent *Slc14A1* gene caused by various mutations related to lineage. In addition, the specific mutations related to hypertension and metabolic syndrome cannot be ignored. Genome-wide association studies established *Slc14A1* as a related gene of bladder cancer and some genotypes are associated with higher morbidity. This chapter aims to introduce the clinical significance of urea transporters.

Keywords Urea · Urea transporter · Jk antigens · Mutations

Urea Transporters and Blood Groups

On April 17 in 1950, Mrs. Kidd gave a birth to a male infant who then suffered from neonatal hemolytic disease due to a previously unidentified antibody passed through placental barrier. This antibody was directed against a new blood group antigen that

J. Ran (✉) · H. Wang
Department of Anatomy and Neuroscience Center, Basic Medical College,
Chongqing Medical University, Yixueyuan Road 1, Chongqing 400016, China
e-mail: ranjianhua@cqmu.edu.cn

H. Wang
e-mail: wanghongkai1993@gmail.com

T. Hu
Department of Nephrology, The Second Affiliated Hospital, Chongqing Medical University,
Yixueyuan Road 1, Chongqing 400016, China
e-mail: hutinghai@163.com

was then named Jk(a) and is expressed on fetal erythrocytes [1]. The Jk(b) gene was assumed to exist by allelomorphic gene theory, and the antigen Jk(b) was successfully found 2 years later by a transfusion reaction [60]. The Kidd blood group system, defined by two codominant alleles, Jk(a) and Jk(b), was established in the 1950s, and it is an important factor in transfusion medicine until the present [46]. Both Jk(a) and Jk(b) are responsible for the three common phenotypes: Jk(a+b−), Jk(a−b+), and Jk(a+b+). The Jk(a−b−) (or JK$_{null}$) phenotype was discovered by a post-transfusional hemolytic disease in 1959 in a Filipina of some Spanish and Chinese ancestry [59]. The Jk(a−b−) phenotype is rare, but occurs with greater incidence in Asians, Finns, Polynesians, etc. [53, 74, 85]. Although Jk(a−b−) persons from each population carry Jk(b)-like alleles (homozygous for adenosine at nt 838), the molecular basis for their Jk(a−b−) phenotype is different. The Jk(a−b−) phenotype results from two different genetic backgrounds: (i) homozygous inheritance of a "silent" allele Jk at the Jk locus [30] and (ii) inheritance of a dominant inhibitor gene In(Jk), unlinked to the Jk locus [44, 53]. Following immunization by transfusion or pregnancy, Jk(a−b−) individuals may produce an antibody called anti-Jk3 (or anti-Jkab), which reacts with all common erythrocytes carrying the Jk(a) and/or Jk(b) antigens causing severe hemolysis, but is unreactive with Jk(a−b−) cells themselves [47].

In 1982, when technicians routinely lysed erythrocytes with urea before using a Technicon Platelet Autocounter II to test a patient with bone marrow aplasia and severe epistaxis, they were confused that the patient's blood sample needed 30-fold time of urea lysis. The subsequent findings exhibited that an increased resistance to urea lysis was associated with the Jk(a−b−) phenotype [20]. It was the first time when a connection between urea and the Kidd blood group system jumped into our field of vision. Meanwhile, in the early 1980s, it was being debated as to whether the Jk gene locus was on chromosome 2 or 7 [49, 62, 70]. And on the basis of genetic linkage theory, the gene locus argument even triggered a bunch of derived questions, such as whether or not insulin-dependent diabetes mellitus is linked to Jk gene [3, 23, 24]. Nonetheless, the arguments came to an end in 1989. After years of development of Human Gene Mapping, a close genetic linkage between JK and the PstI-restriction fragment length polymorphism was detected by the L2.7 genomic DNA probe, and scientists had assigned the latter to chromosome 18 [16, 72].

In 1991, the phenomenon that erythrocytes of the Jk(a−b−) blood type were not permeable to urea was demonstrated [12], which was coincidently similar to the result of previous studies showing that artificial lipid bilayers exhibited a low transmembrane speed of urea flux [14]. This attribution of Jk(a−b−) erythrocytes strongly suggested correlation between Jk antigen and transmembrane movement of urea. In the same year, scientists first detected a urea transporter facilitating the ability of a polar molecule, namely urea, to permeate across the cell membrane in *Xenopus* oocytes [48, 91]. In 1993, a protein of around 40 kDa was directly found by photoaffinity labeling and it, probably the Kidd antigen, could be a protein related to urea transport [52]. In the same year, UT-2 (UT-A2, renamed in later years) was successfully cloned by functional expression in *Xenopus* oocytes microinjected with cDNA from rabbit renal medulla [89]. In 1994, scientists reported the isolation of a human bone marrow-derived cDNA coding for a protein UT-3 (UT-B, renamed

in later years) showing extensive sequence similarity with UT-A2 [56]. In 1995, the UT-B gene was assigned on chromosome 18q12 by in situ hybridization as the Kidd (Jk) blood group locus. The breakthrough was that their experiment finally showed that the Kidd blood group antigen, Jk, and urea transporter, UT-B, are the same protein [54]. They also terminated the derived question that insulin-dependent diabetes mellitus is not connected to Kidd blood group system [55].

Up to now, the morphology and physiology of UT-B have been widely and profoundly researched, and the UT-B null mouse model has been constructed as an imitation of Jk(a−b−) Kidd blood group (introduced in former Chapters). However, the Kidd blood group system itself still shows its clinical significance.

The Kidd blood group system is frequently involved in neonatal hemolytic disease and delayed hemolytic transfusion reactions, just as in its initial discovery [27, 78, 81]. Both anti-Jk(a) and anti-Jk(b) can result in neonatal hemolytic disease, even if the latter is far more common [2, 11, 35, 77].

Based on the 16th edition of the American Association of Blood Banks Technical Manual (2008), Kidd antigen detection is performed using unknown erythrocytes with anti-Jk(a) and anti-Jk(b) by an indirect antiglobulin test or enzyme test. For mass screening of the Jk(a−b−) phenotype, the urea lysis test is suggested [20, 40]. But hemagglutination for Kidd blood group phenotyping is not suitable for multiple transfusion patients, fetus, and newborn infants due to the scarce availability of rare antisera [6, 42, 69]. Therefore, molecular typing of the Jk gene (*Slc14A1* gene) that avoids immunoreaction has been developed and is now well utilized in transfusion medicine. PCR-based determination of the Kidd phenotype has been a lifesaver for some patients whose samples were submitted to the New York Blood Center with confusing serologic results, suggesting better sensitivity than traditional serologic methods [42]. Nowadays, the allele-specific polymerase chain reaction (AS-PCR) technique, high-resolution melting (HRM) analysis, polymerase chain reaction with sequence-specific priming (PCR-SSP) technique, and the like for Kidd blood group genotyping are broadly used on fetus or after multiple transfusions [22, 28, 31, 63, 69, 76].

Aside from transfusion medicine, since UT-B was documented in several tissues as we introduced in Chap. 7, the antibodies in recipients may attack Jk alloantigens (UT-B) as minor histocompatibility antigens expressed on donor's organs after transplantation [38, 68]. It has been reported that antigen Jk(b) is able to cause acute cellular rejection of a transplanted kidney [18, 19, 38]. Even though no post-operation rejection in other organs has been reported yet, we still recommend that surgeons pay attention to the Kidd blood group when they meet a hard-to-explain rejection episode.

Mutations of Urea Transporters in Human

The human *Slc14A1* gene is located at chromosome 18q11-q12 and is organized into 11 exons distributed over 30 kbp (gene database: http://www.ncbi.nlm.nih. gov/gene/6563). The gene region encoding the mature protein begins with exon 4 and then extends to exon 11 [44]. It is known that the Asp280Asn (D280 N) amino

Table 12.1 Mutations of *Slc14A1*

	Mutation	Amino acid change	Population	References
Jk(a)	C582G	Tyr194Stop	Swiss	[29]
	C202T	Gln68Stop	Hispanic-American, Caucasian	[82]
	G327del	Leu109Phe	Japanese	[57]
	G432A	Trp144Stop	Japanese	[57]
	757–759delTCC	Ser253del	Japanese	[57]
	G893A	Gly298Glu	Japanese	[57]
	C956T	Thr319Met	African-American, Indian, Thai, Pakistani	[74, 82]
	C561A	Tyr187Stop	African-American	[26]
	del(exon 4 and 5)	protein not expressed	English, Tunisian, Bosnian	[29, 43, 82]
	IVS8+5 g > a	skipping of exon 8	Chinese	[17]
	IVS5 − 1 g > a	skipping of exon 6	Polynesian	[9]
Jk(b)	G130A	Glu44Lys	Caucasian, Thai	[29, 74]
	G191A	Arg64Gln	African-American, Japanese	[4, 57]
	G194A	Gly65Asp	French-Canadian	[75]
	C222A	Asn74Lys	Taiwanese	[41]
	T437C	Leu146Pro	Chinese	[17]
	G512A	Trp171Stop	Chinese	[17]
	C536G	Pro179Arg	Chinese	[17]
	C561A	Tyr187Stop	Japanese	[57]
	647-648delAC	Asp216Ala	Japanese	[57]
	G719A	Trp240Stop	Japanese	[57]
	T871C	Ser291Pro	Finn	[30, 71]
	G896A	Gly299Glu	Taiwanese, Polynesian, Thai	[41, 74]
	C956T	Thr319Met	African-American, Indian, Thai, Pakistani	[74, 82]
	A723del	Ile262Stop	Hispanic-American	[82]
	IVS5-1 g > c	skipping of exon 6	Chinese	[50]
	IVS5-1 g > a	skipping of exon 6	Taiwanese, Chinese, Filipino, Indonesian, Polynesian, Vietnamese, Japanese	[39, 44, 57, 82, 88]
	IVS7+1 g > t	skipping of exon 7	French	[44]

acid substitution in the UT-B protein determines the erythrocyte Kidd blood group antigen, i.e., Asp280 for Jk(a), Asn280 for Jk(b), and G130A (Glu44Lys) for a weaker version of Jk(a) group, Jk(a)W [45, 83, 86]. A Jk(a)/Jk(b) polymorphism resulted from a G838A transition, causing a D280 N amino acid substitution in the 3rd extracellular loop of the Jk polypeptide [22, 55].

Frequencies of the Jk(a−b−) phenotype in different ethnic groups is dissimilar [21], while several diverse mutations of *Slc14A1* gene with Jk(a−b−) phenotype are also associated with different ethnic lineages [30] (Table 12.1). Although

Jk(a−b−) persons from many populations carry Jk(b)-like alleles, the molecular basis for their Jk(a−b−) phenotype is different. In contrast, some mutations are related to Jk(a)-like alleles and also rely on ethnic group [9]. B.S. (a donor from USA) and L.P. (a donor from Paris) were homozygous for point mutations at conserved 3′-acceptor (*ag* 3 *aa*) and 5′-donor (*gt* 3 *tt*) splice sites of introns 5 and 7 and lead to exons 6 and 7 skipping, respectively [44]. In Polynesian, the mutation is AG to AA located in the 3′-acceptor splice site of intron 5 of Jk(b) causing skipping of exon 6; in Finns, the mutation site is a missense mutation, T871C substitution, that leads to Ser291Pro [30, 71]. A G to A 3′ splice site mutation of intron 5 is associated with skipping exon 6 and was also found in native Chinese [88], while at the same position, a G to C mutation was detected in Chinese resulting in the same consequence [50]. In Taiwan, two novel mutations with one missense mutation C222A (Asn74Lys) in exon 5 and the other missense mutation G896A (Gly299Glu) in exon 9 of the Jk allele led to two heterozygous patterns of Jk(a−b−) genotype [41]. IVS5-1 g > a mutation was detected widely in Taiwanese, Fujian, Filipino, and Indonesian populations [39]. In 2013, a splice mutation of Jk(a), IVS8+5 g > a, resulting in skipping of exon 8 was designated, while a nonsense mutation G512A (Trp171Stop) resulting in a premature stop signal in exon 7, two types of missense point mutations, C536G (Pro179Arg) and T437C (Leu146Pro), were also found in Chinese [17]. In the Swiss Jk(a−b−) samples, a nonsense mutation in exon 7, C582G, resulting in a premature stop codon (Tyr194Stop) was identified [29]. In English, a deletion of 1,603 bp including exons 4 and 5 involves the loss of the translation start codon [29]. In a Tunisian, it was found by genotyping that a 7-kb fragment that normally contains exons 4 and 5 was missing but was displaced by a 136-bp intron 3 sequence located 315-bp and 179-bp upstream from exon 4 [43]. A C956T (Thr319Met) mutation was found in African origin, causing Jk(a−b−) type in an African-American donor [82] and then found in Thais in a subsequent study [74]. Also in an African-American family, C561A (Tyr187Stop) was detected as another Jk(a)-like silent Jk locus [26]. By testing two American siblings of Caucasian origin and one female of Hispanic origin, respectively, two different nonsense mutations, C202T (Gln68Stop) and A723del (Ile262Stop), were identified [82]. In a French-Canadian family, G194A (Gly65Asp) was found as a novel silent mutation [75].

To our knowledge, these mutations are all responsible for deficient urea transport in Jk(a−b−) population. We suggest doctors in other regions of the world test for mutation of the *Slc14A1* gene when they meet Jk(a−b−) patients from an undocumented ethnic group.

Apart from *Slc14A1*, variations of *Slc14A2* are not negligible. In persons of Asian origin, it has been found through genome scan that Val227Ile (rs1123617, G → A) and Ala357Thr (rs3745009, G → A) are significantly associated with blood pressure variation in men but not women [66]. Both Ile227 and Ala357 alleles exhibit a modest protective effect, but mechanisms of difference between genders remain vague. How these polymorphisms contribute to blood pressure variation is considered to be by decreasing the activity of UT-A. Then, the reduction in the reabsorption of urea and water leads to lower blood pressure. Moreover,

subjects carrying both the Ala357/Ala357 genotype in the Ala357Thr polymorphism and either Val227/Ile227 or Ile227/Ile227 genotypes in the Val227Ile polymorphism had the highest mean change in both systolic and diastolic blood pressure after treatment of hypertension by nifedipine gastrointestinal therapeutic system [25]. Interestingly, expression of UT-A is upregulated in hearts and downregulated in kidneys in rats after hypertension [8, 36]. To our knowledge, the potential association herein needs further study.

A genetic study of persons of Asian origin showed that G465C in *Slc14A2* is related to a low risk of metabolic syndrome, revealing a significant difference in triglyceride level [79]. But another study suggested that the *Slc14A2* gene contributes to metabolic syndrome by regulating albumin directly [90]. Based on the above, further studies can delve into the relationship between UT-A and common chronic diseases.

Genetic Variation in the UT-B Gene and the Risk of Urinary Bladder Cancer

Urinary bladder cancer ranks eighth in worldwide cancer incidence and the thirteenth most numerous cause of death from cancer. It is the sixth most common malignancy in men and eighteenth in women, and its frequent recurrence requires regular screening and interventions. Approximately 386,000 new bladder cancer cases (297,000 males and 89,000 females) occurred worldwide in 2008. Rates in males are three to four times those in females [10, 58]. Urinary bladder cancer stands out as a huge burden all over the world, particularly in developing countries [61].

The risk factors associated with the development of bladder cancer include cigarette-smoking, exposure to chemicals such as aromatic amines, chronic bladder inflammation, and age [32, 84]. Most tumors are transitional cell carcinomas (95 %), occurring in industrialized countries. Bladder cancer has historically not been treated as a cancer with a genetic background though a family history of bladder cancer is associated with an approximately two-fold increase in risk [51]. In recent years, some multistage genome-wide association studies (GWAS) have found several genes, TP63, MYC, TERT, PSCA, CLPTMIL, TMEM129, TACC3-FGFR3, APOBEC3A, CBX6, CCNE1, UGT1A, NAT2, GSTM1, that are linked to bladder cancer [33, 34, 64, 67, 87]. In 2011, a new urinary bladder cancer susceptibility locus was discovered from an extension of the European urinary bladder cancer genome-wide association studies—a single-nucleotide polymorphism (SNP) in intron 3, rs17674580, of the UT-B gene *Slc14A1*. It is hypothesized that sequence variants in the *Slc14A1* gene indirectly modify urinary bladder cancer risk by affecting the urine concentration or frequency of urination that affects the time that carcinogens are contacting the urothelium (urogenous contact hypothesis, set in 1987) [5, 65]. Interestingly, at the same time, a meta-analysis of existing GWAS data [67, 87] also identified a novel susceptibility locus that mapped to a region of 18q12.3, marked by rs7238033 and two highly correlated SNPs,

rs10775480/rs10853535, localized to the UT-B gene *Slc14A1*. And they found no evidence of modification of the 18q12.3 locus risk association by smoking status [15]. Coincidently, the latter study group speculated that variations in urine volumes and concentration could modify exposure of bladder epithelium to carcinogens in the urine, which is similar with the urogenous contact hypothesis. To search for more evidence, in 2013, a further study was designed to seek difference between both phenotypes that are T allele versus C allele at rs10775480 [37]. They measured specific gravity representing urine concentration, and differential results were observed. Specifically, carriage of the bladder cancer risk allele resulted in a significant decrease in urinary specific gravity after controlling for all available predictors. Their data suggested that UT-B expressed in the bladder has the ability to influence urine concentration and this mechanism might explain the increased bladder cancer susceptibility associated with rs10775480. However, recent studies in rats found evidence that expression of UT-B in urothelium may be associated with bladder cancer directly. As we introduced previously, UT-B distributes in urothelium so that urea is continuously reabsorbed from the urine across the urothelium via UT-B, and urine is thus altered in its passage through the urinary tract [73]. Additionally, in UT-B null mice, DNA damage and apoptosis were markedly increased, resulted from urea accumulation, an upregulated expression of iNOS and a downregulation of arginase I expression in urothelial cells induced by deletion of UT-B [7]. Research hitherto delving into an association between the urea transporter and carcinoma of bladder or even other bladder disorders are rare. Further studies are desired to reveal precise mechanism.

The expression of the gene *Slc14A1* in humans was affected by castration, in addition to differential expression in the benign and malignant prostate, which suggested that *Slc14A1* might also contribute to prostate carcinoma [80]. Even in cancers out of urinary system, *Slc14A1* stands out unexpectedly. Downregulation of *Slc14A1* in noninvolved tissue of pulmonary adenocarcinoma may mark higher clinical stage [13].

References

 1. Allen FH, Diamond LK, Niedziela B (1951) A new blood-group antigen. nature 167:482
 2. Baek EJ, Park SC, Kwon YH, Kim CR (2013) Haemolytic disease of newborn due to anti-Jka and the duration of antibody persistence. J Paediatr Child Health 49:E101–E102
 3. Barbosa J, Rich S, Dunsworth T, Swanson J (1982) Linkage disequilibrium between insulin-dependent diabetes and the Kidd blood group Jkb allele. J Clin Endocrinol Metab 55:193–195
 4. Billingsley K, Posadas J, Gaur L, Moulds J (2011) Identification of a new JK silencing mutation in the African American population. Transfusion 51:150

5. Braver DJ, Modan M, Chetrit A, Lusky A, Braf Z (1987) Drinking, micturition habits, and urine concentration as potential risk factors in urinary bladder cancer. J Natl Cancer Inst 78:437–440

6. Castilho L, Rios M, Bianco C, Pellegrino J Jr, Alberto FL, Saad ST, Costa FF (2002) DNA-based typing of blood groups for the management of multiply-transfused sickle cell disease patients. Transfusion 42:232–238

7. Dong Z, Ran J, Zhou H, Chen J, Lei T, Wang W, Sun Y, Lin G, Bankir L, Yang B (2013) Urea transporter UT-B deletion induces DNA damage and apoptosis in mouse bladder urothelium. PLoS ONE 8:e76952

8. Duchesne R, Klein JD, Velotta JB, Doran JJ, Rouillard P, Roberts BR, McDonough AA, Sands JM (2001) UT-A urea transporter protein in heart: increased abundance during uremia, hypertension, and heart failure. Circ Res 89:139–145

9. Ekman GC, Hessner MJ (2000) Screening of six racial groups for the intron 5 G– > A 3' splice acceptor mutation responsible for the polynesian kidd (a-b-) phenotype: the null mutation is not always associated with the JKB allele. Transfusion 40:888–889

10. Ferlay J, Shin HR, Bray F, Forman D, Mathers C, Parkin DM (2010) Estimates of worldwide burden of cancer in 2008: GLOBOCAN 2008. Int J Cancer 127:2893–2917

11. Ferrando M, Martinez-Canabate S, Luna I, de la Rubia J, Carpio N, Alfredo P, Arriaga F (2008) Severe hemolytic disease of the fetus due to anti-Jkb. Transfusion 48:402–404

12. Frohlich O, Macey R, Edwards-Moulds J, Gargus J, Gunn R (1991) Urea transport deficiency in Jk (a-b-) erythrocytes. Am J Physiol 260:C778–C783

13. Frullanti E, Colombo F, Falvella FS, Galvan A, Noci S, De Cecco L, Incarbone M, Alloisio M, Santambrogio L, Nosotti M, Tosi D, Pastorino U, Dragani TA (2012) Association of lung adenocarcinoma clinical stage with gene expression pattern in noninvolved lung tissue. Int J Cancer 131:E643–E648

14. Gallucci E, Micelli S, Lippe C (1971) Non-electrolyte permeability across thin lipid membranes. Arch Int Physiol Biochim 79:881–887

15. Garcia-Closas M, Ye Y, Rothman N, Figueroa JD, Malats N, Dinney CP, Chatterjee N, Prokunina-Olsson L, Wang Z, Lin J, Real FX, Jacobs KB, Baris D, Thun M, De Vivo I, Albanes D, Purdue MP, Kogevinas M, Kamat AM, Lerner SP, Grossman HB, Gu J, Pu X, Hutchinson A, Fu YP, Burdett L, Yeager M, Tang W, Tardon A, Serra C, Carrato A, Garcia-Closas R, Lloreta J, Johnson A, Schwenn M, Karagas MR, Schned A, Andriole G Jr, Grubb R 3rd, Black A, Jacobs EJ, Diver WR, Gapstur SM, Weinstein SJ, Virtamo J, Hunter DJ, Caporaso N, Landi MT, Fraumeni JF Jr, Silverman DT, Chanock SJ, Wu X (2011) A genome-wide association study of bladder cancer identifies a new susceptibility locus within SLC14A1, a urea transporter gene on chromosome 18q12.3. Hum Mo Genet 20:4282–4289

16. Geitvik G, Høyheim B, Gedde-Dahl T, Grzeschik K, Lothe R, Tomter H, Olaisen B (1987) The Kidd (JK) blood group locus assigned to chromosome 18 by close linkage to a DNA-RFLP. Hum Genet 77:205–209

17. Guo Z, Wang C, Yan K, Xie J, Shen W, Li Q, Zhang J, Ye L, Zhu Z (2013) The mutation spectrum of the JK-null phenotype in the Chinese population. Transfusion 53:545–553

18. Hamilton MS, Singh V, Warady BA (2006) Plasma cell-rich acute cellular rejection of a transplanted kidney associated with antibody to the red cell Kidd antigen. Pediatr Transplant 10:974–977

19. Hamilton MS, Singh V, Warady BA (2008) Additional case of acute cellular kidney rejection associated with the presence of antibodies to the red blood cell Kidd antigen. Pediatr Transplant 12:918–919

20. Heaton D, McLoughlin K (1982) Jk (a− b−) red blood cells resist urea lysis. Transfusion 22:70–71

21. Henry S, Woodfield G (1995) Frequencies of the Jk(a-b-) phenotype in Polynesian ethnic groups. Transfusion 35:277

22. Hessner MJ, Pircon RA, Johnson ST, Luhm RA (1998) Prenatal genotyping of Jk(a) and Jk(b) of the human Kidd blood group system by allele-specific polymerase chain reaction. Prenat Diagn 18:1225–1231

23. Hodge S, Anderson C, Neiswanger K, Rubin R, Sparkes R, Sparkes M, Crist M, Spence M, Terasaki P, Rimoin D (1983) Association studies between Type 1 (insulin-dependent) diabetes and 27 genetic markers: lack of association between Type 1 diabetes and Kidd blood group. Diabetologia 25:343–347

24. Hodge S, Neiswanger K, Anne Spence M, Sparkes M, Terasaki P, Anderson C, Leigh Field L, Sparkes R, Crist M, Rimoin D (1981) Close genetic linkage between diabetes mellitus and Kidd blood group. Lancet 318:893–895

25. Hong X, Xing H, Yu Y, Wen Y, Zhang Y, Zhang S, Tang G, Xu X (2007) Genetic polymorphisms of the urea transporter gene are associated with antihypertensive response to nifedipine GITS. Methods Find Exp Clin Pharmacol 29:3–10

26. Horn T, Castilho L, Moulds JM, Billingsley K, Vege S, Johnson N, Westhoff CM (2012) A novel JKA allele, nt561C> A, associated with silencing of Kidd expression. Transfusion 52:1092–1096

27. Hussain SS, Ebbs AM, Curtin NJ, Keidan AJ (2007) Delayed haemolytic transfusion reaction due to anti-Jkb in a patient with non-Hodgkin's lymphoma-transient nature of anti-Jkb and the importance of early serological diagnosis. Transfus Med 17:197–199

28. Intharanut K, Grams R, Bejrachandra S, Sriwanitchrak P, Nathalang O (2013) Improved allele-specific PCR technique for Kidd blood group genotyping. J Clin Lab Anal 27:53–58

29. Irshaid NM, Eicher NI, Hustinx H, Poole J, Olsson ML (2002) Novel alleles at the JK blood group locus explain the absence of the erythrocyte urea transporter in European families. Br J Haematol 116:445–453

30. Irshaid NM, Henry SM, Olsson ML (2000) Genomic characterization of the kidd blood group gene: different molecular basis of the Jk(a-b-) phenotype in Polynesians and Finns. Transfusion 40:69–74

31. Irshaid NM, Thuresson B, Olsson ML (1998) Genomic typing of the Kidd blood group locus by a single-tube allele-specific primer PCR technique. Br J Haematol 102:1010–1014

32. Jacobs BL, Lee CT, Montie JE (2010) Bladder cancer in 2010: how far have we come? CA Cancer J Clin 60:244–272

33. Kiemeney LA, Sulem P, Besenbacher S, Vermeulen SH, Sigurdsson A, Thorleifsson G, Gudbjartsson DF, Stacey SN, Gudmundsson J, Zanon C, Kostic J, Masson G, Bjarnason H, Palsson ST, Skarphedinsson OB, Gudjonsson SA, Witjes JA, Grotenhuis AJ, Verhaegh GW, Bishop DT, Sak SC, Choudhury A, Elliott F, Barrett JH, Hurst CD, de Verdier PJ, Ryk C, Rudnai P, Gurzau E, Koppova K, Vineis P, Polidoro S, Guarrera S, Sacerdote C, Campagna M, Placidi D, Arici C, Zeegers MP, Kellen E, Gutierrez BS, Sanz-Velez JI, Sanchez-Zalabardo M, Valdivia G, Garcia-Prats MD, Hengstler JG, Blaszkewicz M, Dietrich H, Ophoff RA, van den Berg LH, Alexiusdottir K, Kristjansson K, Geirsson G, Nikulasson S, Petursdottir V, Kong A, Thorgeirsson T, Mungan NA, Lindblom A, van Es MA, Porru S, Buntinx F, Golka K, Mayordomo JI, Kumar R, Matullo G, Steineck G, Kiltie AE, Aben KK, Jonsson E, Thorsteinsdottir U, Knowles MA, Rafnar T, Stefansson K (2010) A sequence variant at 4p16.3 confers susceptibility to urinary bladder cancer. Nat Genet 42:415–419

34. Kiemeney LA, Thorlacius S, Sulem P, Geller F, Aben KK, Stacey SN, Gudmundsson J, Jakobsdottir M, Bergthorsson JT, Sigurdsson A, Blondal T, Witjes JA, Vermeulen SH, Hulsbergen-van de Kaa CA, Swinkels DW, Ploeg M, Cornel EB, Vergunst H, Thorgeirsson TE, Gudbjartsson D, Gudjonsson SA, Thorleifsson G, Kristinsson KT, Mouy M, Snorradottir S, Placidi D, Campagna M, Arici C, Koppova K, Gurzau E, Rudnai P, Kellen E, Polidoro S, Guarrera S, Sacerdote C, Sanchez M, Saez B, Valdivia G, Ryk C, de Verdier P, Lindblom A, Golka K, Bishop DT, Knowles MA, Nikulasson S, Petursdottir V, Jonsson E, Geirsson G, Kristjansson B, Mayordomo JI, Steineck G, Porru S, Buntinx F, Zeegers MP, Fletcher T, Kumar R, Matullo G, Vineis P, Kiltie AE, Gulcher JR, Thorsteinsdottir U, Kong A, Rafnar T, Stefansson K (2008) Sequence variant on 8q24 confers susceptibility to urinary bladder cancer. Nat Genet 40:1307–1312

35. Kim WD, Lee YH (2006) A fatal case of severe hemolytic disease of newborn associated with anti-Jk(b). J Korean Med Sci 21:151–154

36. Klein JD, Murrell BP, Tucker S, Kim YH, Sands JM (2006) Urea transporter UT-A1 and aquaporin-2 proteins decrease in response to angiotensin II or norepinephrine-induced acute hypertension. Am J Physiol Renal Physiol 291:F952–F959

37. Koutros S, Baris D, Fischer A, Tang W, Garcia-Closas M, Karagas MR, Schwenn M, Johnson A, Figueroa J, Waddell R, Prokunina-Olsson L, Rothman N, Silverman DT (2013) Differential urinary specific gravity as a molecular phenotype of the bladder cancer genetic association in the urea transporter gene, SLC14A1. Int J Cancer 133:3008–3013

38. Lerut E, Van Damme B, Noizat-Pirenne F, Emonds MP, Rouger P, Vanrenterghem Y, Pirenne J, Ansart-Pirenne H (2007) Duffy and Kidd blood group antigens: minor histocompatibility antigens involved in renal allograft rejection? Transfusion 47:28–40

39. Lin M, Yu LC (2008) Frequencies of the JKnull (IVS5-1 g > a) allele in Taiwanese, Fujian, Filipino, and Indonesian populations. Transfusion 48:1768

40. Linz WJ, Muenster S, Watkins J, Moore SB (2003) Transfusion medicine illustrated. Lack of effect of 2 M urea on Jk(a-b-) cells. Transfusion 43:685

41. Liu HM, Lin JS, Chen PS, Lyou JY, Chen YJ, Tzeng CH (2009) Two novel Jk(null) alleles derived from 222C> A in Exon 5 and 896G> A in Exon 9 of the JK gene. Transfusion 49:259–264

42. Lomas-Francis C (2007) The value of DNA analysis for antigens of the Kidd blood group system. Transfusion 47:23s–27s

43. Lucien N, Chiaroni J, Cartron JP, Bailly P (2002) Partial deletion in the JK locus causing a Jk(null) phenotype. Blood 99:1079–1081

44. Lucien N, Sidoux-Walter F, Olives B, Moulds J, Le Pennec PY, Cartron JP, Bailly P (1998) Characterization of the gene encoding the human Kidd blood group/urea transporter protein. Evidence for splice site mutations in Jknull individuals. J Biol Chem 273:12973–12980

45. Lucien N, Sidoux-Walter F, Roudier N, Ripoche P, Huet M, Trinh-Trang-Tan MM, Cartron JP, Bailly P (2002) Antigenic and functional properties of the human red blood cell urea transporter hUT-B1. J Biol Chem 277:34101–34108

46. Lundevall J (1956) The Kidd blood group system investigated with anti-JKa. Acta Pathol Microbiol Scand 38:39–42

47. Marshall CS, Dwyre D, Eckert R, Russell L (1999) Severe hemolytic reaction due to anti-JK3. Arch Pathol Lab Med 123:949–951

48. Martial S, Ripoche P, Ibarra C (1991) Functional expression of urea channels in amphibian oocytes injected with frog urinary bladder mRNA. Biochim Biophys Acta 1090:86–90

49. McAlpine PJ, Bootsma D (1982) Report of the committee on the genetic constitution of chromosomes 2, 3, 4, and 5. Birth Defects Orig Artic Ser 18:121–129

50. Meng Y, Zhou X, Li Y, Zhao D, Liang S, Zhao X, Yang B (2005) A novel mutation at the JK locus causing Jk null phenotype in a Chinese family. Sci China C Life Sci 48:636–640

51. Murta-Nascimento C, Silverman DT, Kogevinas M, Garcia-Closas M, Rothman N, Tardon A, Garcia-Closas R, Serra C, Carrato A, Villanueva C, Dosemeci M, Real FX, Malats N (2007) Risk of bladder cancer associated with family history of cancer: do low-penetrance polymorphisms account for the increase in risk? Cancer Epidemiol Biomarkers Prev 16:1595–1600

52. Neau P, Degeilh F, Lamotte H, Rousseau B, Ripoche P (1993) Photoaffinity labeling of the human red-blood-cell urea-transporter polypeptide components. Possible homology with the Kidd blood group antigen. Eur J Biochem 218:447–455

53. Okubo Y, Yamaguchi H, Nagao N, Tomita T, Seno T, Tanaka M (1986) Heterogeneity of the phenotype Jk (a-b-) found in Japanese. Transfusion 26:237–239

54. Olives B, Mattei MG, Huet M, Neau P, Martial S, Cartron JP, Bailly P (1995) Kidd blood group and urea transport function of human erythrocytes are carried by the same protein. J Biol Chem 270:15607–15610

55. Olivès B, Merriman M, Bailly P, Bain S, Barnett A, Todd J, Cartron J-P, Merriman T (1997) The molecular basis of the Kidd blood group polymorphism and its lack of association with type 1 diabetes susceptibility. Hum Mol Genet 6:1017–1020

56. Olives B, Neau P, Bailly P, Hediger MA, Rousselet G, Cartron JP, Ripoche P (1994) Cloning and functional expression of a urea transporter from human bone marrow cells. J Biol Chem 269:31649–31652

57. Onodera T, Sasaki K, Tsuneyama H, Isa K, Ogasawara K, Satake M, Tadokoro K, Uchikawa M (2013) JK null alleles identified from Japanese individuals with Jk(a− b−) phenotype. Vox Sang

58. Parkin DM (2008) The global burden of urinary bladder cancer. Scand J Urol Nephrol Suppl 42:12–20

59. Pinkerton F, Mermod L, Liles BA, Jack JA, Noades J (1959) The phenotype Jk (a-b-) in the kidd blood group system. Vox Sang 4:155–160

60. Plaut G, Ikin EW, Mourant AE, Sanger R, Race RR (1953) A new blood-group antibody, anti-Jkb. nature 171:431

61. Ploeg M, Aben KK, Kiemeney LA (2009) The present and future burden of urinary bladder cancer in the world. World J Urol 27:289–293

62. Povey S, Morton NE, Sherman SL (1985) Report of the Committee on the Genetic Constitution of Chromosomes 1 and 2. Cytogenet Cell Genet 40:67–106

63. Prager M (2007) Molecular genetic blood group typing by the use of PCR-SSP technique. Transfusion 47:54s–59s

64. Rafnar T, Sulem P, Stacey SN, Geller F, Gudmundsson J, Sigurdsson A, Jakobsdottir M, Helgadottir H, Thorlacius S, Aben KK, Blondal T, Thorgeirsson TE, Thorleifsson G, Kristjansson K, Thorisdottir K, Ragnarsson R, Sigurgeirsson B, Skuladottir H, Gudbjartsson T, Isaksson HJ, Einarsson GV, Benediktsdottir KR, Agnarsson BA, Olafsson K, Salvarsdottir A, Bjarnason H, Asgeirsdottir M, Kristinsson KT, Matthiasdottir S, Sveinsdottir SG, Polidoro S, Hoiom V, Botella-Estrada R, Hemminki K, Rudnai P, Bishop DT, Campagna M, Kellen E, Zeegers MP, de Verdier P, Ferrer A, Isla D, Vidal MJ, Andres R, Saez B, Juberias P, Banzo J, Navarrete S, Tres A, Kan D, Lindblom A, Gurzau E, Koppova K, de Vegt F, Schalken JA, van der Heijden HF, Smit HJ, Termeer RA, Oosterwijk E, van Hooij O, Nagore E, Porru S, Steineck G, Hansson J, Buntinx F, Catalona WJ, Matullo G, Vineis P, Kiltie AE, Mayordomo JI, Kumar R, Kiemeney LA, Frigge ML, Jonsson T, Saemundsson H, Barkardottir RB, Jonsson E, Jonsson S, Olafsson JH, Gulcher JR, Masson G, Gudbjartsson DF, Kong A, Thorsteinsdottir U, Stefansson K (2009) Sequence variants at the TERT-CLPTM1L locus associate with many cancer types. Nat Genet 41:221–227

65. Rafnar T, Vermeulen SH, Sulem P, Thorleifsson G, Aben KK, Witjes JA, Grotenhuis AJ, Verhaegh GW, Hulsbergen-van de Kaa CA, Besenbacher S, Gudbjartsson D, Stacey SN, Gudmundsson J, Johannsdottir H, Bjarnason H, Zanon C, Helgadottir H, Jonasson JG, Tryggvadottir L, Jonsson E, Geirsson G, Nikulasson S, Petursdottir V, Bishop DT, Chung-Sak S, Choudhury A, Elliott F, Barrett JH, Knowles MA, de Verdier PJ, Ryk C, Lindblom A, Rudnai P, Gurzau E, Koppova K, Vineis P, Polidoro S, Guarrera S, Sacerdote C, Panadero A, Sanz-Velez JI, Sanchez M, Valdivia G, Garcia-Prats MD, Hengstler JG, Selinski S, Gerullis H, Ovsiannikov D, Khezri A, Aminsharifi A, Malekzadeh M, van den Berg LH, Ophoff RA, Veldink JH, Zeegers MP, Kellen E, Fostinelli J, Andreoli D, Arici C, Porru S, Buntinx F, Ghaderi A, Golka K, Mayordomo JI, Matullo G, Kumar R, Steineck G, Kiltie AE, Kong A, Thorsteinsdottir U, Stefansson K, Kiemeney LA (2011) European genome-wide association study identifies SLC14A1 as a new urinary bladder cancer susceptibility gene. Hum Mol Genet 20:4268–4281

66. Ranade K, Wu KD, Hwu CM, Ting CT, Pei D, Pesich R, Hebert J, Chen YD, Pratt R, Olshen R, Masaki K, Risch N, Cox DR, Botstein D (2001) Genetic variation in the human urea transporter-2 is associated with variation in blood pressure. Hum Mol Genet 10:2157–2164

67. Rothman N, Garcia-Closas M, Chatterjee N, Malats N, Wu X, Figueroa JD, Real FX, Van Den Berg D, Matullo G, Baris D, Thun M, Kiemeney LA, Vineis P, De Vivo I, Albanes D, Purdue MP, Rafnar T, Hildebrandt MA, Kiltie AE, Cussenot O, Golka K, Kumar R, Taylor JA, Mayordomo JI, Jacobs KB, Kogevinas M, Hutchinson A, Wang Z, Fu YP, Prokunina-Olsson L, Burdett L, Yeager M, Wheeler W, Tardon A, Serra C, Carrato A, Garcia-Closas R, Lloreta J, Johnson A, Schwenn M, Karagas MR, Schned A, Andriole G, Jr., Grubb R, 3rd, Black A, Jacobs EJ, Diver WR, Gapstur SM, Weinstein SJ, Virtamo J, Cortessis VK, Gago-Dominguez M, Pike MC, Stern MC, Yuan JM, Hunter DJ, McGrath M, Dinney CP, Czerniak B, Chen M, Yang H, Vermeulen SH, Aben KK, Witjes JA, Makkinje RR, Sulem

P, Besenbacher S, Stefansson K, Riboli E, Brennan P, Panico S, Navarro C, Allen NE, Bueno-de-Mesquita HB, Trichopoulos D, Caporaso N, Landi MT, Canzian F, Ljungberg B, Tjonneland A, Clavel-Chapelon F, Bishop DT, Teo MT, Knowles MA, Guarrera S, Polidoro S, Ricceri F, Sacerdote C, Allione A, Cancel-Tassin G, Selinski S, Hengstler JG, Dietrich H, Fletcher T, Rudnai P, Gurzau E, Koppova K, Bolick SC, Godfrey A, Xu Z, Sanz-Velez JI, M DG-P, Sanchez M, Valdivia G, Porru S, Benhamou S, Hoover RN, Fraumeni JF, Jr., Silverman DT, Chanock SJ (2010) A multi-stage genome-wide association study of bladder cancer identifies multiple susceptibility loci. Nat Genet 42:978–984

68. Rourk A, Squires JE (2012) Implications of the Kidd blood group system in renal transplantation. Immunohematology 28:90–94
69. Rozman P, Dovc T, Gassner C (2000) Differentiation of autologous ABO, RHD, RHCE, KEL, JK, and FY blood group genotypes by analysis of peripheral blood samples of patients who have recently received multiple transfusions. Transfusion 40:936–942
70. Shokeir M, Ying K, Pabello P (1973) Deletion of the long arm of chromosome no. 7: tentative assignment of the Kidd (Jk) locus. Clin Genet 4:360–368
71. Sidoux-Walter F, Lucien N, Nissinen R, Sistonen P, Henry S, Moulds J, Cartron JP, Bailly P (2000) Molecular heterogeneity of the Jk(null) phenotype: expression analysis of the Jk(S291P) mutation found in Finns. Blood 96:1566–1573
72. Skolnick MH, Willard HF, Menlove LA (1984) Report of the Committee on Human Gene Mapping by Recombinant DNA Techniques. Cytogenet Cell Genet 37:210–273
73. Spector DA, Yang Q, Wade JB (2007) High urea and creatinine concentrations and urea transporter B in mammalian urinary tract tissues. Am J Physiol Renal Physiol 292:F467–F474
74. Sriwanitchrak P, Sriwanitchrak K, Tubrod J, Kupatawintu P, Kaset C, Nathalang O (2012) Genomic characterisation of the Jk(a-b-) phenotype in Thai blood donors. Blood Transfus 10:181–185
75. St-Louis M, Lavoie J, Caron S, Paquet M, Perreault J (2013) A novel JK*02 allele in a French Canadian family. Transfusion 53:3024
76. Tanaka M, Takahahi J, Hirayama F, Tani Y (2011) High-resolution melting analysis for genotyping Duffy, Kidd and Diego blood group antigens. Leg Med (Tokyo) 13:1–6
77. Thakral B, Malhotra S, Saluja K, Kumar P, Marwaha N (2010) Hemolytic disease of newborn due to anti-Jk b in a woman with high risk pregnancy. Transfus Apher Sci 43:41–43
78. Tomar V, Dhingra N, Madan N, Faridi MM (1998) Hemolytic disease of the newborn due to maternal anti-Kidd (anti-Jkb). Indian Pediatr 35:1251–1253
79. Tsai HJ, Hsiao CF, Ho LT, Chuang LM, He CT, Curb JD, Quertermos T, Hsiung CA, Sheu WH (2010) Genetic variants of human urea transporter-2 are associated with metabolic syndrome in Asian population. Clin Chim Acta 411:2009–2013
80. Vaarala MH, Hirvikoski P, Kauppila S, Paavonen TK (2012) Identification of androgen-regulated genes in human prostate. Mol Med Rep 6:466–472
81. Vucelic D, Savic N, Djordjevic R (2005) Delayed hemolytic transfusion reaction due to anti-Jk(a). Acta Chir Iugosl 52:111–115
82. Wester ES, Johnson ST, Copeland T, Malde R, Lee E, Storry JR, Olsson ML (2008) Erythroid urea transporter deficiency due to novel JKnull alleles. Transfusion 48:365–372
83. Wester ES, Storry JR, Olsson ML (2011) Characterization of Jk(a+ (weak)): a new blood group phenotype associated with an altered JK*01 allele. Transfusion 51:380–392
84. Wolff EM, Liang G, Jones PA (2005) Mechanisms of disease: genetic and epigenetic alterations that drive bladder cancer. Nat Clin Pract Urol 2:502–510
85. Woodfield D, Douglas R, Smith J, Simpson A, Pinder L, Staveley J (1982) The Jk (a− b−) phenotype in New Zealand Polynesians. Transfusion 22:276–278
86. Wright EM, Loo DD, Hirayama BA (2011) Biology of human sodium glucose transporters. Physiol Rev 91:733–794
87. Wu X, Ye Y, Kiemeney LA, Sulem P, Rafnar T, Matullo G, Seminara D, Yoshida T, Saeki N, Andrew AS, Dinney CP, Czerniak B, Zhang ZF, Kiltie AE, Bishop DT, Vineis P, Porru S, Buntinx F, Kellen E, Zeegers MP, Kumar R, Rudnai P, Gurzau E, Koppova K, Mayordomo

JI, Sanchez M, Saez B, Lindblom A, de Verdier P, Steineck G, Mills GB, Schned A, Guarrera S, Polidoro S, Chang SC, Lin J, Chang DW, Hale KS, Majewski T, Grossman HB, Thorlacius S, Thorsteinsdottir U, Aben KK, Witjes JA, Stefansson K, Amos CI, Karagas MR, Gu J (2009) Genetic variation in the prostate stem cell antigen gene PSCA confers susceptibility to urinary bladder cancer. Nat Genet 41:991–995

88. Yan L, Zhu F, Fu Q (2003) Jk(a-b-) and Kidd blood group genotypes in Chinese people. Transfusion 43:289–291

89. You G, Smith CP, Kanai Y, Lee WS, Stelzner M, Hediger MA (1993) Cloning and characterization of the vasopressin-regulated urea transporter. Nature 365:844–847

90. Zemunik T, Boban M, Lauc G, Jankovic S, Rotim K, Vatavuk Z, Bencic G, Dogas Z, Boraska V, Torlak V, Susac J, Zobic I, Rudan D, Pulanic D, Modun D, Mudnic I, Gunjaca G, Budimir D, Hayward C, Vitart V, Wright AF, Campbell H, Rudan I (2009) Genome-wide association study of biochemical traits in Korcula Island, Croatia. Croat Med J 50:23–33

91. Zhang RB, Verkman AS (1991) Water and urea permeability properties of Xenopus oocytes: expression of mRNA from toad urinary bladder. Am J Physiol 260:C26–C34

Chapter 13
Active Urea Transport in Lower Vertebrates and Mammals

Lise Bankir

Abstract Some unicellular organisms can take up urea from the surrounding fluids by an uphill pumping mechanism. Several active (energy-dependent) urea transporters (AUTs) have been cloned in these organisms. Functional studies show that active urea transport also occurs in elasmobranchs, amphibians, and mammals. In the two former groups, active urea transport may serve to conserve urea in body fluids in order to balance external high ambient osmolarity or prevent desiccation. In mammals, active urea transport may be associated with the need to either store and/or reuse nitrogen in the case of low nitrogen supply, or to excrete nitrogen efficiently in the case of excess nitrogen intake. There are probably two different families of AUTs, one with a high capacity able to establish only a relatively modest transepithelial concentration difference (renal tubule of some frogs, pars recta of the mammalian kidney, early inner medullary collecting duct in some mammals eating protein-poor diets) and others with a low capacity but able to maintain a high transepithelial concentration difference that has been created by another mechanism or in another organ (elasmobranch gills, ventral skin of some toads, and maybe mammalian urinary bladder). Functional characterization of these transporters shows that some are coupled to sodium (symports or antiports) while others are sodium-independent. In humans, only one genetic anomaly, with a mild phenotype (familial azotemia), is suspected to concern one of these transporters. In spite of abundant functional evidence for such transporters in higher organisms, none have been molecularly identified yet.

L. Bankir (✉)
INSERM UMRS 1138, Centre de Recherche Des Cordeliers, Paris, France
e-mail: lise.bankir@inserm.fr

L. Bankir
Université Pierre et Marie Curie, Paris, France

List of Abbreviations

AUT	Active urea transporter
CD	Collecting duct
FE_{urea}	Fractional excretion of urea
GFR	Glomerular filtration rate
IMCD	Inner medullary collecting duct
P_{urea}	Plasma urea concentration
U/P urea	Ratio of urine urea concentration to plasma urea concentration
UT	Facilitated urea transporter

Introduction

Nitrogen is a major element of all forms of life. Amino acids are the building
blocks of proteins, an abundant constituent of all living organisms. Thus, nitrogen
intake is a crucial issue. Urea is a small organic molecule with two nitrogen atoms.
Some lower organisms can use urea as a source of nitrogen when they possess ure-
ase, an enzyme able to hydrolyze urea into ammonia and carbon dioxide. Higher
organisms face the need either to store and reuse nitrogen in the case of low sup-
ply, or to excrete nitrogen efficiently in the case of excess intake, because there is
no way to store nitrogen in the body. Moreover, all nitrogen metabolism end-prod-
ucts are toxic to some extent. However, in some animal groups, accumulation of
urea in body fluids has been used as a way to prevent desiccation or to counteract
the high osmolarity of seawater.

All biological membranes have a relatively low permeability to urea, a highly
hydrophilic compound. Specific systems of urea transport have been developed
that can be found across the entire tree of living beings, from unicellular organ-
isms up to mammals. They include both facilitated urea transporters (UTs) and
active (energy-dependent) urea transporters (AUTs) (Fig. 13.1). Up to now, a num-
ber of facilitated UTs have been identified and cloned (see Chap. 4). A few active
transporters, able to raise the concentration of urea in unicellular organisms above
that in the surrounding fluid, have been identified and cloned. Other active trans-
porters, able to induce vectorial transport across an epithelium in higher organ-
isms, have been well characterized functionally, but none of them has been cloned
and molecularly identified so far.

Functional studies suggest that there are at least two classes of AUTs with dif-
ferent characteristics. Some AUTs probably have a high capacity, but are able to
establish only a relatively modest transepithelial concentration difference (about
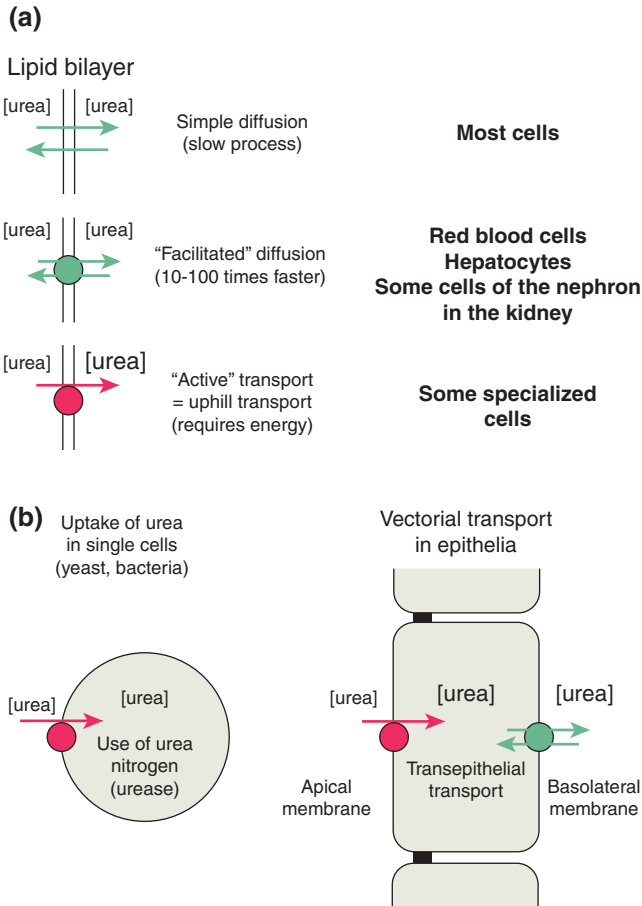
Fig. 13.1 The different ways of urea transport. **a** Urea can be moved through cell membranes in three different ways: (1) Simple diffusion through the lipid bilayer, allowing equilibration of urea concentration between the two compartments. This diffusion is relatively slow because urea is a very hydrophilic molecule. (2) Diffusion along a urea concentration gradient through a facilitated urea transporter inserted into the lipid bilayer. This allows a much faster equilibration between the two compartments. In some epithelia, the transporter is expressed on both the apical and the basolateral membranes of the cells, ensuring a rapid transepithelial flux of urea (3) Active (or secondary active) transport through a protein (or protein complex) that is coupled to an energy source and is thus able to raise urea concentration in one compartment above that in the other, i.e., an "uphill" transport against an unfavorable concentration difference. **b** In single cells (*left*), such an active transport allows an uptake of urea from the medium and is usually associated with the expression of urease in the cell. In epithelial cells (*right*), a facilitated transporter is often located on the opposite membrane, thus allowing transepithelial transport

fivefold to tenfold). See Table 13.1. They may serve either to secrete or to reabsorb urea depending on the function of the tissues in which they are expressed. Other AUTs probably have a low capacity, but are able to maintain a high transepithelial concentration difference (100–1,000-fold) that has been created by another

Table 13.1 Two different families of active urea transporters (*AUTs*)

A. Low affinity, high capacity AUTs		
Animal group	*Organ/localization*	*Function*
Elasmobranchs	Intestine? Kidney?	Absorption/reabsorption of urea?
Some frogs (Amphibians)	Kidney tubules of some frogs	Secretion of urea for urea concentration in urine above its concentration in plasma
Mammals. Ruminants and herbivores. Rats (and possibly humans) when fed a low protein diet	Upper part of IMCD	Reabsorption of urea for nitrogen conservation
Mammals. More likely in carnivores and omnivores	Pars recta of the proximal tubule	Secretion of urea for improved urea excretion and concentration in the urine
Mammals	Testis (seminiferous tubules)?	Secretion of urea driving fluid into the tubule
B. High affinity, low capacity AUTs		
Animal group	*Organ/localization*	*Function*
Marine elasmobranchs	Gill	Conservation of high urea concentration in extracellular fluids
Some terrestrial toads (Amphibians)	Ventral skin	Conservation of high urea concentration in extracellular fluids
Mammals	Terminal IMCD + ureter and bladder urothelium?	Conservation of high urea concentration in bladder urine

A Low-affinity, high-capacity AUTs, able to create a modest difference in urea concentration across an epithelium. By its action, the transporter allows urea to reach a concentration a few times higher (5 ~ 10 fold) in a structure than in the surrounding interstitium. B High-affinity, low-capacity AUTs, able to prevent the dissipation of a large urea concentration difference across an epithelium. The high urea concentration in the fluid is created by another mechanism in another organ (liver for elasmobranchs and toads, kidney in mammals). The AUTs continuously reclaims urea that could diffuse away through epithelia that are in contact with fluids exhibiting a much lower urea concentration (100- ~ 1,000-fold)

IMCD inner medullary collecting duct

mechanism or in another organ (Table 13.1). Functional characterization of these transporters shows that some are coupled to sodium (symports or antiports) while others are sodium-independent. The next sections of this chapter are organized according to the function and localization of these transporters, not to their biochemical characteristics.

Two Notes About Osmolality, Osmolarity, and Osmotic Pressure

1. Although most modern osmometers measure osmolalities (in mosm/kg water), we will prefer in this chapter to use the term osmolarity (in mosm/L) because

living cells sense the concentration of osmoles per unit volume of extra- or intracellular fluids, not per unit weight of these fluids. In any case, in most biological tissues, the numerical difference between osmolality and osmolarity is small because, in the range of solute concentrations observed in living beings, the density of the solutions is not very different from that of pure water.

2. Osmolarity (or osmolality) should be preferred to "osmotic pressure" because this physical osmotic force is not at all a "pressure." It was named in this way because, for a long time, osmolarity was evaluated indirectly as a hydrostatic pressure. In a U-shaped tube, the unknown solution was placed in one side of the tube, separated from pure water in the other side of the tube by a semipermeable membrane. The osmoles present on one side attracted some water through the semipermeable membrane, and this resulted in a difference in height between the two columns. This difference in pressure was expressed in mm of height along the column (also an old way to measure pressures). Now, we should abandon the term "osmotic pressure" and use only "osmolarity" (or osmolality).

Active Urea Transport in Lower Organisms

Some unicellular organisms can use urea as a source of nitrogen by the combination of two associated adaptations. First, they express in their membrane an AUT that can take up urea from the surrounding medium, even if urea is present at very low concentrations (<1 mM). Second, they express in their cytoplasm the enzyme urease that catalyses the hydrolysis of urea into ammonia and carbon dioxide, ammonia being then used for amino acid synthesis. Active urea transport and the use of urea nitrogen for growth have been characterized in the following organisms.

- Plants (e.g., the H$^+$, urea cotransporter **AtDUR3** in *Arabidopsis,* and OsDUR3 in rice) [85, 86, 94, 151].
- Bacteria (e.g., **FmdC** in *Methylophilus methylotrophus* and **Dur3** i*n Candida albicans*) [71, 102, 108].
- Cianobacteria (**urtABC**, an ABC-type transporter that is regulated by the concentration of urea in the medium) [147].
- Fungi (e.g., **PiDur3** in *Paxillus involutus* and **UreA** in *Aspergillus nidulans*) [1, 104, 114].
- Yeast (e.g., **Dur3** in *Saccharomyces cerevisiae*) [41]. Some strains of yeast that are defective for this AUT present a reduced growth rate when grown on 10 mM urea [141].

As an example, Fig. 13.2 shows active urea uptake mediated by PiDur3 in a fungus in the absence or presence of acetohydroxamate acid, a urease inhibitor [104]. A phylogenetic tree has been built (Fig. 13.3), based on AUTs from plants, fungi, and homologues [1].
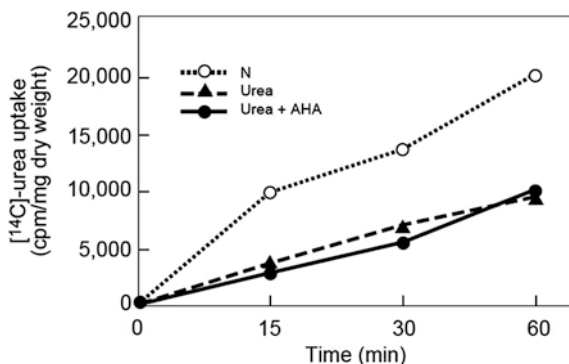
Fig. 13.2 Kinetics of [^{14}C]-urea uptake by the fungus *Paxillus involutus*. After a preliminary period of nitrogen starving, fungal colonies were transferred to a culture medium containing either no urea (-N), or [^{14}C]-urea (1 mM) alone, or with acetohydroxamic acid (*AHA*, 5 mM). Accumulation of radioactive urea was followed for 1 h. Reproduced from [104]
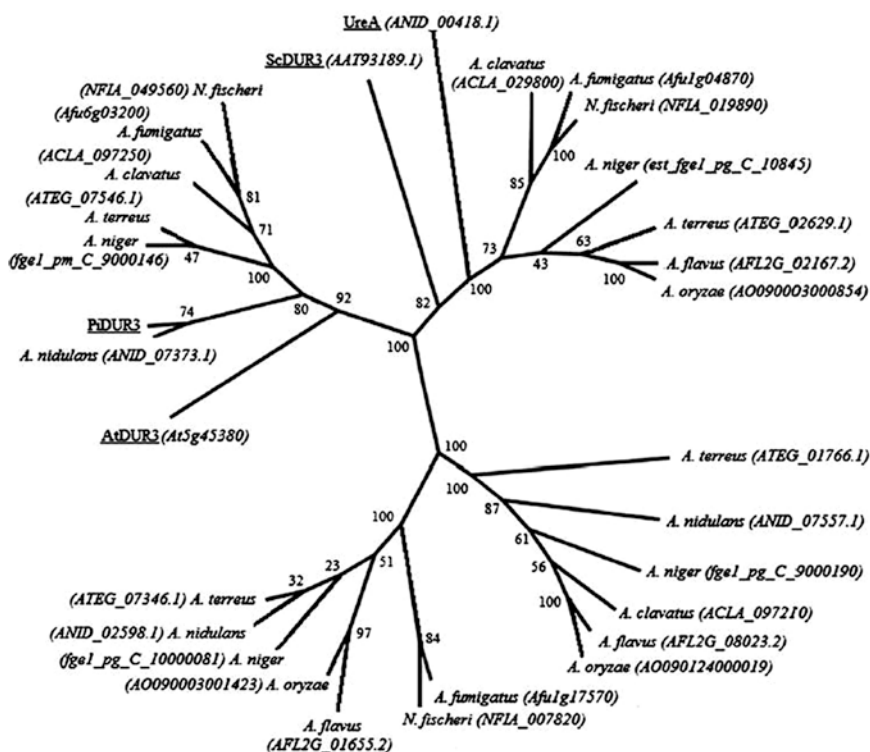
Fig. 13.3 Phylogenetic tree of characterized urea transporters from plants (AtDUR3), fungi (UreA, PiDur3, ScDur3), and homologues in the genus *Aspergillus*. Reproduced from [1]

Active Urea Transport in Lower Vertebrates

Urea is not considered to be a source of nitrogen in vertebrates, except in those that host some bacteria possessing the enzyme urease, which are able to break down urea into ammonia and carbon dioxide (ruminants, see further). Known cases of active urea transport in vertebrates are associated with three different functions. One is the control of blood and extracellular osmolarity in order to conserve urea in body fluids at a relatively high concentration because, in some cases, urea plays the role of an internal osmotic buffer. This is the case in marine animals living in hyperosmotic seawater such as elasmobranchs, and in some terrestrial toads or frogs living in a hot dry environment. The two other functions are related to nitrogen balance in mammals with either the aim to conserve nitrogen by reabsorption of urea in the kidney (for animals feeding on a protein-poor diet), or to facilitate its excretion by active secretion into the urine (for animals feeding on a protein-rich diet). No active urea transport has been reported in reptiles and birds, two groups of animals that are uricotelic (excreting nitrogen wastes as uric acid), not ureotelic, and in which erythrocytes are not highly urea-permeable because they do not express a facilitated UT (like there is in mammals) [93]. Although there is ample functional evidence for the existence of active urea transport in several tissues of pre-vertebrates (elasmobranchs) and lower vertebrates (fish, amphibians), no AUT has been cloned yet.

Elasmobranch Gills

In elasmobranch fishes (rays and sharks), the internal milieu has a high urea concentration (350–500 mM) [26, 59], which contributes to balance the high osmolarity of the surrounding seawater. The transepithelial concentration difference for urea is massive, and thus, urea is permanently at risk of being lost through the gills, which are highly vascularized and exhibit a large area of contact with seawater. Anatomical and functional studies in the dogfish shark (*Squalus acanthias*) have revealed unique characteristics [47]. The basolateral membrane of the gill epithelium shows high levels of cholesterol so that this tissue exhibits the highest reported cholesterol-to-phospholipid molar ratio, probably contributing to reduce solute diffusion through this epithelium. Urea transport studies have revealed the existence, in the basolateral membrane, of phloretin-sensitive, sodium-coupled, secondary active urea transport. A Na^+: urea antiporter is energized by the continual removal of Na^+ from the gill via basolateral Na^+/K^+ATPase [47]. See Fig. 13.4c. This transport system actively brings urea from the fluid lining the gill epithelial cells back into the blood and thus, along with the specialized composition of the membrane, minimizes passive urea leakage across the gills. Elegant perfusion studies by Wood et al. demonstrated that the apical membrane of the gill epithelial cells is the limiting factor in maintaining gill urea impermeability,
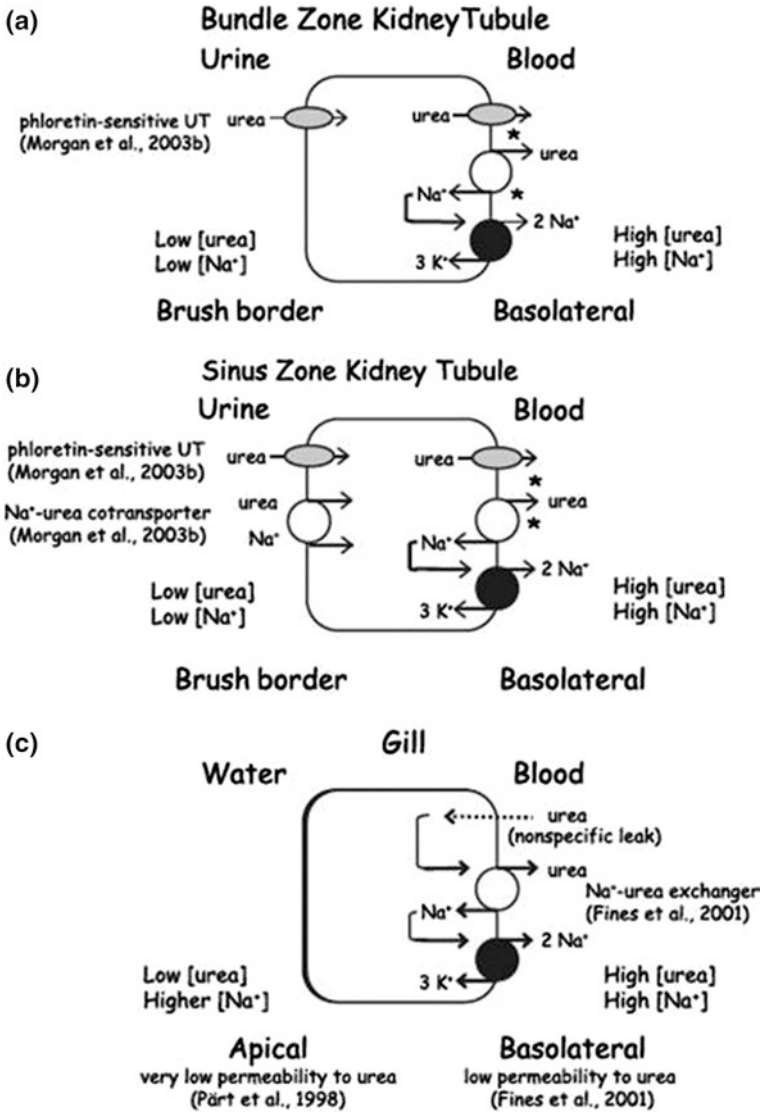
Fig. 13.4 Hypothetical urea transport model of the elasmobranch kidney tubule and gill. Reproduced from [101]. **a** and **b** Kidney tubule in the bundle zone and sinus zone, respectively. Urea would cross the brush border membrane of a sinus zone tubular cell via a Na^+-urea cotransporter and a phloretin-sensitive UT and of a bundle zone tubular cell via a phloretin-sensitive UT. **c**. Gill. In the gill, urea would leak across the basolateral membrane and enter the gill cell. Urea would be pumped out basolaterally in exchange for Na^+, driven by the Na^+, K^+ ATPase. The apical membrane has a very low permeability to urea. Asterisks denote hypothesized transporters in the basolateral membrane that have not been resolved experimentally

suggesting that a urea back-transporter operates at the apical membrane. This transporter can be competitively inhibited by thiourea and acetamide [153]. This enables elasmobranchs to retain urea in the face of an extremely high blood-to-water urea diffusion gradient.

In these cartilaginous fishes, urea may also be lost in the urine, and reabsorption of filtered urea by the kidney is essential for retaining high levels of urea in their internal milieu. The kidney exhibits an extremely complex structure [62, 63], and at least 5 closely related isoforms of facilitated UTs have been identified in selective segments of the nephron and collecting system [72, 73, 75, 136]. But it seems likely that urea conservation by the kidney in elasmobranchs does not rest only on facilitated transporters and countercurrent systems. Experiments in isolated brush-border membrane vesicles of *Raja erinacea* suggest the existence of two different, likely active, transport processes responsible for an uptake of urea (i.e., urea reabsorption) in the elasmobranch kidney [105, 106]. Active urea reabsorption has also been suspected to take place in some parts of the collecting system [128, 131]. See Fig. 13.4a, b (reproduced from [101]).

Active urea transport may also occur in the intestine of marine elasmobranchs. In the dogfish shark, feeding caused a marked switch from a low rate of urea secretion to net urea absorption. This intestinal urea transport occurred at rates comparable to urea reabsorption reported in gills and kidneys and was apparently active [4, 92].

Such active urea transport among marine animals is unique to elasmobranchs. It does not concern teleost fish that do not have a high urea content in their internal milieu [100]. However, a few fish are ureotelic and excrete urea by letting it diffuse through facilitated UTs in the gills, sometimes in a pulsatile fashion, but this does not require active transport [101, 152].

Active Urea Reabsorption in the Skin of Some Terrestrial Amphibians

Some amphibians live in terrestrial biotopes with a high ambient salinity (*Bufo viridis or marinus, Xenopus laevi, Rana crancrivora*). They accumulate urea in their body fluids up to a relatively high concentration (up to 100 mM) in order to maintain their fluid balance (although less high than in marine elasmobranchs) [74, 133]. This urea may be lost by diffusing through their ventral skin that is in contact with the soil or through their skin when immersed in saline water. This ventral skin exhibits a specialized anatomical structure and performs an active, saturable, urea reabsorption that has been well demonstrated in vitro [39, 79, 87, 117]. Adaptation to salty water (100 mM NaCl solution) increases active transport of urea in the skin, and a correlation between the degree of active urea transport across the skin and the capacity of the species to endure dehydrating conditions has been described [53]. This urea transport is energy-dependent and most likely

includes a two-step process [87]. Whether this active urea reabsorption is coupled to sodium or proton transport has been a matter of debate 2–3 decades ago [40, 118, 142, 143] and has not been reevaluated recently to our knowledge.

Active Urea Secretion in the Renal Tubule of Some Frogs

Most fresh water amphibians excrete nitrogen as ammonia that diffuses freely in the water. But a few of them, such as *Rana catesbeinana, Rana pipiens*, *and Rana clamitans,* are ureotelic. Although they are unable to concentrate urine as a whole, urea may be concentrated in their urine more than in the internal milieu, while other solutes are less concentrated. Urea handling by the frog kidney has been the matter of several studies during the years 1950–1975 [27, 48, 49, 95, 96, 130], but did not seem to raise much interest in recent years. Forster showed that urea excretion largely exceeds the amount of urea filtered, due to a saturable urea secretion [48]. Urea clearance can be seven to ten times higher than the GFR [27]. The relative concentration of urea in collecting duct and urine is roughly five to six times higher than that of inulin. An active secretion of urea likely takes place in the proximal and/or distal tubules [130]. As a result of active pumping, kidney slices from *Rana catesbeiana* can accumulate urea to a concentration up to 10 times that of the surrounding fluid [112]. The active UT is probably located in the basolateral membrane of the tubules and could be analogous to that suspected in the mammalian pars recta (see further). Urea secretion results in a very low concentration of urea in the blood and a high urine/plasma concentration ratio. As proposed by Long, the ability to secrete urea and the resulting low plasma urea concentration reduce the osmotic gradient between the frog's interior milieu and the surrounding fresh water [96]. This minimizes the influx of water and thus the energy needed to excrete solute-free water. This situation is opposite to that prevailing in elasmobranchs living in seawater.

Active Urea Transport in Mammals

Mammals excrete most of their nitrogenous wastes in the form of urea. Their urea excretory needs depend on the protein content of their diet and on their eating behavior. Herbivores have a relatively low protein intake and thus need to conserve nitrogen rather than to excrete it. On the opposite, protein intake is quite high in carnivores. But because of their discontinuous large meals, they need to efficiently excrete large loads of urea, alternating with periods of fasting during which they may need to conserve nitrogen. Omnivores, such as rodents, pigs, and humans, who exhibit an intermediate situation with several meals per day, have a more regular need for nitrogen excretion.

The plasma urea level in mammals is kept at a relatively low level (3–10 mM) so that, in carnivores and omnivores, urea is concentrated in the urine far above

its concentration in plasma and body fluids in order to be excreted in a reasonable amount of water. However, there are marked species differences in the urine-to-plasma ratio of urea concentration associated with differences in body size and other factors (Table 13.2). In some desert-adapted rodents, urine urea concentration can be 500-fold higher than that in plasma [11, 14]. Urea is very soluble and can thus be concentrated without risk of precipitation and kidney stones, contrary to uric acid.

Most recent textbooks of renal physiology and nephrology do not include a specific chapter on urea excretion and its possible regulation, although urea represents about 40 % of all urinary solutes in humans (on a Western-type diet) and even more in laboratory rodents [156]. It is usually assumed that urea is freely filtered in the glomeruli and that a variable proportion is reabsorbed passively by diffusion along the nephrons. This reabsorption depends on the urine flow rate. With slower flow and higher concentration, more urea is reabsorbed in the collecting duct, partly because some urea is driven by simple diffusion along the whole CD, due to a greater transepithelial concentration difference and a longer contact time, and partly because of the facilitated diffusion that occurs in the terminal IMCD where the vasopressin-dependent UTs (UT-A1, and UT-A3) are expressed (see Chap. 4). However, as already recognized more than 50 years ago [33, 126, 127], this is too simplistic of a

Table 13.2 Water, urea, and sodium handling in mice, rats, and humans

		Mouse	Rat	Human
Body weight (BW)	kg	0.03	0.3	70
Kidney weight	g/kg BW	13	6.6	4.3
Water and osmoles				
Urine osmolality	mosm/kg H_2O	2,650	1,500	650
Urine output	ml/d	2	12	1,400
Osmolar excretion	mosm/d	5.3	18	900
U/P osmolality	–	8.8	5	2.2
Urea				
Daily urea excretion[a]	mmol/d	3.8	7.5	400
Daily urea excretion	mmol/d/kg BW	130	25	5.7
Plasma urea concentration	mmol/L	9	5	5
Urine urea concentration	mmol/L	1,800	700	285
U/P urea	–	200	140	60
Sodium				
Daily Na excretion[a]	mmol/d	0.2	1.5	130
Daily Na excretion	mmol/d/kg BW	6.6	5	1.8
Plasma Na concentration	mmol/L	140	140	140
Urine Na concentration	mmol/L	60	125	95
U/P Na	–	0.45	0.9	0.68

[a]The daily excretions of urea and sodium depend on the protein and sodium content of the diet, respectively. The figures given here are rounded off and apply to healthy humans consuming a Western-type diet and to normal rats and mice fed a usual rodent diet (values collected from several experimental studies and clinical investigations)

concept. From her pioneer studies, Bodil Schmidt-Nielsen concluded that, in addition to this flow- and vasopressin-dependent reabsorption, urea excretion must be regulated [126, 127]. Both active urea reabsorption and active urea secretion may occur through different transport processes, for the sake of either nitrogen salvaging or more efficient urea excretion, respectively. This is suggested by the very different fractional excretions of urea observed when dogs or sheep are fed low or high protein diets, respectively [125] (Fig. 13.5). A tendency for such regulation is also apparent in humans, but to a much lesser extent [107]. As explained in more detail below, the experimental results suggest that the regulation associated with nitrogen conservation is a slow process, whereas the regulation associated with efficient urea excretion is rapid and probably under the control of peptide hormones.

Urea Reabsorption in the Kidney, As a Strategy for Nitrogen Conservation

Although mammals cannot breakdown urea because they do not express urease in any organ, some mammals can reuse urea nitrogen by virtue of two associated adaptations (Figs. 13.5 and 13.6). One is the ability to reabsorb urea actively from the CD ("uphill" transport), thus reducing its excretion; the other is hosting in their digestive tract bacteria that express urease and are thus able to hydrolyse urea, thus releasing carbon dioxide and ammonia. The former will pass into the blood and be excreted by the lungs, whereas the latter will have two possible fates. Ruminants express a facilitated UT in their rumen [134, 140]. The bacteria will use urea nitrogen diffusing from blood into the rumen to build their own amino acids and proliferate [81].
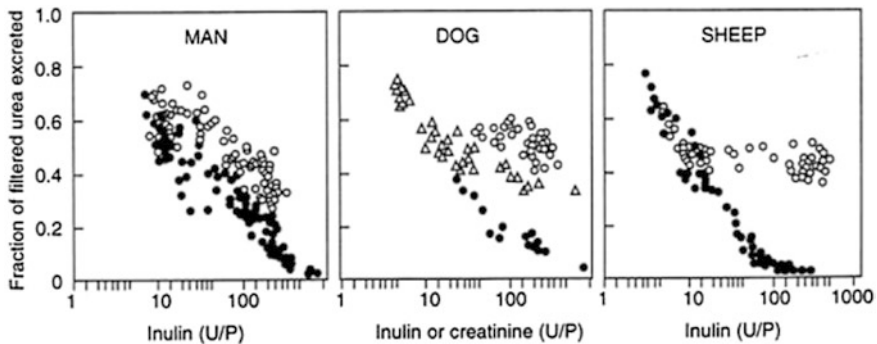
Fig. 13.5 Effects of varying protein intake on the fractional excretion of urea (FE_{urea}), according to the intensity of urine concentration in man, dog, and sheep. Urine concentration is displayed as the urine-to-plasma ratio of inulin or creatinine concentrations (shown in logarithmic scale). Open symbols: high (*circles*) or normal (*triangles*) nitrogen intake. Closed symbols: low nitrogen intake. The low nitrogen intake lowers FE_{urea} in all three species, but the most dramatic effect is seen in the sheep (ruminant). Redrawn and adapted from [125]
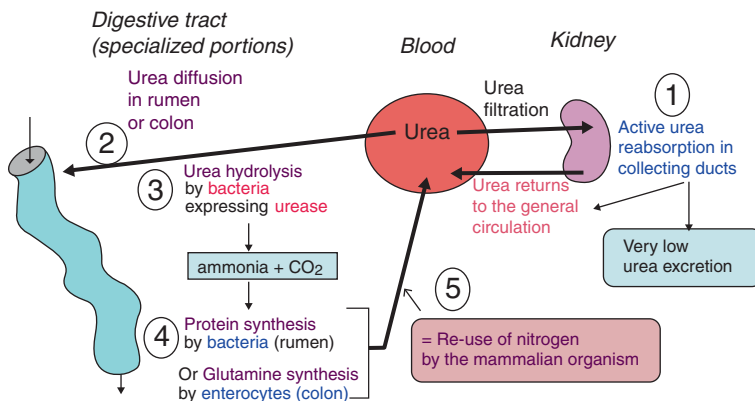
Fig. 13.6 Pathway for reuse of urea nitrogen in mammals (=nitrogen conservation). Filtered urea is reabsorbed in the early inner medullary collecting duct (as shown in low-protein fed rats) by an active transport and returned to the blood, thus reducing its renal excretion (*1*). Urea diffuses passively through facilitated UTs in the digestive tract (rumen in ruminants, or colon in other species) (*2*) where it is hydrolyzed into ammonia and CO_2 by microorganisms expressing urease (*3*). Ammonia nitrogen can be reused for protein synthesis (*4*), thus contributing to nitrogen conservation (*5*)

The bacteria will subsequently be digested in the stomach, and their amino acids absorbed in the intestine, thus making nitrogen available again for the host. In other mammals (including humans), the bacteria able to hydrolyse urea are located in the colon, which expresses a facilitated UT [34, 35, 66, 67, 97, 135, 139, 140]. Ammonia resulting from urea breakdown will be used by the enterocytes of the host to make glutamine that can be further used for nitrogen metabolism (Fig. 13.6).

Because of the very low fractional excretion of urea in sheep, Bodil Schmidt-Nielsen had assumed that active urea reabsorption occurred in their kidney [126, 127]. Sands and colleagues undertook several studies to characterize this urea reabsorption associated with low protein intake. They observed that active urea reabsorption can be induced in rats by feeding them a low protein diet for several weeks (Fig. 13.7). Using microperfusion of isolated segments of the inner medullary collecting duct (IMCD), they showed that this active absorption occurs only in the early portion of the IMCD (closest to the outer medulla), increases with time up to a maximum after 3 weeks, depends on the presence of sodium in the lumen (but not in the bath), and can be inhibited by ouabain [68–70, 76, 78]. This suggests that a low protein diet induces the synthesis and insertion of a sodium–urea cotransporter located in the apical membrane of the early IMCD. Whether this active transport extends into the outer medullary CD has not been evaluated.

In ruminants, the intensity of urea nitrogen recycling is regulated according to the protein content of the diet. With an increasing level of protein intake, nitrogen recycling is reduced along with reductions in urea reabsorption in the kidney, ruminal wall urease activity, and abundance of ruminal facilitated UT [99, 134].

Attempts to clone the active transporter of the IMCD responsible for the urea reabsorption in the rat kidney by either expression cloning or subtracting hybridization have not been successful [7, 30, 123].

Fig. 13.7 Net urea flux measured in isolated perfused initial inner medullary collecting ducts from rats switched from 18 % (week 0) to 8 % protein diet for 1–4 weeks. The capacity to reabsorb urea increases with time and reaches a plateau after 3 weeks. Redrawn after [123]
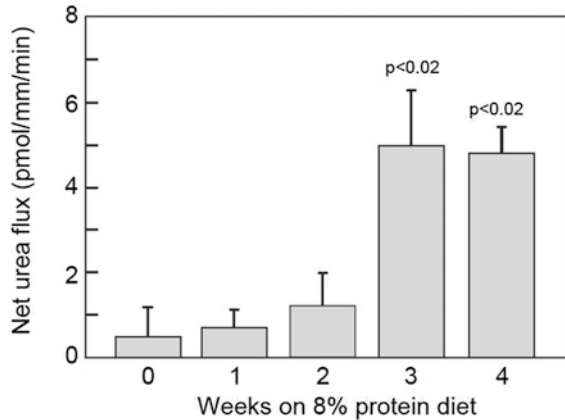
Active urea absorption can also be induced in the same segment of the CD by chronic furosemide treatment. In that case, this transport is stimulated by vasopressin, depends on the presence of sodium in the bath (but not in the perfusate), and is inhibitable by both phloretin and ouabain [77]. These observations suggest that the transporter involved in this case is an absorptive "sodium–urea countertransporter" located in the basolateral membrane of the early IMCD.

Urea Secretion in the Kidney, Leading to Improved Nitrogen Excretion

It has been known for a long time that there is an addition of urea in the loop of Henle of superficial nephrons. This was assumed to result from facilitated diffusion of urea from ascending vasa recta into the thin limbs of Henle's loops that express the facilitated transporter UT-A2 in their lower half. This "recycling" of urea from blood to tubule was considered to play a significant role in the sequestration of urea in the inner medulla [84, 156]. This classical view, which prevailed for several decades, had to be revised when it was observed that mice with genetic deletion of UT-A2 do not show a urine-concentrating defect [146]. Thus, urea addition has to occur in some other place in the loop of Henle. *Note: the "loop of Henle" in micropuncture experiments includes all nephron segments comprised between the late proximal tubule and the early distal tubule accessible at the kidney surface: thus, it includes the pars recta of the proximal tubule, the thin descending limb and the medullary and cortical portions of the thick ascending limb, plus a very short piece of the early distal convoluted tubule.*

On the other hand, several authors have concluded from their observations that active, energy-dependent urea secretion probably occurs in the mammalian kidney [19, 80, 122]. Although 50 % of filtered urea is reabsorbed in the proximal convoluted tubule in the cortex at any level of urine concentration [6], fractional

excretion of urea above 50 % has been reported in a number of studies [32] (see Table 1 in [15]) (Figs. 13.5, 13.8b, 13.10), suggesting that urea is added downstream of the late proximal convoluted tubule. Values above 100 % have even occasionally been reported in rats (Table 13.3), dogs, and humans (see review in [156]) and more recently in mice [45, 156]. Obviously, only a net tubular secretion of urea can account for these observations. This secretion most probably takes place in the pars recta of the proximal tubule [5, 18, 65]. Actually, a modest but significant rate of urea secretion has been found in isolated cortical and medullary pars recta of the rabbit [80]. Studies of rabbit cortical pars recta did not confirm this active transport [82]. However, active secretion is not likely in a herbivore such as the rabbit. Unfortunately, similar studies in pars recta of rats or mice are lacking. However, several authors reported an accumulation of urea in rat cortical slices or in rat medullary rays that suggest active urea uptake by proximal tubule cells [60, 112, 119–121].

In dogs (a carnivore that has a greater load of urea to excrete), urea excretion rate is much greater after a protein meal than after an equivalent infusion of urea, suggesting a specific regulation of this excretion (Fig. 13.8a) [111]. Fractional excretion of urea rises markedly after a protein meal, an effect also reproduced by a glucagon infusion (Fig. 13.8b) [2, 3, 83]. This suggests that glucagon, a hormone known to be secreted after a protein meal, may regulate the intensity of the active urea secretion [15].

Additional evidence for active urea secretion comes from micropuncture studies in rats. The fraction of the filtered load of urea remaining in the last accessible portion of the proximal tubule is about 50 %, whatever the intensity of urine concentration (Fig. 13.9a) [6]. The much higher fraction of urea seen in the early distal tubule means that a marked addition of urea occured in the loop of Henle (between the late proximal and the early distal tubules). However, when solute transport was selectively impaired in the pars recta by cisplatin treatment, the net addition of urea in the loop, observed in normal rats, was abolished and even reversed to a net reabsorption (Fig. 13.9b) [122]. This strongly suggests that the addition of urea into the loop of Henle, previously assumed to take place in the thin descending limb, is rather due to an active secretion into the pars recta.

Active urea secretion probably also occurs in the human kidney. This is suggested by the rare genetic anomaly resulting in azotemia without renal failure [5, 36, 65]. The affected subjects exhibit a selective threefold to fourfold elevation in plasma urea concentration without any other sign of renal dysfunction. The relationship between fractional urea excretion and urine flow rate is shifted down to 30–50 % lower values (Fig. 13.10). This suggests that a large fraction of the excreted urea in normal subjects is due to a tubular process that is missing in these subjects. The defect is best explained by a mutation invalidating the function of a urea transporter contributing to secrete urea in the pars recta of the proximal tubule [15, 58].

Altogether, these observations strongly suggest that active urea secretion in the pars recta is part of normal urea handling by the mammalian kidney. Although it has not been widely accepted up to now, it is not surprising to consider that urea is added to the tubular lumen by active secretion in order to improve the efficiency of its excretion, as is the case for other nitrogenous wastes (uric acid, ammonia). Figure 13.11 depicts the handling of urea according to this new concept [15]. Urea is
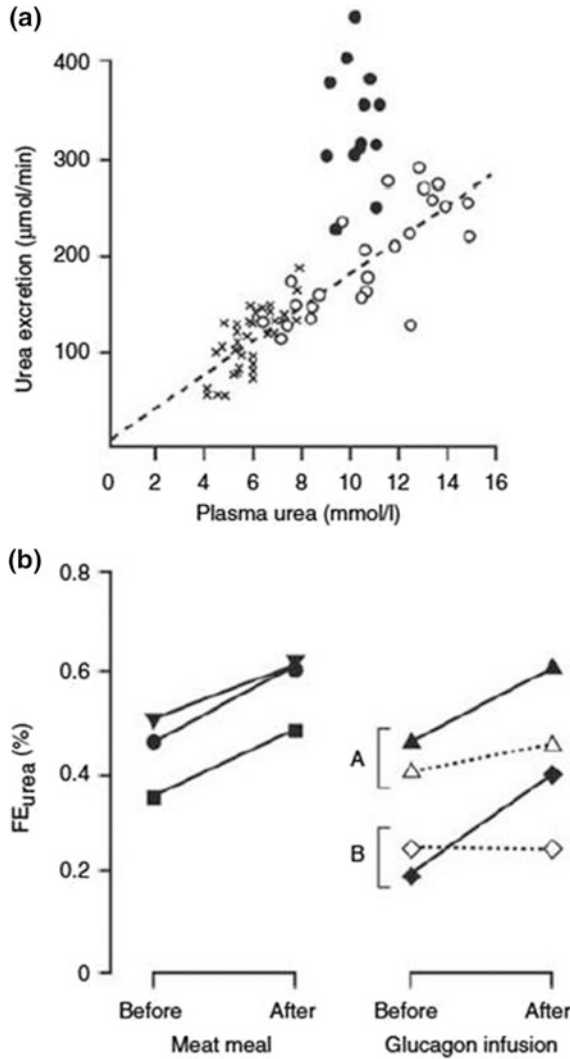
Fig. 13.8 Acute regulation of urea excretion. **a** Relationship between urea excretion and plasma urea concentration in one dog studied in three different conditions (8 ~ 10 experiments in each condition): control (crosses), after a meat meal (closed *circles*) and after an infusion of urea bringing the same amount of nitrogen (open *circles*). The influence of the protein meal clearly differed from that of the urea infusion. Reproduced from O'Connor and Summerill [111]. **b** *Left* influence of a protein meal on FE_urea in three dogs (mean of 8 ~ 10 experiments per dog). Drawn after O'Connor and Summerill [111]. *Right* influence of an acute infusion of glucagon (*solid line*) or vehicle (*dotted line*) in anesthetized rats in two different studies (A and B). Both the meat meal and the infusion of glucagon increased FE_urea by about 30 %. Reproduced from Bankir and Yang [15]. Original data from: O'Connor and Summerill [111] (*top panel* and *left* of *bottom panel*), Ahloulay et al. [3] and Knepper et al. [83] (*right* of *bottom panel* for experimental lines *A* and *B*, respectively)

Table 13.3 Fractional excretion of the main urinary solutes in rats with different urine-concentrating activity

		Low CA	Normal CA	High CA	High/low	ANOVA
Urine flow rate	ml/d	20.3 ± 1.5	11.1 ± 1.0	5.57 ± 0.18	0.27	$p < 0.001$
Urine osmolality	mOsmol/L	762 ± 44	$1,526 \pm 139$	$3,023 \pm 87$	3.97	$p < 0.001$
Inulin clearance	ml/min	1.06 ± 0.10	1.62 ± 0.16	1.93 ± 0.10	1.83	$p < 0.001$
Plasma urea	mM	4.3 ± 0.2	5.2 ± 0.5	7.8 ± 0.3	1,80	$p < 0.01$
FE urea	%	118 ± 18	67 ± 7	43 ± 1	0.37	$p < 0.001$
FE Na	%	1.2 ± 0.1	0.8 ± 0.1	0.7 ± 0.1	0.61	$p < 0.005$
FE K	%	10.1 ± 1.4	6.9 ± 0.6	6.8 ± 0.6	0.68	$p = 0.05$
FE creatinine	%	133 ± 12	107 ± 9	91 ± 6	0.69	$p < 0.05$

Rats in steady state. Data based on two 24-h urine collection in metabolic cages
CA urine-concentrating activity. Fractional excretions (*FEs*) calculated using inulin clearance as a marker of glomerular filtration rate. Data from Bouby et al. [21]. Note that the FE of urea falls much more with increasing CA than that of sodium or potassium (much lower high/low ratio for urea). This is explained by the greater reabsorption of urea that occurs in the collecting duct when urine flow rate declines and to the dose-dependent influence of vasopressin on the terminal inner medullary collecting duct urea transporter

partly reabsorbed in the proximal convoluted tubule, secreted in the pars recta, then reabsorbed to a variable extent along the entire CD and reabsorbed in a vasopressin dose-dependent process in the terminal IMCD. Countercurrent exchange of urea between ascending and descending vasa recta contributes to prevent the dissipation of the urea accumulated in the medulla. A mathematical model of urea handling in the renal medulla showed that this active urea secretion improves the excretion of urea in a minimum amount of water with little consequence on the excretion of sodium and other solutes [88] (see Chap. 3).

The pars recta of the proximal tubule is most likely the site of this urea secretion. It exhibits several anatomical features typical of a secretory segment and is known to secrete organic acids, uric acid, cyclic nucleotides, and xenobiotics. It is surrounded mostly by ascending, venous vasa recta that provide this segment with its nutrient blood supply (capillaries issued from descending, arterial vasa recta are very scarce in the outer stripe of the outer medulla). Importantly, this secreted urea originates in unknown proportions from a mixture of urea present in medullary blood (urea never filtered that remains in plasma after filtration in the juxtamedullary glomeruli) and from urea added to the inner medulla by the vasopressin-dependent action on the terminal IMCD and flowing up in ascending vasa recta blood.

The amount of urea that could be added by secretion has been calculated, based on the micropuncture studies of Safirstein et al. in rats [122] and on studies of subjects with familial azotemia by Armsen et al. [6]. As much as two-thirds of the urea found in the urine of normal individuals may be due to the secretory process missing in azotemic subjects (Figs. 13.9 and 13.10). The calculation published earlier [14] suggests that an extraction by the medullary pars recta of 50 % of non-previously filtered urea flowing in ascending vasa recta blood could account for
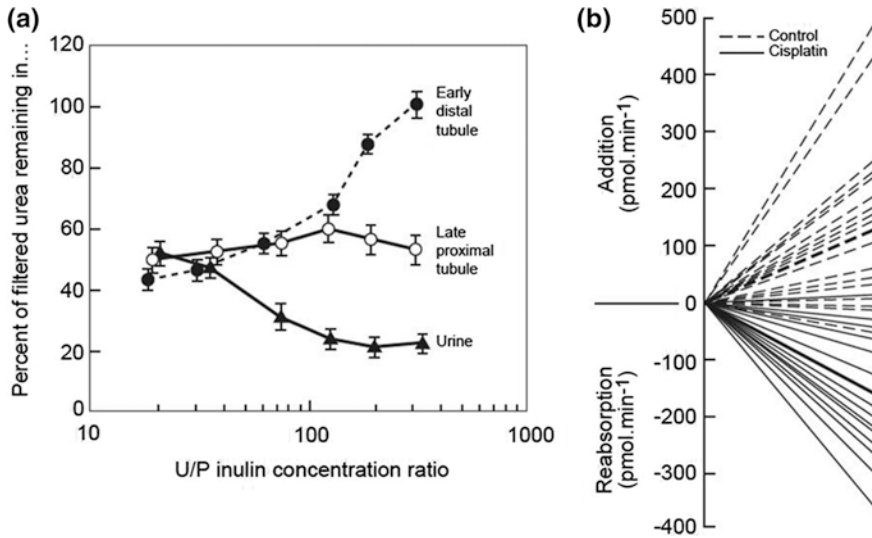
Fig. 13.9 Evidence for urea secretion in the loop of Henle obtained in micropuncture experiments in rats. **a** Fraction of filtered urea remaining in the late proximal tubule, the early distal tubule (close to the macula densa), and in urine of normal rats, plotted against the urine-to-plasma ratio of inulin concentration (an index of water reabsorption and thus of tubular fluid or urine concentration). These data show that: (1) the delivery of urea in the late proximal tubule is equal to about 50 % of the filtered load over the whole range of urine concentration; (2) a very large secretion of urea occurs between the late proximal and the early distal tubule; (3) this addition increases with increasing urine concentration; and (4) the fractional excretion of urea in the urine falls with increasing urine concentration. For each value of the U/P inulin concentration ratio, the difference between early distal tubule and urine represents urea reabsorbed in the distal nephron and collecting duct. This reabsorption increases, and thus, the fractional excretion of urea declines, with increasing urine concentration (see also Fig. 13.10 showing a similar decline in humans). Based on data from [6]. Reproduced from [9]. **b** Net urea movement between the late proximal and the early distal tubule. In control rats (*dashed lines*), a large amount of urea is added to the nephron lumen between these two sites. In contrast, when transport activity is impaired in the pars recta by cisplatin treatment, urea is largely reabsorbed. The magnitude of urea secretion in normal rats is thus equal to the difference between these opposite movements. Adapted from Safirstein et al. [122]

the amount of urea likely secreted in the human kidney. But most likely a lower figure is required as urea secretion may also occur upstream in the medullary rays of the cortex and may also be involved in vasopressin-dependent recycling of urea issued from the IMCD. Red cells could also contribute significantly to supply urea during their relatively slow ascent in venous vasa recta because they express abundant UT-B and may thus quickly equilibrate with surrounding plasma urea.

The transporter responsible for this active urea secretion has not yet been identified. SGLT1, a sodium–glucose cotransporter located in the S3 segment of the proximal tubule, has been shown in vitro to transport urea in addition to glucose [90, 113]. Interestingly, some homology has been found between SGLTs and
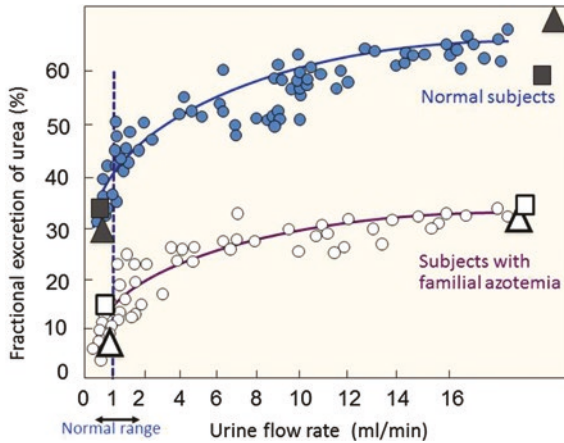
Fig. 13.10 Fractional excretion of urea (FE$_{urea}$) as a function of urine flow rate in healthy subjects and subjects with familial azotemia. In normal subjects, FE$_{urea}$ is relatively high at high urine flows and declines sharply with declining urine flow because of more intense urea reabsorption in the CD. In subjects with familial azotemia, a similar flow-related decline is observed, suggesting that the handling of urea in the CD is normal, but the whole relationship is shifted toward lower values. The marked reduction of FE$_{urea}$ over the whole range of urine flows is probably due to the lack of urea secretion in patients with familial azotemia. Data taken from three independent studies from Germany [5] (*circles*), Italy [36] (*squares*), and USA [65] (*triangles*). Note that the remarkable agreement between the three studies

DUR3, the active urea transporter identified in yeast (see Fig. 13-2 in [155]). In a recent review, we proposed that urea secretion in the mammalian pars recta could possibly occur through SGLT1 [15]. Further studies are needed to evaluate this hypothesis and/or to identify other possible membrane protein(s) that could be responsible for active urea secretion in this nephron segment.

Active Urea Secretion in the Terminal Inner Medullary Collecting Duct and Its Possible Extension in the Whole Urinary Tract, Including Bladder

Intriguingly, secondary active urea secretion has been characterized in vitro in the deepest subsegment of the rat IMCD, which is absent in earlier portions of the IMCD. Studies of isolated perfused terminal IMCDs have shown that it is a sodium–urea counter-transport taking place in the apical membrane [77]. This urea secretion is inhibited by luminal phloretin or triamterene and is stimulated by vasopressin added in the bath.

It is unexpected to find an active urea secretion in a tubule that expresses vasopressin-dependent facilitated UTs on both sides of the epithelium (see Chap. 4).
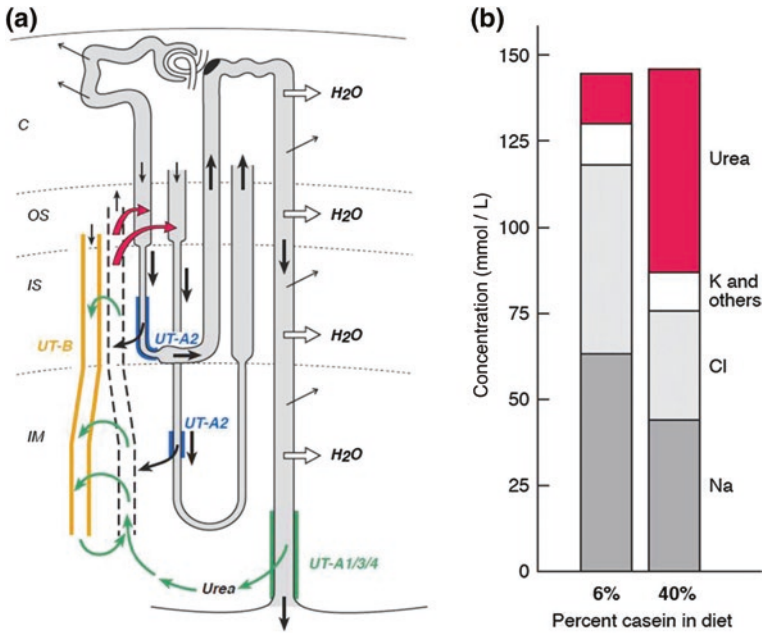
Fig. 13.11 Intrarenal urea handling and influence of protein intake. **a** Urea movements in a superficial and a juxta-medullary nephron (cortical segments of this nephron are not represented), vasa recta and collecting duct. About 50 % of the filtered urea is reabsorbed in the proximal convoluted tubule (*thin black arrows*) (see Fig. 13.9a). Active urea secretion most probably takes place in the pars recta of the proximal tubule (*red arrows*), thus adding significant amounts of urea in the nephron lumen. Some of this urea may be delivered via UT-A2 (*curved black arrows*) (1) to the countercurrent exchanger (*green arrows*) consisting of fenestrated ascending vasa recta (*dotted lines*) and descending vasa recta expressing UT-B and (2) to the IM. Some urea is reabsorbed passively along the whole collecting duct (*thin black arrows*). Concentrated urea is delivered to the terminal IM via UT-A1/3. This urea is taken up by ascending vasa recta but is partly returned to the IM via the countercurrent exchanger and via active secretion into the pars recta of both superficial and juxta-medullary nephrons. Thick *arrows* show the directions of tubule fluid flow. Kidney zones are as follows: *C* cortex, *OS and IS* outer and inner stripes of the outer medulla, respectively, *IM* inner medulla. **b** Results from a micropuncture study of fluid collected from the early distal tubule of rats fed a low or a high protein diet for 7–10 days. Na^+ and Cl^- concentrations were much lower on the high than on the low protein diet, due to more intense reabsorption in the thick ascending limb. But because total osmolality was similar on both diets, another osmole, most likely urea, must account for the difference (i.e., 26 and 67 mM on low and high casein diets, respectively). We assume that part of this urea enters the nephron lumen by an active secretion taking place in the pars recta of the proximal tubule and that this secretion is markedly stimulated on a high protein diet. Drawn after data from Seney et al. [132]

These facilitated UTs are essential for delivering urea to the inner medulla and allowing the production of concentrated urine, as shown by their experimental deletion [43] (see Chap. 9). The amount of urea secreted via this active transporter is negligible compared to the 500-fold higher reabsorption mediated by the facilitated UTs [77]. Thus, the functional role of an active urea secretion in the terminal

IMCD is difficult to understand. Although not proposed by the authors, we postulated in a recent review [15] that this transport system might be similar to that functionally observed in the basolateral membrane of the elasmobranch gill [47] and might extend to the downstream urinary tract (see next section).

Possible Other Sites of Active Urea Transport in Mammals

In the last 20 years, studies of mRNA and protein expression show that facilitated UTs are present in a number of organs in which such transport had not been suspected before. When UTs are expressed on both sides of epithelial or endothelial cells, they allow a rapid equilibration of urea concentration in these cells with the surrounding interstitium. In other cases, when a specific UT is localized only in one of the two membranes of an epithelium, it is conceivable that these cells also express an active UT on their opposite membrane, as is the case, for example, for glucose transport in the proximal convoluted tubule, with the active transporter SGLT2 on the apical membrane and the facilitated transporter GLUT2 on the basolateral membrane [154]. We assume it may be the case in the urinary bladder and in the testis as explained below. We want however to state that this is still speculative. We hope these hypotheses will promote further research in these organs.

Urinary Bladder

In some organs, the presence of a facilitated UT is intriguing. This is the case for the bladder. UT-B is heavily expressed in the basolateral membrane of urothelial cells that line the lumen of the bladder. It is surprising to find a facilitated transporter in an organ that needs to be urea-tight in order to keep highly concentrated urea in the urine for hours (see Fig. 13.12). The presence of UT-B makes more sense if one assumes that an active (or secondary active) urea transporter is expressed on the apical side of urothelial cells, which actively secretes urea into the lumen in order to counteract some urea leakage and thus prevent the dissipation of the high transepithelial gradient. This putative transporter could be the extension in the bladder of the active secretory transporter characterized in the inner most segment of the IMCD [77] (see above). This active transporter could be expressed along the papillary epithelium, the pelvis, ureter, and bladder; those tissues all express UT-B in their basolateral membrane. It might be homologous to the transporter functionally characterized in elasmobranch gills [47] because in both cases, the purpose is to prevent the dissipation of a strong urea concentration gradient between two fluids (urine and blood for the mammalian bladder, and blood and seawater for the elasmobranch gills).

The small urea leakage observed in the ureter or bladder [137, 150] may be the net result of two opposite movements almost compensating for each other, including a passive escape and a partial active recovery. During bladder infections, the bladder
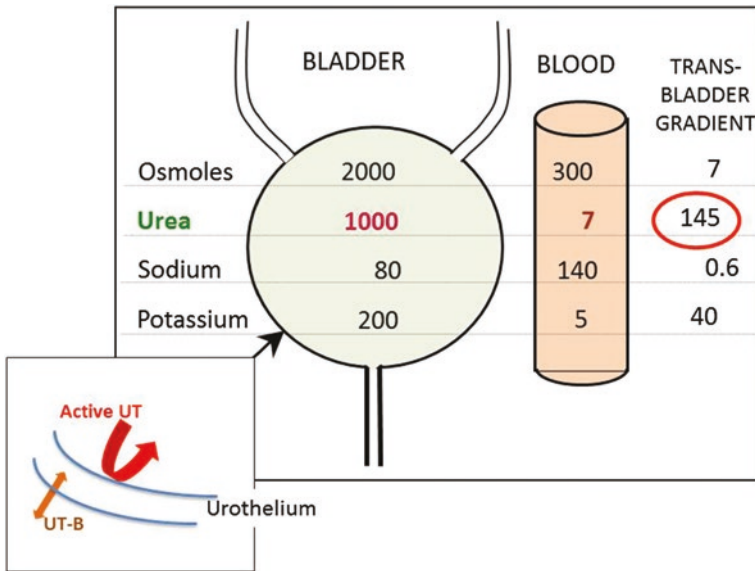
Fig. 13.12 Large urea concentration gradient between bladder and blood. Rounded values corresponding to the situation observed in normal rats. Urea is markedly more concentrated in the urine than in the blood, as shown by the large trans-bladder concentration gradient. Moreover, urine stays for long periods in the bladder, and the facilitated urea transporter UT-B is expressed on the basolateral aspect of urothelial cells. Even with a very specialized urothelium structure, exhibiting a very low permeability to urea, we assume that the bladder could not maintain a high transurothelial gradient without an active urea transporter (*red arrow*) that continuously pumps back the urea that is at risk of diffusing out of the bladder

becomes permeable to solutes. This could partly result from a significant down-regulation of several transporters including this active urea transporter (see review in [15]). The existence of an active urea transporter in the urothelium could explain how bears can prevent a rise in uremia during hibernation. For several months during winter, bears do not eat, drink, defecate, or urinate. Even if the glomerular filtration rate declines markedly, some urine is still formed. But urinary water and solutes are entirely reabsorbed from the bladder [109, 110] returning urinary wastes and water into the blood. Creatininemia goes up, but uremia does not [138]. The leakiness of the urinary bladder could result from a temporary inactivation of transporters that, when active, prevent the dissipation of concentrated solutes from the lumen to the surrounding interstitium and blood. Urea leaking from the bladder can be degraded by the intestinal microflora, allowing reuse of urea nitrogen for the sake of the bear's metabolism. This explains how bears loose very little muscle mass during hibernation [138].

Testis

Also not expected before the availability of molecular tools, facilitated UTs have been found in the testis of rats and mice [46]. UT-A5 is expressed in the

seminiferous tubules, and its progressive expression with age parallels that of seminiferous tubule fluid movement [44]. Interestingly, evidence for active urea transport has also been described in the testis [64, 145], and accumulation of urea above the plasma concentration has been reported in the mouse testis [52]. This makes us assume that active urea secretion might occur in the seminiferous tubes and could induce fluid secretion into the lumen to initiate sperm flow, in a way similar to that observed in the proximal tubule of aglomerular fish [16, 17] or in the mammalian pars recta [55, 56]. The secretion of an osmotically active compound drives water iso-osmotically and thus creates a flow of fluid in the lumen of the structure.

Active Urea Secretion, Vasopressin, and Glomerular Filtration Rate

The catabolism of dietary carbohydrates and lipids produces only CO_2 and H_2O (= metabolic water), which are easily excreted by the lungs and kidneys, respectively. In contrast, the catabolism of proteins produces a number of end-products that are excreted by the kidneys: urea, ammonia, uric acid, phosphates and sulfates, protons, etc. Moreover, because the concentrations of these solutes in plasma and extracellular fluids are relatively low (a few mM or even μM), their renal excretion imposes a need to concentrate them in the urine far above their concentration in the plasma for the sake of water conservation (see Table 2 in [10]).

A single protein-rich meal, or an amino acid infusion, is known to induce a transient rise in glomerular filtration rate (GFR) (often referred to as "hyperfiltration") [20, 54, 57]. A sustained high protein intake (but not a high carbohydrate or lipid intake) induces marked kidney hypertrophy [98] and a permanent increase in GFR [51, 91]. Urinary concentrating ability is also enhanced by a high protein intake, as reported in rats, sheep, dogs, and humans [25, 42, 61, 116, 129]. These changes are absent when a high protein diet is fed to Brattleboro rats with hereditary central diabetes insipidus [24] or in rats with a lithium-induced urinary concentrating defect [31], thus showing that vasopressin and a normal urine-concentrating activity is required for these protein-induced changes [13, 24]. The need to concentrate the protein-derived end-products in the urine probably plays a role in the kidney hypertrophy and hyperfiltration observed in response to protein intake [8, 14]. On the other hand, a chronic stimulation of the urine-concentrating mechanism (by infusion of a vasopressin V2 receptor agonist or by partial water deprivation) increases GFR [21] and induces kidney hypertrophy similar to those induced by a high protein intake, with a marked increase in the medullary thick ascending limb volume and enzymatic activity [12, 13, 22, 23, 25, 144]. Conversely, after the surgical or chemical ablation of the inner medulla, which markedly reduces the ability to concentrate urine, both GFR and kidney weight are reduced (see review in Table 3 of [13]).

The mechanism of the protein-induced increases in GFR and kidney hypertrophy is not fully understood. It probably implies several hormones and a cascade

of mediators. Two possible candidate hormones are glucagon and vasopressin acting in conjunction, as explained below. Glucagon, a hormone secreted after a protein meal, promotes in a coordinated fashion urea formation in the liver and urea excretion by the kidney to get rid of excess amino acid nitrogen [2, 3]. Studies in humans suggest that it probably plays a role in hyperfiltration [38, 50, 54], a way to speed up urea excretion. As explained above, glucagon may also favor active urea secretion in the pars recta. Plasma vasopressin is also increased after a single protein meal [57] or by a high protein intake [29, 37]. This favors the excretion of urea with a significant economy of water [8, 14] Thus, vasopressin, through its action on urea handling in the kidney most probably, plays a role in the protein-induced rise in GFR [8, 10, 14].

This rise in GFR is likely due to a reduction in the tubulo–glomerular feedback operating at the juxtaglomerular apparatus, as shown in the elegant micropuncture study of Seney et al. in rats fed either a high or a low protein intake for 7–10 days [132]. They showed that the sodium and chloride concentrations in the early distal tubule (the closest accessible site to the macula densa) were much lower on a high than on a low protein diet (44 vs 63 mM for sodium and 32 vs 54 mM for chloride). See Fig. 13.11b. But interestingly, they also observed that the osmolality of the tubular fluid was identical in the two conditions (145 mosm/kg H_2O) [132]. This means that another solute was present in the tubular fluid in a much higher concentration on the high than on the low protein diet. Subtracting sodium and chloride from osmolality gives 67 versus 26 mM for the missing solute, respectively. This solute is obviously urea, which is excreted in much larger amount on a high protein intake (Fig. 13.11b). It is well proven that urea, after some reabsorption in the proximal tubule, is added in the loop of Henle so that its flow rate is greater in the early distal tubule than in the late proximal tubule (see Fig. 13.9a, b). The magnitude of this addition increases with urine concentration (Fig. 13.9a) and is larger in desert-adapted rodents than in other species [148]. It is also obviously dependent on the level of protein intake in a given species.

In both wild-type mice and mice with UT-A1/3 knockout, a high protein intake induced a significant rise in GFR [45]. This led the authors to conclude that the tubular recycling of urea released in the deep inner medulla through UT-A1/3 does not participate in the protein-induced rise in GFR [45] (see Chap. 9), as had been previously proposed [14, 21, 156]. In any case, this route of urea recycling was no longer valid because it involved the reintroduction of urea in the thin descending limbs of short-looped nephrons through UT-A2, a hypothesis not confirmed by observations in UT-A2 null mice (see above and [15]). It is now very likely that urea is added by active secretion in the pars recta, a vasopressin-independent step. The protein-induced rise in glucagon may favor this secretion. In mice with UT-A1/3 knockout, the protein-induced hyperfiltration was 25 % lower than in wild-type mice [45]. The lack of significance of this 25 % difference may be due to the small number of mice (5 per group) and the large inter-individual variability of such an in vivo measurement. There is a significant permeability to urea of the terminal IMCD, even in the absence of vasopressin stimulation [124]. This permeability is probably independent of the facilitated UTs and thus may play a

role in UT-A1/3 knockout mice. Noteworthy, the urine/plasma ratio of urea concentration on a 40 % protein diet reached 73 ± 6 in the knockout mice, a value 40 % of that in wild-type mice, suggesting some ability to concentrate urea, even in the absence of the IMCD facilitated UTs (Table 2 in [45]). Moreover, vasopressin (increased by a high protein diet) may further favor a higher urea/Na ratio at the macula densa by its influence on thick ascending limb hypertrophy [12, 23] and increased enzymatic activities (see review in Table 2 of [13]) and by its direct stimulation of sodium reabsorption in this nephron segment [103]. This is supported by a recent mathematical modelization [89]. These enhanced glucagon and vasopressin actions, both occurring upstream of the macula densa, may thus reduce the intensity of the TGF signal, even in mice with UT-A1/3 deletion. These hypotheses need to be confirmed.

When micropuncture is not available, it is not possible to know the urea concentration at the macula densa or in the early distal tubule. In classical clearance experiments, the ratio of the concentration of urea in urine and plasma (urine-to-plasma concentration ratio = U/P urea) provides an index of the relative concentration of urea that probably occurs at the macula densa. In several conditions in rats and humans, striking significant correlations have been observed between GFR (measured by inulin clearance) and the U/P urea ratio or between the change in GFR (=hyperfiltration) and the change in this ratio in response to a glucagon infusion (see figures in [3, 21, 57]). Even if the mechanisms and factors ultimately responsible for the protein-induced rise in GFR are not elucidated yet, a role for a vasopressin-dependent action and its influence on intrarenal urea (and sodium) handling is highly likely because this rise in GFR is highly correlated with the U/P concentration ratio of urea and is not observed in Brattleboro rats lacking vasopressin [24].

Perspectives

There is a marked contrast between the major role of the kidney in the excretion of nitrogen end-products, urea being quantitatively the dominant one, and our relative lack of knowledge about how urea is handled in the kidney and the mechanisms that allow its excretion with a very significant economy of water. The vast amount of information that has been accumulated over the last 20 years about facilitated UTs and the consequences of their invalidation brought very significant knowledge, but provided only a partial picture of urea handling by the mammalian kidney.

The observations reported in this chapter indicate that, without any doubt, several active (or secondary active) urea transporters (or transport systems) exist in the mammalian kidney and possibly in other organs, as well as in several tissues in lower vertebrates. Figure 13.13 shows the localization of these transporters in the mammalian nephron and collecting duct, in parallel with that of the facilitated transporters. In spite of the abundant functional evidence for their existence, no
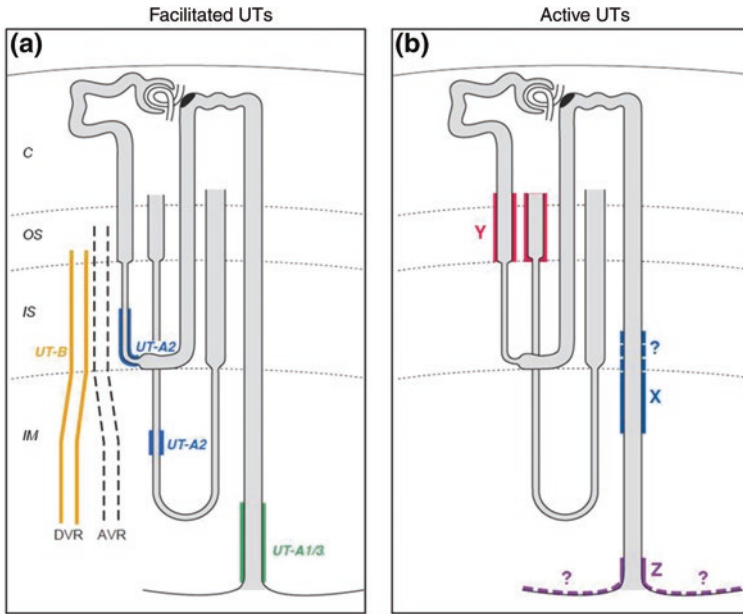
Fig. 13.13 Localization of facilitated UTs (**a**) and active UTs (**b**) along the nephron, collecting duct and vasa recta. The active UTs (*X*, *Y*, and *Z*) have not yet been molecularly characterized, and the sites of their expression are not fully or well delimited (as indicated by quotation marks)

active UT has been identified yet and no indices have been obtained as to their possible molecular structure. Only preliminary studies have attempted to isolate one of them [7, 30, 123].

The search for active UT transporters may be specially difficult if they require the assembly of several subunits to be functional (like is the case for example for Na^+-K^+-ATPase or ENaC). Moreover, they might also transport other solutes and have been misidentified up to now. For example, the uric acid transporter GLUT9 (SLC2A9) was initially considered to be a glucose/fructose transporter [28, 115, 149]. In that case, human genetic diseases helped elucidate the real role of this transporter. For urea, no clue is provided by human genetic studies up to now. No known human disease is associated with abnormal active UT except for familial azotemia (see above). Because this anomaly does not lead to a severe phenotype, it may remain undetected in a number of cases. Mutations in the genes coding for other active UTs either may have no serious consequences on the health of the carriers, or may induce a premature death during embryonic life.

Many other membrane transporters have been initially cloned in lower organisms. The same strategy could be applied here. The search for the high-affinity, low-capacity active UTs might take advantage of the high expression level that probably characterizes the elasmobranch gills. The low-affinity, high-capacity active UT may be easier to isolate from the amphibian kidney. In both cases, the

osmolarity concentration and urea concentration in the surrounding or extracellular fluids are easier to manipulate than in mammals. We hope that this chapter will encourage further research in this field.

References

1. Abreu C, Sanguinetti M, Amillis S, Ramon A (2010) UreA, the major urea/H+ symporter in Aspergillus nidulans. Fungal Genet Biol 47(12):1023–1033
2. Ahloulay M, Bouby N, Machet F, Kubrusly M, Coutaud C, Bankir L (1992) Effects of glucagon on glomerular filtration rate and urea and water excretion. Am J Physiol 263 (Renal Fluid Electrolyte Physiol. 32):F24–F36
3. Ahloulay M, Déchaux M, Laborde K, Bankir L (1995) Influence of glucagon on GFR and on urea and electrolyte excretion: direct and indirect effects. Am J Physiol 269 (Renal Fluid and Electrolyte Physiol. 38):225–235
4. Anderson WG, Dasiewicz PJ, Liban S, Ryan C, Taylor JR, Grosell M, Weihrauch D (2010) Gastro-intestinal handling of water and solutes in three species of elasmobranch fish, the white-spotted bamboo shark, *Chiloscyllium plagiosum*, little skate, *Leucoraja erinacea* and the clear nose skate *Raja eglanteria*. Comp Biochem Physiol A: Mol Integr Physiol 155(4):493–502
5. Armsen T, Glossmann V, Weinzierl M, Edel HH (1986) Familial proximal tubular azotemia. Elevated urea plasma levels in normal kidney function. Dtsch Med Wochenschr 111(18):702–706
6. Armsen T, Reinhardt HW (1971) Transtubular movement of urea at different degrees of water diuresis. Pflugers Arch 326(3):270–280
7. Ashkar ZM, Martial S, Isozaki T, Price SR, Sands JM (1995) Urea transport in initial IMCD of rats fed a low-protein diet: functional properties and mRNA abundance. Am J Physiol 268(6 Pt 2):F1218–F1223
8. Bankir L, Ahloulay M, Bouby N, Machet F, Trinh-Trang-Tan MM (1993) Direct and indirect effects of vasopressin on renal hemodynamics. In: Gross P (ed) Vasopressin. John Libbey Eurotext, London, pp 393–406
9. Bankir L, Ahloulay M, Bouby N, Trinh-Trang-Tan MM, Machet F, Lacour B, Jungers P (1993) Is the process of urinary urea concentration responsible for a high glomerular filtration rate? J Am Soc Nephrol 4(5):1091–1103
10. Bankir L, Bouby N, Ritz E (2013) Vasopressin: a novel target for the prevention and retardation of kidney disease? Nat Rev Nephrol 9(4):223–239
11. Bankir L, de Rouffignac C (1985) Urinary concentrating ability: insights from comparative anatomy. Am J Physiol 249(6 Pt 2):R643–R666
12. Bankir L, Fischer C, Fischer S, Jukkala K, Specht HC, Kriz W (1988) Adaptation of the rat kidney to altered water intake and urine concentration. Pflugers Arch 412(1–2):42–53
13. Bankir L, Kriz W (1995) Adaptation of the kidney to protein intake and to urine concentrating activity: similar consequences in health and CRF. Kidney Int 47(1):7–24
14. Bankir L, Trinh-Trang-Tan MM (2000) Urea and the kidney. In: Brenner BM (ed) The kidney, 6th edn. W B Saunders Company, Philadelphia, pp 637–679

15. Bankir L, Yang B (2012) New insights into urea and glucose handling by the kidney, and the urine concentrating mechanism. Kidney Int 81(12):1179–1198. doi:10.1038/ki.2012.67

16. Beyenbach KW (2004) Kidneys sans glomeruli. Am J Physiol Renal Physiol 286(5):F811–F827

17. Beyenbach KW, Liu PL (1996) Mechanism of fluid secretion common to aglomerular and glomerular kidneys. Kidney Int 49(6):1543–1548

18. Beyer KH, Gelarden RT, Vesell ES (1992) Inhibition of urea transport across renal tubules by parazinoylguanidine and analogs. Pharmacology 44:124–138

19. Beyer KHJ, Gelarden RT (1988) Active transport of urea by mammalian kidney. Proc Natl Acad Sci 85:4030–4031

20. Bosch JP, Lew S, Glabman S, Lauer A (1986) Renal hemodynamic changes in humans. Response to protein loading in normal and diseased kidneys. Am J Med 81(5):809–815

21. Bouby N, Ahloulay M, Nsegbe E, Déchaux M, Schmitt F, Bankir L (1996) Vasopressin increases GFR in conscious rats through its antidiuretic action. J Am Soc Nephrol 7:842–851

22. Bouby N, Bankir L (1988) Effect of high protein intake on sodium, potassium-dependent adenosine triphosphatase activity in the thick ascending limb of Henle's loop in the rat. Clinical science (London, England: 1979) 74 (3):319–329

23. Bouby N, Bankir L, Trinh-Trang-Tan MM, Minuth WW, Kriz W (1985) Selective ADH-induced hypertrophy of the medullary thick ascending limb in Brattleboro rats. Kidney Int 28(3):456–466

24. Bouby N, Trinh-Trang-Tan MM, Coutaud C, Bankir L (1991) Vasopressin is involved in renal effects of high-protein diet: study in homozygous Brattleboro rats. Am J Physiol 260(1 Pt 2):F96–F100

25. Bouby N, Trinh-Trang-Tan MM, Laouari D, Kleinknecht C, Grunfeld JP, Kriz W, Bankir L (1988) Role of the urinary concentrating process in the renal effects of high protein intake. Kidney Int 34(1):4–12

26. Browning J (1978) Urea levels in plasma and erythrocytes of the southern fiddler skate, *Trygonorhina fasciata* guanerius. J Exp Zool 203(2):325–329

27. Carlisky NJ, Jard S, Morel F (1966) In vivo tracer studies of renal urea formation in the bullfrog. Am J Physiol 211(3):593–599

28. Caulfield MJ, Munroe PB, O'Neill D, Witkowska K, Charchar FJ, Doblado M, Evans S, Eyheramendy S, Onipinla A, Howard P, Shaw-Hawkins S, Dobson RJ, Wallace C, Newhouse SJ, Brown M, Connell JM, Dominiczak A, Farrall M, Lathrop GM, Samani NJ, Kumari M, Marmot M, Brunner E, Chambers J, Elliott P, Kooner J, Laan M, Org E, Veldre G, Viigimaa M, Cappuccio FP, Ji C, Iacone R, Strazzullo P, Moley KH, Cheeseman C (2008) SLC2A9 is a high-capacity urate transporter in humans. PLoS Med 5(10):e197

29. Chan AYM, Cheng ML, Keil LC, Myers BD (1988) Functional response of healthy and diseased glomeruli to a large, protein-rich protein meal. J Clin Invest 81:245–254

30. Chen G, Yang Y, Frohlich O, Klein JD, Sands JM (2010) Suppression subtractive hybridization analysis of low-protein diet- and vitamin D-induced gene expression from rat kidney inner medullary base. Physiol Genomics 41(3):203–211

31. Christensen S, Marcussen N, Petersen JS, Shalmi M (1992) Effects of uninephrectomy and high protein feeding on lithium-induced chronic renal failure in rats. Ren Physiol Biochem 15(3–4):141–149

32. Clapp JR (1965) Urea reabsorption by the proximal tubule in the dog. Proc Soc Exp Biol (NY) 120:521–523

33. Clapp JR (1970) The effect of protein depletion on urea reabsorption by the kidney. In: Schmidt-Nielsen B (ed) Urea and the Kidney. Excerpta Medica Foundation, Amsterdam, pp 200–206

34. Collins D, Walpole C, Ryan E, Winter D, Baird A, Stewart G (2011) UT-B1 mediates transepithelial urea flux in the rat gastrointestinal tract. J Membr Biol 239(3):123–130

35. Collins D, Winter DC, Hogan AM, Schirmer L, Baird AW, Stewart GS (2010) Differential protein abundance and function of UT-B urea transporters in human colon. Am J Physiol Gastrointest Liver Physiol 298(3):G345–G351

36. Conte G, DalCanton A, Terribile M, Cianciaruso B, DiMinno G, Pannain M, Russo D, Andreucci VE (1987) Renal handling of urea in subjects with persistent azotemia and normal renal function. Kidney Int 32:721–727

37. Daniels BS, Hostetter TH (1990) Effect of dietary protein intake on vasoactive hormones. Am J Physiol 258 (Regulatory Integrative Comp. Physiol. 27):R1095–R1100

38. DeSanto NG, Coppola S, Anastasio P, Coscarella G, Capasso G, Castellino P, De Mercato R, Bellini L, Strazzullo P, Guadagno P et al (1990) Pancreatectomy abolishes the renal hemodynamic response to a meat meal in man. Nephron 55(1):85–86

39. Dytko G, Smith PL, Kinter LB (1993) Urea transport in toad skin (*Bufo marinus*). J Pharmacol Exp Ther 267:364–449

40. Ehrenfeld J (1998) Active proton and urea transport by amphibian skin. Comp Biochem Physiol A: Mol Integr Physiol 119(1):35–45

41. ElBerry HM, Majumdar ML, Cunningham TS, Sumrada RA, Cooper TG (1993) Regulation of the urea active transporter gene (DUR3) in *Saccharomyces cerevisiae*. J Bacteriol 175(15):4688–4698

42. Epstein FH, Kleeman CR, Pursel S, Hendrikx A (1957) The effect of feeding protein and urea on the renal concentrating process. J Clin Invest 36(5):635–641. doi:10.1172/jci103463

43. Fenton RA (2008) Urea transporters and renal function: lessons from knockout mice. Curr Opin Nephrol Hypertens 17(5):513–518

44. Fenton RA, Cooper GJ, Morris ID, Smith CP (2002) Coordinated expression of UT-A and UT-B urea transporters in rat testis. Am J Physiol Cell Physiol 282(6):C1492–C1501

45. Fenton RA, Flynn A, Shodeinde A, Smith CP, Schnermann J, Knepper MA (2005) Renal phenotype of UT-A urea transporter knockout mice. J Am Soc Nephrol 16(6):1583–1592

46. Fenton RA, Howorth A, Cooper GJ, Meccariello R, Morris ID, Smith CP (2000) Molecular characterization of a novel UT-A urea transporter isoform (UT-A5) in testis. Am J Physiol Cell Physiol 279(5):C1425–C1431

47. Fines GA, Ballantyne JS, Wright PA (2001) Active urea transport and an unusual basolateral membrane composition in the gills of a marine elasmobranch. Am J Physiol Regul Integr Comp Physiol 280(1):R16–R24

48. Forster RP (1954) Active cellular transport of urea by frog renal tubules. Am J Physiol 179(2):372–377

49. Forster RP (1970) Active tubular transport of urea and its role in environmental physiology. In: Schmidt-Nielsen B (ed) Urea and the kidney. Excerpta Medica Foundation, Amsterdam, pp 229–237

50. Friedlander G, Blanchet-Benque F, Nitenberg A, Laborie C, Assan R, Amiel C (1990) Glucagon secretion is essential for aminoacid-induced hyperfiltration in man. Nephrol Dial Transplant 5(2):110–117

51. Friedman AN (2004) High-protein diets: potential effects on the kidney in renal health and disease. Am J Kidney Dis 44(6):950–962

52. Fritz IB, Lyon MF, Setchell BP (1983) Evidence for a defective seminiferous tubule barrier in testes of Tfm and Sxr mice. J Reprod Fertil 67(2):359–363

53. Garcia-Romeu F, Masoni A, Isaia J (1981) Active urea transport through isolated skins of frog and toad. Am J Physiol 241(3):R114–R123

54. Giordano M, Castellino P, McConnell EL, DeFronzo RA (1994) Effect of amino acid infusion on renal hemodynamics in humans: a dose-response study. Am J Physiol 267(5 Pt 2):F703–F708

55. Grantham JJ, Irwin RL, Qualizza PB, Tucker DR, Whittier FC (1973) Fluid secretion in isolated proximal straight renal tubules. Effect of human uremic serum. J Clin Invest 52(10):2441–2450

56. Grantham JJ, Qualizza PB, Irwin RL (1974) Net fluid secretion in proximal straight renal tubules in vitro: role of PAH. Am J Physiol 226(1):191–197

57. Hadj-Aissa A, Bankir L, Fraysse M, Bichet DG, Laville M, Zech P, Pozet N (1992) Influence of the level of hydration on the renal response to a protein meal. Kidney Int 42(5):1207–1216

58. Hays RM (1978) Familial azotemia. N Engl J Med 298:160–161
59. Hazon N, Wells A, Pillans RD, Good JP, Gary Anderson W, Franklin CE (2003) Urea based osmoregulation and endocrine control in elasmobranch fish with special reference to euryhalinity. Comp Biochem Physiol B: Biochem Mol Biol 136(4):685–700
60. Hellerá J, Kleinová M, Janácek K, Rybová R (1985) High concentration of urea in renal cortex. In: Dzúrik R, Lichardus B, Guder W (eds) Kidney metabolism and function. Martinus Nijhoff Publishers, Boston, pp 298–302
61. Hendrikx A, Epstein FH (1958) Effect of feeding protein and urea on renal concentrating ability in the rat. Am J Physiol 195(3):539–542
62. Hentschel H, Mahler S, Herter P, Elger M (1993) Renal tubule of dogfish, Scyliorhinus caniculus: a comprehensive study of structure with emphasis on intramembrane particles and immunoreactivity for H(+)-K(+)-adenosine triphosphatase. The Anatomical record 235(4):511–532
63. Hentschel H, Storb U, Teckhaus L, Elger M (1998) The central vessel of the renal countercurrent bundles of two marine elasmobranchs–dogfish (*Scyliorhinus caniculus*) and skate (*Raja erinacea*)–as revealed by light and electron microscopy with computer-assisted reconstruction. Anat Embryol 198(1):73–89
64. Howards SS, Turner TT (1978) The blood-testis barrier: a morphologic or physiologic phenomenon? Trans Am Assoc Genito-Urinary Surg 70:74–75
65. Hsu CH, Kurtz TW, Massari PU, Ponze SA, Chang BS (1978) Familial azotemia. Impaired urea excretion despite normal renal function. N Engl J Med 298:117–121
66. Inoue H, Jackson SD, Vikulina T, Klein JD, Tomita K, Bagnasco SM (2004) Identification and characterization of a Kidd antigen/UT-B urea transporter expressed in human colon. Am J Physiol Cell Physiol 287(1):C30–C35
67. Inoue H, Kozlowski SD, Klein JD, Bailey JL, Sands JM, Bagnasco SM (2005) Regulated expression of renal and intestinal UT-B urea transporter in response to varying urea load. Am J Physiol Renal Physiol 289(2):F451–F458
68. Isozaki T, Gillin AG, Swanson CE, Sands JM (1994) Protein restriction sequentially induces new urea transport processes in rat initial IMCD. Am J Physiol 266(5 Pt 2):F756–F761
69. Isozaki T, Lea JP, Tumlin JA, Sands JM (1994) Sodium-dependent net urea transport in rat initial inner medullary collecting ducts. J Clin Invest 94(4):1513–1517
70. Isozaki T, Verlander JW, Sands JM (1993) Low protein diet alters urea transport and cell structure in rat initial inner medullary collecting duct. J Clin Invest 92(5):2448–2457
71. Jahns T, Kaltwasser H (1989) Energy-dependent uptake of urea by *Bacillus megaterium*. FEMS Microbiol Lett 48(1):13–17
72. Janech MG, Fitzgibbon WR, Chen R, Nowak MW, Miller DH, Paul RV, Ploth DW (2003) Molecular and functional characterization of a urea transporter from the kidney of the Atlantic stingray. Am J Physiol Renal Physiol 284(5):F996–F1005
73. Janech MG, Fitzgibbon WR, Nowak MW, Miller DH, Paul RV, Ploth DW (2006) Cloning and functional characterization of a second urea transporter from the kidney of the Atlantic stingray, *Dasyatis sabina*. Am J Physiol Regul Integr Comp Physiol 291(3):R844–R853
74. Jorgensen CB (1997) Urea and amphibian water economy. Comp Biochem Physiol A Physiol 117(2):161–170
75. Kakumura K, Watanabe S, Bell JD, Donald JA, Toop T, Kaneko T, Hyodo S (2009) Multiple urea transporter proteins in the kidney of holocephalan elephant fish (*Callorhinchus milii*). Comp Biochem Physiol B: Biochem Mol Biol 154(2):239–247
76. Kato A, Sands JM (1998) Active sodium-urea counter-transport is inducible in the basolateral membrane of rat renal initial inner medullary collecting ducts. J Clin Invest 102(5):1008–1015
77. Kato A, Sands JM (1998) Evidence for sodium-dependent active urea secretion in the deepest subsegment of the rat inner medullary collecting duct. J Clin Invest 101(2):423–428
78. Kato A, Sands JM (1999) Urea transport processes are induced in rat IMCD subsegments when urine concentrating ability is reduced. Am J Physiol 276(1 Pt 2):F62–F71
79. Katz U, Garcia-Romeu F, Masoni A, Isaia J (1981) Active transport of urea across the skin of the euryhaline toad, Bufo viridis. Pflugers Arch 390(3):299–300

80. Kawamura S, Kokko JP (1976) Urea secretion by the straight segment of the proximal tubule. J Clin Invest 58(3):604–612

81. Kiran D, Mutsvangwa T (2010) Effects of partial ruminal defaunation on urea-nitrogen recycling, nitrogen metabolism, and microbial nitrogen supply in growing lambs fed low or high dietary crude protein concentrations. J Anim Sci 88(3):1034–1047

82. Knepper MA (1983) Urea transport in nephron segments from medullary rays of rabbits. Am J Physiol 244(6):F622–F627

83. Knepper MA, Gunter CV, Danielson RA (1976) Effects of glucagon on renal function in protein-deprived rats. Surg Forum 27:29–31

84. Knepper MA, Roch-Ramel F (1987) Pathways of urea transport in the mammalian kidney. Kidney Int 31(2):629–633

85. Kojima S, Bohner A, Gassert B, Yuan L, von Wiren N (2007) AtDUR3 represents the major transporter for high-affinity urea transport across the plasma membrane of nitrogen-deficient *Arabidopsis* roots. Plant J 52(1):30–40

86. Kojima S, Bohner A, von Wiren N (2006) Molecular mechanisms of urea transport in plants. J Membr Biol 212(2):83–91

87. Lacoste I, Dunel-Erb S, Harvey BJ, Laurent P, Ehrenfeld J (1991) Active urea transport independent of H^+ and Na^+ transport in frog skin epithelium. Am J Physiol 261(4 Pt 2):R898–R906

88. Layton AT, Bankir L (2013) Impacts of active urea secretion into pars recta on urine concentration and urea excretion rate. Physiol Rep 1(3). pii: e00034

89. Layton AT, Pannabecker TL, Dantzler WH, Layton HE (2010) Hyperfiltration and inner stripe hypertrophy may explain findings by Gamble and coworkers. Am J Physiol Renal Physiol 298(4):F962–F972

90. Leung DW, Loo DD, Hirayama BA, Zeuthen T, Wright EM (2000) Urea transport by cotransporters. J Physiol 528(Pt 2):251–257

91. Lew SW, Bosch JP (1991) Effect of diet on creatinine clearance and excretion in young and elderly healthy subjects and in patients with renal disease. J Am Soc Nephrol 2(4):856–865

92. Liew HJ, De Boeck G, Wood CM (2013) An in vitro study of urea, water, ion and CO2/HCO3- transport in the gastrointestinal tract of the dogfish shark (*Squalus acanthias*): the influence of feeding. J Exp Biol 216(Pt 11):2063–2072

93. Liu L, Lei T, Bankir L, Zhao D, Gai X, Zhao X, Yang B (2011) Erythrocyte permeability to urea and water: comparative study in rodents, ruminants, carnivores, humans, and birds. J Comp Physiol B Biochem Syst Env Physiol 181(1):65–72

94. Liu LH, Ludewig U, Frommer WB, von Wiren N (2003) AtDUR3 encodes a new type of high-affinity urea/H+ symporter in *Arabidopsis*. Plant Cell 15(3):790–800

95. Long WS (1970) Renal secretion of urea in *Rana Catesbeiana*. In: Schmidt-Nielsen B (ed) Urea and the kidney. Excerpta Medica Foundation, Amsterdam, pp 216–222

96. Long WS (1973) Renal handling of urea in *Rana catesbeiana*. Am J Physiol 224(2):482–490

97. Lucien N, Bruneval P, Lasbennes F, Belair MF, Mandet C, Cartron J, Bailly P, Trinh-Trang-Tan MM (2005) UT-B1 urea transporter is expressed along the urinary and gastrointestinal tracts of the mouse. Am J Physiol Regul Integr Comp Physiol 288(4):R1046–R1056

98. MacKay EM, MacKay LL, Addis T (1928) Factors which determine renal weight. V. The protein intake. Am J Physiol 86:459–465

99. Marini JC, Klein JD, Sands JM, Van Amburgh ME (2004) Effect of nitrogen intake on nitrogen recycling and urea transporter abundance in lambs. J Anim Sci 82(4):1157–1164

100. McDonald MD, Gilmour KM, Walsh PJ (2012) New insights into the mechanisms controlling urea excretion in fish gills. Respir Physiol Neurobiol 184(3):241–248

101. McDonald MD, Smith CP, Walsh PJ (2006) The physiology and evolution of urea transport in fishes. J Membr Biol 212(2):93–107

102. Mills J, Wyborn NR, Greenwood JA, Williams SG, Jones CW (1998) Characterisation of a binding-protein-dependent, active transport system for short-chain amides and urea in the methylotrophic bacterium Methylophilus methylotrophus. Eur J Biochem/FEBS 251(1–2):45–53

103. Molony DA, Reeves WB, Andreoli TE (1987) Some transport characteristics of mammalian renal diluting segments. Miner Electrolyte Metab 13(6):442–450

104. Morel M, Jacob C, Fitz M, Wipf D, Chalot M, Brun A (2008) Characterization and regulation of PiDur3, a permease involved in the acquisition of urea by the ectomycorrhizal fungus *Paxillus involutus*. Fungal Genet Biol 45(6):912–921

105. Morgan RL, Ballantyne JS, Wright PA (2003) Regulation of a renal urea transporter with reduced salinity in a marine elasmobranch, *Raja erinacea*. J Exp Biol 206(Pt 18):3285–3292

106. Morgan RL, Wright PA, Ballantyne JS (2003) Urea transport in kidney brush-border membrane vesicles from an elasmobranch, *Raja erinacea*. J Exp Biol 206(Pt 18):3293–3302

107. Murdaugh HV Jr, Schmidt-Nielsen B, Doyle EM, O'Dell R (1958) Renal tubular regulation of urea excretion in man. J Appl Physiol 13(2):263–268

108. Navarathna DH, Das A, Morschhauser J, Nickerson KW, Roberts DD (2011) Dur3 is the major urea transporter in *Candida albicans* and is co-regulated with the urea amidolyase Dur1,2. Microbiology 157(Pt 1):270–279

109. Nelson RA (1980) Protein and fat metabolism in hibernating bears. Fed Proc 39(12):2955–2958

110. Nelson RA, Jones JD, Wahner HW, McGill DB, Code CF (1975) Nitrogen metabolism in bears: ureametabolism in summer starvation and in winter sleep and role of urinary bladder in water andnitrogen conservation. Mayo Clin Proc 50(3):141–146.

111. O'Connor WJ, Summerill RA (1976) The excretion of urea by dogs following a meat meal. J Physiol 256:93–102

112. O'Dell RM, Schmidt-Nielsen B (1961) Retention of urea by frog and mammalian kidney slices in vitro. J Cell Comp Physiol A 57(3):211

113. Panayotova-Heiermann M, Wright EM (2001) Mapping the urea channel through the rabbit Na(+)-glucose cotransporter SGLT1. J Physiol 535(Pt 2):419–425

114. Pateman JA, Dunn E, Mackay EM (1982) Urea and thiourea transport in *Aspergillus nidulans*. Biochem Genet 20(7–8):777–790

115. Preitner F, Bonny O, Laverriere A, Rotman S, Firsov D, Da Costa A, Metref S, Thorens B (2009) Glut9 is a major regulator of urate homeostasis and its genetic inactivation induces hyperuricosuria and urate nephropathy. Proc Natl Acad Sci USA 106(36):15501–15506

116. Rabinowitz L, Gunther RA, Shoji ES, Freedland RA, Avery EH (1973) Effects of high and low protein diets on sheep renal function and metabolism. Kidney Int 4(3):188–207

117. Rapoport J, Abuful A, Chaimovitz C, Noeh Z, Hays RM (1988) Active urea transport by the skin of *Bufo viridis*: amiloride- and phloretin-sensitive transport sites. Am J Physiol 255(3 Pt 2):F429–F433

118. Rapoport J, Chaimovitz C, Hays RM (1989) Active urea transport in toad skin is coupled to H+ gradients. Am J Physiol 256(5 Pt 2):F830–F835

119. Roch-Ramel F, Chomety F, Peters G (1968) Urea concentrations in tubular fluid and in renal tissue of nondiuretic rats. Am J Physiol 215(2):429–438

120. Roch-Ramel F, Diezi J, Chomety F, Michoud P, Peters G (1970) Disposal of large urea overloads by the rat kidney: a micropuncture study. Am J Physiol 218(6):1524–1532

121. Roch-Ramel F, Peters G (1967) Intrarenal urea and electrolyte concentrations as influenced by water diuresis and by hydrochlorothiazide. Eur J Pharmacol 1:124–139

122. Safirstein R, Miller P, Dikman S, Lyman N, Shapiro C (1981) Cisplatin nephrotoxicity in rats: defect in papillary hypertonicity. Am J Physiol 241(2):F175–F185

123. Sands JM, Martial S, Isozaki T (1996) Active urea transport in the rat inner medullary collecting duct: functional characterization and initial expression cloning. Kidney Int 49(6):1611–1614

124. Sands JM, Nonoguchi H, Knepper MA (1987) Vasopressin effects on urea and H$_2$O transport in inner medullary collecting duct subsegments. Am J Physiol 253(5 Pt 2):F823–F832

125. Schmidt-Nielsen B (1958) Urea excretion in mammals. Physiol Rev 38(2):139–168

126. Schmidt-Nielsen B, Osaki H (1958) Renal response to changes in nitrogen metabolism in sheep. Am J Physiol 193:657–661

127. Schmidt-Nielsen B, Osaki H, Murdaugh HV Jr, O'Dell R (1958) Renal regulation of urea excretion in sheep. Am J Physiol 194(2):221–228

128. Schmidt-Nielsen B, Rabinowitz L (1964) Methylurea and acetamide: active reabsorption by elasmobranch renal tubules. Science (New York, NY) 146(3651):1587–1588
129. Schmidt-Nielsen B, Robinson RR (1970) Contribution of urea to urinary concentrating ability in the dog. Am J Physiol 218(5):1363–1369
130. Schmidt-Nielsen B, Shrauger CR (1963) Handling of urea and related compounds by the renal tubules of the frog. Am J Physiol 205:483–488
131. Schmidt-Nielsen B, Truniger B, Rabinowitz L (1972) Sodium-linked urea transport by the renal tubule of the spiny dogfish *Squalus acanthias*. Comp Biochem Physiol A: Comp Physiol 42(1):13–25
132. Seney FD, Persson AEG, Wright FS (1987) Modification of tubuloglomerular feedback signal by dietary protein. Am J Physiol 252 (Renal Fluid Electrolyte Physiol. 21):F83–F90
133. Shoemaker VH, Nagy KA (1977) Osmoregulation in amphibians and reptiles. Annu Rev Physiol 39:449–471
134. Simmons NL, Chaudhry AS, Graham C, Scriven ES, Thistlethwaite A, Smith CP, Stewart GS (2009) Dietary regulation of ruminal bovine UT-B urea transporter expression and localization. J Anim Sci 87(10):3288–3299
135. Smith CP, Potter EA, Fenton RA, Stewart GS (2004) Characterization of a human colonic cDNA encoding a structurally novel urea transporter, hUT-A6. Am J Physiol Cell Physiol 287(4):C1087–C1093
136. Smith CP, Wright PA (1999) Molecular characterization of an elasmobranch urea transporter. Am J Physiol 276(2 Pt 2):R622–R626
137. Spector DA, Deng J, Stewart KJ (2012) Dietary protein affects urea transport across rat urothelia. Am J Physiol Renal Physiol 303(7):F944–F953
138. Stenvinkel P, Frobert O, Anderstam B, Palm F, Eriksson M, Bragfors-Helin AC, Qureshi AR, Larsson T, Friebe A, Zedrosser A, Josefsson J, Svensson M, Sahdo B, Bankir L, Johnson RJ (2013) Metabolic changes in summer active and anuric hibernating free-ranging brown bears (*Ursus arctos*). PLoS One 8(9):e72934
139. Stewart GS, Fenton RA, Thevenod F, Smith CP (2004) Urea movement across mouse colonic plasma membranes is mediated by UT-A urea transporters. Gastroenterology 126(3):765–773
140. Stewart GS, Graham C, Cattell S, Smith TP, Simmons NL, Smith CP (2005) UT-B is expressed in bovine rumen: potential role in ruminal urea transport. Am J Physiol Regul Integr Comp Physiol 289(2):R605–R612
141. Sumrada R, Gorski M, Cooper T (1976) Urea transport-defective strains of *Saccharomyces cerevisiae*. J Bacteriol 125(3):1048–1056
142. Svelto M, Casavola V, Valenti G, Lippe C (1982) The nature of urea transport across the skin of of Rana esculenta. Bollettino della Societa italiana di biologia sperimentale 58(12):752–755
143. Svelto M, Casavola V, Valenti G, Lippe C (1982) Phloretin sensitive active urea absorption in frog skin. Pflugers Arch 394(3):226–229
144. Trinh-Trang-Tan MM, Bankir L, Doucet A, el Mernissi G, Imbert-Teboul M, Montegut M, Siaume S, Morel F (1985) Influence of chronic ADH treatment on adenylate cyclase and ATPase activity in distal nephron segments of diabetes insipidus Brattleboro rats. Pflugers Arch 405(3):216–222
145. Turner TT, Hartmann PK, Howards SS (1979) Urea in the seminiferous tubule: evidence for active transport. Biol Reprod 20(3):511–515
146. Uchida S, Sohara E, Rai T, Ikawa M, Okabe M, Sasaki S (2005) Impaired urea accumulation in the inner medulla of mice lacking the urea transporter UT-A2. Mol Cell Biol 25(16):7357–7363
147. Valladares A, Montesinos ML, Herrero A, Flores E (2002) An ABC-type, high-affinity urea permease identified in cyanobacteria. Mol Microbiol 43(3):703–715
148. Valtin H (1977) Structural and functional heterogeneity of mammalian nephrons. Am J Physiol 233 (Renal Fluid Electrolyte Physiol. 2):F491–F501

149. Vitart V, Rudan I, Hayward C, Gray NK, Floyd J, Palmer CN, Knott SA, Kolcic I, Polasek O, Graessler J, Wilson JF, Marinaki A, Riches PL, Shu X, Janicijevic B, Smolej-Narancic N, Gorgoni B, Morgan J, Campbell S, Biloglav Z, Barac-Lauc L, Pericic M, Klaric IM, Zgaga L, Skaric-Juric T, Wild SH, Richardson WA, Hohenstein P, Kimber CH, Tenesa A, Donnelly LA, Fairbanks LD, Aringer M, McKeigue PM, Ralston SH, Morris AD, Rudan P, Hastie ND, Campbell H, Wright AF (2008) SLC2A9 is a newly identified urate transporter influencing serum urate concentration, urate excretion and gout. Nat Genet 40(4):437–442
150. Walser BL, Yagil Y, Jamison RL (1988) Urea flux in the ureter. Am J Physiol 255(2 Pt 2):F244–F249
151. Wang WH, Kohler B, Cao FQ, Liu GW, Gong YY, Sheng S, Song QC, Cheng XY, Garnett T, Okamoto M, Qin R, Mueller-Roeber B, Tester M, Liu LH (2012) Rice DUR3 mediates high-affinity urea transport and plays an effective role in improvement of urea acquisition and utilization when expressed in *Arabidopsis*. New Phytol 193(2):432–444
152. Wilkie MP (2002) Ammonia excretion and urea handling by fish gills: present understanding and future research challenges. J Exp Zool 293(3):284–301
153. Wood CM, Liew HJ, De Boeck G, Walsh PJ (2013) A perfusion study of the handling of urea and urea analogues by the gills of the dogfish shark (*Squalus acanthias*). PeerJ 1:e33
154. Wright EM, Hirayama BA, Loo DF (2007) Active sugar transport in health and disease. J Intern Med 261(1):32–43
155. Wright EM, Turk E (2004) The sodium/glucose cotransport family SLC5. Pflugers Arch 447(5):510–518
156. Yang B, Bankir L (2005) Urea and urine concentrating ability: new insights from studies in mice. Am J Physiol Renal Physiol 288(5):F881–F896

Chapter 14
Urea Transport Mediated by Aquaporin Water Channel Proteins

Chunling Li and Weidong Wang

Abstract Aquaporins (AQPs) are a family of membrane water channels that basically function as regulators of intracellular and intercellular water flow. To date, thirteen aquaporins have been characterized. They are distributed wildly in specific cell types in multiple organs and tissues. Each AQP channel consists of six membrane-spanning alpha-helices that have a central water-transporting pore. Four AQP monomers assemble to form tetramers, which are the functional units in the membrane. Some of AQPs also transport urea, glycerol, ammonia, hydrogen peroxide, and gas molecules. AQP-mediated osmotic water transport across epithelial plasma membranes facilitates transcellular fluid transport and thus water reabsorption. AQP-mediated urea and glycerol transport is involved in energy metabolism and epidermal hydration. AQP-mediated CO_2 and NH_3 transport across membrane maintains intracellular acid–base homeostasis. AQPs are also involved in the pathophysiology of a wide range of human diseases (including water disbalance in kidney and brain, neuroinflammatory disease, obesity, and cancer). Further work is required to determine whether aquaporins are viable therapeutic targets or reliable diagnostic and prognostic biomarkers.

C. Li · W. Wang (✉)
Institute of Hypertension and Kidney Research,
Zhongshan School of Medicine, Sun Yat-sen University,
74# Zhongshan Er Road, Guangzhou 510080, China
e-mail: wangwd6@mail.sysu.edu.cn

C. Li
e-mail: lichl3@mail.sysu.edu.cn

Genes and Proteins of Aquaporins

Discovery of Aquaporins

The existence of a water channel protein had been predicted since the early 1950s. The molecular identity of membrane water channels remained elusive until the pioneering discovery of AQP1 by Agre and colleagues around 1988–1992. They purified a novel protein from the red blood cell membrane [32], with a non-glycosylated component of 28 kDa, and a glycosylated component migrating as a diffuse band of 35–60 kDa. This protein was first known as "CHIP28" (channel-like integral protein of 28 kDa), but was later renamed aquaporin-1 or AQP1. Using the *Xenopus laevis* oocyte expression system and AQP1-reconstituted liposomes as mechanisms to study water transporters, Preston and Agre [139], Preston et al. [140], and Zeidal et al. [207] confirmed that CHIP28 functions as a molecular water channel, which is both necessary and sufficient to explain the well-recognized membrane water permeability of the red blood cell. This laid the groundwork for the identification of a number of related water channels by homology cloning and other means, which has led to the understanding that aquaporins (AQPs) play essential roles in transmembrane and transepithelial water transport in the tissues where they are expressed.

General Features of Aquaporins

Aquaporins are present in all membranes where a rapid (or regulated) passage of water molecules (or other small molecules) is required to allow the functions of these cells and membranes to be performed. The water channels have basic roles that alleviate the osmotic stress accompanied by the movement of ions though membranes in signal transduction, energy production, and other cell activities [6]. To date, 13 water channels, AQP0 through AQP12, have been identified and they distribute extensively in human tissues (Table 14.1), implicating important physiological significance in humans.

Sequence analysis of AQP1 demonstrated that AQP protein subunits comprise six α-helix transmembrane domains with two conserved asparagine–proline–alanine (NPA) motifs embedding into the plasma membrane, a signature sequence of water channels, as well as five loops (A through E) and intracellular N- and C-termini. The amino acid sequences of human AQPs are approximately 30–50 % identical. Conformational changes of AQP structure may permit other molecules to pass through the plasma membrane, such as urea, glycerol, H_2O_2, and CO_2.

Classification of Aquaporins

Based on these primary sequences, AQPs are subdivided into three subfamilies—aquaporins, aquaglyceroporins, and superaquaporins (Table 14.1). The first subfamily are the aquaporins, the water selective or specific water channels, also named as "orthodox," "classical" aquaporins, including AQP0, AQP1, AQP2,

Table 14.1 Mammalian aquaporins

Aquaporin	Transport	Exon numbers	Chromosome locus	Organ expression
AQP0	Water	4	12q13	Eye
AQP1	Water	4	7p14	Brain, eye, kidney, heart, lung, gastrointestinal tract, salivary gland, liver, ovary, testis, muscle, erythrocyte, spleen
AQP2	Water	4	12q13	Kidney, ear, ductus deferens
AQP4	Water	4	18q22	Brain, kidney, salivary gland, heart, gastrointestinal tract, muscle
AQP5	Water	4	12q13	Salivary gland, lung, gastrointestinal tract, ovary, eye, kidney
AQP6	Water, urea (±), anion	4	12q13	Brain, kidney
AQP8	Water, urea (±), ammonia	6	16q12	Testis, liver, pancreas, ovary, lung, kidney
Aquaglyceroporins				
AQP3	Water, urea, glycerol, ammonia	6	9p13	Kidney, heart, ovary, eye, salivary gland, gastrointestinal tract, respiratory tract, brain, erythrocyte, fat
AQP7	Water, urea, glycerol, ammonia	6	9p13	Testis, heart, kidney, ovary, fat
AQP9	Water, urea, glycerol	6	15q22	Liver, spleen, testis, ovary, leukocyte
AQP10	Water, urea, glycerol	6	1q21	Gastrointestinal tract
Superaquaporins				
AQP11	Water?	3	11q13	Testis, heart, kidney, ovary, muscle, gastrointestinal tract, leukocytes, liver, brain
AQP12	Unknown	3	2q37	Pancreas

Ishibashi et al. Euro biophysic J, 2012; Litman et al. Handb Exp Pharmacol. 2009

AQP4, AQP5, AQP6, and AQP8. This subfamily of AQPs has been extensively studied and has helped define the gene and protein expression of AQPs in tissue, cellular, and subcellular localizations, as well as their potential roles in physiological and pathophysiological processes. The association of mutations of genes encoding AQPs with human hereditary disorders and detailed phenotype analysis of transgenic mice lacking genes encoding AQPs has also aided our understanding of AQP function, especially in water homeostasis [160, 172].

The second subfamily is represented by aquaglyceroporins, which are permeable to water (to varying degrees), but also to other small uncharged molecules (ammonia, urea, and in particular, glycerol). They also facilitate the diffusion of charged and non-charged molecules of the metalloids, arsenic, and antimony and play a crucial role in metalloid homeostasis [11]. The aquaglyceroporins, including AQP3, AQP7, AQP9, and AQP10, can be distinguished from aquaporins based on amino acid sequence alignments [15]. The first mammalian aquaglyceroporin to be cloned, AQP3, is permeable to glycerol, urea, and water [37, 68, 95, 197]. AQP7 and AQP10 transport water, glycerol, and urea when expressed in Xenopus oocytes [66, 67]. AQP7 has a variant NPA box. The proline in the first NPA box is changed to an alanine, thereby changing the first NPA motif to NAA, whereas a serine replaces the alanine in the second NPA box, resulting in an NPS motif [80]. AQP9 transports water, glycerol, and urea, but also is permeable to a wide range of other solutes in oocytes [170]. AQP9 exhibits high homology to AQP3 (48 %), AQP7 (45 %), and to the amino acid residue region 20–281 of AQP7 (76 %) and has less homology with other aquaporins, including AQP1 (33 %) [3, 170]. However, potentially physiological roles of most aquaglyceroporins in transporting glycerol and urea are less understood.

In addition to aquaporins and aquaglyceroporins, a third subfamily of related proteins was discovered later [68] that have little conserved amino acid sequences around the NPA boxes. They are unclassifiable to the first two subfamilies. Originally, this subfamily included mammalian AQP11 and AQP12 and was called "superaquaporins." Their NPA boxes, however, are quite different from those of previous AQPs (less than 20 % homology at amino acid level), which indicates that they belong to a supergene family of AQPs. Although they are grouped in a single subfamily, there are few homologies between them [62, 63].

Genetic Variations of Aquaporins

Genetic variants of AQPs may result in a disturbance of molecular selectivity and transport by AQPs; disruption of the formation of tetramers or arrays; and misfolding, faulty sorting, or other dysfunction of AQPs [160]. Cellular and human studies of naturally occurring and synthetic mutations have provided great insight into the biology and phenotypic associations of these proteins. While genetic variation in some human AQPs is well characterized, other AQPs are less understood. AQP2 has been most frequently studied due to its many variants and their roles in

nephrogenic diabetes insipidus. Natural human variants have also been character-ized in AQP0, AQP1, and AQP4 [161], which are associated with cataracts, the Colton blood group, and likely water imbalance in the brain, respectively. Natural human variants in AQP3 and AQP7 are shown to be associated with the GIL blood group [149] and abnormal glycerol metabolisms. There are also single uncharac-terized variants in AQPs [160], for which functional significance is still unknown. Improved understanding of the function and variation in AQP genes will lead to novel insights for the diagnosis and treatment of human disease.

Water Transport Property of Aquaporins

While osmotically driven transmembrane water movement can occur via sim-ple diffusion through the lipid bilayer, the selective membrane water permeabil-ity required for rapid and regulated physiologic processes such as secretion and reabsorption requires facilitation through proteinaceous water pores. Many AQP channels are thought to have an exquisite specificity for water (also glycerol, urea, gas, etc.) and are capable of rapidly transporting it in response to changes in tonic-ity; evidence suggests that they make a critical contribution to the regulation of transcellular water flow [28, 80].

Structure of Aquaporins

Overall AQP structure is largely conserved among the various AQP classes, spe-cies, and isoforms, despite significant differences in sequence similarities. Structural studies have provided a relevant insights regarding the determining requirements that enable homotetramer formation, the quaternary structure that actually enables water transport activity in animal AQPs [110, 157].

All the members of the AQP family are small, very hydrophobic, intrinsic membrane proteins, which are present in the membrane as tetramers, each of them constitutes a channel [127, 174]. AQP family proteins have six membrane-spanning helices connected by five loops and have intracellular N- and C-termini (Fig. 14.1a) [1, 74, 127, 174]. Loops B and E feature short helical subunits that penetrate the plasma membrane, and interact with each other at highly con-served Asn-Pro-Ala (NPA) repeats, which are the signature sequences for AQPs (Fig. 14.1a). The six transmembrane domains, and B and E loop helices, form a compact channel, with the interacting NPA repeats marking its narrowest point (Fig. 14.1a). The protein further self-assembles into a tetrameric biological unit, where in addition to the four substrate channels (Fig. 14.2a), an additional tetrameric pore is formed, which is thought to be responsible for the transloca-tion of dissolved gasses and ionic species (Fig. 14.2b) [61]. AQP4, on the other hand, forms larger oligomeric structures in the plasma membrane, also called
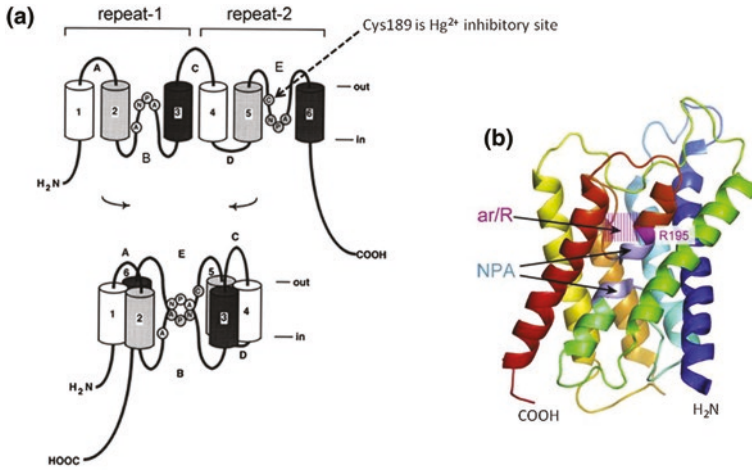
Fig. 14.1 Secondary structure and topology of an aquaporin molecule. **a** AQPs have six membrane-spanning regions, both intracellular amino and carboxy termini, and internal tandem repeats. The tandem repeat structure with two asparagine-proline-alanine (*NPA*) sequences has been proposed to form tight turn structures that interact in the membrane to form the pathway for translocation of water across the plasma membrane. Of the five loops in AQP1, the *B* and *E* loops dip into the lipid bilayer, and form "hemichannels" that connect between the leaflets to form a single aqueous pathway within a symmetric structure that resembles an "hourglass." [Reproduce with permission from (Nielsen et al. 1999)]. **b** A ribbon model of AQP1 using a rainbow color scheme from N-terminal to C-terminal. The narrowest region in the AQP1 pores, termed ar/R, is located close to the extracellular entrance of the pore. The NPA motifs are shown in light blue and the Arg195 is shown in magenta. [Reproduce with permission from (Tani and Fujiyoshi 2014)]

orthogonal arrays (clusters of intramembrane particles in a special systematic/geometric organization) [189], which may suggest a possible role of AQP4 in membrane junction formation in vivo [84, 176]. The AQPs also share another highly conserved sequence, the aromatic/arginine (ar/R) region, which exits at the extracellular side of the channel and constitutes the selectivity filter of the protein (Fig. 14.1b), based on a comparison of the diameter of ar/R between AQP1 and the aquaglyceroporins. In aquaporins, there are two NPA boxes, the "signature" sequence for aquaglyceroporins is the aspartic acid residue in the second NPA box, which expands the pore to accept larger molecules such as glycerol [65].

Mercurial reagents such as $HgCl_2$ inhibit water channel-mediated water permeability. In AQP1, the residue Cys189 is the site of mercurial binding and water transport inhibition (Fig. 14.1a) [74, 140]. This inhibition mechanism was elucidated recently by molecular dynamics simulations [58], which show that the pore is collapsed by conformational changes at the ar/R region, where the mercury-sensitive cysteine residue is located. By binding to cysteine residues, mercury inhibits water and glycerol transport by mammalian AQPs [83], and both nickel and copper cations inhibit glycerol permeability in human lung epithelial cells by interference with the extracellular amino acids Trp128, Ser152, and His241 [208, 210].
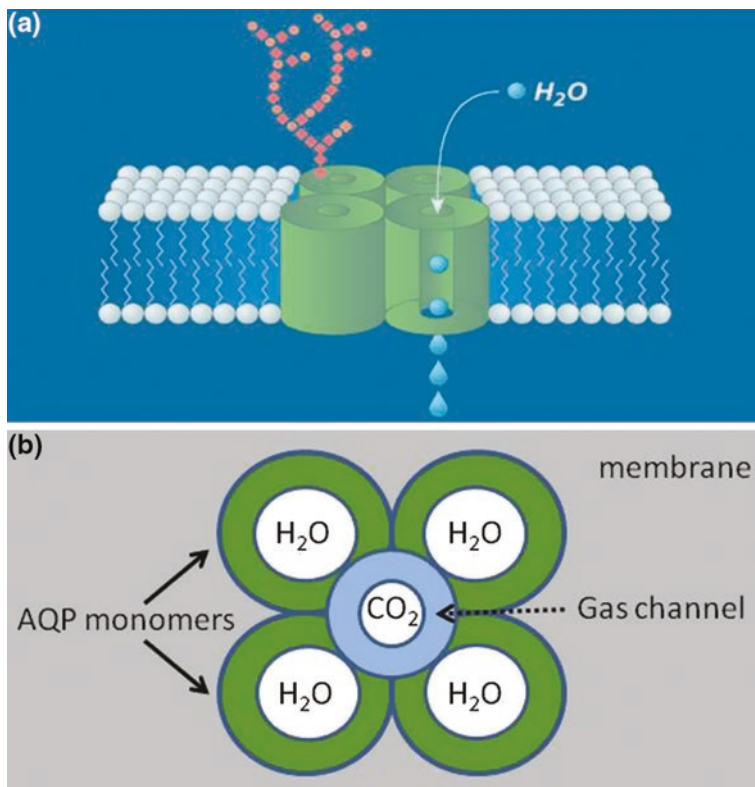
Fig. 14.2 Structures of AQP1 showing the typical AQP fold. **a** AQP1 is a multisubunit oligomer that is organized as a tetrameric assembly of four identical polypeptide subunits with a large glycan attached to only one and each AQP1 monomer transports water (Adapted from Nielsen et al. [127]). **b** AQP1 tetramer in membrane from *top view*. Gas molecules (e.g., CO_2) are thought to entry AQP1 though the central pore

However, it was demonstrated that not all AQPs are inhibited by $HgCl_2$, such as AQP4 [189] and AQP6. The characteristic case is AQP6, whose water permeability is increased in the presence of this mercurial agent [205].

Water Transport by Aquaporins

Molecular dynamic simulations enabled us to understand more details about aquaporin function. Using real-time molecular dynamic simulations of water movement through human AQP1, a two-stage filter model was proposed, in which the NPA motif forms a selectivity-determining region, and the aromatic/arginine (ar/R) region functions as a proton filter [29]. Water flux through AQPs may therefore be roughly considered to occur by single-file permeation. The ordered water structure in the

channel is ensured by the frequent arrangement of hydrogen bond partners along the pore, which also compensate for the loss of solvation when water molecules enter the channel. The dipoles of the two half helices B and E generate an electrostatic field inside the pore, which make the water dipoles rotate by 180° upon permeation [60].

Water transport by aquaporins was first confirmed in biophysical function studies of AQP1. Expression of AQP1 in *X. laevis* oocytes demonstrated that AQP1-expressing oocytes exhibited remarkably high osmotic water permeability, causing the cells to swell rapidly and explode in hypotonic buffer. The osmotically induced swelling of oocytes expressing AQP1 occurs with low activation energy and is reversibly inhibited by $HgCl_2$ or other mercurials. Liposomes reconstituted with AQP1 showed extremely high water permeability which is dramatically and reversibly reduced by $HgCl_2$ [207]. Zeidel et al. also demonstrated that AQP1 proteoliposomes are not permeable to various small solutes or protons, thus revealing that AQP1 is water selective.

Urea, Glycerol, Other Polyols, and Gas Transport Mediated by Aquaporins

The ar/R region in AQP is the selectivity filter for uncharged solutes. Small solutes are filtered through a hydrophobic effect. For larger solutes such as glycerol, steric restraints combined with the arrangement of hydrogen bond donors and acceptors determine channel selectivity. Whether and under which conditions AQPs facilitate gas transport remains under debate [60].

Aquaporins and Urea Transport

The human aquaporins AQP3, AQP7, AQP9, AQP10, and possibly AQP6 are permeable to urea, but the possible role of these aquaporins in urea transport is not fully understood.

The urea transporters (UTs) and the urea-permeable aquaporins are not usually colocalized to the same extent in tissue, with an exception that AQP3 and UT-A3 express in the basolateral membrane of inner medullary principal cells. It is likely that there is no functional overlap of UTs and aquaporins in the kidney. The erythrocyte expresses the urea transporter UT-B [5] and the urea-permeable AQP9 [93]. The ability to transport urea would mitigate osmotic shrinkage of erythrocytes while passing through the kidney, although AQP9 in erythrocytes may function more for the passage of glycerol. The interdependence of the two modes of transport has not been investigated. Interestingly, direct functional evidence for UT-B-facilitated water transport in erythrocytes was demonstrated in double knockout mice lacking both AQP1 and UT-B, suggesting that urea traverses an aqueous pore in the UT-B protein [198], although water movement through UT-B is very unlikely to be physiologically important in erythrocytes. AQP10 is only found in

the small intestine. Initial studies in Xenopus oocytes determined that the shorter form of AQP10 has low water permeability and no permeability to urea or glycerol [52], while the longer form transports water, urea, and glycerol [67]. The function and regulation of AQP10 in urea transport is less extensively studied.

In the kidney, it has been proposed that the urea that is reabsorbed from the thick ascending limbs enters the neighboring proximal straight tubules; thus, complete recycling occurs between the descending limbs and ascending limbs of the loop, with AQP7 acting as a component of the pathway for urea in the proximal straight tubules [64]. However, plasma and urine urea levels in AQP7 knockout mice did not differ from those in wild-type mice [158, 159], and there was also no difference between AQP7 knockout and wild-type mice in the urea content of the papilla, either. To detect small differences in urea levels, a low-protein diet, which limits the urea supply to the kidney, was provided. AQP7 knockout mice did not show impairment in urea accumulation in the papilla even with dehydration when compared with wild-type mice. They also did not show a urine concentrating defect with a low-protein diet and dehydration. Therefore, so far, there is no evidence that AQP7 plays a role in urea recycling in the kidney in vivo.

AQP9 is a urea-permeable protein that is localized at the basolateral membrane of hepatocytes [39]. Ketogenic and high-protein diets, which are associated with increases in plasma β-hydroxybutyrate and urea levels, respectively, do not alter AQP9 levels in rat liver [21], indicating that urea transport is not the primary function of AQP9 in the liver. Consistently, AQP9 null mice do not show any different levels of plasma or tissue urea [148]. A recent study on $AQP9^{-/-}$ and $UT-A1/3^{-/-}$ knockout and $AQP9^{-/-}/UT-A1/3^{-/-}$ double knockout mice show that an unidentified UT-A urea channel constitutes a primary but redundant urea facilitated transporter in murine hepatocytes, in addition to AQP9, for the export of urea to the blood [73]. This suggests that a primary function of AQP9 may be to make glycerol available for gluconeogenesis in hepatocytes, but AQP9 does not contribute to the removal of urea from the liver.

Interestingly, however, AQP3, AQP7, and AQP9 appear to play roles in urea transport in skin. All three AQPs are upregulated in normal human keratinocytes after stimulation with relatively low doses of exogenous urea [47]. Mercury, nickel, and copper cations that are known to inhibit water and glycerol transport by mammalian AQPs and significantly inhibited ^{14}C-labeled urea uptake into keratinocytes, indicating that AQPs also contribute to the net uptake of urea by keratinocytes. The study also suggested that uptake of urea through UTs and AQPs improves epidermal barrier function and plays an important role in keratinocyte differentiation, lipid synthesis, and maintenance of epidermal homeostasis (Fig. 14.3). In pancreas, urea (or glycerol) can activate beta cells via rapid uptake across the beta-cell plasma membrane, probably via AQP7, resulting in cell swelling, volume-regulated anion channel activation, electrical activity, and insulin release [9]. Mice with AQP3 deletion, which have nephrogenic diabetes insipidus under normal conditions, can actually concentrate urine to a high level when given a urea load but at the expense of a reduction in the excretion of other solutes. The capacity of urea to enhance the concentration of non-urea solutes may rest on AQP3 and its capacity to transport both urea and water [214].
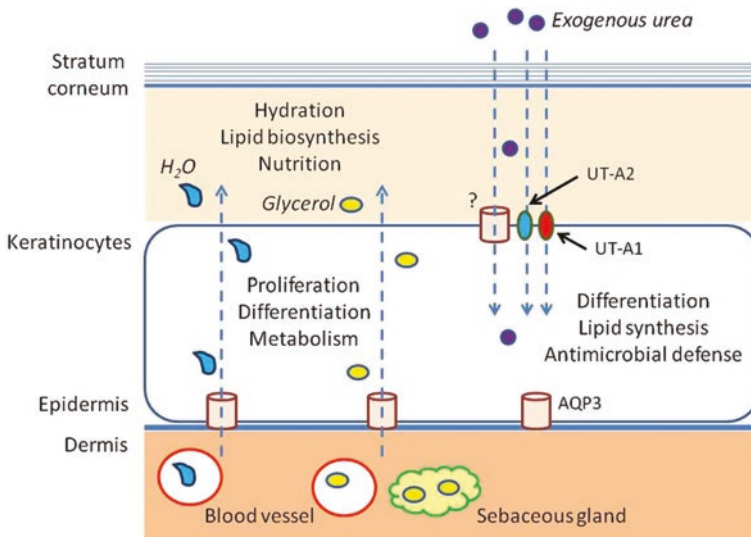
Fig. 14.3 Proposed mechanism of AQP3 function in epidermis. AQP3 facilitates water and glycerol transport from blood and sebaceous glands to keratinocytes. Steady-state glycerol content in epidermis and stratum corneum maintain skin hydration, lipid metabolism, and biosynthesis. AQP3-mediated transport of water and glycerol is also involved in proliferation and differentiation of keratinocytes. UT-A1, UT-A2, and AQP3 facilitates urea uptake in skin, which may induce keratinocyte differentiation and improve barrier and antimicrobial defense function of skin. Urea transporter (*UT*)

Although so far there is no evidence showing that aquaporins play dominant roles in urea transport in normal conditions, it is still unknown whether aquaporins are in coordination with UTs in urea transport in pathophysiological conditions.

Aquaporins and Glycerol Transport

Aquaporin AQP3, AQP7, AQP9, and AQP10, also called aquaglyceroporins, encompass a subfamily of aquaporins that allow the movement of water and other small solutes, especially glycerol, through cell membranes.

Circulating glycerol results from fat lipolysis, diet-derived glycerol or glycerol reabsorbed in the proximal tubules [144]. Glycerol represents an important metabolite for the control of fat accumulation and glucose homeostasis, given that glycerol constitutes the major substrate for hepatic gluconeogenesis during fasting. In addition, glycerol serves as an energy substrate for pancreatic cells and cardiomyocytes via the glycerol-3-phosphate shuttle, a reaction that allows the NADH synthesized in the cytosol by glycolysis to contribute to the oxidative pathway in the mitochondria to generate ATP [57]. Thus, the regulation of glycerol transport by aquaglyceroporins contributes to the control of energy production, metabolism, and homeostasis, as well as insulin secretion and other functions.

Aquaglyceroporins display characteristic subcellular localization in murine 3T3-L1 adipocytes. AQP3 is present in the plasma membrane and cytoplasm, AQP7 resides predominantly in the cytoplasm upon the lipid droplets, whereas AQP9 is constitutively expressed in the plasma membranes [144]. The main function of aquaglyceroporins in adipocytes is the control of glycerol uptake and release, which is involved in lipogenesis and lipolysis [102], and is regulated by lipogenic (mainly insulin) and lipolytic (by leptin and catecholamines) hormones. The liver plays another central role in glycerol metabolism, where glycerol enters hepatocytes via AQP9, and is converted into glycerol-3-phosphate for gluconeogenesis and triglyceride synthesis. AQP9 is localized at the sinusoidal plasma membrane that faces the portal vein and therefore constitutes the most important glycerol channel in hepatocytes [21, 39] (Fig. 14.4). Therefore, promoting AQP3 and AQP7-facilitated glycerol efflux from adipose tissue, while reducing the glycerol influx into hepatocytes via AQP9 may prevent the excessive lipid accumulation and the subsequent aggravation of hyperglycemia in human obesity [102, 113, 144] (see below).

Aquaporins and Ammonia Transport

Several AQPs are able to transport ammonia (NH_4^+) [92], including AQP3, AQP7, AQP8, AQP9, and AQP10. The ammonia-permeable aquaporins have a distinct ar/R region, a major size-limiting filter, compared to the aquaporins permeable to water. In these AQPs, the amino acid residues of this filter allow larger substrates
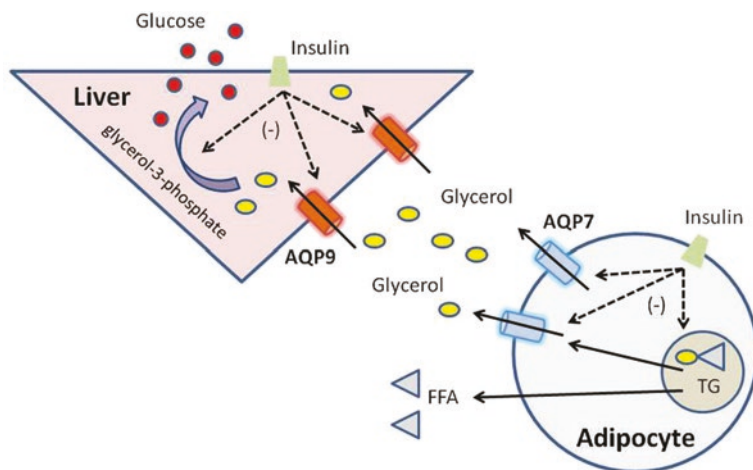
Fig. 14.4 Coordinated regulation of adipose tissue AQP7 and liver AQP9 in glycerol metabolism. AQP7 facilitates glycerol exit from adipocytes, preventing intracellular glycerol and triglyceride accumulation. AQP9 in the liver contributes to the entry of portal glycerol into hepatocytes, where glycerol is one of the substrates for gluconeogenesis. Insulin inhibits expression of AQP7 and AQP9, suppresses release of glycerol from the adipose and transport of glycerol to the liver as well as gluconeogenesis in the liver

to pass. In mammals, the membrane proteins of the Rhesus-type (Rh) were found to function as ammonia transporters as well as giving rise to the antigens of the red blood cells [92]. Ammonium is potentially toxic, yet is an essential component in amino acid metabolism. As a consequence, transport of ammonia has to be regulated precisely so that plasma ammonia concentration is kept low. Interestingly, the ammonia-permeable aquaporins and the Rh proteins RhAG, RhBG, and RhCG are found colocalized in tissues involved in ammonia transport. In the liver, RhBG is localized to the basolateral membrane of the perivenous hepatocyte together with AQP9 [21]. In the kidney, RhBG is found basolaterally in the collecting duct [186] where it overlaps to some degree with AQP3. These facts may suggest coordination between AQPs and Rh proteins during ammonia transport. The parallel location of the ammonia-permeable aquaporins and the Rh group of proteins applies to the cells associated with either nitrogen homeostasis or high rates of anabolism.

As it is located in basolateral membrane of principal cells in cortical and outer medullary collecting ducts, AQP3 could play a direct role in the final steps of acid secretion via NH_4^+, which take place across the collecting duct epithelium [92]. In a well-established metabolic acidosis rodent model induced by NH_4Cl in drinking water, AQP3 protein was significantly upregulated [132]. It is, therefore, expected that AQP3 knockout mice may have impaired urinary acidification.

Permeability of AQP7 to glycerol and ammonia suggests a role in carbohydrate and amino acid metabolism in adipose, liver, and skeletal muscles. In the liver, AQP8 can be found in the mitochondria of hepatocytes [19], suggesting a direct role for the uptake of NH_4^+ to supply the urea cycle. In hepatocyte mitochondrial, AQP8 was recently shown to facilitate the mitochondrial uptake of ammonia and its metabolism into urea. This mechanism may be relevant to hepatic ammonia detoxification and in turn, avoid the deleterious effects of hyperammonemia [162], although an early study did not support the physiological significance of NH_3 transport facilitated by AQP8 in mice [201]. In the liver, AQP9 localized in the hepatocyte plasma membrane facing the sinusoids [21, 148] and may mediate ammonium transport from the blood into the periportal hepatocytes for metabolism; urea produced in the urea cycle may leave the cell again via AQP9 [21, 148].

Aquaporin and Transport of Other Polyols

AQP9 shows a unique feature of being permeable to mannitol, sorbitol [171], purines (adenine), pyrimidines (uracil, 5-fluorouracil), and monocarboxylates (lactate, β-hydroxybutyrate). It is interesting to note that the coefficient of AQP9 diffusion for lactate and β-hydroxybutyrate is dependent on pH with a significantly increased permeation in low pH [170], suggesting that monocarboxylates can be transported via AQP9 only in the protonated form.

Aquaporin and H_2O_2 Transport

Reactive oxidative species (ROS) activate components of diverse signaling pathways and trigger the expression of specific genes required for cellular and metabolic adaptation. H_2O_2, one of the most abundant and stable ROS molecules in organisms, possesses reducing and oxidizing properties that are important for its multiple intracellular and intercellular functions. Evidence shows that several AQPs may mediate H_2O_2 transport across the plasma membrane. Silencing AQP8-inhibited H_2O_2 entry into HeLa cells and also inhibited the H_2O_2 spikes and phosphorylation of downstream proteins induced by epidermal growth factor [8]. Studies on human hepatoma HepG2 cells suggest that mitochondrial AQP8 facilitates mitochondrial H_2O_2 release and that its defective expression causes ROS-induced mitochondrial depolarization via the mitochondrial permeability transition mechanism and cell death [105, 106]. Endogenous AQP3 expression modulates intracellular H_2O_2 accumulation and thus influences downstream cell signaling cascades [112]. AQP3-mediated H_2O_2 uptake is also required for chemokine-dependent T cell migration in sufficient immune response [49]. Taken together, AQP-mediated H_2O_2 transport indicates broad implications for the controlled use of this potentially toxic small molecule for beneficial physiological functions.

Aquaporins as Gas Transporters

In the plasma membrane, AQP1 exists as a homotetramer with each subunit containing an individually functional water pore. At the center of the four monomers lies a fifth pore composed mainly of hydrophobic amino acids that may provide a path for non-polar molecules [54, 157, 184], such as gas (Fig. 14.2b). Several aquaporins including AQP1, AQP3, AQP4, AQP5, AQP8, and AQP9 each have a characteristic CO_2, NO, and NH_3 permeability.

CO_2 Early studies showed that influx, permeability, and transport of CO_2 were increased by several fold in oocytes injected with AQP1 mRNA and in proteoliposomes containing purified AQP1, suggesting that CO_2 uses the single water channel to traverse the channel protein [27, 138]. Also, the rate of CO_2 transport was blocked by mercurial agents and by substituting Ser for Cys189 in AQP1[120, 138], indicating that blocking the aquapores causes conformational changes in the central pore, making it less permeable to CO_2, as mercurial agents inhibit AQP1 by binding to Cys189, which is located in the water pore itself. By using ^{18}O-labeled HCO_3^- to examine the CO_2 permeability of wild-type versus AQP1-null human red blood cells, one study showed that CO_2 permeability was reduced by $\sim$60 % in the AQP1-null red blood cells [41], supporting the hypothesis that AQP1 facilitates CO_2 movement across the plasma membrane. Insertion of human AQP1 into cholesterol-containing membranes causes a physiologically and highly significant increase in

membrane CO_2 permeability. This suggests that both cholesterol and AQP1 protein are necessary for CO_2 permeability across biological membranes [72].

However, some investigators showed that AQP1-dependent CO_2 transport has no physiological relevance [42, 191]. Lung gas exchange has been studied in vivo in AQP1-deficient mice that have been ventilated with 5 % CO_2 in oxygen. No difference in CO_2 transport could be observed between AQP1-deficient mice and wild-type mice [191]. The reason for the unexpected finding is still unclear, but a limitation of CO_2 release to the alveolar lumen caused by the lack of AQP1 could be one of explanations, especially when the contact time of red blood cells to pulmonary capillaries is short.

AQP1 is abundantly expressed in the proximal tubules of the kidney, where it takes up 70–80 % of the filtered HCO_3^-. The transport of CO_2 across the apical membrane of the proximal tubule is the first step in the reabsorption of HCO_3^- [54], however, evidence about a role of AQP1 as a CO_2 (or NH_3) channel in renal acid–base regulation is still lacking (Fig. 14.5).

NO Nitric oxide is a gas that plays important roles in cardiovascular, renal, and central nervous system (CNS) physiology. It is known that NO produced by the endothelial cells of the vasculature relaxes adjacent vascular smooth muscle cells, and thus regulates blood flow and blood pressure. It means that NO must exit the endothelial cells and enter the vascular muscle cells where it acts; the process was previously thought to occur by free diffusion through the lipid bilayer of the cell membrane. This conception was later challenged by an observation which showed that AQP1, expressing in both endothelial cells and vascular smooth muscle cells, facilitated NO transport and increased NO influx rate across the cell membrane in Chinese hamster ovary cells transfected to express AQP1 and in the lipid bilayer inserted with human AQP1 [55]. Free diffusion of NO between cells still occurs in the absence of AQP1, although more slowly. Studies from the same group later demonstrated that NO transport into vascular smooth muscle cells and out of endothelial cells is diminished in cells lacking AQP1. NO-dependent relaxation is impaired in thoracic aortas from AQP1-deficient mice. In addition, NO stimulated by acetylcholine induced relaxation was decreased in vessels isolated from AQP1-deficient mice when compared with wild-type mice, indicating that endothelium-dependent relaxation was impaired in the absence of AQP1 [53]. Decrease of NO transport in endothelia of AQP1-deficient mice raised the question of whether these mice are hypertensive, indeed they have lower blood pressure than controls. This discrepancy is likely explained by the fact that these mice have a urine concentrating defect which might mask the hypertensive phenotype dictated by defective NO-dependent relaxation in the systemic vasculature [54]. However, a more recent study demonstrated that AQP1 deletion decreased baseline blood pressure by increased prostanoid-dependent relaxation in resistance vessels, but not the endothelial NO-dependent relaxation [116]. In addition to AQP1, evidence shows that AQP4, a major AQP located in the brain, is also permeable to NO through its central pore. Interestingly, the central pore of AQP4 appears to serve as a better gas conduction pathway than that of AQP1 [185]. As AQP4 forms high-density arrays in cells near NO sources (e.g., neurons that synthesize neuronal NO
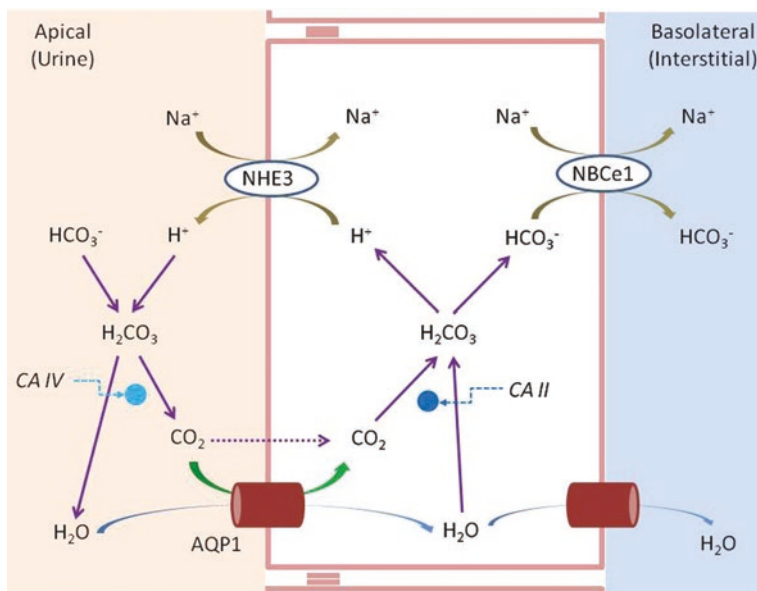
Fig. 14.5 Potential physiological role of AQP1 in mediating CO_2 transport in the epithelium of renal proximal tubule (*PT*). The cells of the PT secrete H^+ into the tubule lumen using the Na^+–H^+ exchanger NHE3 at the apical membrane. The secreted H^+ in the lumen titrate filtered HCO_3^- to form H_2O and CO_2, catalyzed by luminal carbonic anhydrase IV (*CA IV*). AQP1 mediates H_2O reabsorption, meanwhile, it may also facilitate transporting CO_2 into the epithelial cells of the PT, where it is converted back to HCO_3^- by soluble carbonic anhydrase II (*CA II*). CO_2 can also freely diffuse across plasma membrane of epithelial cells in the PT. In turn, HCO_3^- is extruded across the basolateral membrane into the interstitium via the electrogenic Na^+/HCO_3^- cotransporter (NBCe1)

synthase, nNOS) in the brain, it would be of interest to investigate whether AQP4 might play a role in the control of NO flow in the CNS.

NH3 NH$_3$ transport by AQPs has not been extensively studied. AQP1, AQP3, AQP8, and AQP9 have been shown to facilitate NH$_3$ transport in Xenopus oocytes and lipid bilayers expressing AQPs, respectively [59, 118, 153]. AQP-facilitated movement of NH$_3$ across the plasma membrane may be more closely correlated with ammonia transport.

Physiology of Aquaporins

AQPs are relatively ubiquitous in mammalian organs and are usually not restricted to a sole tissue. They are expressed in a wide range of tissues (Table 14.1), often spatially located within a certain region of the cell. This enables them to play central roles in the flow of water, glycerol, urea, ammonia, and gas through those tissues [46].

Aquaporins

AQP0 AQP0 is present in the eye lens fiber cells and its mutation provokes cataract formation. Lowering internal Ca^{2+} concentration or inhibiting calmodulin increased AQP0 water permeability. As the Ca^{2+} concentration throughout the layers of the lens differs, it is possible that the water permeability of AQP0 also varies among the layers of the lens in a physiologically significant manner [20, 122].

AQP1 AQP1 is mostly expressed in red blood cells, brain, lung, and kidney and is associated with water reabsorption and fluid secretion [14]. AQP1 is expressed in cholangiocytes, the cells that line bile ducts and secrete water in response to the hormone secretin [129]. When cholangiocytes were stimulated with secretin, there was an increase in the amount of AQP1 on the plasma membrane and a decrease in the amount of intracellular AQP1 [107]. In the lung, AQP1 is expressed in the endothelial cells of the capillaries where gas exchange occurs [129]. AQP1 has also been suggested to be involved in cerebrospinal fluid secretion and reabsorption [164] (see below). In the kidney, AQP1 protein is highly expressed in proximal tubules, descending thin limbs, and vasa recta [129] (Fig. 14.6). The transepithelial osmotic water permeability (P_f) in isolated S2 segments of the proximal tubule was found to be about fivefold lower in AQP1 knockout mice than in wild-type mice, highlighting the main role of AQP1 in transcellular water reabsorption in this nephron segment [154]. Transgenic mice with knockout of the AQP1 gene [97] have polyuria and a urinary concentrating defect that was not sensitive to vasopressin treatment, however, it could be partially corrected by delivery of an adenovirus encoding AQP1 [193]. In humans, AQP1 encodes the Colton blood group antigen. Colton-null subjects have a reduced ability to concentrate urine when subjected to water deprivation, which is in agreement with the data obtained in AQP1 knockout mice [76].

AQP1 also plays an important role in angiogenesis, cell migration, and cell growth. AQP1 is strongly expressed in tumor cells and promotes cell migration and tumor cell angiogenesis [123, 173]. AQP1 deletion reduces endothelial cell migration, limiting tumor angiogenesis and growth [151]. A recent study showed that reduction of AQP1 expression via chemical downregulation blocked angiogenesis and slowed the progression of tumors [12]. Not only AQP1, but other AQPs such as AQP3 and AQP4, may facilitate cell migration (see below). AQP-facilitated cell migration might be relevant not only to angiogenesis but also to tumor spread, glial scarring, wound healing, and other physiological phenomenon.

AQP2 AQP2 is expressed in principal cells of the collecting ducts and is abundant both in the apical plasma membrane and subapical vesicles [126] (Fig. 14.6). AQP2 is the primary target for vasopressin regulation of collecting duct water permeability [125, 188]. AQP2 mutations can cause an autosomal form of hereditary nephrogenic diabetes insipidus in humans [31]. Lack of functional AQP2 expression in AQP2 gene knockout mice [146] produces a severe urine concentration defect, papillary atrophy and hydronephrosis, and results in postnatal death.
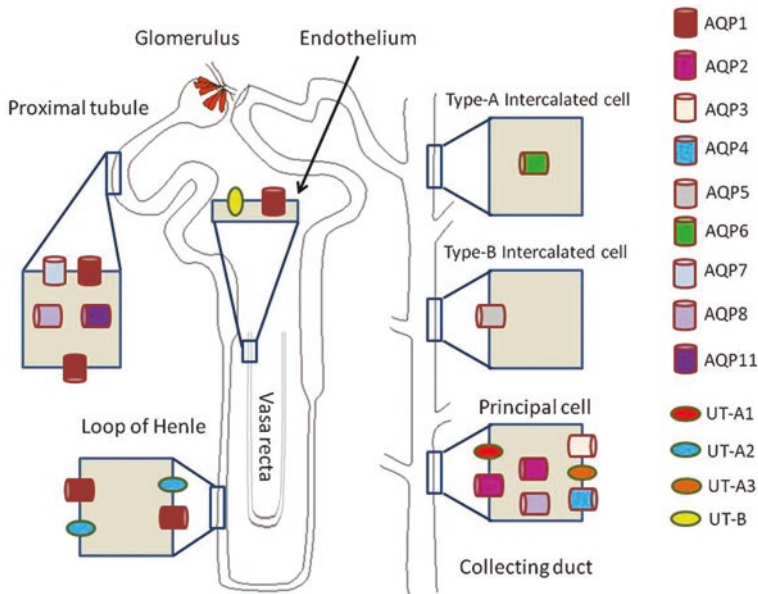
Fig. 14.6 Expression of renal aquaporins along the nephron and collecting ducts. Blood is filtered by glomeruli, and most of the filtrate is reabsorbed through AQP1 in the proximal tubule and descending thin limbs of Henle. AQP1 is also expressed in endothelia of the descending vasa recta, facilitating the removal of water. In the connecting tubule and collecting duct, AQP2 is mainly expressed at the apical membrane and intracellular vesicles of principal cells, while AQP3 and AQP4 are present at the basolateral membrane of the principal cells, representing exit pathways for water reabsorbed via AQP2. AQP5 is apically expressed in type-B intercalated cells in the collecting ducts. AQP6, AQP8, and AQP11 are localized in intracellular membranes only. AQP6 is localized to intercalated cells of the collecting duct, while AQP8 and AQP11 are expressed in proximal tubules. Several urea transporters are colocalized with AQPs in the kidney, UT-A1 is expressed in the apical membrane, whereas UT-A3 is present at the basolateral membrane of the principal cells. UT-A2 is localized in descending thin limbs of Henle, UT-B is expressed in endothelia of the descending vasa recta

AQP2 expression in principal cells of the collecting ducts is regulated by vasopressin when binding to its V2 receptor (Fig. 14.7). Under conditions of normal hydration, AQP2 is confined to the cytoplasm of the collecting duct cells. When the body is dehydrated and needs to retain water, AQP2 relocates to the apical membrane, thus enabling water reabsorption from the tubule into the cell. Vasopressin binds to the vasopressin V2 receptor on the basolateral plasma membrane of the collecting duct principal cells and initiates the signal transduction. Vasopressin binding to the V2 receptor promotes the disassembly of the bound hetertrimeric G-protein, Gs, into Gα and Gβγ subunits, Gsα then stimulates adenylyl cyclase, resulting in an increase in intracellular cyclic adenosine monophosphate (cAMP) levels. Increased cAMP activates protein kinase A, which phosphorylates AQP2 at serine 256. As a consequence of AQP2 phosphorylation, subapical storage vesicles that contain AQP2 translocate from the cytoplasm of
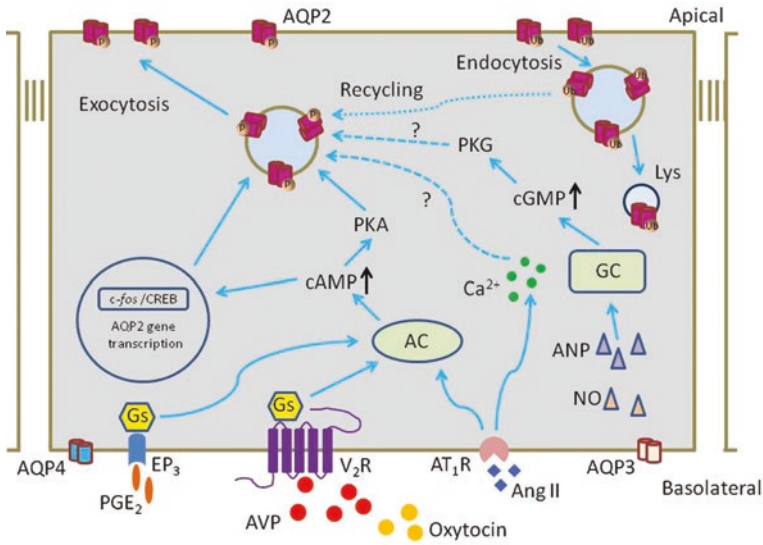
Fig. 14.7 Regulation of AQP2-mediated water reabsorption. Vasopressin (*AVP*) binds to the vasopressin type-2 receptor (*V2R*), present on the basolateral membrane of renal collecting duct principal cells. This induces a signaling cascade, involving Gs protein mediated activation of adenylyl cyclase (*AC*), a rise in intracellular cAMP, activation of protein kinase A (*PKA*), and subsequent phosphorylation of AQP2. This results in the redistribution of AQP2 from intracellular vesicles to the apical membrane. On the long term, vasopressin also increases AQP2 expression via phosphorylation of the cAMP responsive element binding protein (*CREB*), which stimulates transcription from the AQP2 promoter. Once water balance is restored, AVP levels drop and AQP2 is internalized via ubiquitination. Internalized AQP2 can either be targeted to recycling pathways or to degradation via lysosomes (*Lys*). Driven by the transcellular osmotic gradient, water enters principal cells through AQP2 and passes through the basolateral plasma membrane via AQP3 and AQP4 to the blood. Oxytocin or prostagladin E2 (*PGE2*) may bind V2R or PGE2 receptor (EP3), respectively, and result in AQP2 trafficking and expression via the AC-cAMP-PKA pathway in principal cells of the collecting duct. Atrial natriuretic peptide (*ANP*) and nitric oxide (*NO*) induce elevation of intracellular cGMP levels and lead to AQP2 membrane insertion, probably via guadenylate cyclase (*GC*)-protein kinase G (*PKG*)-mediated phosphorylation of serine 256 on the AQP2. Angiotensin II (*Ang II*), by binding its type 1 receptor (*AT1R*) in the basolateral membrane of principal cells, induces AQP2 trafficking and protein expression via both cAMP-PKA and calcium-calmodulin pathways

principal cells to the apical membrane and fuse with it. Relocation of phosphorylated AQP2 to the cell membrane increases the cell water permeability, resulting in water reabsorption [84, 127, 131]. Upon removal of the vasopressin stimulus, AQP2 is shuttled back to the cell cytoplasm, a process that restores the water impermeability of the cell [125, 127]. Long-term regulation of AQP2 abundance by vasopressin occurs over a period of hours to days [125, 127]. In addition to vasopressin, several other factors have recently been reported to affect AQP2 trafficking, such as atrial natriuretic peptide (ANP) [17, 180], protagladin E_2 [209], aldosterone [124], angiotensin II [90, 181], oxytocin [91], and others (Fig. 14.7).

AQP4   AQP4 is permeable to water and is expressed in astroglial cells at the blood–brain barrier and in the spinal cord, kidney collecting duct, airways, skeletal muscle, stomach, and retina [194]. Unlike AQP3 in cortical collecting ducts, AQP4 is present in principal cells [168] (Fig. 14.6), with the greatest abundance in inner medullary collecting ducts. Targeted disruption of AQP4 in mice results in a 75 % reduction in the osmotic water permeability of the inner medullary collecting duct [26]. However, AQP4-null mice have only a mild urinary concentrating defect [96], indicating a likely greater water reabsorption by AQP3 in cortical collecting duct. AQP3/AQP4 double knockout mice show more severe polyuria than AQP3-knockout mice, although they still have residual water reabsorption ability [95, 167]. As a major aquaporin located in CNS, AQP4 is found play an important pathophysiological role in brain edema and neuromyelitis optica (NMO) (see below). In contrast, studies on AQP4 deficient mice provide evidence against a significant role of AQP4 in skeletal muscle physiology [196].

AQP5   AQP5 is permeable to water and is expressed in glandular epithelia, corneal epithelium, alveolar epithelium, and the gastrointestinal tract [46]. Saliva production in the parotid gland involves the re-localization of AQP5 into the plasma membrane of the secretory cells [70]. Defective cellular trafficking of AQP5 in salivary [163] and lacrimal [169] glands has been associated with Sjörgren's syndrome, which is characterized by deficient secretion of tears and saliva. A recent study [141] demonstrated that AQP5 is also expressed in type-B intercalated cells in the kidney connecting tubules and collecting ducts (Fig. 14.6), where AQP5 co-localizes with the apical transporter pendrin. However, AQP5 knockout mice develop "grossly normal" with no kidney phenotype [94]. Further studies are thus required to uncover a possibly unexpected role for AQP5 in the kidney.

AQP6   AQP6 is thought to be involved in chloride permeability and is expressed in intracellular vesicles of acid-secreting type-A intercalated cells in renal collecting ducts, where it is colocalized with H^+-ATPase (Fig. 14.6). This localization suggests that AQP6 may be regulated by low pH [206]. AQP6 expression in oocytes has revealed low water permeability during basal conditions, while in the presence of $HgCl_2$, a rapid increase in water permeability and ion conductance is observed [206]. In addition, reductions in pH (below 5.5) quickly and reversibly increase anion conductance and water permeability in AQP6 expressing oocytes [206].

AQP8   AQP8 is a water channel found in intracellular domains of the proximal tubule and the collecting duct cells [40] (Fig. 14.6). AQP8-null mice did not show a urinary concentrating defect and specifically, urine osmolality was not significantly different in AQP1-null mice versus mice lacking both AQP8 and AQP1 [190, 195, 202]. This observation suggests that AQP8 may not be physiologically relevant to renal function; however, mitochondrial AQP8 was recently demonstrated in playing an important role in the adaptive response of proximal tubules to acidosis [115]. AQP8 is also expressed in liver, pancreas intestine, salivary gland, testis, and heart [46].

Aquaglyceroporins

AQP3 AQP3 is expressed in different tissues including kidney, skin, gastrointestinal tract, adipose, and airway epithelium. It is permeable to glycerol and may be important for proper lipid metabolism [147]. AQP3 is the most abundant skin aquaglyceroporin. Both water and glycerol transport by AQP3 appears to play an important role in hydration of mammalian skin epidermis. Glycerol transport by AQP3 is also involved in the metabolism of lipids in skin as well as in the regulation of proliferation and differentiation of keratinocytes [13, 18, 119]. The role of glycerol was confirmed when either systemic or topical glycerol replacement was shown to reverse all of the effects of the lack of AQP3 in mouse skin [51].

In the kidney, AQP3 is localized in the basolateral plasma membranes of cortical and outer medullary collecting duct principal cells [69] (Fig. 14.6), where they are thought to mediate the basolateral exit of water that enters apically via AQP2. AQP3-deficient mice are severely polyuric [95] and fail to respond appropriately to dDAVP, demonstrating that basolateral membrane water transport can also become a rate-limiting factor for water reabsorption [95].

AQP7 AQP7 is involved in water and glycerol permeability and is expressed mainly in adipose tissue, and in testis, heart, skeletal muscle, and kidney proximal tubule [156]. AQP7 is permeated by water and glycerol [66] and is expressed in the brush border of the proximal tubule S3 segment [64, 121], where AQP7 is colocalized with AQP1 (Fig. 14.6). AQP7 null mice have reduced water permeability in the proximal tubule brush border membrane [158], whereas they do not exhibit a urinary concentrating defect or water-balance abnormality, which is not surprising since AQP1 represents the major water channel in this segment of the nephron. AQP7 null mice have a severe loss of glycerol in the urine, confirming that AQP7 is a major transporter for glycerol reabsorption in the proximal tubule [158]. Interestingly, the serum level of glycerol was normal when compared with wild-type animals, indicating that a systemic compensative mechanism may play a role in keeping normal plasma glycerol levels in AQP7 knockout mice [158]. Additionally, studies have suggested an important role of AQP7 in energy metabolism (see below).

AQP9 AQP9 is expressed in liver, white blood cells, testis, and brain and is involved in water and small solute permeability [39], its permeability to glycerol and lactate indicates that it may play a role in energy metabolism. AQP9 is expressed in the liver where it is proposed to play a role in glycerol uptake for gluconeogenesis during fasting [21]. Plasma concentrations of glycerol and triglycerides were slightly increased in AQP9 null mice. When AQP9 null mice were mated with leptin-resistant diabetic mice, the double mutants had dramatically increased plasma glycerol levels and reduced blood glucose levels after fasting [148]. Red blood cells from AQP9 null mice have dramatically reduced glycerol permeability but the water permeability remains unchanged [93], thus the physiological role for AQP9 in red blood cells is still not clear.

AQP10 AQP10 is thought to be involved in water, glycerol, and urea permeability when expressed in Xenopus oocytes [67] and is expressed in small intestine [46, 62]. A recent study showed that AQP10 silencing in human differentiated adipocytes resulted in a 50 % decrease of glycerol and osmotic water permeability, suggesting that AQP10 in human adipose tissue, together with AQP7, is particularly important for the maintenance of normal or low glycerol content inside the adipocyte, thus protecting humans from obesity [85].

Superaquaporins

AQP11 AQP11 is expressed in kidney, testis, liver, brain, intestine, heart, and adipose tissue. AQP11 is suggested to be vital for kidney (Fig. 14.6) and liver development and endoplasmic reticulum stress in the kidney cells [145, 147]. AQP11 knockout mice die at a young age with polycystic kidneys [117], which is similar to human polycystic kidney diseases (PKD). Therefore, these transgenic mice might be considered a new animal model providing an alternative pathway for studying cystogenesis in PKD.

AQP12 AQP12 seems to be expressed specifically in pancreatic acinar cells, although the role of AQP12 remains to be clarified [62, 148]. When using cholecystokinin-8 to induce pancreatitis, AQP12 null mice show more severe pathological damage and larger exocytotic vesicles in the pancreatic acini than wild-type mice, indicating that AQP12 may function in controlling the proper secretion of pancreatic fluid following rapid and intense stimulation [133].

Clinical Significance of Aquaporins

Dysregulation of Renal Aquaporins in Water-balance Disorders

Several clinically important water-balance disorders are associated with dysregulation of AQP2, according to results from animal models of various disease states. Such disease states can be divided into urine concentrating defects and urine diluting defects.

Urine concentrating defect The amount of AQP2 in collecting duct cells is decreased in a variety of polyuric disorders [84, 127]. There are two significant inherited forms of diabetes insipidus (DI): central and nephrogenic. In central (or neurogenic) DI, production or secretion of vasopressin in the hypothalamus is impaired. The Brattleboro rat provides an excellent model of this condition. These animals have a total or near-total lack of vasopressin production and substantially decreased expression levels of vasopressin-regulated AQP2 compared with the parent strain. Infusion of vasopressin for several days can restore kidney

AQP2 protein levels to normal [33]. These deficits are likely to be the most important cause of the polyuria from which these patients with central DI suffer, and they will be reversed by treatment with desmopressin, which is a vasopressin V2-selective agonist. The second form of DI is called nephrogenic DI (NDI) and is caused by the inability of the kidney to respond to vasopressin stimulation. The most common hereditary cause (95 % of the cases) is an X-linked disorder associated with mutations of the vasopressin V2 receptor making the collecting duct cells insensitive to vasopressin [10]. Interestingly, most cases of non-X-linked NDI appear to be associated with mutations in the AQP2 gene [30]. In a mouse model of human NDI, an Hsp90 inhibitor, identified in a small screen of known protein folding "correctors," partially rescued defective AQP2 cellular processing and partially restored urinary concentration function, indicating a potential therapeutic utility of this inhibitor in treating human NDI [192, 203].

In humans, acquired forms of NDI are much more common. Dysregulation of AQP2 plays a fundamental role in many acquired forms of NDI, such as sustained lithium intake [84, 108, 127], ureteral obstruction [44, 45, 88, 89], hyperthyroidism [183], hypokalemia [109], and hypercalcemia [36, 178]. Each of these four syndromes is associated with depletion of AQP2 protein from the collecting ducts and a defect in urinary concentration. Interestingly, hypercalcemia [177, 179] is also associated with downregulation of the Na–K–2Cl cotransporter (NKCC2) in the thick ascending limb, which could reduce sodium and chloride reabsorption in the thick ascending limb and hence decrease medullary osmolality, also contributing to the polyuria and impaired urinary concentration.

Urine diluting defect Increased expression of renal AQP2 protein is seen in several extracellular fluid (ECF)-expanded states, such as congestive heart failure (CHF) [130, 187], hepatic cirrhosis [43], and glucocorticoid deficiency [182]. Severe heart failure is characterized by defects in renal handling of water and sodium, resulting in ECF expansion and hyponatremia. In CHF, a marked increase in the abundance of the AQP2 protein in the collecting ducts is observed, consistent with an increase in apical water permeability. The rats with CHF manifest significantly increased plasma vasopressin levels, presumably owing to non-osmotic factors related to arterial underfilling. Administration of a V2 receptor antagonist significantly increases urine output and plasma osmolality, in parallel with a significant reduction in AQP2 expression. Based on this model, V2 receptor antagonists (vaptans) are now being used clinically to ameliorate the hyponatremia seen in severe CHF [143].

Aquaporins and Central Nervous System

Aquaporins and brain edema At least three AQPs are expressed in the CNS. AQP1 is located in the epithelia of the choroid plexus [134] and dorsal root ganglia [155], and AQP9 is expressed in the substantia nigra [4]. AQP4 is found in the glia [128] and neurons.

AQP1 expression is restricted to the choroid plexus region of the brain under normal conditions. Osmotically induced water transport was reduced fivefold in AQP1 null mice along with a decrease in intracranial pressure and a 25 % decrease in CSF production [134]. Hydrocephalus is associated with CSF flow abnormalities, and AQP1 modulation was suggested as a therapeutic route for its treatment [164].

AQP4 is associated with the pathophysiology of brain edema. Astrocytes are the most abundant glial cells within the brain and AQP4 is highly concentrated in astrocytic end-feet [28, 128], which function as part of the blood–brain barrier (BBB) water exchange mechanism. Compared with littermate controls, glial-conditional AQP4 knockout mice show a 31 % reduction in brain water uptake after systemic hypoosmotic stress and a delayed postnatal reabsorption of brain water [48].

Because AQP4 allows bidirectional water flux through cell membranes, it is not surprising that it facilitates water transport to and from the CNS. Experiments demonstrate the role of AQP4 in facilitating cellular water uptake as well as the clearance of ECF from the brain. Deletion of AQP4 impairs cell water uptake in several disease models such as acute cerebral ischemia [104], water intoxication [104, 200], and traumatic brain injury, in which water moves into the cell resulting in cytotoxic brain edema (Fig. 14.8a). Transgenic AQP4 overexpression in mice worsens brain swelling in water intoxication [199]. AQP4 null mice showed less brain water content and a remarkably improved degree of neurological deficits as compared to wild-type mice in acute liver failure, in which brain edema and astrocyte swelling induced by elevated ammonia levels is a hallmark [142]. Consistent with this, silencing the AQP4 gene in cultured astrocytes prevented ammonia-induced cell swelling [142]. Vasogenic edema, which is created via leakage of isoosmolar fluid through a defective BBB into the brain extracellular space, is usually seen in another subset of CNS pathologies such as brain tumors, cold brain injury, and persistent ischemia. In these models, AQP4 facilitates the reabsorption of edema fluid from the extracellular space (Fig. 14.8b). Deletion of AQP4 resulted in worsening of cerebral edema, as assessed by brain wet to dry weight ratio and intracranial pressure, together with a lower neurological score [135, 136]. The bimodal role of AQP4 in the development of vasogenic and cytotoxic edema, thus should be noted when formulating strategies targeting AQP4 in edema therapy.

Aquaporins and neuromyelitis optica The involvement of AQP4 in NMO is quite unexpected. NMO is a clinical syndrome characterized by optic neuritis and myelitis. If untreated, NMO usually takes a relapsing course and often results in blindness and paralysis. The discovery of circulating IgG autoantibodies to AQP4 in 70–80 % of patients with NMO (termed NMO-IgG or AQP4-Ab) [86, 87] and subsequent investigations into the pathogenic impact of this new reactivity have led to the recognition of NMO as a unique autoimmune disease that is distinct from classic multiple sclerosis.

There is now strong evidence that AQP4-IgG is pathogenic in NMO. Administration of human NMO-IgG produces NMO-like pathology in rats with pre-existing neuroinflammation [7]. Naïve mice or rats injected intracranially with human NMO-IgG, with or without complement, develop characteristic NMO
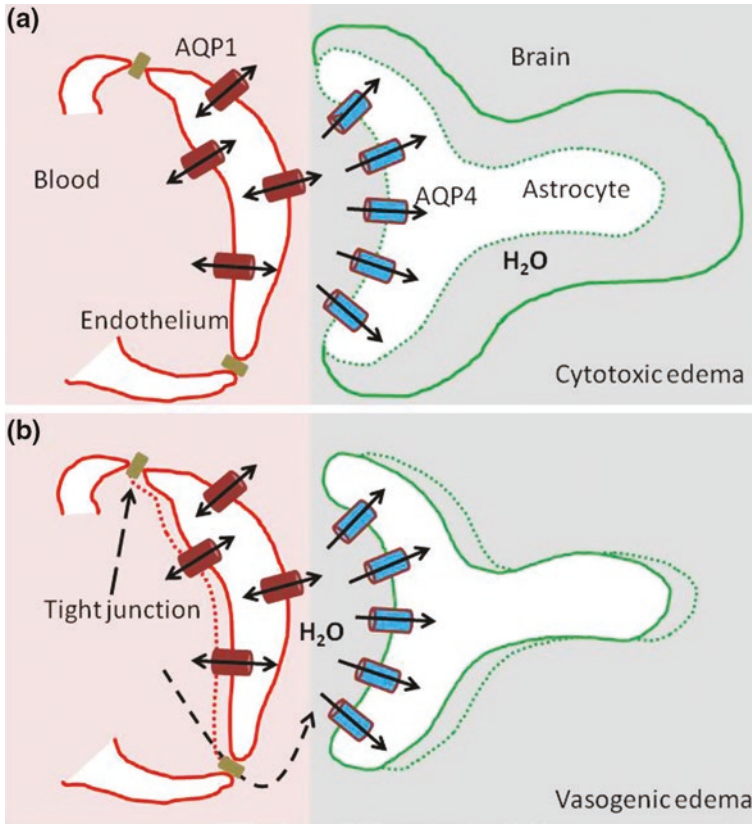
Fig. 14.8 Mechanism of brain edema formation in cytotoxic and vasogenic edema. **a** In cytotoxic edema, AQP4 facilitates water uptake of perivascular astrocyte end-feet, resulting in astrocyte swelling and subsequent compression of the adjacent neurons. *Dotted line* astrocyte end-feet before swelling and *solid line* astrocyte end-feet after swelling. **b** In vasogenic edema, the endothelial tight junction is damaged, leading the disruption of the blood–brain barrier (*BBB*) seal. In this condition, AQP4 facilitates clearance of excess brain water from the extracellular space. *Dotted line* relative position of endothelium and astrocyte end-feet when extracellular fluid accumulates; *solid line* relative position of endothelium and astrocyte end-feet after extracellular fluid is cleared; *black arrow* water movement

lesions, with neuroinflammation, loss of glial fibrillary acidic protein and AQP4 immunore-activity, myelin loss, perivascular deposition of activated complement or vasculocentric complement deposition, granulocyte [212] and macrophage infiltration, BBB disruption, microglial activation, and neuron death [2, 152]. It is therefore thought that IgG binding to AQP4 in astrocytes initiates an inflammatory cascade involving leukocytes infiltration, cytokine release, complement, and natural killer cell–mediated astrocyte damage and BBB breakdown [173]. The consequent neuroinflammation and myelin loss produce neurological deficits.

NMO-IgG seropositivity is highly specific for NMO, and, in some studies, NMO-IgG levels correlate with disease activity [173].

Assay of serum NMO-IgG in NMO was an excellent example of aquaporin-based diagnostics. A NMO-IgG seropositivity is nearly 100 % sensitive and specific for NMO in one report [100], and the most recent data demonstrated that a cell-based assay test based on the use of the large orthogonal arrays of particles forming isoform AQP4-M23 with a C-terminal fluorescent tag is a better test for NMO diagnosis [137].

AQP4-based therapeutics in NMO is an exciting area. Recent proof-of-concept studies have demonstrated that high-affinity, nonpathogenic, recombinant NMO antibodies (aquaporumabs) can block NMO-IgG binding to AQP4 and prevent consequent cell killing and development of NMO lesions in ex vivo and in vivo animal models [173, 175].

Aquaporins and Obesity

Adipocytes serve a crucial role as an energy supplier under starvation to maintain whole body energy homeostasis and contribute to survival during longer starvation. However, over-nutrition and lack of exercise have resulted in over-accumulation of fat, causing an increase in life-style related diseases, such as diabetes, dyslipidemia, hypertension, and atherosclerosis, which are commonly recognized as the metabolic syndrome [103]. The involvement of AQP7 in adipocyte and AQP9 in liver metabolism suggests the possibility of new strategies for therapy of obesity and metabolic syndrome and further studies may refine our understanding of metabolic syndrome.

AQP7 is expressed in mammal adipose tissue [77, 78]. AQP7 mRNA levels are decreased by feeding and are increased by fasting in parallel with plasma glycerol levels, which are opposite to plasma insulin levels. Indeed, the insulin negative response element is identified in the promoter region of the AQP7 gene [77, 78], indicating that AQP7 mRNA expression is closely regulated by insulin at the transcriptional level, suggesting that adipose AQP7 seems to be associated with glucose metabolism [103]. In 3T3-L1 adipocytes, AQP7 is localized at the periphery of the nucleus under steady-state conditions and may rapidly translocate to the plasma membrane following stimulation with the lipolysis inducer adrenaline [77]. This may mediate efficient release of glycerol from adipocytes into the bloodstream, as 3T3-L1 adipocytes with AQP7 loss of function mutations correlated with higher triglyceride content [99].

The role of AQP7 in glycerol metabolism was also supported by observations of AQP7 knockout mice. AQP7 knockout mice showed low plasma glycerol concentrations under the fasting state and impaired plasma glycerol elevation in response to β3-adrenergic agonist or longer starvation challenge when compared with wild-type mice [101]. Also, AQP7-knockout mice exhibited obesity with increases of fat weight after 12 weeks of age [56] and showed insulin resistance in accordance

with obesity. Adipose intracellular glycerol contents and activity of glycerol kinase, a key enzyme in the conversion of glycerol to glycerol-3-phosphate, were elevated in AQP7 knockout mice when compared with those of wild-type mice. These studies suggest that AQP7 deficiency in adipose tissue may promote fatty acid uptake, and finally cause triglyceride accumulation. The association of AQP7 and energy metabolism is also shown in humans. In severely obese women, adipose tissue AQP7 expression levels were significantly reduced and plasma glycerol concentrations were lower [22]. Loss-of-function genetic defects of AQP7 are associated with an inability to elevate plasma glycerol during exercise [79].

AQP9 is considered the sole glycerol channel in liver and is localized at the sinusoidal plasma membrane facing the portal vein [39]. Administration of streptozotocin results in an increase in AQP9 mRNA [81] and protein [21] levels in insulin deficient mice, which indicates that insulin may suppress AQP9 expression and thus reduce glycerol intake from plasma. AQP9 mRNA level is increased by fasting and is decreased by feeding [81], which could be attributed to opposite insulin levels in these two conditions. Interestingly, in accordance with increased AQP9 gene and protein in fasting, hepatic key enzymes involved in gluconeogenesis (e.g., glycerol kinase and PEPCK) show increased expression. In feeding condition, gene expression of AQP9 and glycerol kinase is lower than normal. An important role of AQP9 in hepatic glycerol and glucose metabolism is also demonstrated in AQP9 knockout mice [148]. AQP9$^{-/-}$ mice exhibited a significant increase in plasma glycerol and triglyceride levels compared to AQP9$^{+/-}$ mice. When crossed with db/db mice, which are a type 2 diabetes model mice, the blood glucose levels of db/db AQP9$^{-/-}$ mice were lower than db/db AQP9$^{+/-}$ mice under 3-h fasting conditions, probably due to failed gluconeogenesis in the liver.

It is becoming clear that in the fasting condition, glycerol (produced by lipolysis) is transferred from adipose tissue to the plasma by AQP7, and plasma glycerol is then taken up by the liver via AQP9 to provide a substrate for hepatic glucose synthesis (gluconeogenesis) [21, 81]. In the fed state, a rise in plasma insulin concentration results in the suppression of lipolysis and the reduction of adipose AQP7, and thus decreases glycerol release from adipocytes. Feeding also reduces liver AQP9 level and suppresses glycerol-based gluconeogenesis [103]. The coordination between AQP7 in adipose and AQP9 in the liver indicates the importance of aquaglyceroporins in physiological and pathophysiological glucose metabolism (Fig. 14.4).

Aquaporins and Oncology

AQPs are involved in cell migration, which has implications for tumor angiogenesis, local invasion, and metastasis. Extensive studies have shown that tumor cells express AQPs and a positive correlation exists between histological tumor grade and AQP expression. AQPs are also involved in tumor edema formation and angiogenesis in several solid and hematological tumors. AQP inhibition in endothelial

and tumor cells might limit tumor growth and spread, therefore, AQPs are potentially pharmacological targets in anticancer therapies.

AQP1 gene disruption was closely associated with a significant decrease in angiogenesis and neoplasticity [151]. Xenograft models of subcutaneous melanoma tumors showed decreased tumor growth and reduced microvascularization in AQP1 null mice compared to wild-type controls. Significant tumor necrosis was also observed in xenograft models using AQP1 null mice [61]. Also, abnormal expression of AQP1 in brain tumor cells is responsible for the invasiveness and rapid growth of the tumor [150].

Besides AQP1, high AQP4 expression has been found in invasive astrocytomas [164]. Recent studies demonstrated that AQP4 overexpression in the peritumoral tissue surrounding invasive gliomas is associated with the rate-limited growth of those tumors [111]. This study was later supported by a finding showing that siRNA downregulation of AQP4 slowed proliferation and invasiveness of LN229 tumor models [34, 35].

AQP3 expression appears to be associated with tumorgenesis, proliferation, and metastasis. AQP3 was found in high expression levels in human skin squamous cell carcinomas [50], bronchioloalveolar carcinomas [98], and esophageal and oral squamous cell carcinoma [82]. AQP3 null mice were shown to be resistant to tumorigenesis in a rodent skin cancer model [50] and AQP3 inhibition by siRNA was found to improve the efficacy of cryotherapy in prostate cancer [71]. Emerging evidence suggests that expression of AQP1, AQP3, AQP4, AQP5, and AQP7 is altered in mammary tumors and in breast cancer cell lines although it is not yet clear whether this is a cause or a consequence of neoplastic development [114].

Several recent studies found the increased expression of AQP5 in lung cancer cells (particularly pulmonary adenocarcinomas) [213], colon cancer tissues [75], and myelogenous leukemia cells [23]. AQP5 expression has also been linked to proliferation of the human ovarian cancer cell line [204] and metastasis of non-small cell lung cancer. Interestingly, the apparent activation of the EGFR/ERK/p38 MAPK signaling pathway by AQP5 in lung cancer cells [213] indicates a potential target for oncotherapy.

The emerging roles of AQPs facilitating water movement in tumor cells are not only important in the mechanistic understanding of the cell migration, angiogenesis, and proliferation process, but may also have a wide range of potentially therapeutic implications [61, 173]. Further work is required to determine whether aquaporins are viable therapeutic targets or reliable diagnostic and prognostic biomarkers.

Aquaporins in Several Other Diseases

As discussed above, glycerol and water (and maybe also urea) transport through AQP3 has an important function in skin hydration, barrier function, and wound healing. In rodent atopic dermatitis models, upregulation of AQP3 enhanced proliferation of human keratinocytes, which was involved in epidermal hyperplasia, a

characteristic of atopic dermatitis [119]. This finding suggests that AQP3 inhibition by topical agents may be beneficial for the treatment of epidermal hyperplasia in atopic dermatitis.

The importance of AQPs in ocular diseases is evident from the finding that genetic defects in AQP0 are associated with hereditary cataracts. AQP1 and AQP4 appear to be involved in intraocular pressure formation, which suggest that inhibition of these AQPs could be a potential treatment of glaucoma [211]. Impaired cellular trafficking and expression of AQP5 in lacrimal glands [169] has been linked to the Sjörgren's syndrome. AQP-mediated water transport in the inner ear [38, 165, 166], which is essential for maintaining function of hearing and equilibrium, is regulated at least in part via the vasopressin-AQP2 system. Endolymphatic hydrops, a morphological characteristic of Meniere's disease, is thought to be caused by abnormal regulation of AQP2 in the inner ear. A recent delicate experiment demonstrated an unexpected role of AQP2 in promoting renal epithelial cell migration and in maintaining structural and functional integrity of the mammalian kidney [24]. Integrin is widely expressed in ureteric bud derivatives and collecting duct epithelial cells in developing kidney and is critical to kidney development and repair. By regulating the intracellular trafficking and subsequent cell surface presentation of integrin β1, AQP2 modulates epithelial cellular migration and ultimately contributes to kidney epithelial morphogenesis. This study suggests an important role of AQP2 in the development of various segments of the renal tubule.

AQPs are also expressed throughout the respiratory tract to facilitate water transport. AQP5 deletion in submucosal glands in upper airways reduced fluid secretion and increased protein content [16], indicating that AQP5 could be a therapy target for reducing fluid secretion in bronchitis and rhinitis. In the gastrointestinal tract, downregulation of AQP3 and AQP8 gene and protein expression in ileum and colon was associated with an increase in intestinal inflammation and injury in a rodent colitis model [215]. In addition to mediating glycerol transport to the liver, AQP9 is also postulated to have a significant role in spermatogenesis and uterine implantation of blastocysts [25].

References

1. Agre P, King LS, Yasui M, Guggino WB, Ottersen OP, Fujiyoshi Y, Engel A, Nielsen S (2002) Aquaporin water channels–from atomic structure to clinical medicine. J Physiol 542:3–16
2. Asavapanumas N, Ratelade J, Verkman AS (2013) Unique neuromyelitis optica pathology produced in naive rats by intracerebral administration of NMO-IgG. Acta Neuropathol 127:539–551
3. Badaut J (2010) Aquaglyceroporin 9 in brain pathologies. Neuroscience 168:1047–1057
4. Badaut J, Petit JM, Brunet JF, Magistretti PJ, Charriaut-Marlangue C, Regli L (2004) Distribution of Aquaporin 9 in the adult rat brain: preferential expression in catecholaminergic neurons and in glial cells. Neuroscience 128:27–38
5. Bagnasco SM (2006) The erythrocyte urea transporter UT-B. J Membr Biol 212:133–138

6. Benga G (2012) The first discovered water channel protein, later called aquaporin 1: molecular characteristics, functions and medical implications. Mol Aspects Med 33:518–534

7. Bennett JL, Lam C, Kalluri SR, Saikali P, Bautista K, Dupree C, Glogowska M, Case D, Antel JP, Owens GP, Gilden D, Nessler S, Stadelmann C, Hemmer B (2009) Intrathecal pathogenic anti-aquaporin-4 antibodies in early neuromyelitis optica. Ann Neurol 66:617–629

8. Bertolotti M, Bestetti S, Garcia-Manteiga JM, Medrano-Fernandez I, Dal Mas A, Malosio ML, Sitia R (2013) Tyrosine kinase signal modulation: a matter of H_2O_2 membrane permeability? Antioxid Redox Signal 19:1447–1451

9. Best L, Brown PD, Yates AP, Perret J, Virreira M, Beauwens R, Malaisse WJ, Sener A, Delporte C (2009) Contrasting effects of glycerol and urea transport on rat pancreatic beta-cell function. Cell Physiol Biochem 23:255–264

10. Bichet DG (1996) Vasopressin receptors in health and disease. Kidney Int 49:1706–1711

11. Bienert GP, Schussler MD, Jahn TP (2008) Metalloids: essential, beneficial or toxic? Major intrinsic proteins sort it out. Trends Biochem Sci 33:20–26

12. Bin K, Shi-Peng Z (2011) Acetazolamide inhibits aquaporin-1 expression and colon cancer xenograft tumor growth. Hepatogastroenterology 58:1502–1506

13. Bollag WB, Xie D, Zheng X, Zhong X (2007) A potential role for the phospholipase D2-aquaporin-3 signaling module in early keratinocyte differentiation: production of a phosphatidylglycerol signaling lipid. J Invest Dermatol 127:2823–2831

14. Bondy C, Chin E, Smith BL, Preston GM, Agre P (1993) Developmental gene expression and tissue distribution of the CHIP28 water-channel protein. Proc Natl Acad Sci USA 90:4500–4504

15. Borgnia M, Nielsen S, Engel A, Agre P (1999) Cellular and molecular biology of the aquaporin water channels. Annu Rev Biochem 68:425–458

16. Borok Z, Verkman AS (2002) Lung edema clearance: 20 years of progress: invited review: role of aquaporin water channels in fluid transport in lung and airways. J Appl Physiol 93:2199–2206 (1985)

17. Bouley R, Breton S, Sun T, McLaughlin M, Nsumu NN, Lin HY, Ausiello DA, Brown D (2000) Nitric oxide and atrial natriuretic factor stimulate cGMP-dependent membrane insertion of aquaporin 2 in renal epithelial cells. J Clin Invest 106:1115–1126

18. Boury-Jamot M, Sougrat R, Tailhardat M, Le Varlet B, Bonte F, Dumas M, Verbavatz JM (2006) Expression and function of aquaporins in human skin: is aquaporin-3 just a glycerol transporter? Biochim Biophys Acta 1758:1034–1042

19. Calamita G, Moreno M, Ferri D, Silvestri E, Roberti P, Schiavo L, Gena P, Svelto M, Goglia F (2007) Triiodothyronine modulates the expression of aquaporin-8 in rat liver mitochondria. J Endocrinol 192:111–120

20. Carbrey JM, Agre P (2009) Discovery of the aquaporins and development of the field. Handb Exp Pharmacol 190:3–28

21. Carbrey JM, Gorelick-Feldman DA, Kozono D, Praetorius J, Nielsen S, Agre P (2003) Aquaglyceroporin AQP9: solute permeation and metabolic control of expression in liver. Proc Natl Acad Sci USA 100:2945–2950

22. Ceperuelo-Mallafre V, Miranda M, Chacon MR, Vilarrasa N, Megia A, Gutierrez C, Fernandez-Real JM, Gomez JM, Caubet E, Fruhbeck G, Vendrell J (2007) Adipose tissue expression of the glycerol channel aquaporin-7 gene is altered in severe obesity but not in type 2 diabetes. J Clin Endocrinol Metab 92:3640–3645

23. Chae YK, Kang SK, Kim MS, Woo J, Lee J, Chang S, Kim DW, Kim M, Park S, Kim I, Keam B, Rhee J, Koo NH, Park G, Kim SH, Jang SE, Kweon IY, Sidransky D, Moon C (2008) Human AQP5 plays a role in the progression of chronic myelogenous leukemia (CML). PLoS ONE 3:e2594

24. Chen Y, Rice W, Gu Z, Li J, Huang J, Brenner MB, Van Hoek A, Xiong J, Gundersen GG, Norman JC, Hsu VW, Fenton RA, Brown D, Lu HA (2012) Aquaporin 2 promotes cell migration and epithelial morphogenesis. J Am Soc Nephrol 23:1506–1517

25. Cho YS, Svelto M, Calamita G (2003) Possible functional implications of aquaporin water channels in reproductive physiology and medically assisted procreation. Cell Mol Biol (Noisy-le-grand) 49:515–519

26. Chou CL, Ma T, Yang B, Knepper MA, Verkman AS (1998) Fourfold reduction of water permeability in inner medullary collecting duct of aquaporin-4 knockout mice. Am J Physiol 274:C549–C554

27. Cooper GJ, Boron WF (1998) Effect of PCMBS on CO_2 permeability of Xenopus oocytes expressing aquaporin 1 or its C189S mutant. Am J Physiol 275:C1481–C1486

28. Day RE, Kitchen P, Owen DS, Bland C, Marshall L, Conner AC, Bill RM, Conner MT (2013) Human aquaporins: regulators of transcellular water flow. Biochim Biophys Acta 1840:1492–1506

29. de Groot BL, Grubmuller H (2001) Water permeation across biological membranes: mechanism and dynamics of aquaporin-1 and GlpF. Science 294:2353–2357

30. Deen PM, Marr N, Kamsteeg EJ, van Balkom BW (2000) Nephrogenic diabetes insipidus. Curr Opin Nephrol Hypertens 9:591–595

31. Deen PM, Verdijk MA, Knoers NV, Wieringa B, Monnens LA, van Os CH, van Oost BA (1994) Requirement of human renal water channel aquaporin-2 for vasopressin-dependent concentration of urine. Science 264:92–95

32. Denker BM, Smith BL, Kuhajda FP, Agre P (1988) Identification, purification, and partial characterization of a novel Mr 28,000 integral membrane protein from erythrocytes and renal tubules. J Biol Chem 263:15634–15642

33. DiGiovanni SR, Nielsen S, Christensen EI, Knepper MA (1994) Regulation of collecting duct water channel expression by vasopressin in Brattleboro rat. Proc Natl Acad Sci USA 91:8984–8988

34. Ding T, Gu F, Fu L, Ma YJ (2010) Aquaporin-4 in glioma invasion and an analysis of molecular mechanisms. J Clin Neurosci 17:1359–1361

35. Ding T, Ma Y, Li W, Liu X, Ying G, Fu L, Gu F (2011) Role of aquaporin-4 in the regulation of migration and invasion of human glioma cells. Int J Oncol 38:1521–1531

36. Earm JH, Christensen BM, Frokiaer J, Marples D, Han JS, Knepper MA, Nielsen S (1998) Decreased aquaporin-2 expression and apical plasma membrane delivery in kidney collecting ducts of polyuric hypercalcemic rats. J Am Soc Nephrol 9:2181–2193

37. Echevarria M, Windhager EE, Tate SS, Frindt G (1994) Cloning and expression of AQP3, a water channel from the medullary collecting duct of rat kidney. Proc Natl Acad Sci USA 91:10997–11001

38. Eckhard A, Muller M, Salt A, Smolders J, Rask-Andersen H, Lowenheim H (2014) Water permeability of the mammalian cochlea: functional features of an aquaporin-facilitated water shunt at the perilymph–endolymph barrier. Pflugers Arch

39. Elkjaer M, Vajda Z, Nejsum LN, Kwon T, Jensen UB, Amiry-Moghaddam M, Frokiaer J, Nielsen S (2000) Immunolocalization of AQP9 in liver, epididymis, testis, spleen, and brain. Biochem Biophys Res Commun 276:1118–1128

40. Elkjaer ML, Nejsum LN, Gresz V, Kwon TH, Jensen UB, Frokiaer J, Nielsen S (2001) Immunolocalization of aquaporin-8 in rat kidney, gastrointestinal tract, testis, and airways. Am J Physiol Renal Physiol 281:F1047–F1057

41. Endeward V, Musa-Aziz R, Cooper GJ, Chen LM, Pelletier MF, Virkki LV, Supuran CT, King LS, Boron WF, Gros G (2006) Evidence that aquaporin 1 is a major pathway for CO_2 transport across the human erythrocyte membrane. FASEB J 20:1974–1981

42. Fang X, Yang B, Matthay MA, Verkman AS (2002) Evidence against aquaporin-1-dependent CO_2 permeability in lung and kidney. J Physiol 542:63–69

43. Fernandez-Llama P, Jimenez W, Bosch-Marce M, Arroyo V, Nielsen S, Knepper MA (2000) Dysregulation of renal aquaporins and Na–Cl cotransporter in CCl4-induced cirrhosis. Kidney Int 58:216–228

44. Frokiaer J, Christensen BM, Marples D, Djurhuus JC, Jensen UB, Knepper MA, Nielsen S (1997) Downregulation of aquaporin-2 parallels changes in renal water excretion in unilateral ureteral obstruction. Am J Physiol 273:F213–F223

45. Frokiaer J, Marples D, Knepper MA, Nielsen S (1996) Bilateral ureteral obstruction down-regulates expression of vasopressin-sensitive AQP-2 water channel in rat kidney. Am J Physiol 270:F657–F668

46. Gomes D, Agasse A, Thiebaud P, Delrot S, Geros H, Chaumont F (2009) Aquaporins are multifunctional water and solute transporters highly divergent in living organisms. Biochim Biophys Acta 1788:1213–1228

47. Grether-Beck S, Felsner I, Brenden H, Kohne Z, Majora M, Marini A, Jaenicke T, Rodriguez-Martin M, Trullas C, Hupe M, Elias PM, Krutmann J (2012) Urea uptake enhances barrier function and antimicrobial defense in humans by regulating epidermal gene expression. J Invest Dermatol 132:1561–1572

48. Haj-Yasein NN, Vindedal GF, Eilert-Olsen M, Gundersen GA, Skare O, Laake P, Klungland A, Thoren AE, Burkhardt JM, Ottersen OP, Nagelhus EA (2011) Glial-conditional deletion of aquaporin-4 (Aqp4) reduces blood-brain water uptake and confers barrier function on perivascular astrocyte endfeet. Proc Natl Acad Sci USA 108:17815–17820

49. Hara-Chikuma M, Chikuma S, Sugiyama Y, Kabashima K, Verkman AS, Inoue S, Miyachi Y (2012) Chemokine-dependent T cell migration requires aquaporin-3-mediated hydrogen peroxide uptake. J Exp Med 209:1743–1752

50. Hara-Chikuma M, Verkman AS (2008) Prevention of skin tumorigenesis and impairment of epidermal cell proliferation by targeted aquaporin-3 gene disruption. Mol Cell Biol 28:326–332

51. Hara M, Verkman AS (2003) Glycerol replacement corrects defective skin hydration, elasticity, and barrier function in aquaporin-3-deficient mice. Proc Natl Acad Sci USA 100:7360–7365

52. Hatakeyama S, Yoshida Y, Tani T, Koyama Y, Nihei K, Ohshiro K, Kamiie JI, Yaoita E, Suda T, Hatakeyama K, Yamamoto T (2001) Cloning of a new aquaporin (AQP10) abundantly expressed in duodenum and jejunum. Biochem Biophys Res Commun 287:814–819

53. Herrera M, Garvin JL (2007) Novel role of AQP-1 in NO-dependent vasorelaxation. Am J Physiol Renal Physiol 292:F1443–F1451

54. Herrera M, Garvin JL (2011) Aquaporins as gas channels. Pflugers Arch 462:623–630

55. Herrera M, Hong NJ, Garvin JL (2006) Aquaporin-1 transports NO across cell membranes. Hypertension 48:157–164

56. Hibuse T, Maeda N, Funahashi T, Yamamoto K, Nagasawa A, Mizunoya W, Kishida K, Inoue K, Kuriyama H, Nakamura T, Fushiki T, Kihara S, Shimomura I (2005) Aquaporin 7 deficiency is associated with development of obesity through activation of adipose glycerol kinase. Proc Natl Acad Sci USA 102:10993–10998

57. Hibuse T, Maeda N, Nakatsuji H, Tochino Y, Fujita K, Kihara S, Funahashi T, Shimomura I (2009) The heart requires glycerol as an energy substrate through aquaporin 7, a glycerol facilitator. Cardiovasc Res 83:34–41

58. Hirano Y, Okimoto N, Kadohira I, Suematsu M, Yasuoka K, Yasui M (2010) Molecular mechanisms of how mercury inhibits water permeation through aquaporin-1: understanding by molecular dynamics simulation. Biophys J 98:1512–1519

59. Holm LM, Jahn TP, Moller AL, Schjoerring JK, Ferri D, Klaerke DA, Zeuthen T (2005) NH3 and NH4+ permeability in aquaporin-expressing Xenopus oocytes. Pflugers Arch 450:415–428

60. Hub JS, Grubmuller H, de Groot BL (2009) Dynamics and energetics of permeation through aquaporins. What do we learn from molecular dynamics simulations? Handb Exp Pharmacol, pp 57–76

61. Huber VJ, Tsujita M, Nakada T (2012) Aquaporins in drug discovery and pharmacotherapy. Mol Aspects Med 33:691–703

62. Ishibashi K (2009) New members of mammalian aquaporins: AQP10–AQP12. Handb Exp Pharmacol, pp 251–262

63. Ishibashi K, Hara S, Kondo S (2009) Aquaporin water channels in mammals. Clin Exp Nephrol 13:107–117

64. Ishibashi K, Imai M, Sasaki S (2000) Cellular localization of aquaporin 7 in the rat kidney. Exp Nephrol 8:252–257

65. Ishibashi K, Kondo S, Hara S, Morishita Y (2011) The evolutionary aspects of aquaporin family. Am J Physiol Regul Integr Comp Physiol 300:R566–R576

66. Ishibashi K, Kuwahara M, Gu Y, Kageyama Y, Tohsaka A, Suzuki F, Marumo F, Sasaki S (1997) Cloning and functional expression of a new water channel abundantly expressed in the testis permeable to water, glycerol, and urea. J Biol Chem 272:20782–20786

67. Ishibashi K, Morinaga T, Kuwahara M, Sasaki S, Imai M (2002) Cloning and identification of a new member of water channel (AQP10) as an aquaglyceroporin. Biochim Biophys Acta 1576:335–340

68. Ishibashi K, Sasaki S, Fushimi K, Uchida S, Kuwahara M, Saito H, Furukawa T, Nakajima K, Yamaguchi Y, Gojobori T et al (1994) Molecular cloning and expression of a member of the aquaporin family with permeability to glycerol and urea in addition to water expressed at the basolateral membrane of kidney collecting duct cells. Proc Natl Acad Sci USA 91:6269–6273

69. Ishibashi K, Sasaki S, Fushimi K, Yamamoto T, Kuwahara M, Marumo F (1997) Immunolocalization and effect of dehydration on AQP3, a basolateral water channel of kidney collecting ducts. Am J Physiol 272:F235–F241

70. Ishikawa Y, Yuan Z, Inoue N, Skowronski MT, Nakae Y, Shono M, Cho G, Yasui M, Agre P, Nielsen S (2005) Identification of AQP5 in lipid rafts and its translocation to apical membranes by activation of M3 mAChRs in interlobular ducts of rat parotid gland. Am J Physiol Cell Physiol 289:C1303–C1311

71. Ismail M, Bokaee S, Morgan R, Davies J, Harrington KJ, Pandha H (2009) Inhibition of the aquaporin 3 water channel increases the sensitivity of prostate cancer cells to cryotherapy. Br J Cancer 100:1889–1895

72. Itel F, Al-Samir S, Oberg F, Chami M, Kumar M, Supuran CT, Deen PM, Meier W, Hedfalk K, Gros G, Endeward V (2012) CO_2 permeability of cell membranes is regulated by membrane cholesterol and protein gas channels. FASEB J 26:5182–5191

73. Jelen S, Gena P, Lebeck J, Rojek A, Praetorius J, Frokiaer J, Fenton RA, Nielsen S, Calamita G, Rutzler M (2012) Aquaporin-9 and urea transporter-A gene deletions affect urea transmembrane passage in murine hepatocytes. Am J Physiol Gastrointest Liver Physiol 303:G1279–G1287

74. Jung JS, Preston GM, Smith BL, Guggino WB, Agre P (1994) Molecular structure of the water channel through aquaporin CHIP. The hourglass model. J Biol Chem 269:14648–14654

75. Kang SK, Chae YK, Woo J, Kim MS, Park JC, Lee J, Soria JC, Jang SJ, Sidransky D, Moon C (2008) Role of human aquaporin 5 in colorectal carcinogenesis. Am J Pathol 173:518–525

76. King LS, Choi M, Fernandez PC, Cartron JP, Agre P (2001) Defective urinary-concentrating ability due to a complete deficiency of aquaporin-1. N Engl J Med 345:175–179

77. Kishida K, Kuriyama H, Funahashi T, Shimomura I, Kihara S, Ouchi N, Nishida M, Nishizawa H, Matsuda M, Takahashi M, Hotta K, Nakamura T, Yamashita S, Tochino Y, Matsuzawa Y (2000) Aquaporin adipose, a putative glycerol channel in adipocytes. J Biol Chem 275:20896–20902

78. Kishida K, Shimomura I, Kondo H, Kuriyama H, Makino Y, Nishizawa H, Maeda N, Matsuda M, Ouchi N, Kihara S, Kurachi Y, Funahashi T, Matsuzawa Y (2001) Genomic structure and insulin-mediated repression of the aquaporin adipose (AQPap), adipose-specific glycerol channel. J Biol Chem 276:36251–36260

79. Kondo H, Shimomura I, Kishida K, Kuriyama H, Makino Y, Nishizawa H, Matsuda M, Maeda N, Nagaretani H, Kihara S, Kurachi Y, Nakamura T, Funahashi T, Matsuzawa Y (2002) Human aquaporin adipose (AQPap) gene. Genomic structure, promoter analysis and functional mutation. Eur J Biochem 269:1814–1826

80. Krane CM, Goldstein DL (2007) Comparative functional analysis of aquaporins/glyceroporins in mammals and anurans. Mamm Genome 18:452–462

81. Kuriyama H, Shimomura I, Kishida K, Kondo H, Furuyama N, Nishizawa H, Maeda N, Matsuda M, Nagaretani H, Kihara S, Nakamura T, Tochino Y, Funahashi T, Matsuzawa Y

(2002) Coordinated regulation of fat-specific and liver-specific glycerol channels, aquaporin adipose and aquaporin 9. Diabetes 51:2915–2921

82. Kusayama M, Wada K, Nagata M, Ishimoto S, Takahashi H, Yoneda M, Nakajima A, Okura M, Kogo M, Kamisaki Y (2011) Critical role of aquaporin 3 on growth of human esophageal and oral squamous cell carcinoma. Cancer Sci 102:1128–1136

83. Kuwahara M, Gu Y, Ishibashi K, Marumo F, Sasaki S (1997) Mercury-sensitive residues and pore site in AQP3 water channel. Biochemistry 36:13973–13978

84. Kwon TH, Nielsen J, Moller HB, Fenton RA, Nielsen S, Frokiaer J (2009) Aquaporins in the kidney. Handb Exp Pharmacol, pp 95–132

85. Laforenza U, Scaffino MF, Gastaldi G (2013) Aquaporin-10 represents an alternative pathway for glycerol efflux from human adipocytes. PLoS ONE 8:e54474

86. Lennon VA, Kryzer TJ, Pittock SJ, Verkman AS, Hinson SR (2005) IgG marker of optic-spinal multiple sclerosis binds to the aquaporin-4 water channel. J Exp Med 202:473–477

87. Lennon VA, Wingerchuk DM, Kryzer TJ, Pittock SJ, Lucchinetti CF, Fujihara K, Nakashima I, Weinshenker BG (2004) A serum autoantibody marker of neuromyelitis optica: distinction from multiple sclerosis. Lancet 364:2106–2112

88. Li C, Wang W, Knepper MA, Nielsen S, Frokiaer J (2003) Downregulation of renal aquaporins in response to unilateral ureteral obstruction. Am J Physiol Renal Physiol 284:F1066–F1079

89. Li C, Wang W, Kwon TH, Isikay L, Wen JG, Marples D, Djurhuus JC, Stockwell A, Knepper MA, Nielsen S, Frokiaer J (2001) Downregulation of AQP1, -2, and -3 after ureteral obstruction is associated with a long-term urine-concentrating defect. Am J Physiol Renal Physiol 281:F163–F171

90. Li C, Wang W, Rivard CJ, Lanaspa MA, Summer S, Schrier RW (2011) Molecular mechanisms of angiotensin II stimulation on aquaporin-2 expression and trafficking. Am J Physiol Renal Physiol 300:F1255–F1261

91. Li C, Wang W, Summer SN, Westfall TD, Brooks DP, Falk S, Schrier RW (2008) Molecular mechanisms of antidiuretic effect of oxytocin. J Am Soc Nephrol 19:225–232

92. Litman T, Sogaard R, Zeuthen T (2009) Ammonia and urea permeability of mammalian aquaporins. Handb Exp Pharmacol, pp 327–358

93. Liu Y, Promeneur D, Rojek A, Kumar N, Frokiaer J, Nielsen S, King LS, Agre P, Carbrey JM (2007) Aquaporin 9 is the major pathway for glycerol uptake by mouse erythrocytes, with implications for malarial virulence. Proc Natl Acad Sci USA 104:12560–12564

94. Ma T, Song Y, Gillespie A, Carlson EJ, Epstein CJ, Verkman AS (1999) Defective secretion of saliva in transgenic mice lacking aquaporin-5 water channels. J Biol Chem 274:20071–20074

95. Ma T, Song Y, Yang B, Gillespie A, Carlson EJ, Epstein CJ, Verkman AS (2000) Nephrogenic diabetes insipidus in mice lacking aquaporin-3 water channels. Proc Natl Acad Sci USA 97:4386–4391

96. Ma T, Yang B, Gillespie A, Carlson EJ, Epstein CJ, Verkman AS (1997) Generation and phenotype of a transgenic knockout mouse lacking the mercurial-insensitive water channel aquaporin-4. J Clin Invest 100:957–962

97. Ma T, Yang B, Gillespie A, Carlson EJ, Epstein CJ, Verkman AS (1998) Severely impaired urinary concentrating ability in transgenic mice lacking aquaporin-1 water channels. J Biol Chem 273:4296–4299

98. Machida Y, Ueda Y, Shimasaki M, Sato K, Sagawa M, Katsuda S, Sakuma T (2011) Relationship of aquaporin 1, 3, and 5 expression in lung cancer cells to cellular differentiation, invasive growth, and metastasis potential. Hum Pathol 42:669–678

99. Madeira A, Camps M, Zorzano A, Moura TF, Soveral G (2013) Biophysical assessment of human aquaporin-7 as a water and glycerol channel in 3T3-L1 adipocytes. PLoS ONE 8:e83442

100. Mader S, Lutterotti A, Di Pauli F, Kuenz B, Schanda K, Aboul-Enein F, Khalil M, Storch MK, Jarius S, Kristoferitsch W, Berger T, Reindl M (2010) Patterns of antibody binding to aquaporin-4 isoforms in neuromyelitis optica. PLoS ONE 5:e10455

101. Maeda N, Funahashi T, Hibuse T, Nagasawa A, Kishida K, Kuriyama H, Nakamura T, Kihara S, Shimomura I, Matsuzawa Y (2004) Adaptation to fasting by glycerol transport through aquaporin 7 in adipose tissue. Proc Natl Acad Sci USA 101:17801–17806

102. Maeda N, Funahashi T, Shimomura I (2008) Metabolic impact of adipose and hepatic glycerol channels aquaporin 7 and aquaporin 9. Nat Clin Pract Endocrinol Metab 4:627–634

103. Maeda N, Funahashi T, Shimomura I (2013) Cardiovascular-metabolic impact of adiponectin and aquaporin. Endocr J 60:251–259

104. Manley GT, Fujimura M, Ma T, Noshita N, Filiz F, Bollen AW, Chan P, Verkman AS (2000) Aquaporin-4 deletion in mice reduces brain edema after acute water intoxication and ischemic stroke. Nat Med 6:159–163

105. Marchissio MJ, Frances DE, Carnovale CE, Marinelli RA (2012) Mitochondrial aquaporin-8 knockdown in human hepatoma HepG2 cells causes ROS-induced mitochondrial depolarization and loss of viability. Toxicol Appl Pharmacol 264:246–254

106. Marchissio MJ, Frances DE, Carnovale CE, Marinelli RA (2014) Evidence for necrosis, but not apoptosis, in human hepatoma cells with knockdown of mitochondrial aquaporin-8. Apoptosis 19:851–859

107. Marinelli RA, Pham L, Agre P, LaRusso NF (1997) Secretin promotes osmotic water transport in rat cholangiocytes by increasing aquaporin-1 water channels in plasma membrane. Evidence for a secretin-induced vesicular translocation of aquaporin-1. J Biol Chem 272:12984–12988

108. Marples D, Christensen S, Christensen EI, Ottosen PD, Nielsen S (1995) Lithium-induced downregulation of aquaporin-2 water channel expression in rat kidney medulla. J Clin Invest 95:1838–1845

109. Marples D, Frokiaer J, Dorup J, Knepper MA, Nielsen S (1996) Hypokalemia-induced downregulation of aquaporin-2 water channel expression in rat kidney medulla and cortex. J Clin Invest 97:1960–1968

110. Mathai JC, Agre P (1999) Hourglass pore-forming domains restrict aquaporin-1 tetramer assembly. Biochemistry 38:923–928

111. McCoy ES, Haas BR, Sontheimer H (2010) Water permeability through aquaporin-4 is regulated by protein kinase C and becomes rate-limiting for glioma invasion. Neuroscience 168:971–981

112. Miller EW, Dickinson BC, Chang CJ (2010) Aquaporin-3 mediates hydrogen peroxide uptake to regulate downstream intracellular signaling. Proc Natl Acad Sci USA 107:15681–15686

113. Miranda M, Escote X, Ceperuelo-Mallafre V, Alcaide MJ, Simon I, Vilarrasa N, Wabitsch M, Vendrell J (2010) Paired subcutaneous and visceral adipose tissue aquaporin-7 expression in human obesity and type 2 diabetes: differences and similarities between depots. J Clin Endocrinol Metab 95:3470–3479

114. Mobasheri A, Barrett-Jolley R (2013) Aquaporin water channels in the mammary gland: from physiology to pathophysiology and neoplasia. J Mammary Gland Biol Neoplasia 19:91–102

115. Molinas SM, Trumper L, Marinelli RA (2012) Mitochondrial aquaporin-8 in renal proximal tubule cells: evidence for a role in the response to metabolic acidosis. Am J Physiol Renal Physiol 303:F458–F466

116. Montiel V, Leon Gomez E, Bouzin C, Esfahani H, Romero Perez M, Lobysheva I, Devuyst O, Dessy C, Balligand JL (2013) Genetic deletion of aquaporin-1 results in microcardia and low blood pressure in mouse with intact nitric oxide-dependent relaxation, but enhanced prostanoids-dependent relaxation. Pflugers Arch 466:237–251

117. Morishita Y, Matsuzaki T, Hara-chikuma M, Andoo A, Shimono M, Matsuki A, Kobayashi K, Ikeda M, Yamamoto T, Verkman A, Kusano E, Ookawara S, Takata K, Sasaki S, Ishibashi K (2005) Disruption of aquaporin-11 produces polycystic kidneys following vacuolization of the proximal tubule. Mol Cell Biol 25:7770–7779

118. Musa-Aziz R, Chen LM, Pelletier MF, Boron WF (2009) Relative CO_2/NH_3 selectivities of AQP1, AQP4, AQP5, AmtB, and RhAG. Proc Natl Acad Sci USA 106:5406–5411
119. Nakahigashi K, Kabashima K, Ikoma A, Verkman AS, Miyachi Y, Hara-Chikuma M (2011) Upregulation of aquaporin-3 is involved in keratinocyte proliferation and epidermal hyperplasia. J Invest Dermatol 131:865–873
120. Nakhoul NL, Davis BA, Romero MF, Boron WF (1998) Effect of expressing the water channel aquaporin-1 on the CO_2 permeability of Xenopus oocytes. Am J Physiol 274:C543–C548
121. Nejsum LN, Elkjaer M, Hager H, Frokiaer J, Kwon TH, Nielsen S (2000) Localization of aquaporin-7 in rat and mouse kidney using RT-PCR, immunoblotting, and immunocytochemistry. Biochem Biophys Res Commun 277:164–170
122. Nemeth-Cahalan KL, Kalman K, Froger A, Hall JE (2007) Zinc modulation of water permeability reveals that aquaporin 0 functions as a cooperative tetramer. J Gen Physiol 130:457–464
123. Nico B, Ribatti D (2010) Aquaporins in tumor growth and angiogenesis. Cancer Lett 294:135–138
124. Nielsen J, Kwon TH, Praetorius J, Frokiaer J, Knepper MA, Nielsen S (2006) Aldosterone increases urine production and decreases apical AQP2 expression in rats with diabetes insipidus. Am J Physiol Renal Physiol 290:F438–F449
125. Nielsen S, Chou CL, Marples D, Christensen EI, Kishore BK, Knepper MA (1995) Vasopressin increases water permeability of kidney collecting duct by inducing translocation of aquaporin-CD water channels to plasma membrane. Proc Natl Acad Sci USA 92:1013–1017
126. Nielsen S, DiGiovanni SR, Christensen EI, Knepper MA, Harris HW (1993) Cellular and subcellular immunolocalization of vasopressin-regulated water channel in rat kidney. Proc Natl Acad Sci USA 90:11663–11667
127. Nielsen S, Frokiaer J, Marples D, Kwon TH, Agre P, Knepper MA (2002) Aquaporins in the kidney: from molecules to medicine. Physiol Rev 82:205–244
128. Nielsen S, Nagelhus EA, Amiry-Moghaddam M, Bourque C, Agre P, Ottersen OP (1997) Specialized membrane domains for water transport in glial cells: high-resolution immunogold cytochemistry of aquaporin-4 in rat brain. J Neurosci 17:171–180
129. Nielsen S, Smith BL, Christensen EI, Agre P (1993) Distribution of the aquaporin CHIP in secretory and resorptive epithelia and capillary endothelia. Proc Natl Acad Sci USA 90:7275–7279
130. Nielsen S, Terris J, Andersen D, Ecelbarger C, Frokiaer J, Jonassen T, Marples D, Knepper MA, Petersen JS (1997) Congestive heart failure in rats is associated with increased expression and targeting of aquaporin-2 water channel in collecting duct. Proc Natl Acad Sci USA 94:5450–5455
131. Noda Y, Sohara E, Ohta E, Sasaki S (2010) Aquaporins in kidney pathophysiology. Nat Rev Nephrol 6:168–178
132. Nowik M, Kampik NB, Mihailova M, Eladari D, Wagner CA (2010) Induction of metabolic acidosis with ammonium chloride (NH4Cl) in mice and rats–species differences and technical considerations. Cell Physiol Biochem 26:1059–1072
133. Ohta E, Itoh T, Nemoto T, Kumagai J, Ko SB, Ishibashi K, Ohno M, Uchida K, Ohta A, Sohara E, Uchida S, Sasaki S, Rai T (2009) Pancreas-specific aquaporin 12 null mice showed increased susceptibility to caerulein-induced acute pancreatitis. Am J Physiol Cell Physiol 297:C1368–C1378
134. Oshio K, Watanabe H, Song Y, Verkman AS, Manley GT (2005) Reduced cerebrospinal fluid production and intracranial pressure in mice lacking choroid plexus water channel Aquaporin-1. FASEB J 19:76–78
135. Papadopoulos MC, Manley GT, Krishna S, Verkman AS (2004) Aquaporin-4 facilitates reabsorption of excess fluid in vasogenic brain edema. FASEB J 18:1291–1293

136. Papadopoulos MC, Verkman AS (2013) Aquaporin water channels in the nervous system. Nat Rev Neurosci 14:265–277
137. Pisani F, Sparaneo A, Tortorella C, Ruggieri M, Trojano M, Mola MG, Nicchia GP, Frigeri A, Svelto M (2013) Aquaporin-4 autoantibodies in *Neuromyelitis optica*: AQP4 isoform-dependent sensitivity and specificity. PLoS ONE 8:e79185
138. Prasad GV, Coury LA, Finn F, Zeidel ML (1998) Reconstituted aquaporin 1 water channels transport CO_2 across membranes. J Biol Chem 273:33123–33126
139. Preston GM, Agre P (1991) Isolation of the cDNA for erythrocyte integral membrane protein of 28 kilodaltons: member of an ancient channel family. Proc Natl Acad Sci USA 88:11110–11114
140. Preston GM, Carroll TP, Guggino WB, Agre P (1992) Appearance of water channels in Xenopus oocytes expressing red cell CHIP28 protein. Science 256:385–387
141. Procino G, Mastrofrancesco L, Sallustio F, Costantino V, Barbieri C, Pisani F, Schena FP, Svelto M, Valenti G (2011) AQP5 is expressed in type-B intercalated cells in the collecting duct system of the rat, mouse and human kidney. Cell Physiol Biochem 28:683–692
142. Rama Rao KV, Verkman AS, Curtis KM, Norenberg MD (2013) Aquaporin-4 deletion in mice reduces encephalopathy and brain edema in experimental acute liver failure. Neurobiol Dis 63C:222–228
143. Robertson GL (2011) Vaptans for the treatment of hyponatremia. Nat Rev Endocrinol 7:151–161
144. Rodriguez A, Catalan V, Gomez-Ambrosi J, Fruhbeck G (2011) Aquaglyceroporins serve as metabolic gateways in adiposity and insulin resistance control. Cell Cycle 10:1548–1556
145. Rojek A, Fuchtbauer EM, Fuchtbauer A, Jelen S, Malmendal A, Fenton RA, Nielsen S (2013) Liver-specific Aquaporin 11 knockout mice show rapid vacuolization of the rough endoplasmic reticulum in periportal hepatocytes after amino acid feeding. Am J Physiol Gastrointest Liver Physiol 304:G501–G515
146. Rojek A, Fuchtbauer EM, Kwon TH, Frokiaer J, Nielsen S (2006) Severe urinary concentrating defect in renal collecting duct-selective AQP2 conditional-knockout mice. Proc Natl Acad Sci USA 103:6037–6042
147. Rojek A, Praetorius J, Frokiaer J, Nielsen S, Fenton RA (2008) A current view of the mammalian aquaglyceroporins. Annu Rev Physiol 70:301–327
148. Rojek AM, Skowronski MT, Fuchtbauer EM, Fuchtbauer AC, Fenton RA, Agre P, Frokiaer J, Nielsen S (2007) Defective glycerol metabolism in aquaporin 9 (AQP9) knockout mice. Proc Natl Acad Sci USA 104:3609–3614
149. Roudier N, Ripoche P, Gane P, Le Pennec PY, Daniels G, Cartron JP, Bailly P (2002) AQP3 deficiency in humans and the molecular basis of a novel blood group system, GIL. J Biol Chem 277:45854–45859
150. Saadoun S, Papadopoulos MC, Davies DC, Bell BA, Krishna S (2002) Increased aquaporin 1 water channel expression in human brain tumours. Br J Cancer 87:621–623
151. Saadoun S, Papadopoulos MC, Hara-Chikuma M, Verkman AS (2005) Impairment of angiogenesis and cell migration by targeted aquaporin-1 gene disruption. Nature 434:786–792
152. Saadoun S, Waters P, Bell BA, Vincent A, Verkman AS, Papadopoulos MC (2010) Intracerebral injection of neuromyelitis optica immunoglobulin G and human complement produces neuromyelitis optica lesions in mice. Brain 133:349–361
153. Saparov SM, Liu K, Agre P, Pohl P (2007) Fast and selective ammonia transport by aquaporin-8. J Biol Chem 282:5296–5301
154. Schnermann J, Chou CL, Ma T, Traynor T, Knepper MA, Verkman AS (1998) Defective proximal tubular fluid reabsorption in transgenic aquaporin-1 null mice. Proc Natl Acad Sci USA 95:9660–9664
155. Shields SD, Mazario J, Skinner K, Basbaum AI (2007) Anatomical and functional analysis of aquaporin 1, a water channel in primary afferent neurons. Pain 131:8–20
156. Skowronski MT, Lebeck J, Rojek A, Praetorius J, Fuchtbauer EM, Frokiaer J, Nielsen S (2007) AQP7 is localized in capillaries of adipose tissue, cardiac and striated muscle: implications in glycerol metabolism. Am J Physiol Renal Physiol 292:F956–F965

157. Smith BL, Agre P (1991) Erythrocyte Mr 28,000 transmembrane protein exists as a multi-subunit oligomer similar to channel proteins. J Biol Chem 266:6407–6415

158. Sohara E, Rai T, Miyazaki J, Verkman AS, Sasaki S, Uchida S (2005) Defective water and glycerol transport in the proximal tubules of AQP7 knockout mice. Am J Physiol Renal Physiol 289:F1195–F1200

159. Sohara E, Rai T, Sasaki S, Uchida S (2006) Physiological roles of AQP7 in the kidney: lessons from AQP7 knockout mice. Biochim Biophys Acta 1758:1106–1110

160. Sorani MD, Manley GT, Giacomini KM (2008) Genetic variation in human aquaporins and effects on phenotypes of water homeostasis. Hum Mutat 29:1108–1117

161. Sorani MD, Zador Z, Hurowitz E, Yan D, Giacomini KM, Manley GT (2008) Novel variants in human Aquaporin-4 reduce cellular water permeability. Hum Mol Genet 17:2379–2389

162. Soria LR, Marrone J, Calamita G, Marinelli RA (2013) Ammonia detoxification via ureagenesis in rat hepatocytes involves mitochondrial aquaporin-8 channels. Hepatology 57:2061–2071

163. Steinfeld S, Cogan E, King LS, Agre P, Kiss R, Delporte C (2001) Abnormal distribution of aquaporin-5 water channel protein in salivary glands from Sjörgren's syndrome patients. Lab Invest 81:143–148

164. Tait MJ, Saadoun S, Bell BA, Papadopoulos MC (2008) Water movements in the brain: role of aquaporins. Trends Neurosci 31:37–43

165. Takeda T, Sawada S, Takeda S, Kitano H, Suzuki M, Kakigi A, Takeuchi S (2003) The effects of V2 antagonist (OPC-31260) on endolymphatic hydrops. Hear Res 182:9–18

166. Takumida M, Takumida H, Kakigi A, Egami N, Nishioka R, Anniko M (2013) Localization of aquaporins in the mouse vestibular end organs. Acta Otolaryngol 133:804–813

167. Tamma G, Procino G, Svelto M, Valenti G (2012) Cell culture models and animal models for studying the patho-physiological role of renal aquaporins. Cell Mol Life Sci 69:1931–1946

168. Terris J, Ecelbarger CA, Marples D, Knepper MA, Nielsen S (1995) Distribution of aquaporin-4 water channel expression within rat kidney. Am J Physiol 269:F775–F785

169. Tsubota K, Hirai S, King LS, Agre P, Ishida N (2001) Defective cellular trafficking of lacrimal gland aquaporin-5 in Sjörgren's syndrome. Lancet 357:688–689

170. Tsukaguchi H, Shayakul C, Berger UV, Mackenzie B, Devidas S, Guggino WB, van Hoek AN, Hediger MA (1998) Molecular characterization of a broad selectivity neutral solute channel. J Biol Chem 273:24737–24743

171. Tsukaguchi H, Weremowicz S, Morton CC, Hediger MA (1999) Functional and molecular characterization of the human neutral solute channel aquaporin-9. Am J Physiol 277:F685–F696

172. Verkman AS (2006) Roles of aquaporins in kidney revealed by transgenic mice. Semin Nephrol 26:200–208

173. Verkman AS (2012) Aquaporins in clinical medicine. Annu Rev Med 63:303–316

174. Verkman AS, Mitra AK (2000) Structure and function of aquaporin water channels. Am J Physiol Renal Physiol 278:F13–F28

175. Verkman AS, Phuan PW, Asavapanumas N, Tradtrantip L (2013) Biology of AQP4 and anti-AQP4 antibody: therapeutic implications for NMO. Brain Pathol 23:684–695

176. Walz T, Fujiyoshi Y, Engel A (2009) The AQP structure and functional implications. Handb Exp Pharmacol, pp 31–56

177. Wang W, Kwon TH, Li C, Frokiaer J, Knepper MA, Nielsen S (2002) Reduced expression of Na-K-2Cl cotransporter in medullary TAL in vitamin D-induced hypercalcemia in rats. Am J Physiol Renal Physiol 282:F34–F44

178. Wang W, Li C, Kwon TH, Knepper MA, Frokiaer J, Nielsen S (2002) AQP3, p-AQP2, and AQP2 expression is reduced in polyuric rats with hypercalcemia: prevention by cAMP-PDE inhibitors. Am J Physiol Renal Physiol 283:F1313–F1325

179. Wang W, Li C, Kwon TH, Miller RT, Knepper MA, Frokiaer J, Nielsen S (2004) Reduced expression of renal Na+ transporters in rats with PTH-induced hypercalcemia. Am J Physiol Renal Physiol 286:F534–F545

180. Wang W, Li C, Nejsum LN, Li H, Kim SW, Kwon TH, Jonassen TE, Knepper MA, Thomsen K, Frokiaer J, Nielsen S (2006) Biphasic effects of ANP infusion in conscious, euvolumic rats: roles of AQP2 and ENaC trafficking. Am J Physiol Renal Physiol 290:F530–F541

181. Wang W, Li C, Summer S, Falk S, Schrier RW (2010) Interaction between vasopressin and angiotensin II in vivo and in vitro: effect on aquaporins and urine concentration. Am J Physiol Renal Physiol 299:F577–F584

182. Wang W, Li C, Summer SN, Falk S, Cadnapaphornchai MA, Chen YC, Schrier RW (2006) Molecular analysis of impaired urinary diluting capacity in glucocorticoid deficiency. Am J Physiol Renal Physiol 290:F1135–F1142

183. Wang W, Li C, Summer SN, Falk S, Schrier RW (2007) Polyuria of thyrotoxicosis: downregulation of aquaporin water channels and increased solute excretion. Kidney Int 72:1088–1094

184. Wang Y, Cohen J, Boron WF, Schulten K, Tajkhorshid E (2007) Exploring gas permeability of cellular membranes and membrane channels with molecular dynamics. J Struct Biol 157:534–544

185. Wang Y, Tajkhorshid E (2010) Nitric oxide conduction by the brain aquaporin AQP4. Proteins 78:661–670

186. Weiner ID, Verlander JW (2003) Renal and hepatic expression of the ammonium transporter proteins, Rh B Glycoprotein and Rh C Glycoprotein. Acta Physiol Scand 179:331–338

187. Xu DL, Martin PY, Ohara M, St John J, Pattison T, Meng X, Morris K, Kim JK, Schrier RW (1997) Upregulation of aquaporin-2 water channel expression in chronic heart failure rat. J Clin Invest 99:1500–1505

188. Yamamoto T, Sasaki S, Fushimi K, Ishibashi K, Yaoita E, Kawasaki K, Marumo F, Kihara I (1995) Vasopressin increases AQP-CD water channel in apical membrane of collecting duct cells in Brattleboro rats. Am J Physiol 268:C1546–C1551

189. Yang B, Brown D, Verkman AS (1996) The mercurial insensitive water channel (AQP-4) forms orthogonal arrays in stably transfected Chinese hamster ovary cells. J Biol Chem 271:4577–4580

190. Yang B, Folkesson HG, Yang J, Matthay MA, Ma T, Verkman AS (1999) Reduced osmotic water permeability of the peritoneal barrier in aquaporin-1 knockout mice. Am J Physiol 276:C76–C81

191. Yang B, Fukuda N, van Hoek A, Matthay MA, Ma T, Verkman AS (2000) Carbon dioxide permeability of aquaporin-1 measured in erythrocytes and lung of aquaporin-1 null mice and in reconstituted proteoliposomes. J Biol Chem 275:2686–2692

192. Yang B, Gillespie A, Carlson EJ, Epstein CJ, Verkman AS (2001) Neonatal mortality in an aquaporin-2 knock-in mouse model of recessive nephrogenic diabetes insipidus. J Biol Chem 276:2775–2779

193. Yang B, Ma T, Dong JY, Verkman AS (2000) Partial correction of the urinary concentrating defect in aquaporin-1 null mice by adenovirus-mediated gene delivery. Hum Gene Ther 11:567–575

194. Yang B, Ma T, Verkman AS (1995) cDNA cloning, gene organization, and chromosomal localization of a human mercurial insensitive water channel. Evidence for distinct transcriptional units. J Biol Chem 270:22907–22913

195. Yang B, Song Y, Zhao D, Verkman AS (2005) Phenotype analysis of aquaporin-8 null mice. Am J Physiol Cell Physiol 288:C1161–C1170

196. Yang B, Verbavatz JM, Song Y, Vetrivel L, Manley G, Kao WM, Ma T, Verkman AS (2000) Skeletal muscle function and water permeability in aquaporin-4 deficient mice. Am J Physiol Cell Physiol 278:C1108–C1115

197. Yang B, Verkman AS (1997) Water and glycerol permeabilities of aquaporins 1–5 and MIP determined quantitatively by expression of epitope-tagged constructs in Xenopus oocytes. J Biol Chem 272:16140–16146

198. Yang B, Verkman AS (2002) Analysis of double knockout mice lacking aquaporin-1 and urea transporter UT-B. Evidence for UT-B-facilitated water transport in erythrocytes. J Biol Chem 277:36782–36786

199. Yang B, Zador Z, Verkman AS (2008) Glial cell aquaporin-4 overexpression in transgenic mice accelerates cytotoxic brain swelling. J Biol Chem 283:15280–15286
200. Yang B, Zhang H, Verkman AS (2008) Lack of aquaporin-4 water transport inhibition by antiepileptics and arylsulfonamides. Bioorg Med Chem 16:7489–7493
201. Yang B, Zhao D, Solenov E, Verkman AS (2006) Evidence from knockout mice against physiologically significant aquaporin 8-facilitated ammonia transport. Am J Physiol Cell Physiol 291:C417–C423
202. Yang B, Zhao D, Verkman AS (2006) Evidence against functionally significant aquaporin expression in mitochondria. J Biol Chem 281:16202–16206
203. Yang B, Zhao D, Verkman AS (2009) Hsp90 inhibitor partially corrects nephrogenic diabetes insipidus in a conditional knock-in mouse model of aquaporin-2 mutation. FASEB J 23:503–512
204. Yang JH, Yu YQ, Yan CX (2011) Localisation and expression of aquaporin subtypes in epithelial ovarian tumours. Histol Histopathol 26:1197–1205
205. Yasui M (2009) pH regulated anion permeability of aquaporin-6. Handb Exp Pharmacol, pp 299–308
206. Yasui M, Hazama A, Kwon TH, Nielsen S, Guggino WB, Agre P (1999) Rapid gating and anion permeability of an intracellular aquaporin. Nature 402:184–187
207. Zeidel ML, Ambudkar SV, Smith BL, Agre P (1992) Reconstitution of functional water channels in liposomes containing purified red cell CHIP28 protein. Biochemistry 31:7436–7440
208. Zelenina M, Bondar AA, Zelenin S, Aperia A (2003) Nickel and extracellular acidification inhibit the water permeability of human aquaporin-3 in lung epithelial cells. J Biol Chem 278:30037–30043
209. Zelenina M, Christensen BM, Palmer J, Nairn AC, Nielsen S, Aperia A (2000) Prostaglandin E(2) interaction with AVP: effects on AQP2 phosphorylation and distribution. Am J Physiol Renal Physiol 278:F388–F394
210. Zelenina M, Tritto S, Bondar AA, Zelenin S, Aperia A (2004) Copper inhibits the water and glycerol permeability of aquaporin-3. J Biol Chem 279:51939–51943
211. Zhang D, Vetrivel L, Verkman AS (2002) Aquaporin deletion in mice reduces intraocular pressure and aqueous fluid production. J Gen Physiol 119:561–569
212. Zhang H, Verkman AS (2013) Eosinophil pathogenicity mechanisms and therapeutics in neuromyelitis optica. J Clin Invest 123:2306–2316
213. Zhang Z, Chen Z, Song Y, Zhang P, Hu J, Bai C (2010) Expression of aquaporin 5 increases proliferation and metastasis potential of lung cancer. J Pathol 221:210–220
214. Zhao D, Bankir L, Qian L, Yang D, Yang B (2006) Urea and urine concentrating ability in mice lacking AQP1 and AQP3. Am J Physiol Renal Physiol 291:F429–F438
215. Zhao G, Li J, Wang J, Shen X, Sun J (2014) Aquaporin 3 and 8 are down-regulated in TNBS-induced rat colitis. Biochem Biophys Res Commun 443:161–166